STUDIES ON Cu(II) AND Ni(II) COMPLEXES WITH MIXED S,N-DONOR LIGANDS : BIOINORGANIC PERSPECTIVES

By

SUBRATA MANDAL

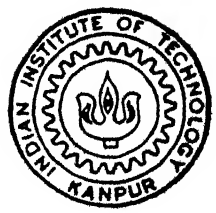

DEPARTMENT OF CHEMISTRY

INDIAN INSTITUTE OF TECHNOLOGY KANPUR

August, 1992

STUDIES ON Cu(II) AND Ni(II) COMPLEXES WITH MIXED S,N-DONOR LIGANDS : BIOINORGANIC PERSPECTIVES

A Thesis Submitted
in Partial Fulfilment of the Requirements
for the Degree of
DOCTOR OF PHILOSOPHY

[redacted]

SUBRATA MANDAL

to the

DEPARTMENT OF CHEMISTRY
INDIAN INSTITUTE OF TECHNOLOGY KANPUR

August, 1992

Dedicated to
my parents

DEPARTMENT OF CHEMISTRY
INDIAN INSTITUTE OF TECHNOLOGY, KANPUR INDIA

CERTIFICATE - 1

This is to certify that Mr. SUBRATA MANDAL has satisfactorily completed all the courses required for the Ph.D. Degree program. These courses include :

Chem 505 Principles of Organic Chemistry

Chem 524 Modern Physical Methods in Chemistry

Chem 525 Principles of Physical Chemistry

Chem 545 Principles of Inorganic Chemistry

Chem 541 Advanced Inorganic Chemistry I

Chem 646 Bioinorganic Chemistry

Chem 800 General Seminar

Chem 801 Graduate Seminar

Chem 900 Post-Graduate Research

Mr. Subrata Mandal successfully completed his Ph.D. qualifying examination ~~in~~ 18th September 1989.

24/8/92

(S.S. Katiyar)
Professor and Head
Department of Chemistry
I.I.T. Kanpur

24/8/92

(B.D. Gupta)
Professor and Convenor
Departmental Post Graduate Commit
Department of Chemistry
I.I.T. Kanpur

CERTIFICATE - II

It is certified that the work contained in the theis entitled `STUDIES ON Cu(II) AND Ni(II) COMPLEXES WITH MIXED S,N-DONOR LIGANDS : BIOINORGANIC PERSPECTIVES' by *Subrata Mandal*, has been carried out under my supervision and the same has not been submitted elsewhere for a degree.

P. K. Bharadwaj 29/8/92

(Dr. P.K. Bharadwaj)
Department of Chemistry
Indian Institute of Technology, Kanpur

August, 1992.

A C K N O W L E D G E M E N T

I feel immense gratitude and indebtedness to Dr. P.K. Bharadwaj, who provided invaluable guidance, inspiration, numerous suggestions and took keen interest in the progress of the research work and preparation of the manuscript of the thesis. Without his active involvement, many hurdles faced during this work wouldn't have been overcome. Working with him has indeed been a memorable and educative experience for me. It was his encouragement and faith in me which generated self confidence to be able to meet any challenge boldly and independently.

A special word of thanks to Prof. S. Sarkar, Dr. R.N. Mukherjee, Dr. J. Iqbal and Dr. S. Manogaran for generously extending their laboratory facilities. It was an extremely enjoyable experience for me working with my colleagues Mr. K. Ragunathan, Dr. R. Shukla, Dr. B.R. Srinivasan, Dr. Surendranath, Messers G. Mandal, Prasenjit, Atul K. Verma, Ish Dhawan and Sunil Paliwal, Ms. Poonam, Jayati, Annapurna and Latha for their whole hearted cooperation and congenial company. I sincerely thank all of them.

It has been a pleasure to be in the company of friends like Messers M. Ray, S. Mahapatra, S. Das, T.K. Lal, Debashis, P. Tarakeswar, Jayaraman, S. George, Tamil, Bhisma, Naren,M. Reddy, R.S. Singh, P. Kumar, S. Roy, S. Kumar, Balakrishnan, Ilangovan, Kashi & D. Kundu, Dr. J.K. Dey, Mrs. D. Bharadwaj, Ms. Indrani and B. Bhatia. I am grateful to all of them for their help, cooperation and pleasant association.

I am thankful to Messers N. Ahmed, Kannaujia, Bhavsar and Rajagopalan for recording the spectra for me. I wish to thank Mr. Panth and A.K. Ganguli for their help in the preparation of this thesis.

I find myself at a loss for words in expressing my heartfelt gratitude to my adored parents, brother, elder sister and other family members for providing tremendous moral support and encouragement for completion of my work.

Finally, the financial support from the authorities of I.I.T. Kanpur is gratefully acknowledged.

SUBRATA MANDAL

SYNOPSIS

The thesis entitled "Studies on Cu(II) and Ni(II) complexes with Mixed N,S-Donor Ligands : Bioinorganic Perspectives" has been divided into six chapters.

Chapter I gives a general account of modelling the active sites of some copper and nickel containing proteins. Active sites of most of the copper proteins are intrinsic in nature. It is, therefore, difficult to have model copper complexes which can mimic all aspects of structure and bonding of these sites. However, model copper complexes can be synthesized which may serve as electronic structural analogues. These electronic structural analogues can duplicate specific features of the active sites' properties and can provide an important data base to facilitate interpretation of data obtained on native active sites. Modelling the copper proteins' active sites can be effectively done by studying separately copper-nitrogen, copper-thioether and copper-thiolate bondings. A good amount of data are available on copper-nitrogen bonding. Comparatively less is known about copper-thiolate bonding although its bioinorganic scope is enormous. In this chapter, brief discussions on the above three types of bondings are presented. A short description on the present status of modelling the nickel centre of some hydrogenases is also presented.

Chapter II discusses the scope of the present work. Emphasis is given on synthesizing Cu(II)-thiolato complexes with different coordination geometries. The following points are discussed :

(i) no thiolato complex has been reported todate that can show rhombic EPR spectral characteristics of the stellacyanin class of blue proteins.

(ii) no hexacoordinated Cu(II) complex having thiolate ligation has been described in the literature. Suitably designed hexadentate ligands are capable of forming tetragonal Cu(II) complexes which can lower the Cu(III)/Cu(II) couple so that oxidation of Cu(II)-thiolates can be easily achieved. This is important because in the catalytic cycles of some copper proteins, involvement of Cu(III) has been implicated.

(iii) A new route of synthesizing stable Cu(II)-thiolates is important from the points of view of synthetic inorganic chemistry as well as bio-inorganic chemistry of copper.

(iv) Hexadentate tripodal ligands bearing S and N donors for ligation to Ni(II) should provide an alternative approach to model the nickel centre present in some hydrogenases.

Chapter III has been divided into two parts. Part A describes synthesis of tetradentate ligands with the donor sets, N_2S^*S (S^* = thioether) and N_2S^*O both of which form tetragonal Cu(II) complexes based on electronic and EPR spectral, room temperature magnetic susceptibility and electrochemical studies. Part B concerns with the isolation and characterization of two pseudotetrahedral CuN_2S_2 complexes which show high positive potential ($E_{1/2} \approx 0.5$V vs. SCE) for the Cu(II)/Cu(I) couple. One of the complexes show rhombic EPR spectrum in acetonitrile glass like the ones obtained with stellacyanin class of blue proteins. The rhombic nature has been suggested as due to mixing of about 5% of d_z2 orbital into the ground state wavefunction. Similar mixing

has been suggested to account for the rhombic nature of stellacyanin EPR spectrum.

Chapter IV presents a number of hexacoordinated Cu(II)-thiolates having the chromophore, $CuN_2S^*_2S_2$ (S^* = thioether) where the four sulfurs are equatorially bonded. This bonding arrangement destabilizes the singly occupied $d_{x^2-y^2}$ so that the electron loss from this orbital becomes easier giving rise to oxidized Cu(II)-thiolate species. Each of the complexes shows well defined cyclic responses with $E_{1/2}$ of about 0.5 V vs. SCE. One of the complexes actually show reversible oxidative response. Various control experiments, to sort out possible ligand oxidations, are described. A characteristic feature in the electronic spectrum of each complex is an intense absorption ($\epsilon_{max} \approx$ 3000-5000 $dm^3mol^{-1}cm^{-1}$) around 600 nm attributable to σ(thiolate) $\rightarrow$ Cu(II) LMCT transition.

Chapter V describes a new route of synthesizing Cu(II)-thiolates having the chromophore, CuN_2S_2 by reacting $[Cu(CH_3CN)_4]BF_4$ with 10-membered macrocyles having a disulfide linkage besides two amino groups in the ring. X-ray structural studies have been carried out to confirm the formation of the starting macrocycles. Molecular structure of a rearrangement product is also described in this chapter.

Chapter VI presents the synthesis of two new tripodal ligands with the donor set, S_3N_3. These tripodal ligands form 1:1 complexes with Ni(II) salts with the coordination geometry distorted from octahedral. Molecular structure of one NiS_3N_3 complex is described and is correlated with the solution electronic spectrum.

CONTENTS

CHAPTER 6

CHAPTER 1

INTRODUCTION

The chemistry of copper was dominated, not so long ago, by four-coordinate square planar complexes of copper(II), even to the extent of ignoring copper(III) altogether in most inorganic chemistry texts. The demands of biochemistry led to an upsurge in interest in copper chemistry. As new copper proteins are discovered or the electronic structure and bonding of the already known proteins are being probed continually, studies of model complexes become more crucial. Copper containing proteins are involved in a wide variety of biochemical functions including copper transport [1] (ceruloplasmin), copper storage [2] (metallo thionein), protective roles [3] (superoxide dismutase), oxygenase catalysis [4] (galactose oxidase), oxygen transport [5] (hemocyanin), electron transport [6] (plastocyanin), terminal oxidase for O_2 respiration [7] (cytochrome C oxidase), oxidation of amine [8] (amine oxidase) etc. The incredibly diverse roles of these proteins depend upon variation in the chemical nature and geometrical disposition of the ligation at the binding sites.

The use of spectroscopic techniques to probe the metal binding sites remains a subject of considerable current interest. Even in the cases where crystallographic studies have revealed the structural details of the binding sites, spectroscopic, electrochemical and reactivity with various substrate molecules are still required to establish how the redox and chemical

properties are tuned by the interactions of the available metal and ligand orbitals.

However, the active sites in many of these copper proteins are intrinsic [9] in nature, i.e., they are formed through intimate interactions of the copper ions with the amino acid residues of the proteins. An intrinsic active site generates an unusual coordination environment at the metal binding site due to conformationally imposed constraints upon amino acid side chains that comprise the ligands for the metal ion. The imposition of an irregular geometry onto a metal ion at the active site is designed by nature to achieve a condition energetically favourable [10] to carry out its assigned biological role(s). However, this leads to two important problems : (i) spectroscopic studies of the native proteins may yield data that are difficult to interpret and (ii) it is quite unrealistic to expect to synthesize a complex which is a detailed model for an intrinsic active site. It is possible, however, to generate small, well-defined electronic structural analogues which duplicate specific protein features and can be studied in detail to provide a data base to facilitate interpretation of data obtained on the native protein systems. The best way to approach such a difficult problem is to divide it into a set of simpler problems. In case of copper proteins, this objective can be achieved by studying copper(II) complexes with ligands containing one type of donor atoms followed by ligands having mixed donors. The donor atoms that provide ligation at the active sites of the copper proteins include nitrogen, oxygen and sulfur with oxygen being less common.

A brief review of copper-nitrogen and copper-sulfur bonding has been made in this chapter. This is to have the right perspectives for the work described in this thesis. Discussion are limited to mononuclear complexes and are not claimed to be exhaustive. The present thesis describes the synthesis and characterization of copper (II) complexes with ligands having nitrogen (amine, imine and amide) and sulfur (thiolate and thioether) donors. However, emphasis has been given on Cu(II)-thiolato complexes. Hence, for brevity, only copper-thiolate bonding will be dicussed in detail.

1.1 Copper (II)-Nitrogen Bonding

One or more histidine imidazole ligands are present at the binding sites of nearly all copper containing proteins. The structural features of such bonding have been established by crystallographic studies of plastocyanin [11], azurin [12], basic blue protein [13], amicyanin [14], ascorbate oxidase [15],glactose oxidase [16] and superoxide dismutase [17]. Other evidences have been used to infer copper(II)-imidazole interactions in stellacyanin [18], serum albumin [19], cytochrome C oxidase [20], ceruloplasmin [21], hemocyanin [22], etc. Electronic spectral [23], circular dichroism [24] and magnetic circular dichroism [25] alongwith EPR [26] and ENDOR [27] studies on native proteins as well on models have been carried out to probe the important role of Cu(II)-imidazole interactions in biological systems. Early work in this area has been reviewed by Sundberg and Martin [28] while references to more recent literature are given in the study

of Cu(II)-histidine systems by Casella and Gullotti [29]. Harvey Schugar's group has significantly contributed [30] to our understanding of Cu(II) imidazole bonding and its bioinorganic significance. Electronic structure and the positions of LMCT absorptions have been quantified [30] by a combination of spectroscopic and molecular orbital studies of systematically perturbed imidazoles and their complexes with copper(II) having more or less tetragonal geometry. Appearance of these LMCT bands has been shown to be dependent on the orientation of the imidazole rings [31] relative to that of the half-filled d-vacancy on copper(II). Tetrahedral or pseudotetrahedral copper (II) complexes can be useful probes to answer important questions about the active sites of copper-proteins that embody this structural feature. Simple monodentate or bidentate ligands favourably form square planar Cu(II) complexes. Introducing rigidity in the ligand framework via ligand design can, however, impose a non-planar coordination geometry. The geometrically constraining bidentate ligand 2,2'-bis(2-imidazolyl) biphenyl (Fig. 1.1) is able to form pseudotetrahedral CuN_4 complexes [32] with both Cu(II) and Cu(I). X-band EPR parameters for the copper (II) complex doped into the isostructural Zn(II) complex are remakably similar to those for Cu(II) doped into the pseudotetrahedral Zn(II) site of superoxide-dismutase . The neat Cu(II) complex gives an absorption band at 22700 cm^{-1} assigned as π(imH) $\rightarrow$ Cu(II) LMCT transition which compares favourably in energy and intensity with the corresponding absorptions observed for plastocyanin and Cu(II)-doped Zn superoxide-dismutase. Cyclic

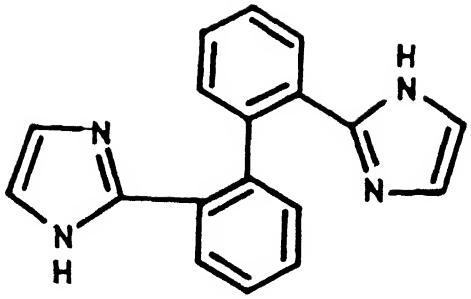

Fig 1.1 2,2'-bis (2-imidazolyl) biphenyl ligand

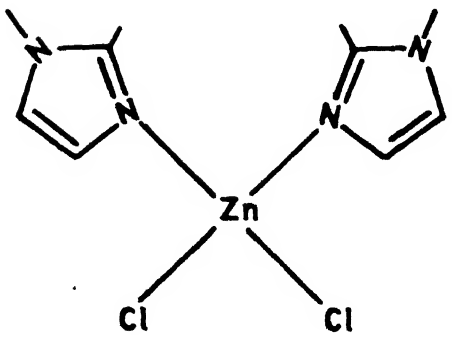

Fig 1.2 Pseudotetrahedral $[Zn(1,2\text{-}Me_2Im)_2\ Cl_2]$ complex

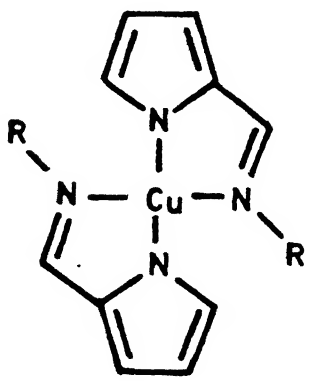

Fig 1.3 Copper(II) complex with a pyrrole-2-carboxaldehyde Schiff base ligand

voltammetric studies in acetonitrile revealed a reversible Cu(II)/Cu(I) couple at RT with $E_{1/2}$ = + 0.11 V vs SCE. The positive Cu(II)/Cu(I) potential is reflective of its structure distorted from regular planar geometry favoured by Cu(II). This distorted structure is a compromise geometry acceptable to both oxidation states as found in native blue proteins' active sites. A pseudotetrahedral Cu(II)-doped Zn (1,2-dimethylimidazole)$_2$Cl$_2$ complex (Fig. 1.2) has been characterized by X-ray crystallography [33]. This complex exhibits [34] rhombic EPR spectrum similar to that observed in case of structurally uncharacterized blue copper protein, stellacyanin. Single crystal optical and EPR studies on this complex combined with ligand field and SCF-X_α-SW calculations indicate that the rhombically split g and A values can be explained through admixture of about 3% d_z2 character in the ground state wave function. In contrast to the C_{3v} effective symmetry found in plastocyanin, stellacyanin is predicted to have C_{2v} effective symmetry. The rhombic splitting seen in the EPR spectrum of stellacyanin is calculated [35] to be due to 2-5% mixing of d_z2 into the ground state. Thus, spectroscopic questions regarding distorted tetrahedral imidazole-containing Cu(II) chromophores present in the blue protein active sites may profitably be pursued by studying model compounds of this type. To achieve this goal, chelating ligands containing a number of pyrazole units have also been used. This is because pyrazoles have electronic structures similar [36] to imidazoles and polydentate pyrazole ligands are easier to synthesize than the imidazole analogs. Thus, a large number of CuN_4 complexes with

pyrazoles are known which have been subjected to electronic and EPR spectral studies [37,38]. Detailed assignment of LMCT transitions in pyrazole -Cu(II) systems is, however, potentially complicated [39] by the relatively small separation of π-symmetry orbitals in the free ligand of about 0.7 eV (the corresponding separation in imidazole is about 1.2 eV).

Electronic and EPR spectral and electrochemical studies are available [40] on a series of pyrrole-2-carboxaldehyde Schiff base copper(II) complexes (Fig. 1.3) where coordination geometry is systematically varied from square planar to pseudotetrahedral. Smooth correlations could be observed among d-d band energies, $g_{\parallel}$ and $A_{\parallel}$ values. As the dihedral angle between the chelate rings increases from 0^{o} (square planar) through 90^{o} (tetrahedral), $g_{\parallel}$ increases, $|A_{\parallel}|$ decreases and redox potentials shift systematically to more positive values. Relatively fewer studies are available on copper(II) complexes with simple aliphatic/aromatic amines. Electronic and EPR spectral studies on the copper(II) complexes of ethylenediamine and its alkyl derivatives have been reported [41]. Correlations between the position of LMCT bands and first ionization potential of the free amines have been made. However, cyclic voltammetric data are not available on these complexes. In the preparation of pseudotetrahedral CuN_4 complexes, bidentate and polydentate N-donor ligands have been used [42,43]. These complexes show dihedral angles ranging upto ~72^{o} but the tetrahedral limit of 90^{o} has remained elusive.

1.2 Copper(II)-Thioether Bonding

Although the synthesis and characterization of Cu(II)-thioether complexes remains a subject of some interest, the bio-inorganic relevance of these systems is considerably less compared to complexes with ligands having nitrogen and thiolate donors. A number of copper blue proteins have copper-thioether ligation at their active sites. However, the electronic spectral consequences of copper(II)-thioether ligation in these centres are not profound [44]. One of the reasons being substantial elongation of this bond from its typical length that ranges within (2.3 - 2.4Å) as found in Cu(II) complexes [45]. Simple thioethers are poor ligands [46] for copper(II). Therefore, chelating ligands having thioethers in addition to other types of donors have been used. A significant number of Cu(II)-thioether complexes with various geometries are thus known. A particularly interesting thioether complex was synthesized [47] with the ligand 1,3-bis (5-phenyl-2-imidazolyl)-2-thiopropane. This tetragonal $[CuN_4S^*_2]^{2+}$ complex has four equatorial Cu-N bonds and two long axial Cu-S^* bonds of 2.824(5)Å each. The blue protein plastocyanin has a copper-thioether bond of length 2.9 Å.

A large number of Cu(II)-complexes with macrocylic thioethers are also known which are irrelevant here and, therefore, not discussed.

1.3 Copper(II)-Thiolate Bonding

Ligation of thiolate sulphur to copper at the active sites of quite a number of copper proteins has been established.

Cu(II)-thiolate bonding has been shown to be present by x-ray crystallography in case of single copper proteins like plastocyanin [11], azurin [12], pseudoazurin [48], basic blue protein [13] from cucumber (CBP), bacterial blue protein [14], amicyanin from T.Versutur and in a multicopper protein, ascorbate oxidase [16]. In case of other monocopper blue proteins like stellacyanin, rusticyanin or multicopper oxidases like tree and fungal laccases, ceruloplasmin etc., copper-thiolate bonding could be established by various spectroscopic studies [49]. Non-blue proteins like the Cu_A site in cytochrome C oxidase [50] also contains two cysteine thiolates bonded to Cu(II). In addition, Cu(II) ion has been used as a spectroscopic probe for active sites of different metalloproteins [51]. In these cases as well, the presence of Cu(II)-thiolate bonding at the active sites could be established spectroscopically. Thus, the bio-inorganic significance of Cu(II)-thiolate bonding is enormous. Particularly, the blue protein active sites (type 1 site) have spectroscopic signatures attributable to a significant extent to the presence of strong Cu(II)-thiolate bonding [52].

All these type 1 sites show an intense absorption band centred around 600 nm (molar Cu absorptivity lie in the range, 2000-6000) attributable to σ(thiolate) $\rightarrow$Cu(II) LMCT transition. The electronic consequences, when thiols are converted to thiolates and coordinate Cu(II) in a type 1 geometry have been comprehensively described [53] by Solomon and coworkers. Their SCF-X_α calculations on hypothetical $CuN_2(NH_3)(CH_3S)(CH_3SCH_3)$ systems have contributed significantly to our knowledge of the

electronic structure and bonding of the type 1 active site. The HOMO of free methanethiolate consists of two degenerate orbitals which are about 91% sulfur p_x and p_y and the rest 9% CH_3 character. The third orbital is 2.2 eV deeper in binding energy and has about 59% sulfur p_z character. It is this orbital that forms the σ-bond between sulfur and the methyl group. Upon complexation, the degenerate orbitals are converted into local π-symmetry and σ-symmetry orbitals separated in energy by ~1.6 eV while the third orbital lie lower by ~2 eV. This scenario is illustrated in Fig. 1.4. Moreover, these orbitals interact strongly with the Cu d-orbitals but do not interact to any significant extent with other ligands. As this picture unfolds, thiolate LMCT involves excitation from three occupied MOs having mixed S-Cu character into an acceptor orbital similarly constituted. Thus, taking the calculated orbital energies at the face value, a strong σ(thiolate) $\longrightarrow$ Cu(II) LMCT absorption is expected to be flanked on either side (by ~60 - 80 nm) by weaker π(thiolate) $\longrightarrow$Cu(II) LMCT transitions if electron reorganisation and correlation effects are ignored. In plastocyanin spectrum (Fig. 1.5) this theoretical predictions have been observed experiementally.

EPR spectral studies on the blue proteins have revealed that subtle yet important differences exist amongst the blue proteins type 1 centres [54]. Proteins like plastocyanin shows essentially an axial EPR spectrum; only a small rhombic splitting can sometimes be detected. On the other hand, proteins like stellacyanin or CBP exhibits EPR spectrum which is rhombically

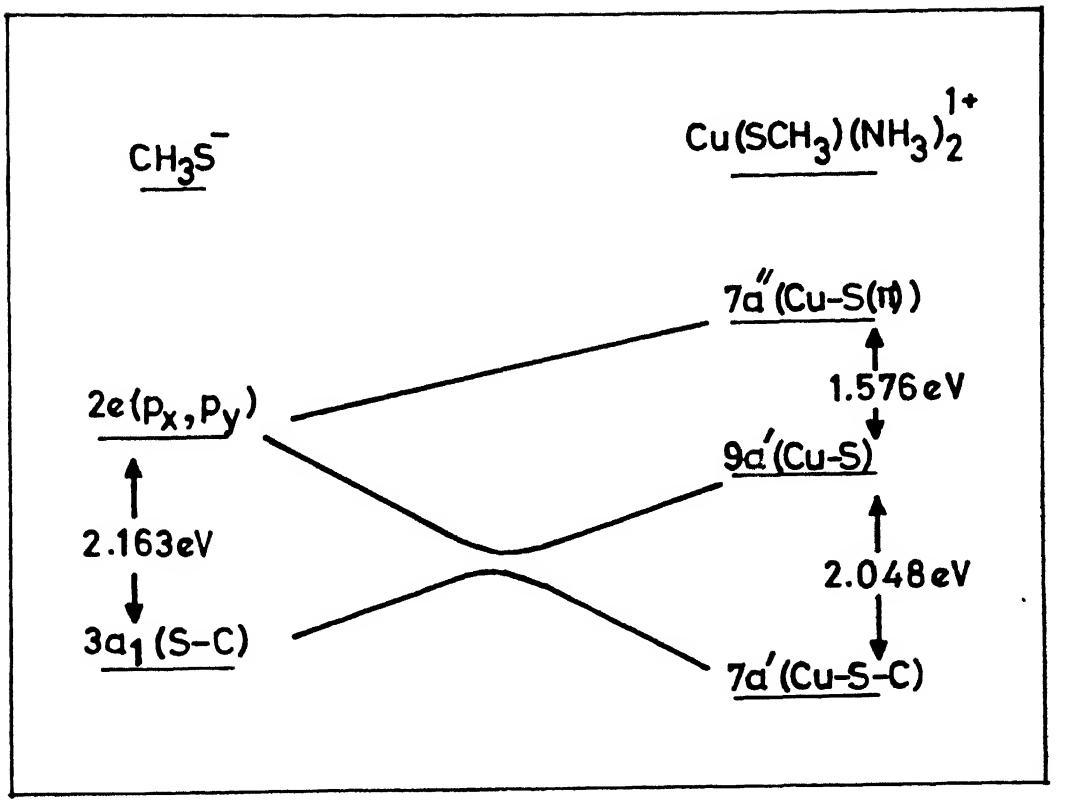

Fig 1.4 Interection of the three highest energy orbitals of methanethilate with a Cu(II) ion

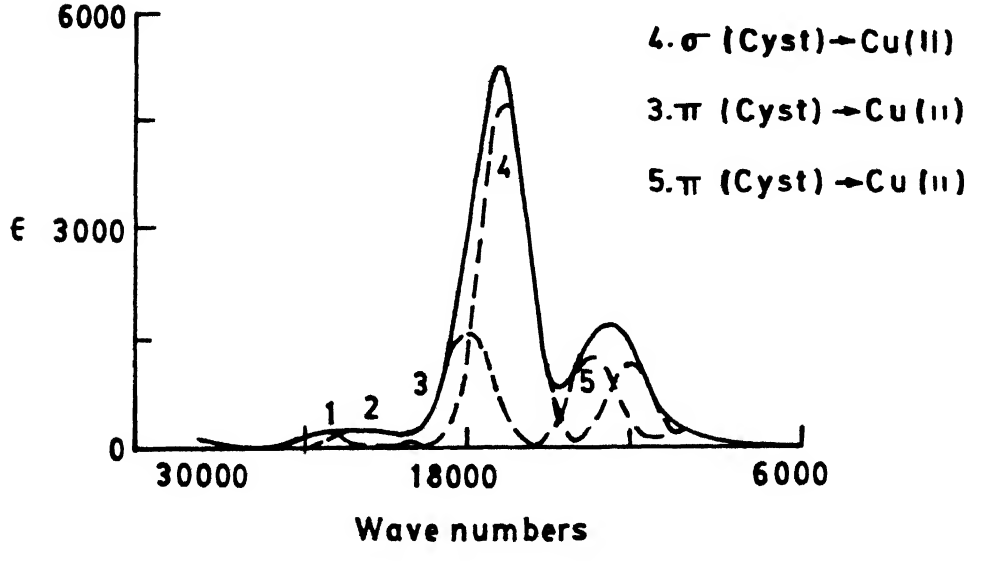

Fig 1.5 Visible spectrum of plastocyanin around 600 nm

distorted. To have a quantitative idea, plastocyanin shows (g_x-g_y) = 0.017 whereas for stellacyanin, (g_x-g_y) = 0.057. However, all the known blue sites show a very small hyperfine coupling in the parallel region ($A_{\parallel}$). The ground electronic state description should, therefore, be different for the two classes of blue proteins. SCF-X_{α} studies [53] suggest that in case of plastocyanin, extensive delocalization of the single d-electron onto sulfur pπ (cys 84) orbitals gives the almost axial EPR spectra with a small $A_{\parallel}$ value. In case of stellacyanin, however, about 3% mixing of the d_z2 orbital into the ground state wavefunction can account for its EPR parameters [54].

In case of non-blue proteins like the Cu_A site in cytochrome C oxidase, the Cu(II)-thiolate bond had been described as very covalent in character [50]. The reaction between Cu(II) and thiolates has other important biological significance as well. For example, the thiol D-penicillamine is effective in removing excess of copper from patients suffering from Wilson's disease [55]. Also it has been suggest that use of D-penicillamine in the treatment of rheumatoid arthritis may be related to its affinity [56] for copper ions.

Obviously, synthesis of stable Cu(II)-thiolato complexes is an area of continued interest. The problem lies, however, in the thermodynamic instability of Cu(II)-thiolate systems which readily undergo decomposition giving Cu(I), disulfides and other products [57]. Surmounting this instability a number of systems have been isolated and characterized in the solid state which are discussed next. Of course, quite a few Cu(II)-thiolate systems

have been studied in solution as well [58,59]. However, little is known about their coordination geometry; also the assumptions that single solution complexes are present have not been seriously tested.

Australian workers synthesized and X-ray crystallographically characterized [60] the first Cu(II)-thiolato complex in 1977. The ligand used was a tetradentate N_2S_2-donor derived from Schiff base condensation of o-mercapto-benzalehyde with ethylenediamine. The structure consists of monomeric cis-CuN_2S_2 units. While detailed structure is not available, the EPR shows rhombic splitting signifying the geometry somewhat distorted from planarity. Complete electronic spectral data are also not available and might be obscured by strong near-UV absorptions of the ligand. Since that time, quite a few Cu(II)-thiolates have been synthesized following different strategies.

One such strategy involves anchoring a Cu(II) ion in a suitable macrocycle and then allow it to react with a thiol/thiolate to inhibit the formation of any binuclear intermediate of the type $[Cu_2(SR)_2]$, which provides the redox complimentary pathway to the disulfide product. Following this strategy, a number of Cu(II)-thiolates have been isolated and characterized whose structural data are collected in Table 1.1. A stable Cu(II)-thiolate formed in the reaction of the macrocyclic tetramine complex, $Cu(tetb)^{2+}$ with o-mercaptobenzoate has approximately trigonal bipramidal geometry (Fig. 1.6) where thiolate sulfur occupy an equatorial position [61]. The complex

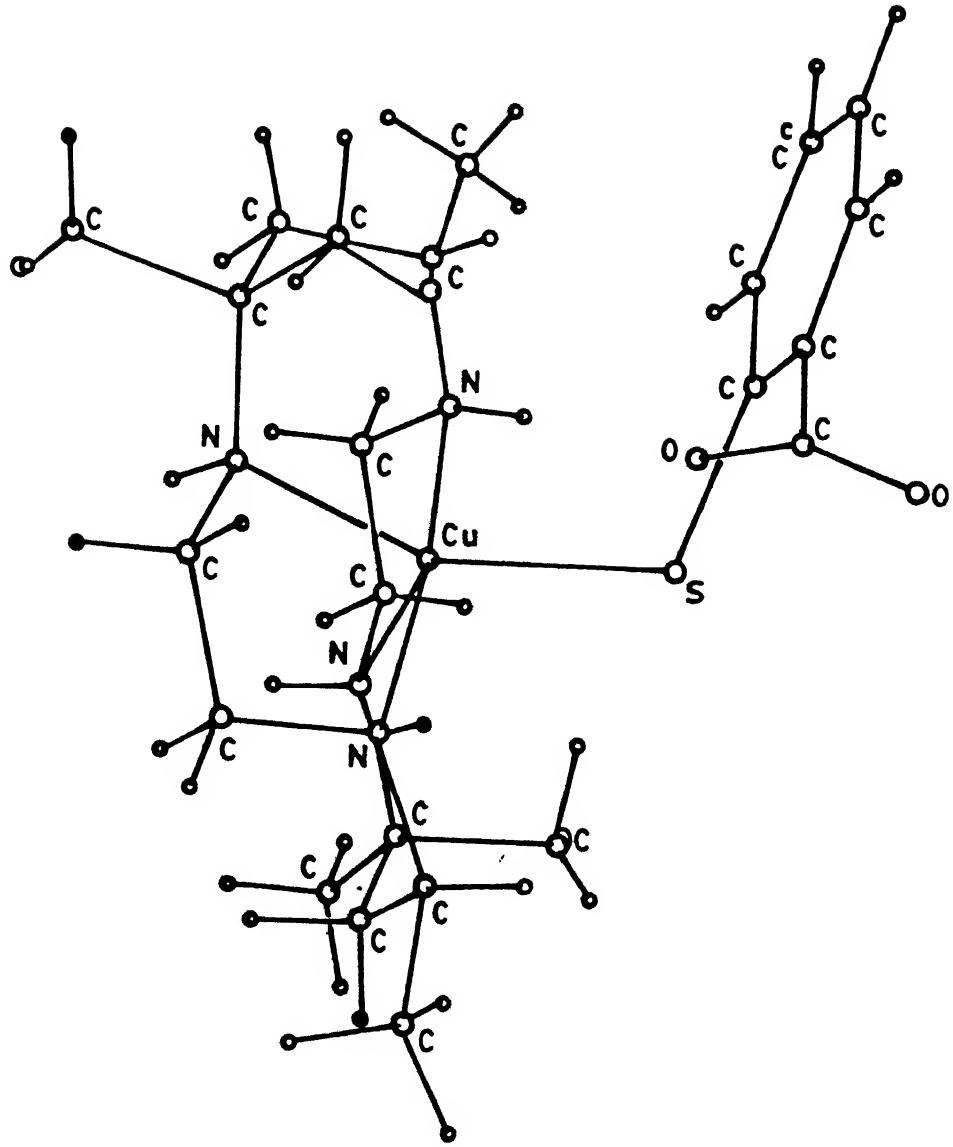

Fig 1.6 A perspective view of the complex, Cu(tetb) o-mercaptobenzoate

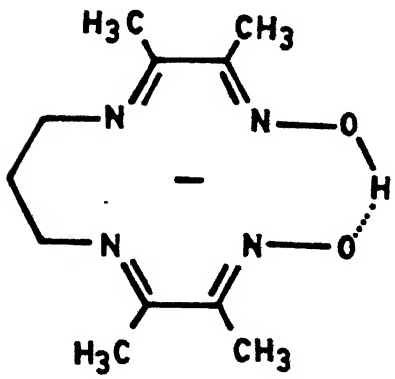

Fig 1.7 Monoanionic tetramine ligand

Table 1.1

Structural Data of CuN_4S Complexes

Complex	Geometry	Bond length A				Ref
		$Cu-S^a$	$Cu-S^e$	$Cu-N^a$	$Cu-N^e$	
1. Cu(Tetb) ($SC_6H_4CO_2$-p)	Trigonal-bipyramidal	--	2.359	2.012	2.162	61
2. Cu(Tetb) (SCH_2CH_2-CO_2)	Trigonal-bipyramidal	--	2.314	2.016	2.161	66
3. Cu(Tetb) ($SSCH_2CO_2$)	Trigonal-bipyramidal	--	2.328	2.062	2.068	67
4. Cu(Cyclam) $(SC_6F_5)_2$	Tetragonal	2.940	--	--	2.008	62
5. Cu(N_4-dione dioxime) (SC_6H_5)	Square-pyramidal	--	2.424	--	1.979	63
6. Cu(N_4-dione dioxime) (SC_6H_5Cl-p)	Square-pyramidal	2.424	--	--	1.976	63
7. $Cu_2(Cyclop)_2$ (SC_6H_4Me-p)	Square-pyramidal	2.471	--	--	1.961	64

shows a strong absorption near 360nm assigned as σ-(thiolate) $\rightarrow$Cu(II) LMCT absorption while the weaker flanking absorption at lower energy has been assigned as π(thiolate) $\rightarrow$Cu(II) transition. The lower energy π-tansition is split owing to a weak bonding and antibonding interaction of the sulfur orbitals with the π-system of the benzene ring. With another macrocyclic complex, $Cu(cyclam)^{2+}$, pentafluorothio-phenolate forms [62] a tetragonal CuN_4S_2 complex where the axially disposed thiolates are weakly bonded (Cu-S = 2.94Å). The optical and ESR spectra of this complex reveal no characteristic effects of thioate coordination. Two approximately square pyramidal CuN_4S complexes have been reported [63] by Anderson et.al. where the four equatorial N-donors are supplied by the monoanionic tetramine ligand shown in Fig. 1.7 and the apical S-donor is either thiophenolate (Fig. 1.8) or p-chlorothiophenolate. Both complexes show absorptions at ~350 ($\epsilon_{max} \simeq 5400$) and ~430nm ($\epsilon_{max} \simeq 5200$). These absorptions overlap with an intense UV absorption from the ligands and the true molar extinction coefficients must be significantly smaller. These complexes show a cyclic response with $E_{1/2} \approx -0.85V$ vs. SHE. The parent $[Cu(N_4)]BF_4$ complex exhibits a cyclic response with $E_{1/2} = -0.49V$ vs SHE. Thus, it appears clear that binding of the thiolates is associated with a stabilisation of the Cu(II) state by approximately 350 mV. Japanese workers reported [64] an interesting thiolate bridge Cu(II) dimer in which a single p-methylbenzenethiolate serves as the apical ligand for two CuN_4 unit similar to the one shown in Fig. 1.9 except that the two oxime oxygens are linked with a BF_2 fragment. The electronic

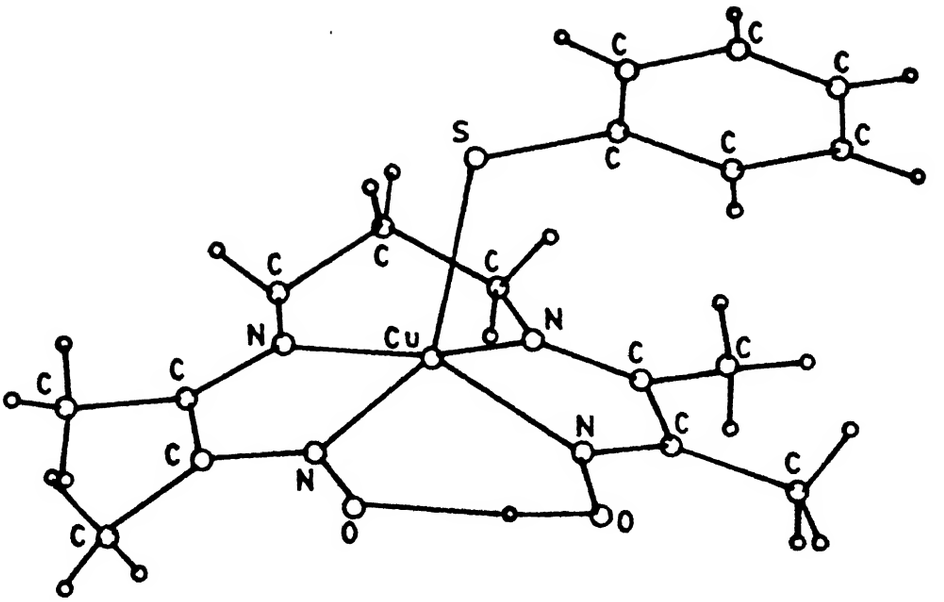

Fig 1.8 Square-pyramidal CuN_4S complex

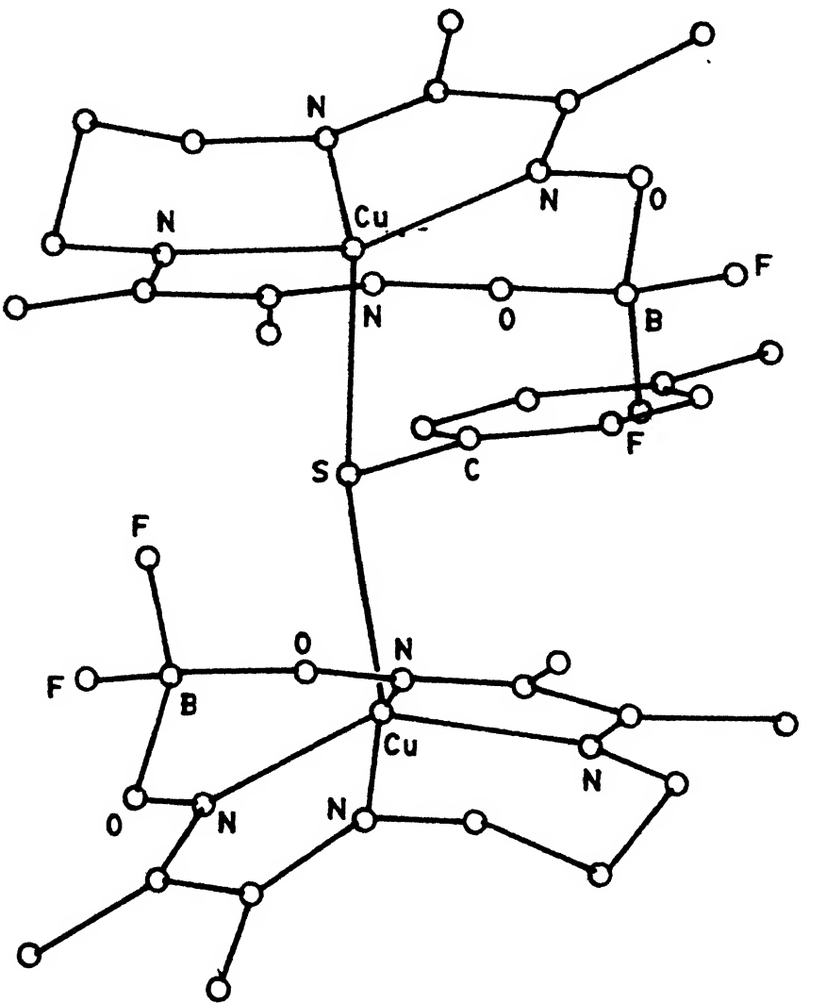

Fig 1.9 Thiolato-bridged dimeric Cu(II) complex

specturm is reminescent of those exhibited by the monomers [63] of Anderson et.al. All of the above structurally characterized complexes contain ligation by aromatic thiolates. The observed thiolate LMCT absorptions are potentially complicated due to "through space" interactions between $S3_p$ orbitals and the highest occupied MOs of the aromatic π-system [65]. These interactions are apparent in the photoelectron spectra of the free ligands, but are not quantified in the LMCT absorptions which originate from ligand orbitals perturbed in this manner due to paucity of such complexes.

Aliphatic thiolates also give similar complexes although they are much less stable. A green coloured trigonal bipyramidal complex [66] of $Cu(tetb)^{2+}$ and 3-mercaptopropinate has been characterized in the solid state (Fig 1.10). The equatorial Cu-S distance is shorter than those reported for the aromatic thiolate complexes (Table 1.1). Green methanolic solutions of this complexes rapidly decomposes. However, electronic spectra of the polycrystalline $Cu(tetb)^{2+}$ complexes with 2-mercaptobenzoate and 3-mercaptopropionate are similar except low intensity of the presumed π(thiolate)$\rightarrow$Cu(II) LMCT band. With mercaptoacetate, $Cu(tetb)^{2+}$ forms a complex [67] which is a rarely documented example of a ligating hydropersulfide i.e. $[SSCH_2CO_2]^{2-}$. The coordination geometry around Cu(II) is similar to what is present in case of the complex with 3-mercaptopropionate. The observed electronic spectral pattern of modestly intense near UV LMCT absorptions is reminiscent of peroxide $\rightarrow$ metal LMCT absorptions [68].

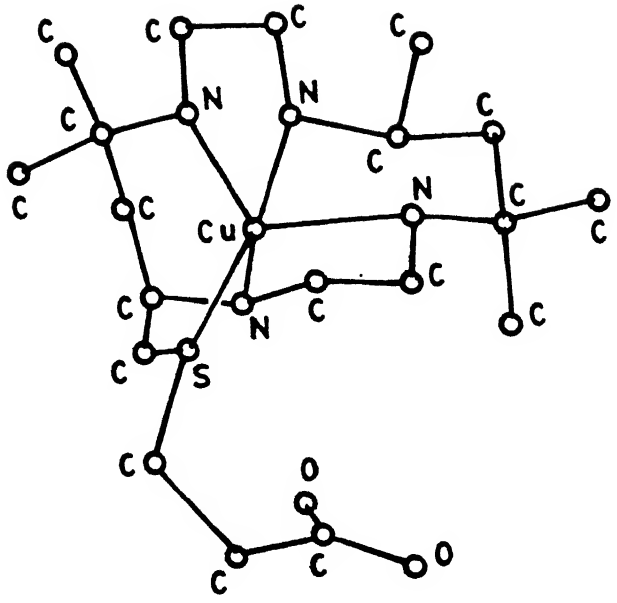

Fig 1.10 A perspective view of the complex, Cu(tetb) 3-mercaptopropionate

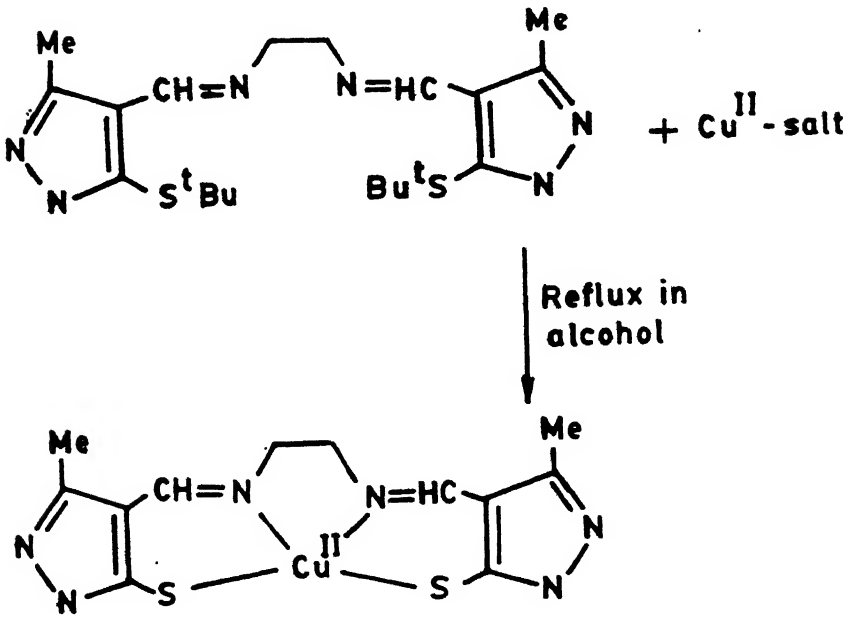

Fig 1.11 Synthesis of Cu(II)-thiolates by breaking the S-^{t}Bu linkage

Another strategy of synthesizing stable Cu(II)-thiolates makes use of the Lewis acidity of Cu(II) ion [69]. In this method, a polydentate ligand where the thiols are protected as t-butyl mercaptides, is allowed to reflux with a Cu(II)-salt in alcohol. During reflux, Cu(II) cleaves the S-^{t}Bu linkage and gets bonded to the free thiolates (Fig. 1.11). This method not only is easy but also gives the products in high yields. Using this synthetic strategy Toftlund and coworkers [69-71] have been able to isolate a good number of cis-CuN_2S_2 complexes. A representative structure of such a CuN_2S_2 complex is shown in Fig. 1.12. Positions of the ligand field bands in these complexes have been shown to be dependent on the coordination geometry. As the geometry distorts from planarity towards tetrahedral, the ligand field bands shift to lower energies as expected. However, the positions of LMCT transitions involving thiolate and Cu(II) are not so well documented in their studies. Also, the EPR spectral data have been sporadically reported and redox behaviour of these systems have not been mentioned.

Trispyrazolylborate ligands form complexes with Cu(II) where one site of copper is vacant. This site can be occupied by a suitable thiol giving a Cu(II)-thiolate complex with the chromophore, CuN_3S. This synthetic strategy has been used by at least two groups who have prepared tetrahedral/pseudotetrahedral complexes (Fig. 1.13). One such complex, $CuN_3(SR)$ [N_3 = hydrotris (3,5-dimethyl-1-pyraroloyl) borate; SR ≡ p-nitrobenzenethiolate] has a strong absorption with λ_{max} near 590nm and shows an axial EPR spectrum in THF glass [72]. However, the hyperfine splitting

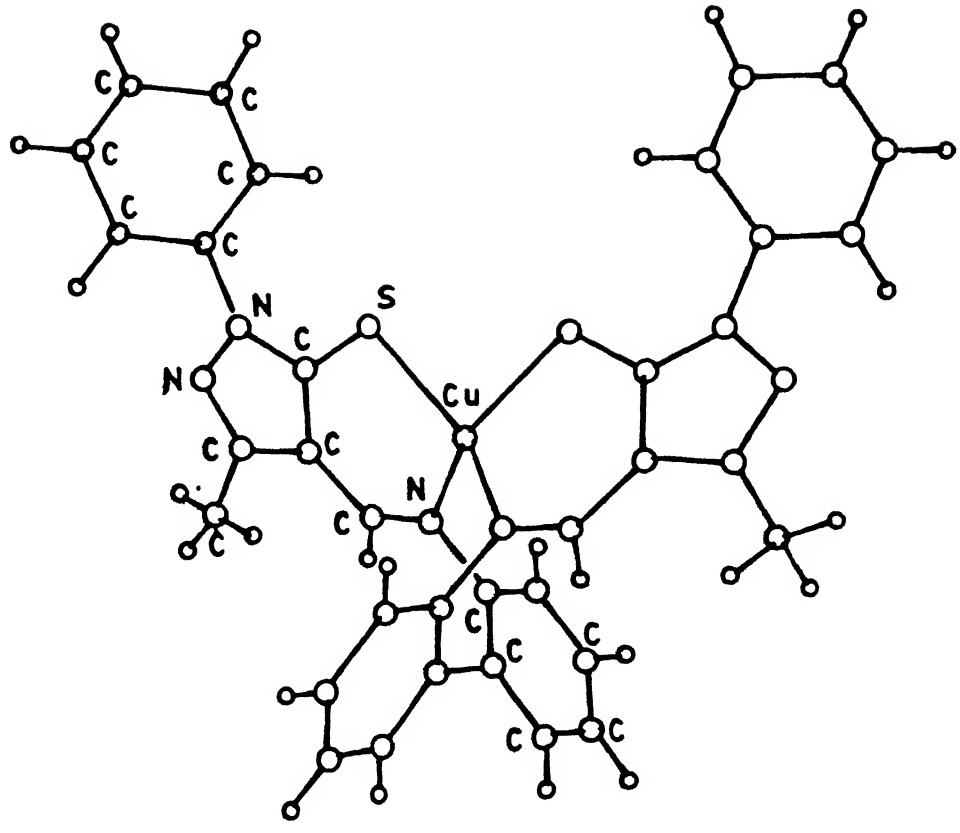

Fig 1.12 A pseudotetrahedral CuN_2S_2 complex

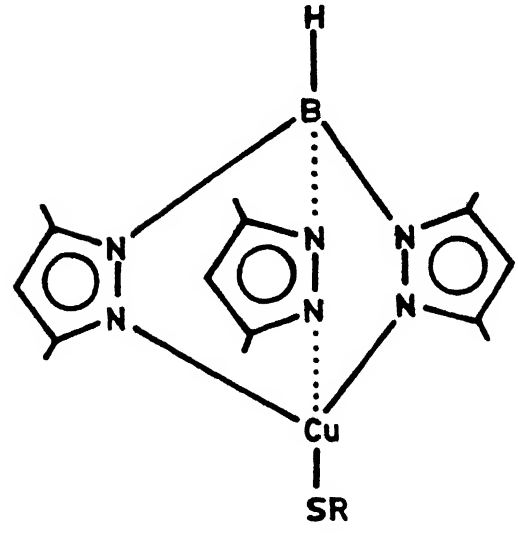

Fig 1.13 A Cu(II) complex with the chromophore CuN_3S

in the parallel region is about $170x10^{-4}$ cm^{-1} which is much higher than what is observed for the type 1 site (Table 1.3). The reaction of $KHB(3.5\text{-}iPr_2pz)_3$ with 1 equivalent of $CuCl_2.2H_2O$ in dry acetone gives $Cu(Cl)(HB(3,5\text{-}iPr_2pz)_3$. This monochloro compound when allowed to react with ^tBuSH gives [73] a deep-blue solution. This solution shows a strong absorption band at 608nm ($\epsilon \geq 3500$ $M^{-1}cm^{-1}$) and also gives an axial EPR signal with $A_{\parallel}$ being about $65x10^{-4}$ cm^{-1}. The structure proposed is illustrated in Fig. 1.14.

Murray and coworkers [74] followd by Casella and coworkers [75] have synthesized Cu(II)-thiolates starting from polydentate ligands containing one or two terminal pyridine thione groups. This group assumes the tautomeric pyridinium thiolate form when bound to Cu(II) (Fig. 1.15). Using this method, a number of complexes with chromophores CuN_2S^*S (Fig. 1.16) and CuN_2S_2 have been synthesized as electronic structural analogues of the type 1 sites where coordination geometry ranges from planar towards distorted tetrahedral. The LMCT transitions involving thiolate sulfur and Cu(II) occur at different energies as shown in Table 1.4. Also, these transitions are frequently associated with ligand based transitions so that real extinction coefficients due to S $\rightarrow$Cu(II) absorptions will be much less than the values reported. The EPR spectra are either axial or slightly rhombic in nature with $A_{\parallel}$ values are in the normal range found for tetragoanl Cu(II) complexes. These complexes exhibit quasi-reversible Cu(II)/Cu(I) couples. The $E_{1/2}$ values have been found to be dependent not only on the nature of the donors but also on the

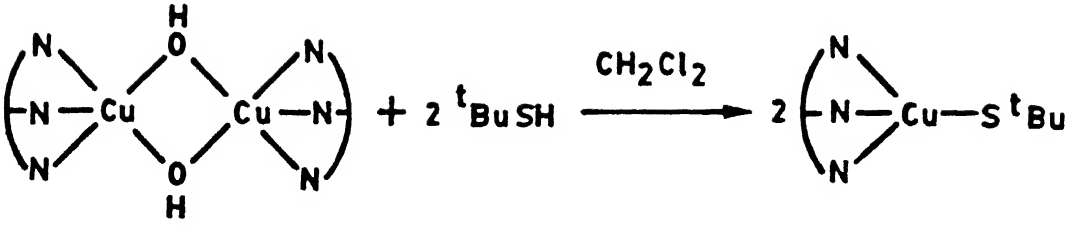

Fig 1.14 A distorted tetrahedral CuN_3S complex

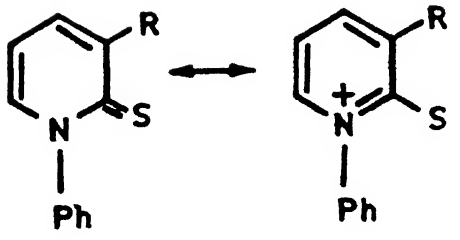

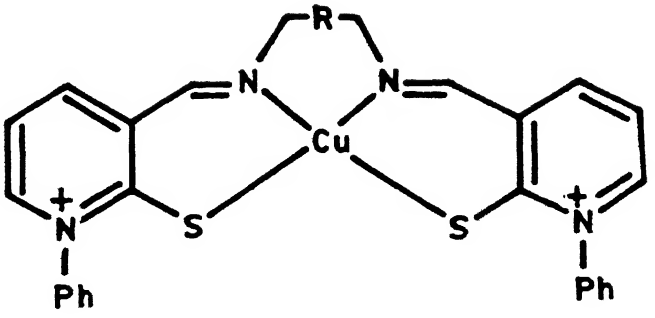

Fig 1.15 Interaction between Cu(II) and a pyridine-thione derivative

Table 1.2

Electronic and EPR Spectral Data for Some Type 1 Sites and Model CuN_3S Complexes

Compound	σ-(Thiolate)$\rightarrow$ Cu λ_{max}/ nm(ϵ_{max} $dm^3mol^{-1}cm^{-1}$)	$g_{\parallel}$	$g_{\perp}$	$A_{\parallel}^{Cu}$	Ref
Plastocyanin(Spinach)	597 (4900)	2.226	2.053	63	22
Stellacyanin (Rhus vermicifera)	605 (4050)	2.287	2.051	35	35
Azurin(Pseudomonas aeraginosa)	625 (3500)	2.260	2.05	60	22
$Cu(HB(3,5\text{-}Me_2pz)_3(SC_6H_4NO_2\text{-}p)$	588 (3900)	2.286	2.067	160	72
$Cu(HB(3,5\text{-}ipr_2pz)_3(S^tBu)$	608 (≥3500)	2.21	2.07	65	73

Unit for $A_{\parallel}$ values is 1×10^{-4} cm^{-1}

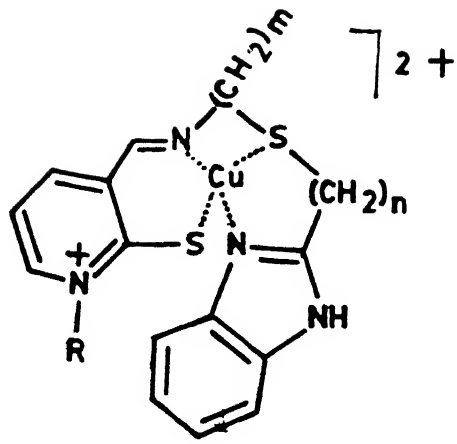

Fig 1.16 A perspective view of a Cu(II) complex with the chromophore, CuN_2S^*S

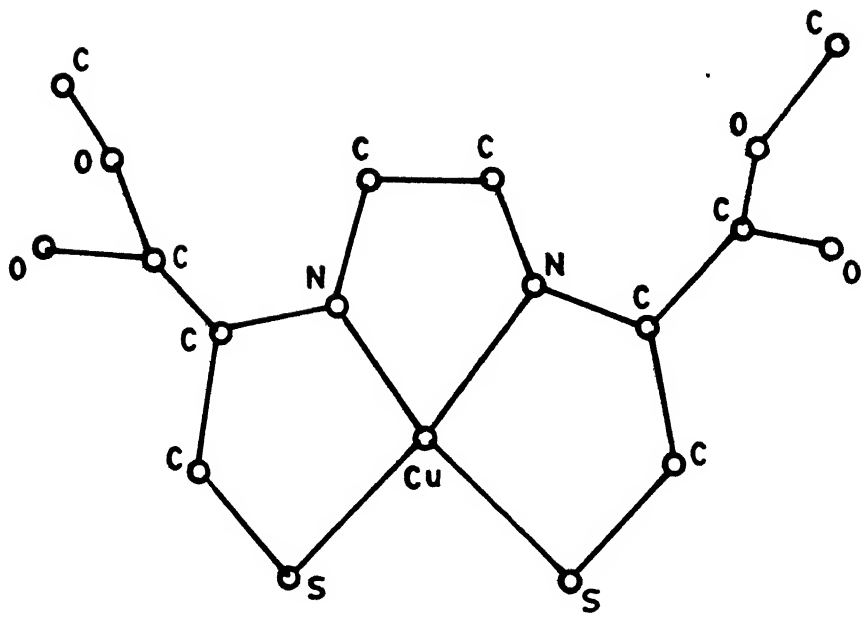

Fig 1.17 A perspective view of the CuN_2S_2 complex with the tetradentate dicysteine derivative

Table 1.3

Thiolate $\rightarrow$Cu(II) LMCT Absorptions of σ- and π - Summery of Some CuN_2S^*S and CuN_2S_2 Complexes

Complex	λ_{max}/nm(ϵ_{max}/$dm^3 mol^{-1} cm^{-1}$)		Ref
	σ- symmetry	π-symmetry	
$[CuL_1][ClO_4]$	410(4700)	520(1500)	75
$[CuL_2][ClO_4]$	430(3500)	525(900)	75
$[CuL_3][ClO_4]$	435(4000)	530(1350)	75
$[CuL'_1]$	420(3600)	500(1200)	75
$[CuL'_2]$	410(5000)	480(2800)	75
$[CuL'_3]$	425(11,000)	490(4500)	75

Ligands L_1, L_2 and L_3 are derived from the condensation of (IR)-3-hydroxymethylenebornane-2-thione and 2-aminothia alkyl benzimidazoles (N_2S^*S). The carbon chain increases progressively from 2 to 4. Ligands L'_1, L'_2 and L'_3 are obtained from condensation of (IR)-3-hydroxymethlenebornane-2-thione and symmetric diamines (N_2S_2). Length of the Carbon chain between imines is varied from 2 to 4 as one goes from L'_1 to L'_3.

Higher energy π-symmetry transition is not observed.

coordination geometry. As the geometry distorts from planarity, the ligand field strength decreases and the Cu(II)/Cu(I) potential shifts towards the positive direction as expected.

On the basis of spectroscopic studies, there is compelling evidence that the EPR detectable Cu_A site in cytochrome C oxidase embodies ligation by two cysteine thiolates and has considerable Cu(I)-thiyl radical character [50] rather than Cu(II)-thiolate character. The EPR spectra of the Cu_A site show small g values; one of them actually falls below 2.0 and Cu-hyperfine splittings are not resolved. The ligand [76] shown complexed to Cu(II) in Fig. 1.17 has two L-cysteine methylester units linked by an ethylene bridge through nitrogens. The facile redox decomposition undergone by Cu(II) complexes of cysteine is somehow blocked and the resulting red-brown Cu(II) complex is infinitely stable in the solid state. The corresponding diacid also exhibits sluggish decomposition in the solution phase. The observed Cu-S distances (2.230, 2.262 Å) are shorter than most of the thiolates discussed above while the Cu-N distances (2.058, 2.002 Å) are typical. The geometry is very slightly distorted from planarity as the dihedral angle of 21^{o} indicates (for square planar geometry the dihedral angle is 0^{o}). An interesting structural feature with potentially significant electronic consequences is the short S ....S contact of 3.40Å. This separation is less than the van der Waals contact of 3.7Å, but not as short as those reported (2.734-2.82Å) for Mo(VI) complexes having $N_2O_2S_2$ donor sets [77]. The EPR parameters observed in DMF glass or in polycrystalline Cu(II)-doped into the Ni(II) analogue

agree well with those reported for the rapidly frozen metastable species [57b] formulated as bis Cu(II) complexes of L-cysteine or D-penicillamine (Table 1.4). LMCT transitions involving thiolates are found to appear at ~ 350 and ~400 nm while one ligand field band appears at 550 nm. Intensity of this band is quite high probably due to intensity stealing from charge transfer transitions. While this complex is formed by treating $Cu(teta)^{2+}$ with the ligand, other complexes result if the starting Cu(II) complex is different. Thus with $Cu(en)_2^{2+}$ a mixed-valent pentamer is formed [78]. The pentamer is composed of three CuN_2S_2 monomers (as shown in Fig. 1.17) suitably oriented to create trigonal planar coordination sites for two Cu(I) ions. All three CuN_2S_2 units show small distortions from planarity; the Cu(II)-S distances span the range 2.237-2.266Å and Cu(II)-N distances are in the range, 1.965-2.055Å. Cu(I)-S distances lie in the range 2.232-2.291Å. Effective magnetic moment per Cu(II) is found to be between 1.74-1.79μ_B which can be fitted to the Kambe model [79] for a triangular cluster having a small intracluster ferromagnetic exchange ($J=0.2594\ cm^{-1}$) and T.I.P of $\approx 3.836 \times 10^{-5}$ cgs. X-band EPR spectrum in polycrystalline or in glycol/water glass shows an isotropic signal with g = 2.02 while electronic spectral data are reminiscent of those exhibited by the simple monomer.

The recent findings of the presence of nickel-sulfur and nickel-nitrogen bonds at the active sites of several hydrogenases [79] and carbon-monoxide dehydrogenases [80] have stimulated interest in nickel chemistry with mixed sulfur and nitrogen donor ligands [81-84]. In the "as prepared" form of the enzyme, Desulfovibrio gigas [85], the EPR spectrum with g values of 2.31,

Table 1.4

EPR Data of Cu(II)-Thiolato Complexes

Thiol	$g_{\parallel}$	$g_{\perp}$	$A_{\parallel}^{Cu}$	$A_{\perp}^{Cu}$	Ref
D - Penicillamine	2.116	2.038	173	49	57b
L - Cysteine	2.118	2.037	174	50	57b
Cysteamine	2.117	2.037	173	50	57b
2-Dimethylamino ethanethiol	2.116	2.036	173	49	57b
N,N′-Ethylenebis (L-cysteine)	2.126	2.039	182	49	76

Unit for $A_{\parallel}$ values is 1×10^{-4} cm^{-1}

2.23 and 2.02 (Ni A spectrum) has been attributed to trivalent nickel in an approximately tetragonal environment. Upon incubation with H_2, this spectrum becomes replaced by a spectrum with g values of 2.19, 2.16, and 2.02 (Ni C spectrum), which corresponds to a Ni(III) intermediate form of the enzyme. At longer incubation times, an EPR-silent state ascribed to Ni(II) is reached. Also, XANES data suggests [86] a pseudooctahedral Ni environment. The most noteworthy characteristics of the Ni-sites are the existence of Ni(III) states and the low Ni(III)/Ni(II) redox potentials, ca -150 to-400 mV vs SHE. Efforts are on by different workers [81-84] to synthesize octahedral/distorted octahedral Ni(II) complexes with mixed S,N-donor ligands (Table 1.5). However, mimicking the active site properties remain largely unachievable.

Table 1.5

Synthetic Models for Nickel Hydrogenases

Complex	Chromophore	Geometry	Ni(III)/Ni(II) Redox Couple (in V)	Ref
$[Ni(pdtc)_2]^{2-}$	N_2S_4	Tetragonal	-0.09	82
$[Ni(phma)]^{2-}$	N_2S_2	Square Planar	-0.24	82
$[Ni(dtc)_3]^{1-}$	S_6	Tetragonal	-0.32	82
$[Ni(ema)]^{2-}$	N_2S_2	Square Planar	-0.34	82
$[Ni(emi)]^{2-}$	N_2S_2	Square Planar	-0.42	82
$[Ni(nbdt)_2]^{2-}$	S_4	Square Planar	-0.76	81
$[Ni(emb)]^{2-}$	N_2S_2	Square Planar	-0.04	81b

pdtc = Pyridine-2,6-bis-(thiocarboxylate)
H_4phma = N,N′-1,2-phenylene-bis-(2-mercaptoacetamide)
dtc = Dithiocarbamate
H_4ema = N,N′-ethylene-bis-(2-mercaptoacetamide)
H_4emi = N,N′-ethylene-bis-(2-mercaptoisobutyramide)
nbdt = Norborane-2,3-dithiolate
emb = N,N′-Ehylene-bis-(o-mercaptobenzamide)

CHAPTER 2

SCOPE OF THE WORK

Synthesis of copper(II) complexes with ligands bearing nitrogen, thioether and thiolate donors is an area of considerable current interest both from chemical and biological points of view. A large number of copper(II) complexes with imidazoles, pyrazoles, amines etc. have been studied in detail which have contributed significantly to our knowledge about copper-nitrogen bonding as present at the active sites of several copper proteins. In contrast, much less data are available on copper-sulfur (thiolate/thioether) bonding although such bonding is very common in copper proteins. The peculiar spectroscopic properties exhibited by the blue copper proteins and the underlying electronic structure and bonding at the blue active sites may be profitably pursued by model Cu(II)-thiolates. This is because such spectral properties are attributed to strong Cu(II)-thiolate bonding interactions [52]. Based on EPR parameters, the blue sites may be subdivided [54] into two classes (i) protein like plastocyanin, shows essentially axial EPR spectra whereas (ii) stellacyanin, basic blue protein from cucumber etc. show EPR spectra which are rhombically split. As an example, poplar plastocyanin shows a spectrum where the difference $(g_x-g_y) \approx 0.017$ while for stellacyanin, $(g_x-g_y) = 0.057$. However, all the blue sites show very small hyperfine splittings in the parallel region ($A_{\parallel}$) in contrast to model tetracoordinate Cu(II) complexes [9].

Theoretical studies indicate [54] that for the plastocyanin class of proteins the almost axial EPR spectra with small $A_{\parallel}$ values can be accounted for by assuming delocalization of the single electron from Cu(II) to thiolate sulfur. The details of ground electronic state description in plastocyanin have been probed [53] by an SCF-X_{α} study of a hypothetical $Cu(CH_3S)(NH_3)_2(CH_3SCH_3)$ model. These calculations indicate that the unpaired electron in the type 1 site of plastocyanin spends about 40% of the time in the $d_{x^2-y^2}$ orbital on copper and about 36% of the time in $S3_{p\pi}$ orbitals. On the other hand, for the stellacyanin class of proteins, significant rhombic distortion alongwith small $A_{\parallel}$ values are attributable [54] to the mixing of d_{z^2} orbital into the ground state ($d_{x^2-y^2}$) to the extent of about 2-5%. To substantiate these theoretical results small molecular weight model complexes should be studied. However, no Cu(II)-thiolate complex is known to date which can emulate the EPR spectral characteristics of the stellacyanin class of proteins. A pseudotetrahedral Cu(1,2-dimethylimidazole)Cl_2 complex in the Zn(II) host lattice has been subjected to detailed EPR spectral studies [35]. The results indicate that for a Cu(II) complex having C_{2v} local symmetry, rhombic splitting is possible and the amount of such splitting can be correlated with the amount of dz^2 mixing into the ground state wavefunction. Thus, for obvious reasons, it is important to synthesize and study pseudotetrahedral Cu(II)-thiolates. Moreover, Cu(II)-thiolates with distorted geometries are likely to show interesting redox properties. Because, a distorted geometry would be a compromise structure for

both Cu(II) and Cu(I) ions so that their interconversion would be easier. For most of the thiolate complexes reported as discussed in chapter 1, redox data are not available. And for cases where such data are reported, the Cu(II)/Cu(I) couples have either negative or very low positive values.

Tetracoordinated Cu(II)-complexes with the chromophore CuN_2S^*S like the one present at the active sites of several blue proteins viz., plastocyanin, CBP, ascorbate oxidase etc. should be studied. This is to probe the combined effects of such a donor set on the spectral and electrochemical behaviour of the resulting complexes.

To date, no hexacoordinated Cu(II) complexes with donors that include one or more thiolates have been reported. Due to the Jahn-Teller effect being operational such complexes will be of tetragonal symmetry. The tetragonality, T, may be defined as [87]

$$T = \frac{0.5\ (R_x + R_y)}{R_z},$$

where R is the bond length along the axis denoted by the subscript.

For moderate to strong tetragonal distortions, the singly occupied d-orbital, i.e., $d_{x^2-y^2}$ will be destabilized so that electron loss from the complex with the formation of Cu(III) species might be possible. If the ligand is hexadentate, it can completely surround the metal ion and should be able to inhibit ready decomposition of the oxidized species. This way, it might

be just possible to have metastable Cu(III)-thiolate species. Apart from being novel from the point of view of synthetic chemistry, such complexes might prove useful in studying the reaction mechanisms of some copper proteins. Although, no copper protein is known to have Cu(III)-thiolate bonding at the active site, its formation during catalytic cycles cannot be ruled out [88]. Thus, studies of Cu(III)-thiolate species become more important as it can provide an important data base not available in the literature.

The problem in the isolation of stable Cu(II)-thiolato complexes lies in the facile redox decomposition of Cu(II)-thiolates when a Cu(II) salt is allowed to react with a thiol. Surmounting this redox instability, a number of Cu(II)-thiolato complexes have been isolated following different synthetic strategies as mentioned in the previous chapter. The strategy adopted by Toftlund and coworkers [69] is attractive as it makes a wide variation of ligand design possible. The method involves cleaving the S-^{t}Bu linkage(s) of a polydentate ligand utilizing Lewis acidity of the Cu(II) ion. This method has been used only sporadically. A variety of ligands should be designed and synthesized where the thiol groups are protected as their tertiary butyl derivatives. This will lead to interesting Cu(II) thiolato complexes. It is also highly desirable to probe the possibilities for the synthesis of Cu(II)-thiolates following a new strategy. This is not only important from the point of view of synthetic chemistry but also might allow to synthesize

Cu(II)-thiolato complexes with desired coordination geometries not possible following existing methods.

Since the discovery of nickel at the active sites of several hydrogenases and carobon-monoxide dehydrogenases, several groups are involved in synthesizing hexacoordinated nickel complexes with mixed S and N donor ligands as mentioned in chapter 1. As a new approach to model these sites, efforts should be made to synthesize tripodal ligands with hexadentate S, N-donors as ligands for nickel. Tripodal ligands are capable of forming complexes with metal ions that can exhibit unusual coordination, high thermodynamic stability, and kinetic inertness [89].

CHAPTER 3

In this chapter, synthesis and characterization of two different sets of stable tetracoordinated copper(II) thiolato complexes are described. In Part A, a copper(II) complex with a new tetradentate ligand (L_1) bearing one methionine thioether, one thiolate and two amino nitrogens (Fig. 3.1) is discussed. To facilitate characterization of this complex, the oxygen analogue (L_2) of the thiolate ligand has been prepared which also forms a four-coordinate Cu(II)-complex. This study is undertaken to have a copper(II) complex with the same chromophore as present [49] in some type 1 active sites, e.g. in monocopper proteins like plastocyanin, CBP, amicyanin etc. or in multicopper proteins like tree and fungal laccases, ascorbate oxidase, ceruloplasmin etc. The search for synthetic models for these type 1 sites must tackle the problem of the redox instability of copper(II)-thiolate bonding. In the present case, the thiol was protected as its t-butyl derivative. For complexation, the ligand with protected thiol is allowed to reflux with a Cu(II) salt which cleaves the S-^{t}Bu linkage and forms the corresponding Cu(II)-thiolato complex. This method was first adopted by Toftlund and coworkers [69]. Casella and coworkers have synthesized [90] a few CuN_2S^*S complexes with tetradentate ligands derived either from the condensation of 1-allyl or 1-aryl-3-formyl-2(1H)-pyridinethione with aminoallylthioalkyl benzimidazoles or from the condensation of (IR)-3-hydroxymethylene-bornane-2-thione and several 2-aminothia-allyl benzimidazoles. These complexes are either

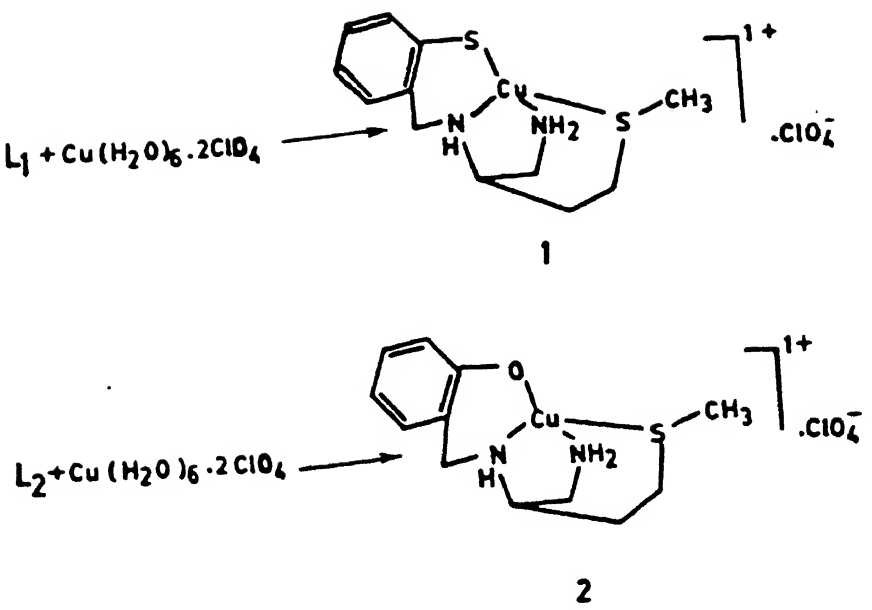

Fig 3.1 Synthetic scheme for the complexes 1 and 2

tetragonal or slightly distorted thereof as deduced from their spectral characteristics [75,90]. However, in all these complexes, the thiolate sulfur is directly linked to the pyridinium moeity and so the electronic structure of the thiolate complex is potentially complicated.

In **Part B**, a pair of pseudotetrahedral CuN_2S_2 complexes are discussed. The two new tetradentate ligands, L_3 and L_4 have been synthesized by Schiff base condensation of diisobutyraldehyde disulfide with 2-mercaptoethylamine and 2-mercaptoaniline respectively (Fig. 3.2). The thiol is protected in each case by forming its t-butyl derivative before the Schiff base condensation reaction. A CuN_4 analogue (Fig.3.3) has also been prepared by condensing the dialdehyde with 2-dimethylaminoethyl amine. The three tetradentate ligands were designed to enforce a pseudotetrahedral coordination geometry onto Cu(II). Examination of molecular models revealed that a tentradentate ligand with a large bite angle and proper substituents should be able to impose a coordination which will be substantially distorted from planarity.

EPR studies [35] of the blue protein active sites have revealed that subtle yet important differences exist between blue proteins like plastocyanin, azurin etc. in one hand and stellacyanin, basic blue protein from cucumber (CBP), etc., on the other. Plastocyanin class of blue proteins show essentially axial EPR spectra. Only a small rhombic splitting ($g_x - g_y$ = 0.017) could be detected in the Q band spectrum of polar plastocyanin.

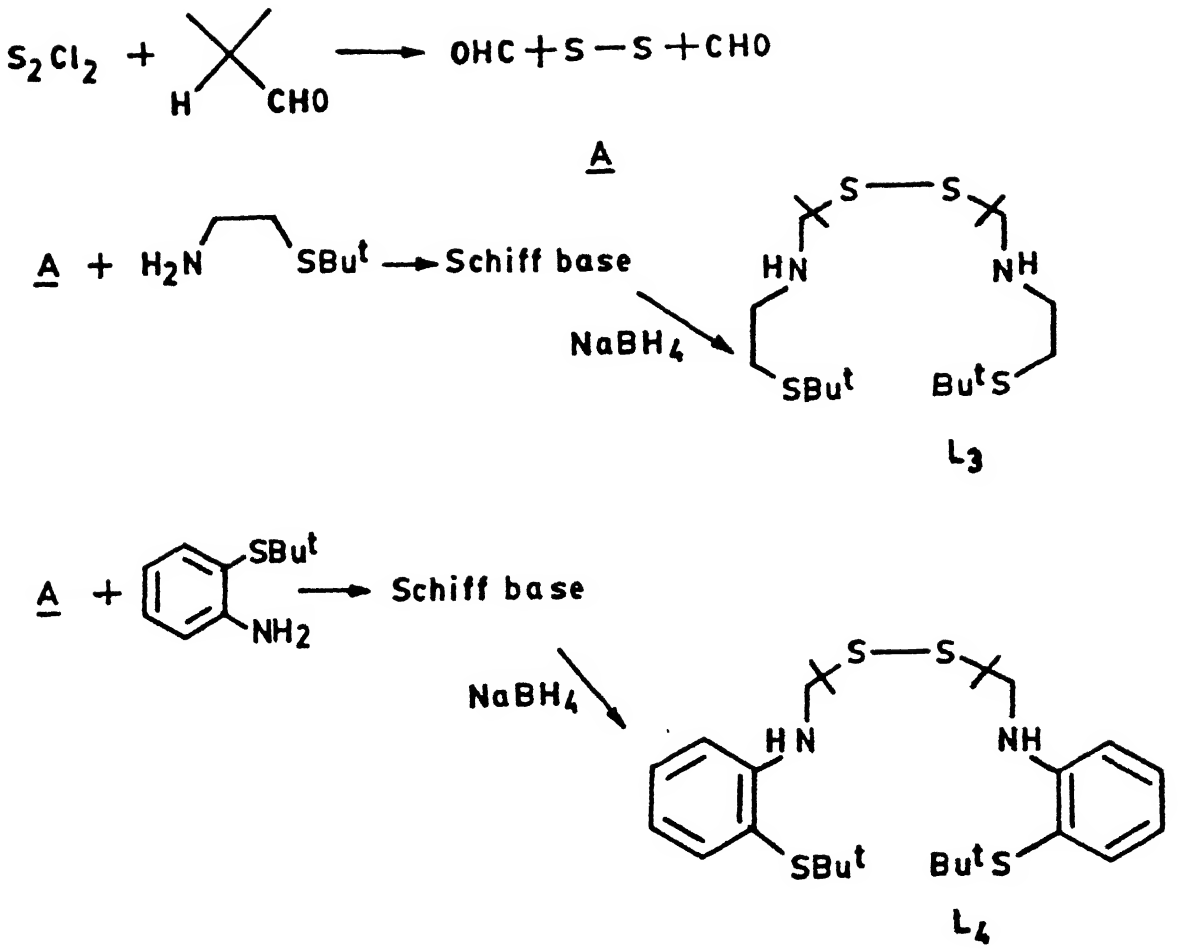

Fig 3.2 Synthetic scheme for the ligands L_3 & L_4

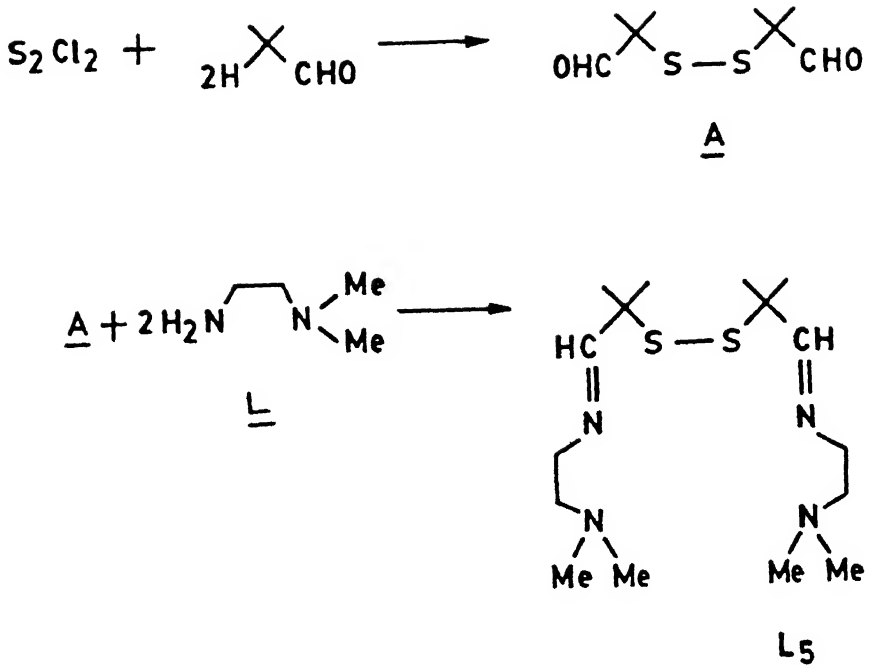

Fig 3.3 Synthetic scheme for the ligands L_5

Stellacyanin class of proteins show significant rhombic splitting ($g_x - g_y$ = 0.057 for stellacyanin). Both classes of proteins show small hyperfine coupling in the parallel region. The ground electronic states should, therefore, be different for the two classes of proteins. For plastocyanin, extensive delocalization of the single d-electron into sulfur P_π (Cys 84) orbital results [44] in the unusual EPR parameters while in case of stellacyanin, about 3-5% mixing of d_z2 orbital into the ground state wave function has been suggested [34] as the principal cause for significant rhombic splitting. For pseudotetrahedral non-thiolate model copper(II) complexes as well, a significant amount of g split could be observed which has been attributed to d_z2 mixing into the ground state [34,91]. Besides, the high redox potentials observed for these blue sites are reflective of their structures much distorted from a regular planar geometry favoured by copper(II). The Cu(II)/Cu(I) potential may be raised by any one or a combination of the two factors which lead to lowering of ligand field stabilization energy (LFSE) : (i) decreasing ligand -donor ability and (ii) constraining the geometry of the metal center to the one that favours copper(I) e.g. tetrahedral. With strong donors like amines and thiolates, a copper(II) complex with the geometry distorted from planarity will be able to show high positive value for the Cu(II)/Cu(I) couple. In order to address the peculiar EPR spectral characteristics as well as high redox potential values for the Cu(II)/Cu(I) couple exhibited by these proteins, the two CuN_2S_2 complexes are studied. The CuN_4 complex is included to facilitate interpretation of data obtained on

CuN_2S_2 complexes.

Synthesis and characterizaion of CuN_2S^*S and CuN_2S^*O complexes (Part A) are discussed first followed by pseudotetrahedral CuN_2S_2 and CuN_4 complexes (Part B).

3.1 Experimental Section

3.1.1 Solvents and Reagents

All the solvents and tertiary butanol used were obtained from Glaxo Laboratories and were purified prior to use following standard procedures [92].

Reagent grade DL-methionine, 2-nitrobenzaldehyde, salicylaldehyde, tertiary butylthiol, copper(II) perchlorate, anhydrous potassium carbonate, 2-mercaptoaniline, cysteamine, lithium aluminum hydride and 2-dimethylaminoethyl amine were acquired from Aldrich and used as received. Sulfur monochloride was obtained from Fluka and used as received. Isobutyraldehyde was from Merck and was used after distillation at atmospheric pressure.

3.1.2 Measurements

The elements carbon, hydrogen, nitrogen and sulphur were analyzed by standard microanalytical techniques at the Indian Institute of Technology, Kanpur or at the Central Drug Research Institute, Lucknow, India.

Infrared spectra were recorded either on a model 580 grating or on a model FTIR 1600 Perkin-Elmer spectrophotometer. KBr pellets were used for solid samples and nujol mull for liquid or semisolid samples. A polystyrene film was used as the reference.

^{1}H-NMR data were recorded either on a Bruker WP-80FT (80MHz) instrument or on a PMX-60 JEOL (60MHz) instrument using TMS (tetramethyl silane) as internal standard. Deuterated solvents like $CDCl_3$, CD_3CN, d^6-DMSO were used to dissolve the samples. Only a few representative ^{1}H-NMR spectra are provided while all ^{1}H-NMR data are given. Magnetic susceptibility measurements were made at room temperature on a Cahn Faraday Balance using $[CoHg(SCN)_4]$ as the standard.

Cyclic voltammetric measurements were performed by using a PAR model 370-4 electrochemistry system : 174A, polarographic analyzer; 175, universal programmer; and RE 0074, X-Y recorder. Potentials are reported at 298 K relative to a saturated calomel reference electrode (SCE) and are uncorrected for junction potentials. A sealed all-glass cell was used. The auxiliary electrode, which consisted of a platinum flag sealed in soft glass, and the reference electrode were separated from the working solution by means of a fritted bridge filled with the same solvent and supporting electrolyte. Uncompensated solution resistance in the cell configuration was minimized by placing the tip of the reference electrode as close to the working electrode as possible and using an approximately constant ratio of $[NBu_4]ClO_4$ supporting

electrolyte and solute concentration (≃100:1). A PAR G0021 glassy carbon electrode was used as the working electrode. The system was calibrated against ferrocene, [$Fe(\eta\text{-}C_5H_5)_2$] [93], and tris (2,2′ bipyridine) iron(II) Perchlorate, [$Fe(dipy)_3$][ClO_4]$_2$ [94]. All measurements were made under an atmosphere of nitrogen. Solvents used was either CH_3CN or DMF in pure and dry condition.

Electron paramagnetic resonance (EPR) spectra were recorded on a varian E-109 spectrometer operating at X-band using DPPH as the external standard. EPR spectra were taken at room temperature and in liquid nitrogen temperature as well. Conductivity data were collected on an Elico Model CM-82T conductivity bridge for dilute solution [~10^{-3}M]. Melting points were recorded using an electrical melting point apparatus (PERFIT) and were uncorrected. The electronic spectra were recorded on a Perkin Elmer Lambda-2 UV-VIS spectrophotometer at room temperature.

3.2 Syntheses of Ligands

Syntheses of ligands is shown schematically in Fig. 3.4.

3.2.1 Synthesis of 2-t-Butylthiobenzaldehyde

It was prepared following a reported procedure [95].o-Nitrobenzaldehyde (20 g, 0.13 mol) was mixed with anhydrous potassium carbonate (20 g, 0.14 mol), t-butylthiol (25 ml, 0.33 mol) and freshly distilled dimethylformamide(25 ml). The resulting mixture was allowed to reflux. Color of the mixture

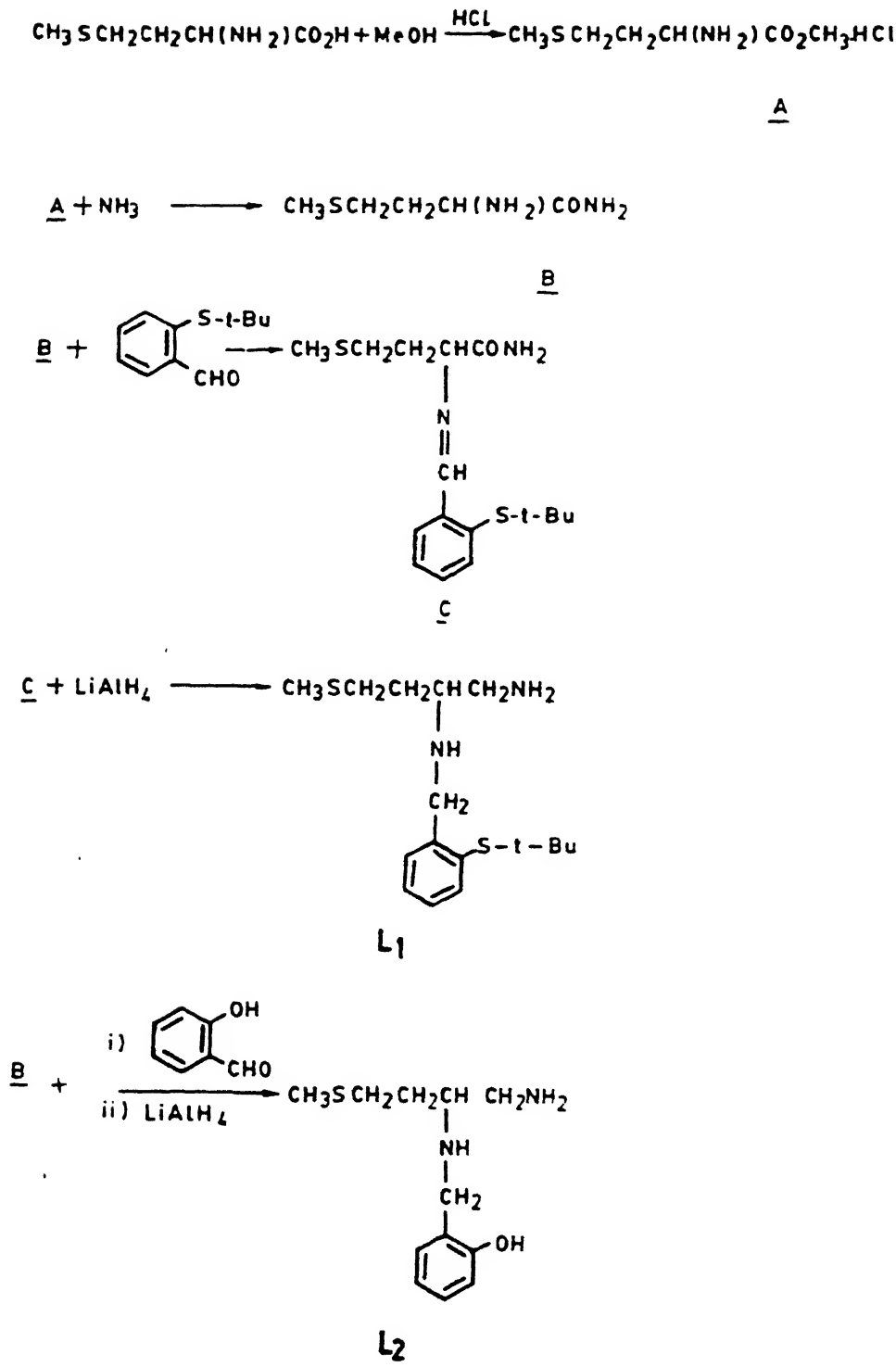

Fig 3.4 Synthetic scheme for the ligands, L_1 and L_2

gradually changed from orange to dark brown. The solution was allowed to reflux for a total of 30 hours. It was then cooled and poured into water (500 ml) with constant stirring. The aqueous solution was shaken with (5x100 ml) portions of diethyl ether and the ether extracts were collected. The combined extract washed successively with water (4x500 ml), 2% sodium hydroxide solution (4x200 ml) and finally with (2x100 ml) water. The ether layer was dried over anhydrous magnesium sulphate, and then evaporated off completely to obtain a dark brown liquid. The desired product was obtained as a pale yellow oil upon fractional distillation (160^{o}C; 1 mm of Hg) in ~90% yield.

^{1}H-NMR (80 MHz, $CDCl_3$, δ_{TMS} ppm) : 10.81 (s, 1H) CHO, 7.52 (m, 4H) aromatic, 1.2 (s, 9H) t-butyl (Fig 3.5).

3.2.2 Synthesis of DL-methionineamide hydrochloride

This was synthesized following the method of Bosnich et. al. [96]. Dry methanol (150 ml) was saturated with dry HCl gas under cold condition (0^{o}C) and then DL-methionine (10 g, 0.067 mole) was added to it with stirring in cold condition. The reaction mixture was refluxed for 13 hours, cooled to room temperature, and the solvent was evaporated off to yield the methylester hydrochloride in nearly quantitative yield. The methylester hydrochloride was dissolved in dry methanol (80 ml) and the solution was cooled in an ice both. The cold solution was saturated with dry ammonia and allowed to stand for 5 hours at 0^{o}C. After 5 hours, ammonia gas was again passed through the

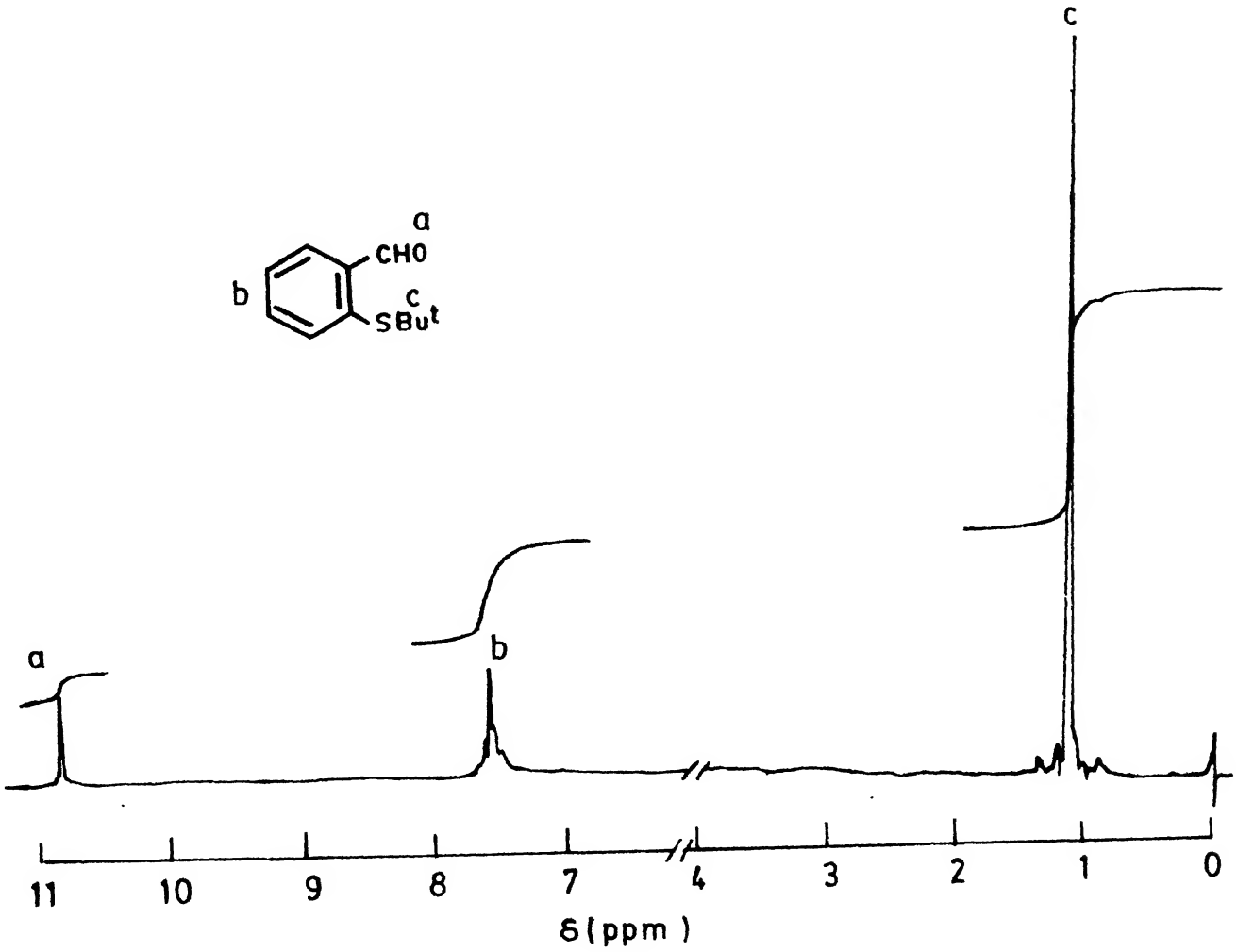

Fig 3.5 ^1H NMR (80MHz) spectrum of 2-t-butylthibenzaldehyde in $CDCl_3$.

solution for 30 minutes and then kept at $0^{o}C$ for 2.5 days. Ammonia gas was introducted again into the cold solution for 30 minutes and left undisturbed for a further period of 2.5 days. After the solution was allowed to stand for a total of 5 days, the methanol was evaporated off to yield a white solid. The white solid was taken in hot distilled water (4 ml) and then quickly diluted with ethanol (110 ml). The mixture was allowed to stand at $5^{o}C$ for 18 hours during which time white crystals slowly separated out. The crystals were collected by filtration, washed with small amounts of ice cold ethanol followed by ether and dried in a vacuum desiccator. Yield 72%.

3.2.3 Synthesis of the Schiff Base, L_1'

The Schiff base, L_1' was synthesized by refluxing 2-t-butylmercaptobenzaldehyde (2.4 g, 0.012 mol) in dry benzene (60 ml) and methionineamide hydrochloride (2.3 g, 0.012 mol) in dry methanol (20 ml). Within 1/2 hours, a clear golden yellow solution formed which attained a deep orange yellow color after 5 hours. The hot solution was treated with activated charcoal and evaporated in a rotary evaporator to obtain a yellow semi-solid. IR spectrum of this species gave a strong band at 1655 cm^{-1} indicating the presence of the imine linkage. Other selected bands obsereved 1670 $cm^{-1}(\nu_{C=O})$ & 3490 $cm^{-1}(\nu_{NH})$. ^{1}H-NMR (80 MHz, $CDCl_3$, δ_{TMS} ppm) : 8.5 (s, H) imine, 7.2 (m, 4H) aromatic, 6.4 (s br, 2H) NH_2 4.16 (t, 1H) CH, 2.5 (m, 4H) aliphatic CH_2, 2.1 (s, 3H) CH_3, 1.2 (s, 9H) t-butyl (Fig. 3.6).

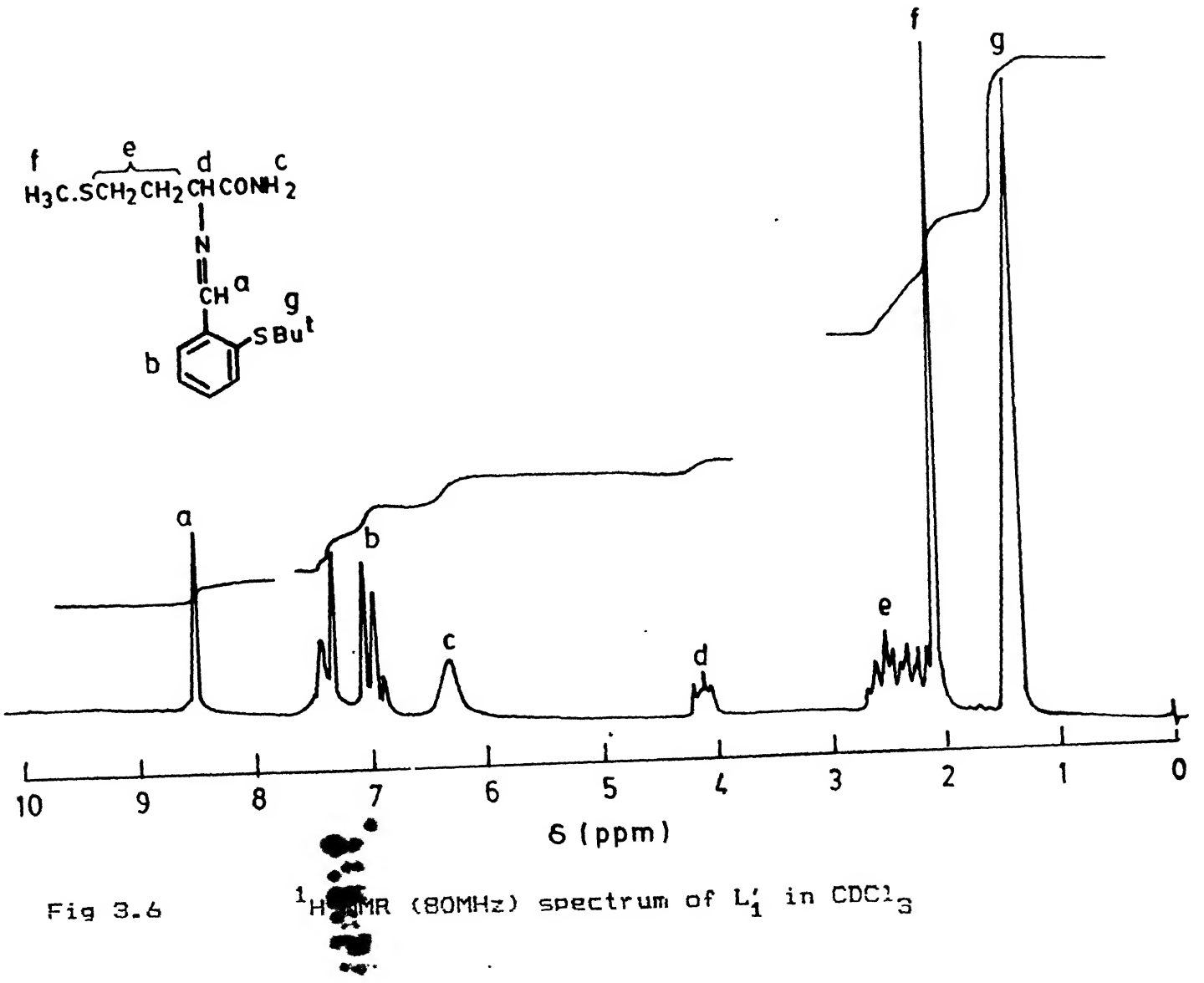

Fig 3.6 ^1H NMR (80MHz) spectrum of L_1' in $CDCl_3$

3.2.4 Synthesis of the ligand, L_1

The Schiff base (3.3 g,0.01 mol) isolated from the previous reaction, was taken in dry THF (150 ml). Into the slurry thus obtained was slowly added $LiAlH_4$(1.2 g, 0.03 mol) in small portions. A vigorous reaction started immediately. The reaction mixture was carefully refluxed for 16 hours. Then it was cooled to room temperature and excess $LiAlH_4$ was quenched by adding distilled water (5 ml) in drops through the reflux condenser. The the reaction mixture was extracted with ether (4x25 ml) and the combined extracts were dried over anhydrous sodium sulfate. Upon evaporation of ether in a rotary evaporator, the desired ligand was obtained as a yellow semisolid in 85% yield. IR spectrum of this species did not show any absorption due to imine linkage. ^1H NMR (80 MHz, $CDCl_3$, δ_{TMS} ppm) : 7.3 (m, 4H) aromatic, 6.55 (s br, 3H) NH, 4.84 (s, 2H) CH_2-NH, 3.7-2 (m, 7H) aliphatic CH(s), 2.0 (s, 3H) CH_3, 1.2 (s, 9H) t-butyl (Fig. 3.7).

3.2.5 Synthesis of the Schiff base, L_2'

This Schiff base was synthesized by refluxing salicyldehyde (1.6 g, 0.013 mol) and methionineamide hydrochloride (2.3 g, 0.012 mol) in dry benzene. After 5 hours of reflux the solution was allowed to cool to room temperature. Benzene was evaporated off in rotary evaporator to obtain a golden yellow liquid which on keeping at 5^oC for 2 hours, gave a pale-yellow solid in 80% yield. m.pt, 80^oC, I.R of this compound showed a strong peak at 1650 cm^{-1} ($\nu_{C=N}$)besides other selected peaks at 1665 ($\nu_{C=O}$)and 3201 cm^{-1}(ν_{NH}). ^1H-NMR (80 MHz, $CDCl_3$, δ_{TMS} ppm) :

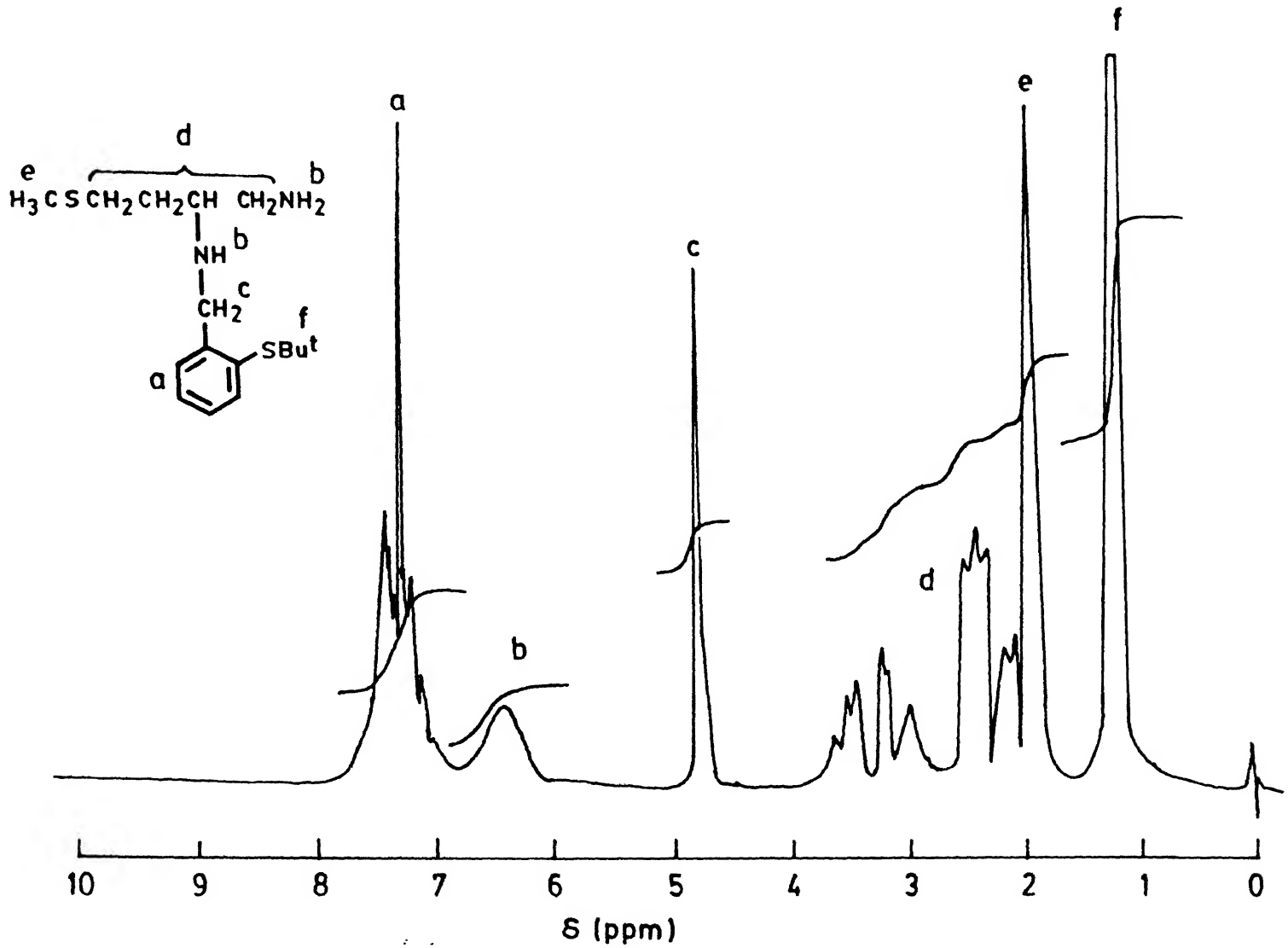

Fig 3.7 ^1H NMR (80MHz) spectrum of L_1 in $CDCl_3$

8.55 (s, H) imine, 7.21 (m, 4H) aromatic, 6.4 (s br, 2H) NH_2, 4.16 (t, 1H) CH, 2.5 (m, 4H) aliphatic CH_2, 2.1 (s, 3H) CH_3 (Fig. 3.8).

3.2.6 Synthesis of the Ligand, L_2

The Schiff base, L_1' (2 g, 0.008 mol) was dissolved in dry THF (150 ml). To the resulting solution slowly added $LiAlH_4$ (0.912 g, 0.024 mol) in small portions. A vigorous reaction started immediately. The reaction mixture was carefully refluxed for 16 hours. Then it was cooled to room temperature and the excess $LiAlH_4$ was quenched by adding water (~5 ml) in drops through the reflux condenser. The product was extracted with ether (4x25 ml) and the light combined ehereal extracts were dried over anhydrous sodium sulfate. Ether was removed in a rotary evaporator to obtain a light yellow semi-solid in high yield (90%). IR spectrum did not show any absorption due to imine linkage. ^{1}H-NMR (80 MHz, $CDCl_3$, δ_{TMS} ppm) : 7.0 (m, 4H) aromatic, 4.67 (s br, 3H) NH, 4.0 (s, 2H)CH_2NH, 3.7-2.1 (m, 7H) aliphatic CH, 2.1 (S, 3H) CH_3 (Fig. 3.9).

3.3 Syntheses of Complexes

Syntheses of complexes is shown schematically in Fig. 3.1.

3.3.1 Synthesis of the Complex, 1

This complex was synthesized by breaking the sulfur-tertiarybutyl linkage utilizing the Lewis acidity of copper(II) [69].

Ligand L_1 (3.3 g, 0.01 mol) was taken in dry methyl alcohol (30 ml) and copper(II) perchlorate hexahydrate (3.6 g,

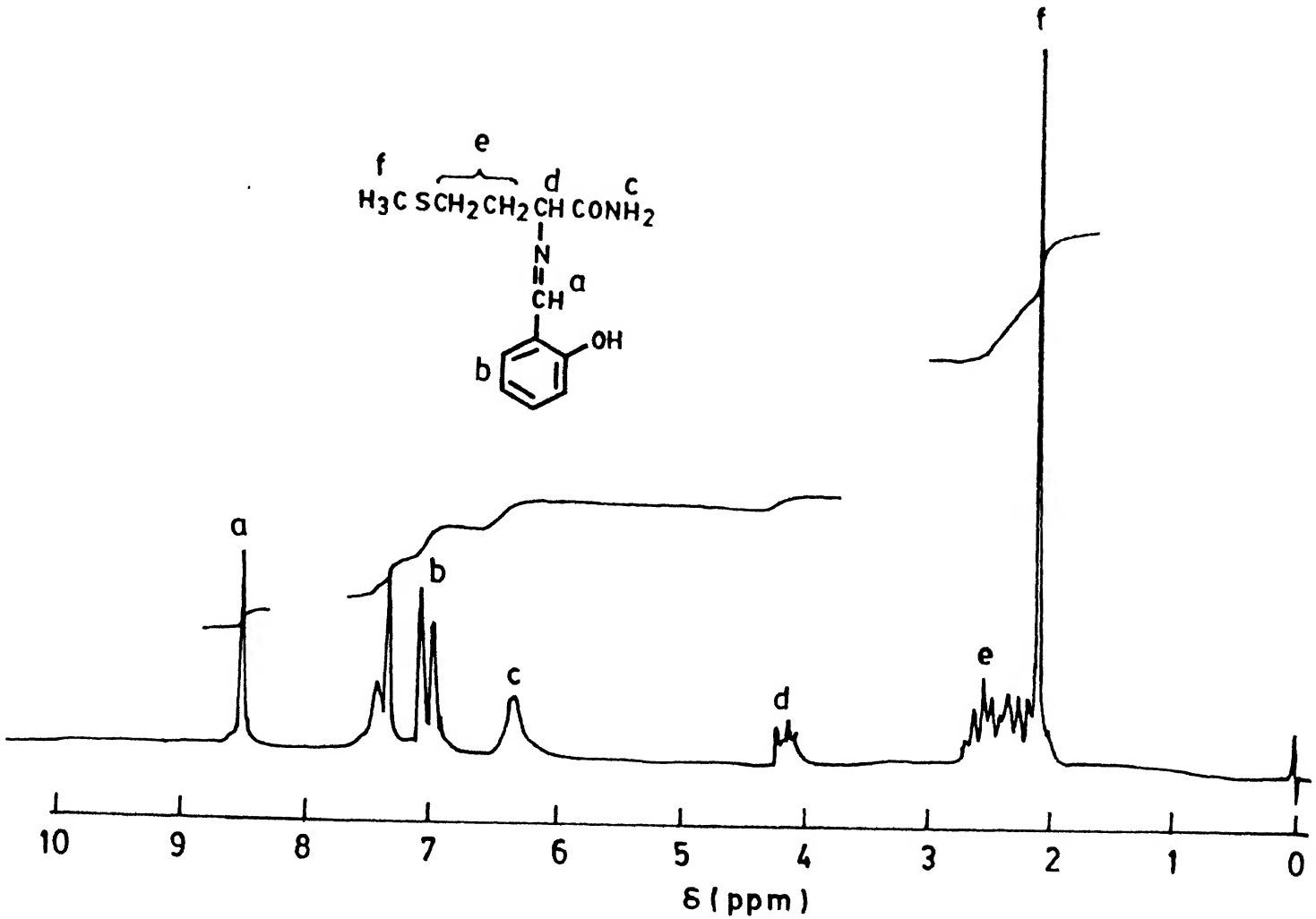

Fig 3.8 ^{1}H NMR (80MHz) spectrum of L'_2 in $CDCl_3$

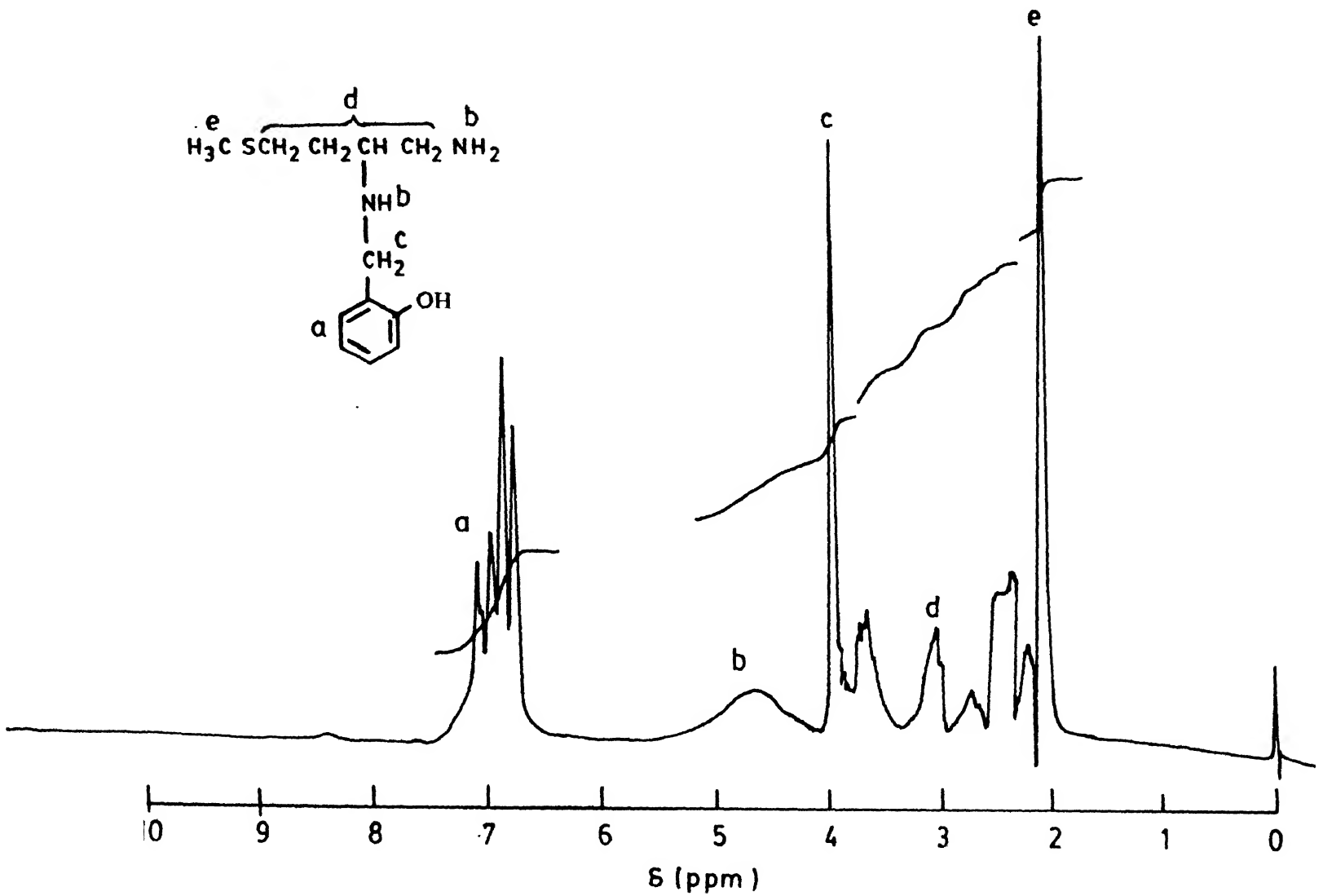

Fig 3.9 ^1H NMR (80MHz) spectrum of L_2 in $CDCl_3$

0.01 mol) was added to it. The color of the reaction mixture immediately changed to deep green. Upon refluxing for 1 hour, color changed to dark brown and a brown crystalline solid separated. The solution was allowed to cool to room temperature and filtered. The solid was washed with 5 ml of dry methyl alcohol followed by ether (10 ml) and air dried. The whole operation was done in an argon atmosphere. Yield 75%. The yield of the product decreased slowly with the increase in time of refluxing due to the oxidative effect of perchlorate.

3.3.2 Synthesis of the Complex, 2

Ligand L_2 (2.4 g, 0.01 mol) was dissolved in dry methyl alcohol (20 ml) and to this was added solid copper(II) perchlorate hexa hydrate (3.6 g, 0.01 mol). Color of the solution immediately changed to dark green. The solution was warmed for 10 minutes and then filtered after cooling to room temperature. Upon slow evaporation, a green crystalline solid separated in approximately 85% yield. Analytical data for the complexes are given in Table 3.1.

CAUTION : Care must be taken when treating organic compounds with copper(II) perchlorate as potentially explosive mixture may be formed.

3.4 Results and Discussion

IR spectra (Table 3.2) of complexes 1 and 2 in the region 1200-900 cm^{-1} show a strong and broad absorption at 1100 cm^{-1} which indicates the presence of uncoordinated ClO_4^- anion [97]. Molar conductance values for 1 and 2 in acetonitrile (Table

Table 3.1

Microanalytical Data for the Complexes 1 and 2

Complex	Empirical formula	Anal % Calcd				Found			
		C	H	N	S	C	H	N	S
1.	$C_{12}H_{19}N_2O_4S_2ClCu$	34.45	4.57	6.69	15.33	35.15	4.39	6.64	14.87
2.	$C_{12}H_{19}N_2O_5SClCu$	35.82	4.76	6.96	7.97	35.36	4.69	6.86	8.01

3.2) are found to be 122 and 131 ohm^{-1} cm^2 respectively which indicate that both behave as 1:1 electrolytes in that solvent [98].

Both 1 and 2 show only irreversible cyclic voltammograms taken in freshly prepared CH_3CN solutions. The situation does not improve upon varying the scan rate from 50 mVs^{-1} to 500 mVs^{-1}.

Magnetic moment values (Table 3.2) for 1 and 2 are 2.07 and 2.09 B.M. respectively at room temperature after applying diamagnetic corrections. The values are typical of discrete mononuclear copper(II) complexes [99]. EPR spectral results on 1 and 2 are given in Table 3.3. In the solid state, both give axial spectra with two lines in the parallel region (Fig. 3.10 and 3.11). The spectral shape does not change on lowering the temperature. In acetonitrile solution at RT, a characteristic four-line spectrum is obtained for each which changes to the one obtained in the solid state at liquid nitrogen temperature. The spectra are consistent with the presence of discretre tetrgonal copper(II) complexes [100]. Attempts to dope Cu(II) in a suitable diamagnetic host lattice so as to get magnetically dilute samples remain unsuccessful.

Both the complexes (Figs. 3.12 and 3.13) show a number of charge transfer transitions in addition to ligand field bands (Table 3.3). For four coordinate copper(II) complexes the d-d bands may occur in the range 500-850 nm depending upon the stereochemistry and nature of donor atoms as well [101]. On the basis of the absorption intensities, the broad band at 760 nm in 1 and the one at 610 nm in 2 are assigned to d-d transition(s). Ligand field band positions do not change with change of solvent

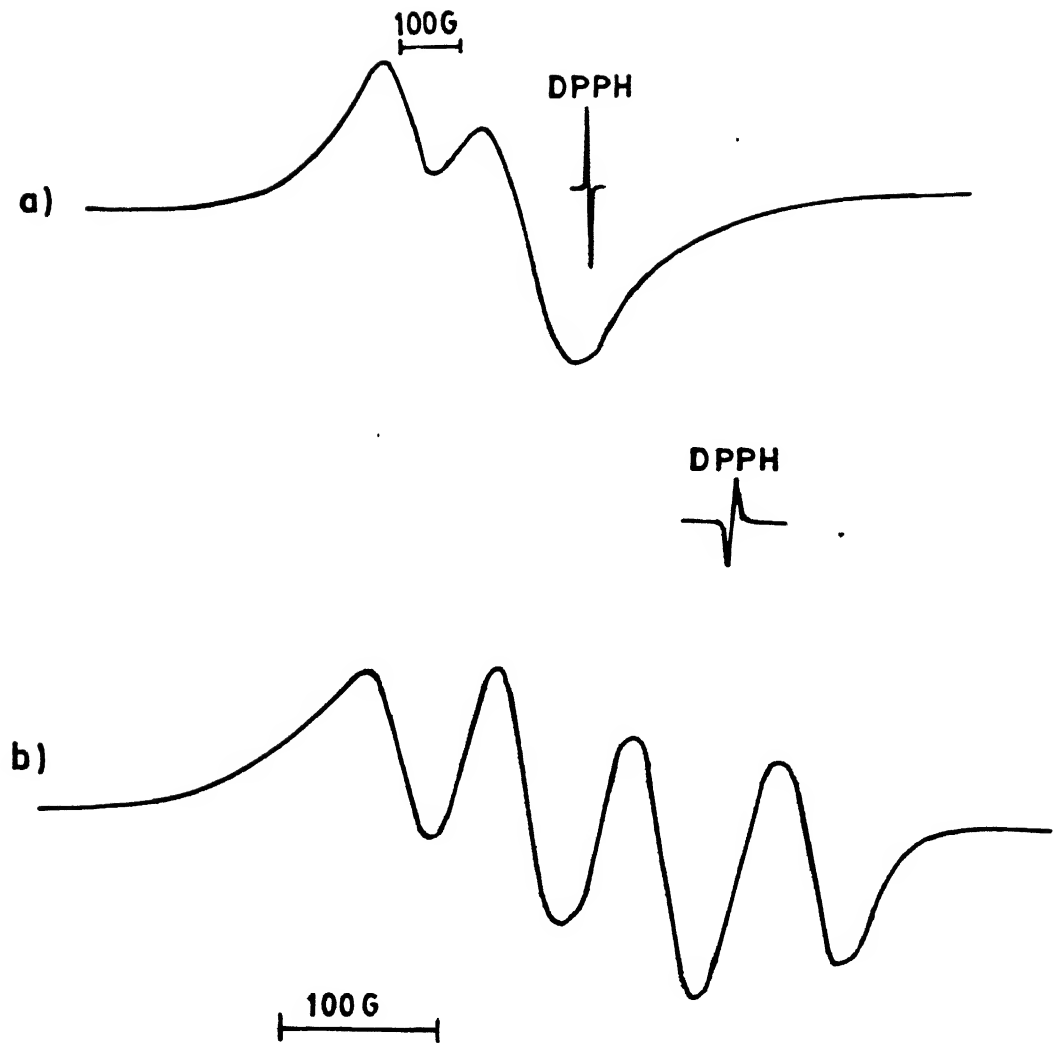

Fig 3.10 EPR spectra (R.T) of complex 1, a) solid state b) solution in CH_3CN

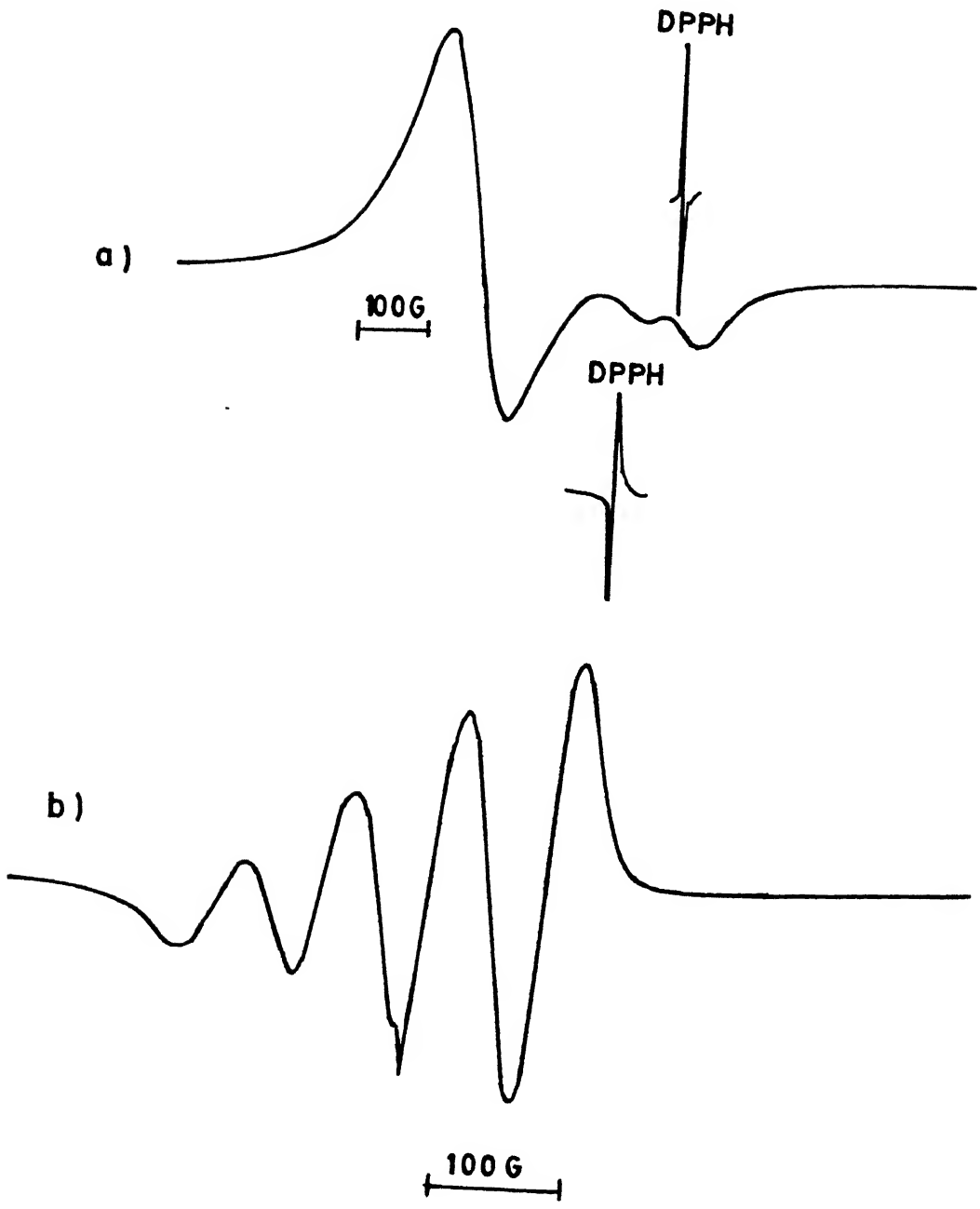

Fig 3.11 EPR spectra (R.T) of complex 2, a) solid state b) solution in CH_3CN

from acetonitrile to methenol or DMF. A large number of Cu(II)-amine complexes [41. 102] have been assigned tetragonal structures; if, in analogy 1 and 2 are assumed to be tetragonal, then the strong absorptions that occur at 280 and 270 nm respectively may be assigned to σ(N) → Cu(II)LMCT transitions. For 1 intraligand transitions also contribute significantly to the 280 nm absorption. This cannot be quantified as the corresponding Zn (II) complex does not form. Studies on tetracoordinate mixed aminothioether complexes [103] of copper(II) revealed that σ(thioether) →Cu(II) LMCT absorptions occur as a strong band in the region 320-390 nm and the π(thioether) →Cu(II) transitions may either be weak or absent and should occur at lower energies. It is, therefore, reasonable to assign the strong band at 390 nm in the case of 1 to σ(thioether) →Cu(II) LMCT absorption; this band occurs at 380 nm in the case of 2. This assignment agrees well with the separation of about 125 nm between σ(N)→Cu(II) and σ(thioether) →Cu(II) transitions [103]. For 2, however, the peak at 380 nm is assigned also to Cu(II)→phenolate MLCT transition (vide infra). For tetragonal thiolato complexes, the σ(thiolate) →Cu(II) transitions occur [104] around 350 nm and the band at 345 nm for 1 is assigned to σ(thiolate→Cu(II) LMCT absorption. However, unlike a thioether, a thiolate has two π-symmetry lone pairs on sulphur which may give rise to π-symmetry LMCT transitions on either side of the σ-transition [9]. For tetragonal Cu(II)-thiolato complexes, the lower energy π-transition occurs at approximately 450 nm. The 510 nm band in 1 is well separated from the ligand field band so this band is assigned to π(thiolate) →Cu(II) LMCT transition. In that case,

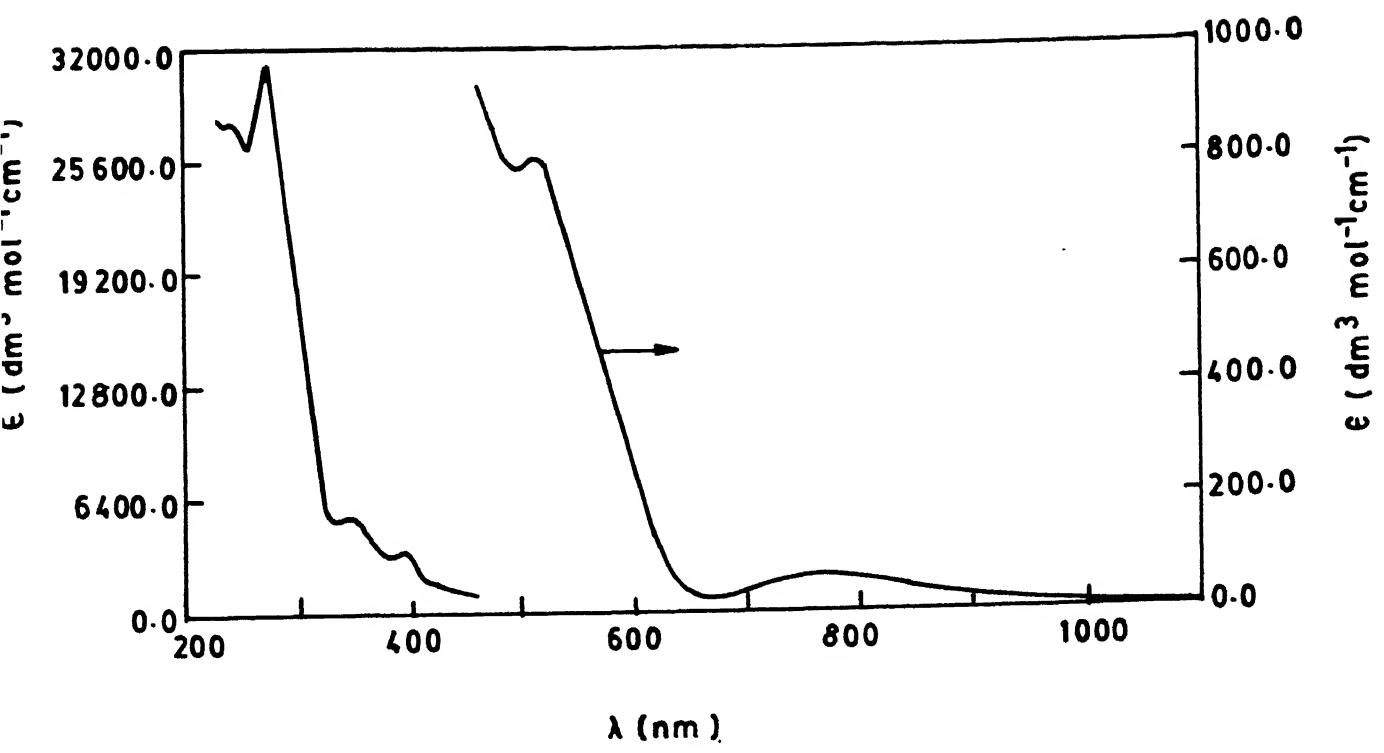

Fig 3.12 Electronic spectrum of complex 1 in CH_3CN

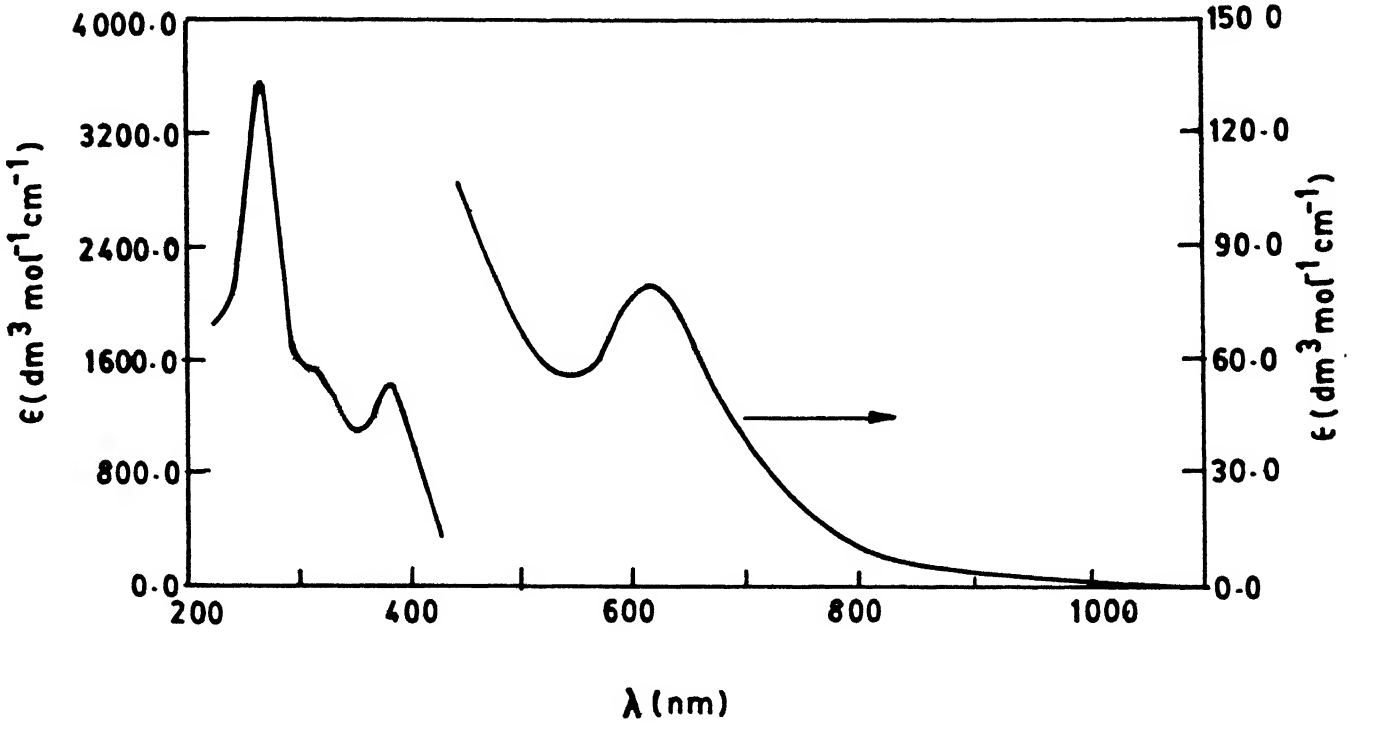

Fig 3.13 Electronic spectrum of complex 2 in CH_3CN

Table 3.3

Electronic and EPR Spectral Data(RT) for the Complexes 1 and 2

Compound	λ_{max}/nm (ϵ_{max}/$dm^3 mol^{-1} cm^{-1}$)	Assignments	EPR Data	
			Solid	Solution
1	760(65)	d-d	$g_{\parallel}$ = 2.23 $g_{\perp}$ = 2.02	g_{av} = 2.08
	510(800)	π(thiolate)→Cu(II)LMCT		
	390(3500)	σ(thioether)→Cu(II)LMCT		
	345(5470)	σ(thiolate)→Cu(II)LMCT		
	280(>30000)	σ(N)→Cu(II)LMCT + Ligand based transition		
2	610(80)	d-d	$g_{\parallel}$ = 2.03 $g_{\perp}$ = 2.24	g_{av} = 2.10
	380(1400)	(Phenolate)→Cu(II)MLCT + σ(thioether)→Cu(II)LMCT		
	315(1500)	(Phenolate)→Cu(II)MLCT		
	270(3450)	σ(N)→Cu(II)LMCT		

this transition is significantly red-shifted which is possible due to "through space" interaction between S3p orbitals and HOMO of the aromatic π-system [65]. The band at 315 nm for 2 is assigned as Cu(II) $\rightarrow$(phenolate) MLCT transition together with the one at 380 nm based on literature reports [59. 105] on Cu(II)-phenolato complexes.

3.5 Syntheses of Ligands Related to Part B

Syntheses of the ligands are shown schematically in Figs. 3.2 and 3.3.

3.5.1 Synthesis of Di-isobutylraldehyde disulfide

The dialdehyde was prepared by homolytic cleavage of S-Cl bond by isobutylraldehyde following a published procedure [106]. Sulfur monochloride (20 g, 0.15 mol) in dry CCl_4 (24 ml) was added dropwise to a solution of freshly distilled isobutylraldehyde (21.4 g, 0.30 mol) mixed with 40 ml of dry CCl_4 maintaining the temperature at 40-45^{o}C throughout. At the beginning, the temperature of the reaction mixture increased rapidly and cooling was necessary. As soon as sulfur monochloride came into contact with isobutylraldehyde, copius evolution of HCl gas occurred which was driven out of the reaction vessel by occasional passage of dinitrogen gas through the flask. Total addition time was 3 hours after which the reaction mixture was maintained at 40^{o}C for 48 hours for completion of the reaction. To collect the product, carbontetrachloride was evaporated off and the resulting pale yellow thick liquid was washed several times

with distilled water and finally allowed to distil under reduced pressure. The dialdehyde was obtained as a pale yellow oily liquid (15 mm, 90-100^{o}C) in 81% yield. ^{1}H-NMR (80 MHz, $CDCl_3$, δ_{TMS} ppm) : 9.0 (s, 2H) CHO, 1.1 (s, 12H) CH_3.

3.5.2 Synthesis of S-tertiary butyl cysteamine

This was prepared following a published procedure [107]. A mixture containing cysteamine (7.7 g, 100 mmol), tetiarybutyl alcohol (15 ml) and 50 ml of 2(N) hydrochloric acid was refluxed using a long condenser for 15 hours. Tertiary butyl alcohol and almost half of the water used was removed under reduced pressure. The resulting white solid was treated with excess of saturated potassium hydroxide solution in water and extracted (4x25 ml) in ether. The ether extract after drying over anhydrous sodium sulphate, evaporated off completely to get a colorless oily liquid in about 65% yield. ^{1}H-NMR (60 MHz, $CDCl_3$, δ_{TMS} ppm) : 5.2 (s br, 2H) NH_2, 2.85 (t, 4H) CH_2, 1.2(s, 9H) t-butyl.

3.5.3 Synthesis of S-tertiary butyl 2-amino thiophenol

This was synthesized following the above procedure by refluxing 2-aminothiophenol (5.4 g, 43.2 mmol), tertiary butyl alcohol (12 ml) and 25 ml of 2(N) hydrochloric acid for 14 hours using a long condenser. The product was obtained as a yellow semisolid in about 70% yield. ^{1}H-NMR (60 MHz, $CDCl_3$, δ_{TMS} ppm) : 7.2 (m, 4H) aromatic, 4.4 (s br, 2H) NH_2, 1.2 (s, 9H) t-butyl (Fig. 3.14).

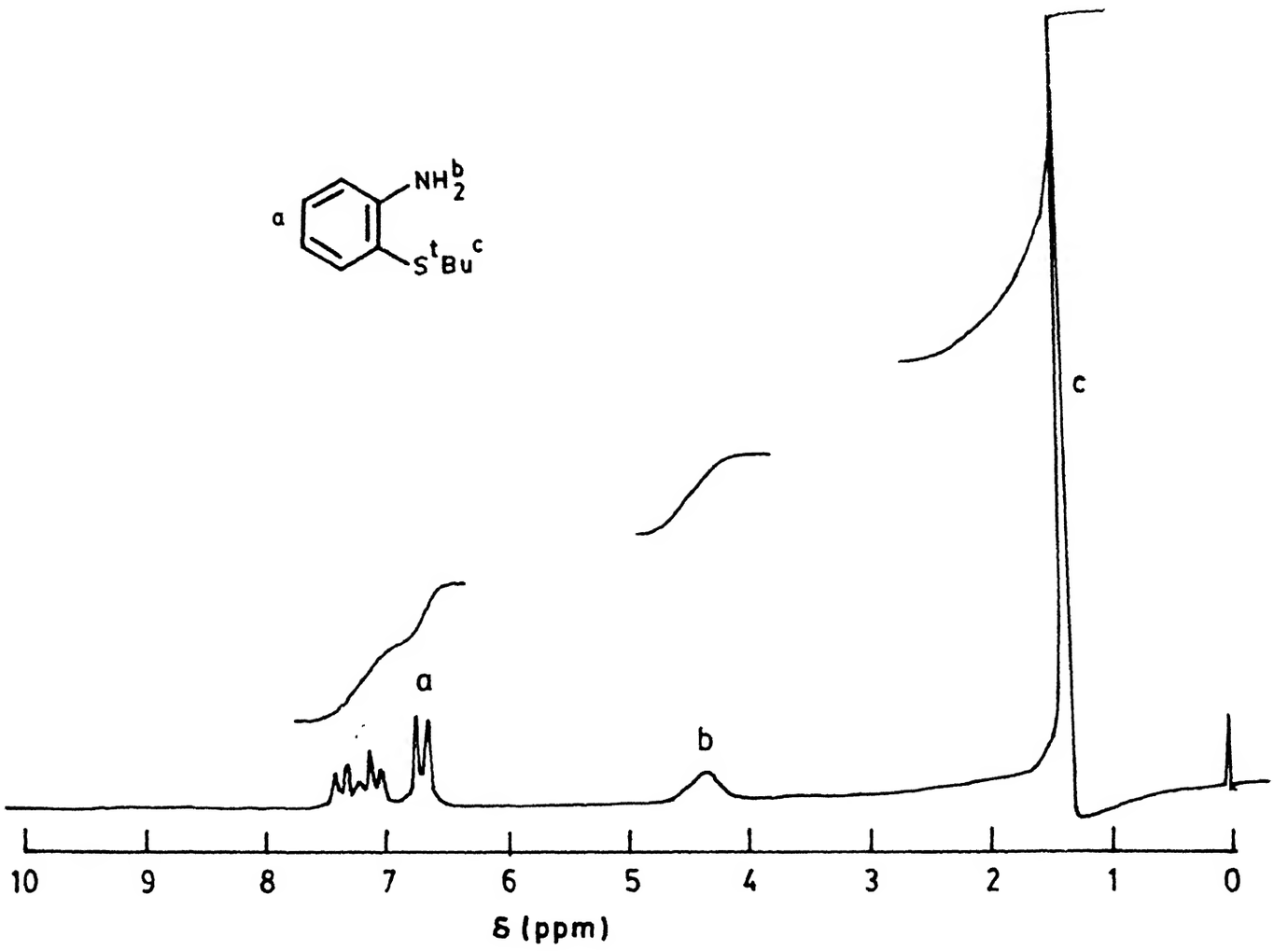

Fig 3.14 ^{1}H-NMR (60 MHz) spectrum of S-tertiary butyl -2-aminothiophenol in $CDCl_3$

3.5.4 Synthesis of the Ligand, L_3

Di-isobutylraldehyde disulphide (1.2 g; 5.7 mmol) was allowed to reflux with S-protected mercaptoethylamine (1.5 g; 11.4 mmol) in dry ethanol (20 ml) for 6 hours. The Schiff base that formed was reduced with $NaBH_4$ by refluxing for 2 hours. After the reflux, ethanol was removed in a rotary evaporator, the residue shaken with 20 ml of water, followed by extraction with $CHCl_3$ and finally removal of $CHCl_3$ under reduced pressure yielded L_1 as a pale yellow thick liquid. Yield 87% This was used subsequently for complexation without further purification. ^{1}H-NMR (60 MHz, $CDCl_3$, δ_{TMS} ppm) : 4.5 (s br, 2H) NH, 2.9 (m, 8H) $4CH_2$, 2.3 (s, 4H) $2CH_2$, 1.2 (s, 18H) t-butyl, 1.0 (s, 12H) $4CH_3$ (Fig. 3.15)

3.5.5 Synthesis of Ligand, L_4

The ligand L_4 could be obtained in 83% yield as a pale yellow oily liquid following the above procedure starting from S-t-butyl-2-mercaptoaniline and diisobutyraldehyde disulfied. This product used for complexation without further purification. ^{1}H-NMR (60 MHz, $CDCl_3$, δ_{TMS} ppm) : 7.1 (m, 8H) aromatic, 4.5 (s, 4H) CH_2, 3.8 (s br, 2H) NH, 1.2 (s, 18H) t-butyl, 1.0 (s, 12H) $4CH_3$ (Fig. 3.16).

3.5.6 Synthesis of Ligand, L_5

This ligand was synthesized by the Schiff base condensation reaction between di-isobutyraldehyde disulfide and 2-dimethylaminoethyl amine in ethanol. Diisobutyraldehyde

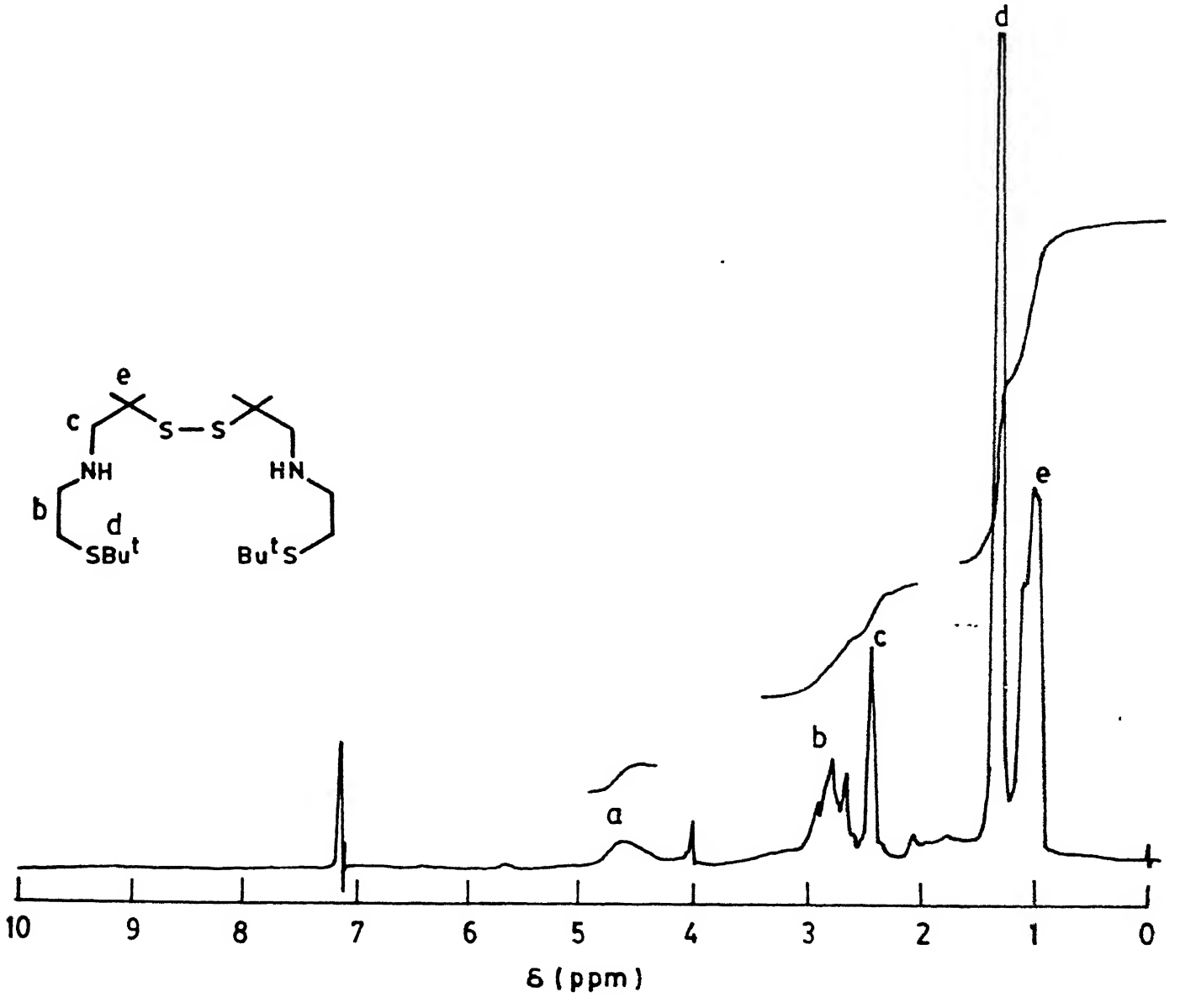

Fig 3.15 ^{1}H-NMR (60 Mhz) spectrum of L_3 in $CDCl_3$

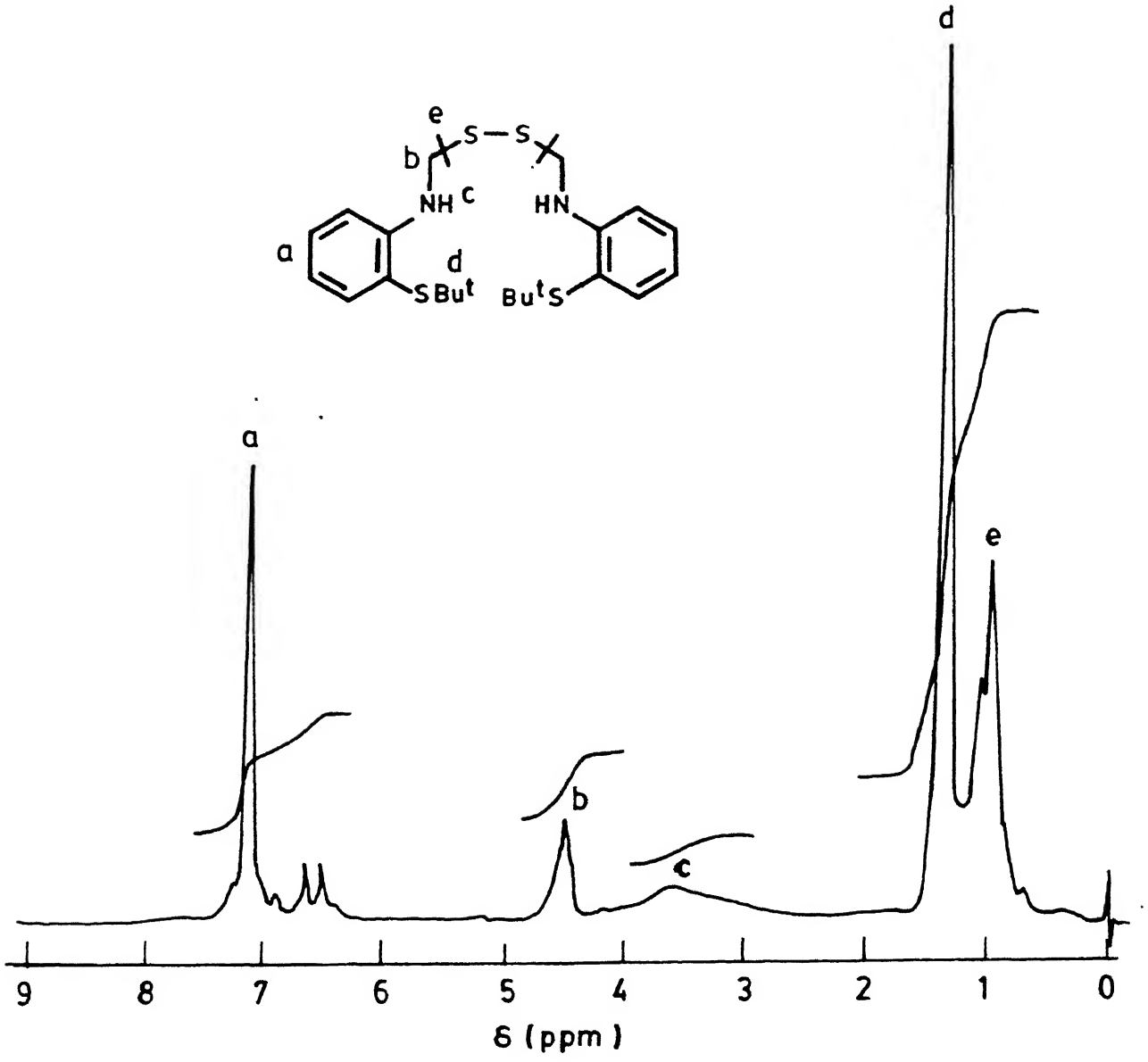

Fig 3.16 ^{1}H-NMR (60MHz) spectrum of L_4 in $CDCl_3$

disulfide (2 g, 0.01 mol) was allowed to reflux in dark and in an atmosphere of purified N_2 with 2-dimethylaminoethyl amine (1.7 g, 0.02 mol) in ethanol (20 ml). Color of the reaction mixture changed to orange from light yellow after 2 hours of reflux. After removal of ethanol in rotary evaporator it was pumped on for 2 hours. The thick orange liquid was used for complexation wtihout further purification. Infrared spectrum showed a strong absorption at 1650 cm^{-1} indicating the presence of the imine linkage.

3.6 Syntheses of the Complexes

3.6.1 Synthesis of the Complex, 3

Ligand L_3 (2.5 g, 6.1 mmol) dissolved in 40 ml ethanol and treated with a solution of $CuCl_2.2H_2O$ (1.0 g, 5.8 mmol) in 20 ml of ethanol. The light green solution thus obtained was allowed to reflux for 1 hour when the color changed to dark green. The entire operation was done in an atmosphere of nitrogen. The solution was concentrated to ~ 15 ml by passing nitrogen gas through and then filtered using a Schlenk-line. To the solution added about 25 ml of ether which caused a dark green solid to separate. This was collected by filtration. Yield 64%. The solid dissolved in acetronitrile (40 ml), filtered and allowed for slow evaporation in a stream of dry nitrogen gas. Dark green crystals in the form of needles appeared which were collected by filtration and dried in vacuum. Yield 52%; crystals were too small to be used in x-ray crystallographic studies.

3.6.2 Synthesis of the Complex, 4

This complex was synthesized in 65% yield as a dark blue-green crystalline solid following the above procedure. ligand L_4 (2.5 g, 4.9 mmol) and $CuCl_2.2H_2O$ (0.8 g, 4.9 mmol) were refluxed together in a total of 50 ml of ethanol for 1 hour.

3.6.3 Synthesis of the Complex, 5

The ligand L_5 (0.93 g, 3 mmol) dissolved in ethylacetate (15 ml) and to this was added solid copper(II) perchlorate hexahydrate (1 g, 3 mmol) with constant stirring at RT. Color of the reaction mixture turned dark green. After 30 minutes of stirring, the solution was filtered and the volume reduced to about 6 ml. The concentrated solution was kept at 5^oC for 5 hour. Green crystalline solid separated which was collected by filtration and dried under vacuum. Yield 45% .

3.6.4 Synthesis of the Complex, 6

$Cu(H_2O)_6(ClO_4)_2$ was allowed to stir at RT with 2-dimethylaminoethyl amine in 1:2 molar ratio in ethanol to obtain a dark blue solution which on slow evaporation yielded dark blue plates of 6 in 80% yield. Analytical data for the complexes are given in Table 3.4.

3.7 Results and Discussion

Both the complexes 3 and 4 behave as non-electrolyte (Table 3.5) in dichloromethane, acetonitrile and methyl alcohol.

Table 3.4

Microanalytical Data for the Complexes 3, 4, 5 and 6

Complex	Emperical formula	Anal % Calcd.				Found			
		C	H	N	S	C	H	N	S
3.	$C_{12}H_{26}N_2S_4Cu$	36.94	6.71	7.18	32.87	36.36	6.49	7.25	32.43
4.	$C_{20}H_{26}N_2S_4Cu$	49.40	5.39	5.76	26.37	49.12	5.66	5.80	26.19
5.	$C_{16}H_{34}N_4S_2O_8Cl_2Cu$	31.55	5.58	9.20		31.90	6.11	9.02	
6.	$C_8H_{24}N_4O_8Cl_2Cu$	21.89	5.48	12.76		21.49	5.31	12.62	

Table 3.5

Selective Infrared Bands, Yield, Color and Conductivity Data for the Complexes 3, 4, 5, and 6

Complex	Infrared bands (cm^{-1})	Yield %	Color	Conductance ($ohm^{-1}cm^{2}mol^{-1}$) (in acetonitrile)
3.	3270,s,br(ν_{NH})	60	Green	5
4.	3310,s,br(ν_{NH})	65	Dark blue green	4
5.	1610,s,($\nu_{C=N}$)	42	Green	263
6.	3370,s,br(ν_{NH})	80	Dark blue	266

Moreover, the qualitative test for the chloride ion is negative when copper(II) chloride is used for complex formation with the ligands (L_3 and L_4) indicating complete cleavage of S-tertiarybutyl linkage and subsequent replacement of the chloride ions by thiolates.

Magnetic moment values after diamagnetic corrections for the complexes 3 and 4 are listed in (Table 3.6). The values are indicative of discrete Cu(II) complexes [99].

3.7.1 Electron Paramagnetic Resonance

EPR spectral results for complexes 3 and 4 are listed in (Table 3.6). Complex 3 in the solid state or in solution at liquid nitrogen temperature exhibits an EPR spectrum which is significantly rhombic-distorted. The EPR spectra of 3 in the solid state and in acetonitrile glass are shown in (Figs. 3.17 & 3.18). For complex 4, only a broad signal is obtained in the solid state or in acetonitrile glass. The solvent molecules are not bonded to copper(II) in either of the complexes (3 and 4) as the analysis of electronic spectral data showed (vide infra). The EPR parameters for 3 listed are those obtained by spectral simulation. The highest symmetry appropriate for CuN_2S_2 complex that should show [108] rhombic splitting is C_{2v}. In this point group, both $d_{x^2-y^2}$ and d_{z^2} orbitals transform in the A_1 representation. Therefore, the metal part of the ground state wave function should be a mixture of both these orbitals. In this symmetry, the g shifts (from the free electron value) are given by

Table 3.6

Magnetic Moment (R T) and EPR Spectral Data (80 K) for the Complexes 3, 4, 5, and 6

Complex	μ_{eff}/μ_B	$g_{\parallel}$	$g_{\perp}$	g_{av}	$A_{\parallel}$	g_x	g_y	g_z	A_x	A_y	A_z	Ref
CBP						2.02	2.08	2.21	60	10	55	34
Stellacyanin						2.02	2.08	2.29	57	-29	-35	"
Plastocyanin						2.04	2.06	2.23	-17	-17	-63	"
Zn[Cu](1,2-Me_2Im)$_2$$Cl_2$						2.042	2.144	2.365	45	28	65	"
3.	2.10					2.014	2.11	2.235	67	11	97	
4.	2.05			2.10[a]								
5.	2.01	2.23[a]		2.038[a]	150							
6.	2.07	2.218[a]		2.005	185							

a = solid state; unit for $A_{x,y,z}$ is 1 x 10^{-4} cm^{-1}

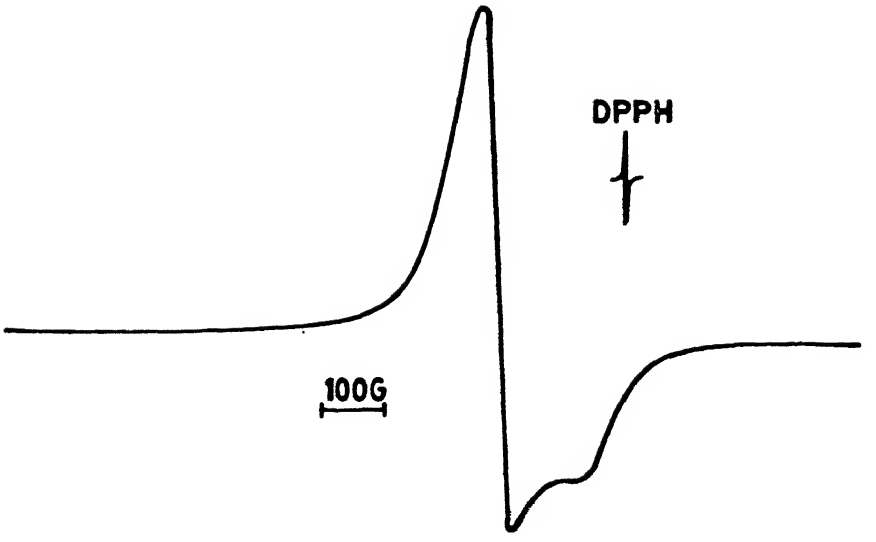

Fig 3.17 EPR spectrum of complex 3 in solid state at liquid nitrogen temperature

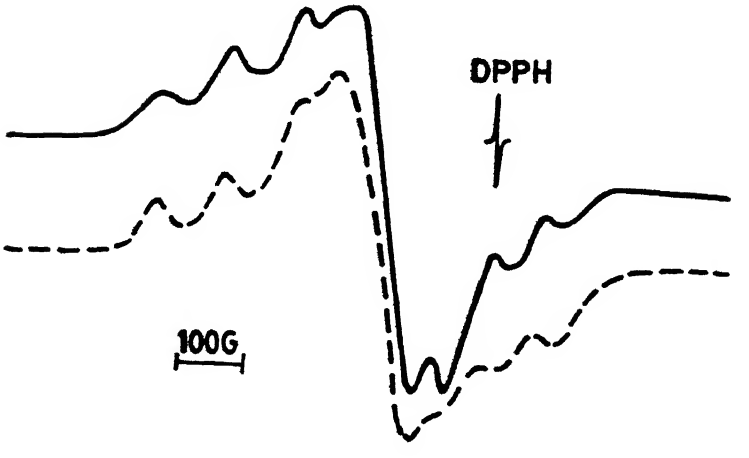

Fig 3.18 EPR spectrum of complex 3 in acetonitrile glass at liquid nitrogen temperature. Broken line represents the simulated spectrum

[108].

$$g_x = -2\lambda K_x^2 (a-3^{1/2}b)^2/E_{xz} \quad (1)$$

$$g_y = -2\lambda K_y^2 (a+3^{1/2}b)^2/E_{yz} \quad (2)$$

$$g_z = -8\lambda K_z^2 a^2/E_{xy} \quad (3)$$

Here $K_{x,y,z}$ are the orbital reduction factors [109], λ is the spin orbit coupling of copper(II) ion, a and b are the coefficients of $d_{x^2-y^2}$ and d_{z^2} in the ground state wavefunction respectively while the denominators represent d-d transition energies i.e. E_{xy} is the energy difference between the ground state and d_{xy} and so on. As these equations indicate, three possible mechanisms can split g_x and g_y which are (i) differences in E_{xz} and E_{yz} values, (ii) differences in reduction factors i.e., excited state delocalization and (iii) magnitude of a and b i.e., d_{z^2} mixing into the ground state wave function. Detailed calculations [34] on copper(II)-doped Zn (1,2-dimethylimidazole)$_2$Cl$_2$ host lattice having a pseudotetrahedral structure suggest that for a difference of about 125 nm between E_{xz} and E_{yz} values, the difference (g_x-g_y) can be as much as 0.004. In absence of polarized electronic spectral data on 3, it is not possible to designate the two ligand field transitions observed. In any case, the band positions (Table 3.7) put an upper limit of about 55 nm between the two transition energies, viz, E_{xz} and E_{yz}. Therefore, point (i) above cannot account for such a large split in the g values. The major contributing factor(s) towards the rhombic splitting for 3 should be either due to d_{z^2} mixing into the ground state wavefunction or

extensive excited state delocalization or both.

In probing the EPR spectral characteristics of plastocyanin, it has been argued in favour of an anisotropic delocalization over the cysteine sulfur p_π orbital [53] However, the extent of g split in plastocyanin is small (0.017) compared to stellacyanin (0.057). The extensive g split in stellacyanin cannot be accounted for considering orbital reduction factors alone due to their small effects. On the other hand, the difference (g_x-g_y) is quite sensitive to the amount of dz^2 mixing [34]. For Stellcyanin, observed g split could be explained satisfactorily taking into consideration of about 3% mixing of d_z2 into the ground state. This amount of mixing can also account for the differences between A_x and A_y values observed in stellacyanin. To evaluate the extent of d_z2 mixing neglecting the orbital reduction factors, a parameter R_g may be defined [110] as

$$R_g = \frac{2(g_x-g_y)}{g_x+g_y} \qquad (4)$$

For stellacyanin, R_g is 0.9 while for the Cu(II)-doped Zn (1,2-dimethylimidazole) Cl_2 this value is 1.1 and for complex 3, the value of R_g is calculated to be 1.6. This arameter is a steep function [34] of the extent of d_z2 mixing. For 3 a mixing of the order of 4-5% can satisfactorily account for the g split observed. For the copper(II)-doped complex above, about 3% mixing is suggested for the observed g split (0.102). For a 4-5% mixing, the difference, (A_x-A_y) should be about $60\times10^{-4}cm^{-1}$ which is very

close to the value obtained for complex 3.

3.7.2 Absorption Spectra

Electronic spectral data for the complexes (3 and 4) at room temperature are collected in (Table 3.7) and the spectra are shown in (Figs. 3.19 and 3.20). To probe possible solvent coordination, dichloromethane, acetonitrile and dimethyl formamide were used as solvents. In acetonitrile or dimethyl formamide, the spectral features were same as in non-coordinating dichloromethane. Therefore, if there is solvent coordination, it must be a very weak one. The bands with λ_{max} at 815 and at 760 nm are assigned as ligand field transitions. These are significantly red shifted compared to those for CuN_2S_2 chromophores having almost planar geometry [75,76,111,112]. Tetracoordinated copper(II) can exist in a large number of sterochemistries [113]. As the geometry distorts from planarity (dihedral angle 0^o) towards tetrahedral (dihedral angle 90^o) for the same chromphore, the d-orbital splittings decrease and consequently the ligand field bands shift towards lower energies. To probe this aspect of red-shift of the ligand field bands, the complexes 5 and 6 have been synthesized and charecterized. Complex 6 will be square planar while 5 should be distorted from planarity. Indeed, it is found (Table 3.7) that for 6 a broad ligand field transition occurs at 595 nm while in case of 5 (Fig. 3.21) it occurs as a broad band centred at 730 nm showing a red-shift of 135 nm. Attempts have been made [40,114] to relate the band maxima with the value of the dihedral angle. Any conclusions based on such

Table 3.7

Electronic Spectral and Electrochemical Redox Potential Data* for the Complexes 3, 4, 5, and 6

Complex	$\lambda_{max/nm}(\epsilon_{max}/dm^3mol^{-1}cm^{-1})$	E_{Pc}	E_{Pa}	$E_{1/2}$	ΔE_P (mV)
3	815(510),760(540),415(2825) 345(3415), 280(5000)	0.45	0.56	0.51	120
4	810(515),670(930),470(2420) 335(3125), 290(5040)	0.5	0.6	0.55	100
5	730(25),280(1750)	0.14	0.22	0.28	80
6	595(30), 280(1600)	-0.35	-0.215	- .18	100

*Potential values are in volts; the standar electrode is the saturated colomel electrode (SCE)

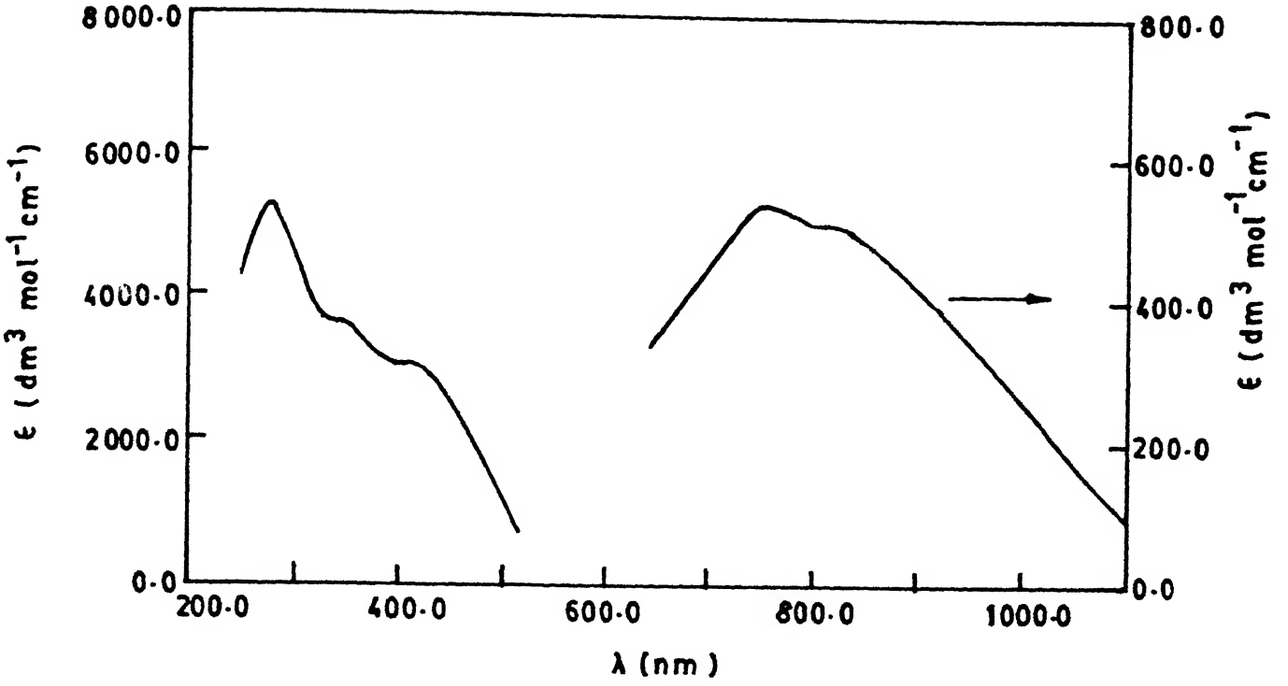

Fig 3.19 Electronic spectrum of complex 3 in CH_3CN

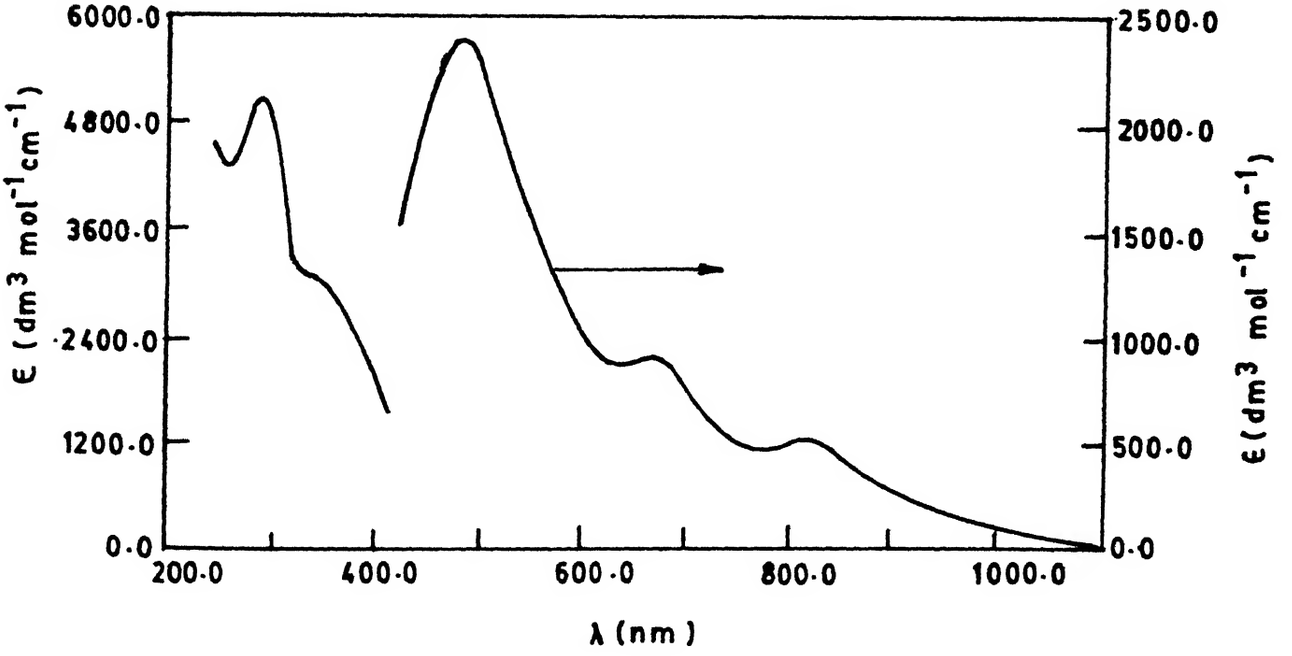

Fig 3.20 Electronic spectrum of complex 4 in CH_3CN

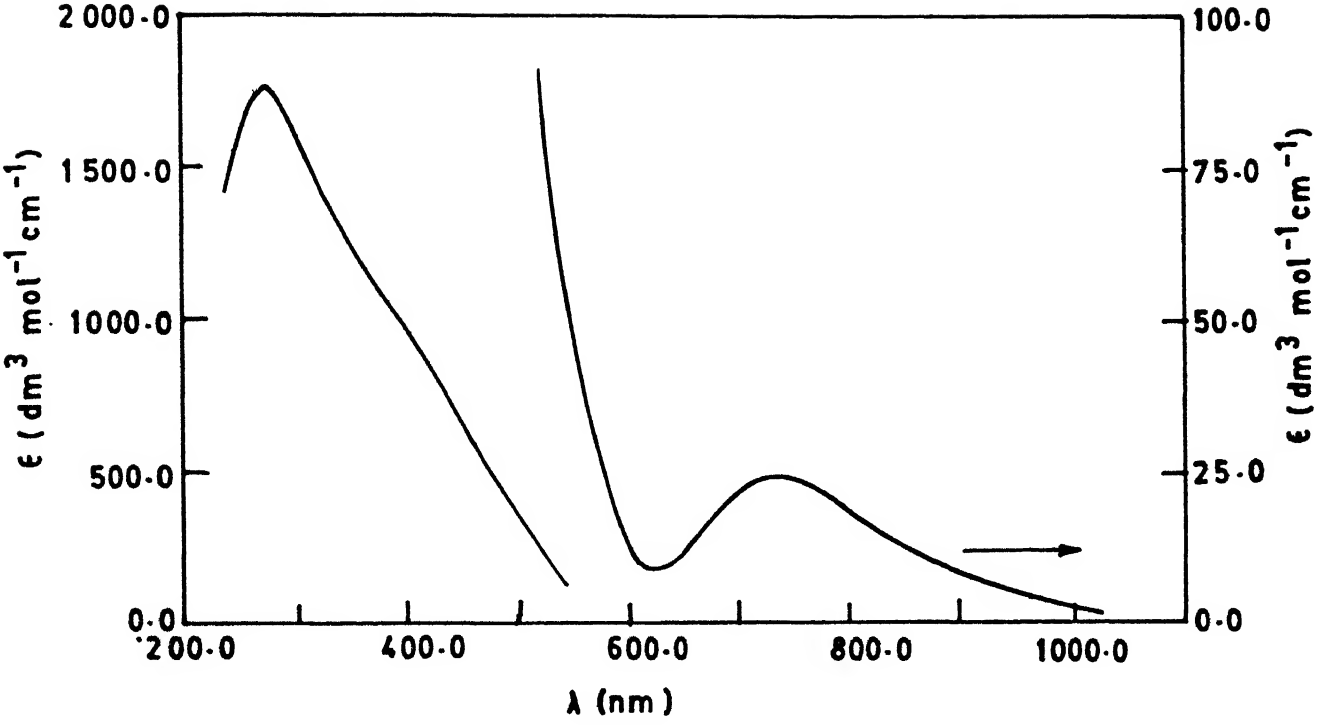

Fig 3.21 Electronic spectrum of complex 5 in CH_3CN

correlations should be made only for closely related ligands. As the data shown in (Table 3.7) indicate, d-d band positions in 3 and 4 occur at energies as in case of CuN_2S_2 chromophores [75,115] where the dihedral angle is near 50^o or slightly more. Somewhat higher intensities observed for the ligand field bands in the present cases are possible due to intensity borrowing from the nearby charge transfer transitions [76].

Charge transfer transitions involving amines and copper(II) are available [41-43,102]. The parent complex, $[Cu(en)_2(ClO_4)_2$ absorbs at 240 nm attributable to σ(N)$\rightarrow$ Cu(II) LMCT transition. Alkylation of the nitrogen atoms lowers the ionization potential [116] of the amine and results in a systematic red-shift of this band showing a linear relationship between the two parameters [40]. Therefore, the strong peak with λ_{max} at 280 nm in complex 3 is attributed to σ(N) $\rightarrow$Cu(II) LMCT absorption. In case of complex 4, the peak at 290 nm is similarly assigned. For complex 4, the intensity of this band is very high (Table 3.7). The free S-protected ligand (L_4) absorb strongly in this region. Aliphatic disulfides absorb [117] at energies higher than 280 nm. The prominent absorption at 350 nm and the weaker one at 470 nm are too low in energy to be σ(N) $\rightarrow$ Cu(II) LMCT bands originating from a secondary amine. These transitions are, therefore, attributable to thiolate $\rightarrow$ Cu(II) LMCT transitions. When a thiolate is bonded to copper(II), the LMCT involves three transitions - one intense σ(thiolate $\longrightarrow$ Cu(II) flanked on either side by weaker π(thiolate) $\rightarrow$ Cu(II) [53]. For CuN_2S_2 complexes, the σ(thiolate) $\rightarrow$Cu(II) LMCT transition occur near 350 nm

[76,115] and hence, the peaks near 350 nm are similarly assigned for both 3 and 4. In that case, the weaker absorption near 470 nm is assignable to π(thiolate) -› Cu(II) LMCT transition. The higher energy π-transition involving thiolate and copper(II) is not seen in either case which is mixed with other C T transitions.

3.7.3 Electrochemistry

Each of the complexes (3 and 4) show a well defined response in its cyclic voltammogram as shown in Fig. 3.22. The redox data in acetonitrile at room temperature (R.T) are collected in (Table 3.7). The following results were obtained : For complex 3, the response is quasi-reversible (ΔE_p = 120 mV) with $E_{1/2}$ = 0.51 V vs SCE. The ratio i_{Pa}/i_{Pc}, is equal to 1.0 within experimental error and independent of scan rates (25, 50, 100, 200 mVs^{-1}), the ΔE_p value increases steadily although by a small magnitude as the scan speed is increased and finally the ratio $i_{Pc}/V^{1/2}$ (V is the scan rate) is found to be practically constant. For complex 4, the response is again quasi-reversible (ΔE_p = 100 mv) with $E_{1/2}$ = 0.55 V vs SCE and is independent of scan rates employed, the ratio i_{Pa}/i_{Pc} is 1.0 within experimental error for all the scan rates while the ratio, $i_{Pc}/V^{1/2}$ is constant. The peaks are assignable to the Cu(II)/Cu(I) couple as shown below.

$$[Cu(II)L_3] + e^- = [Cu(I)L_3]^- \qquad (4)$$

$$[Cu(II)L_4] + e^- = [Cu(I)L_4]^- \qquad (5)$$

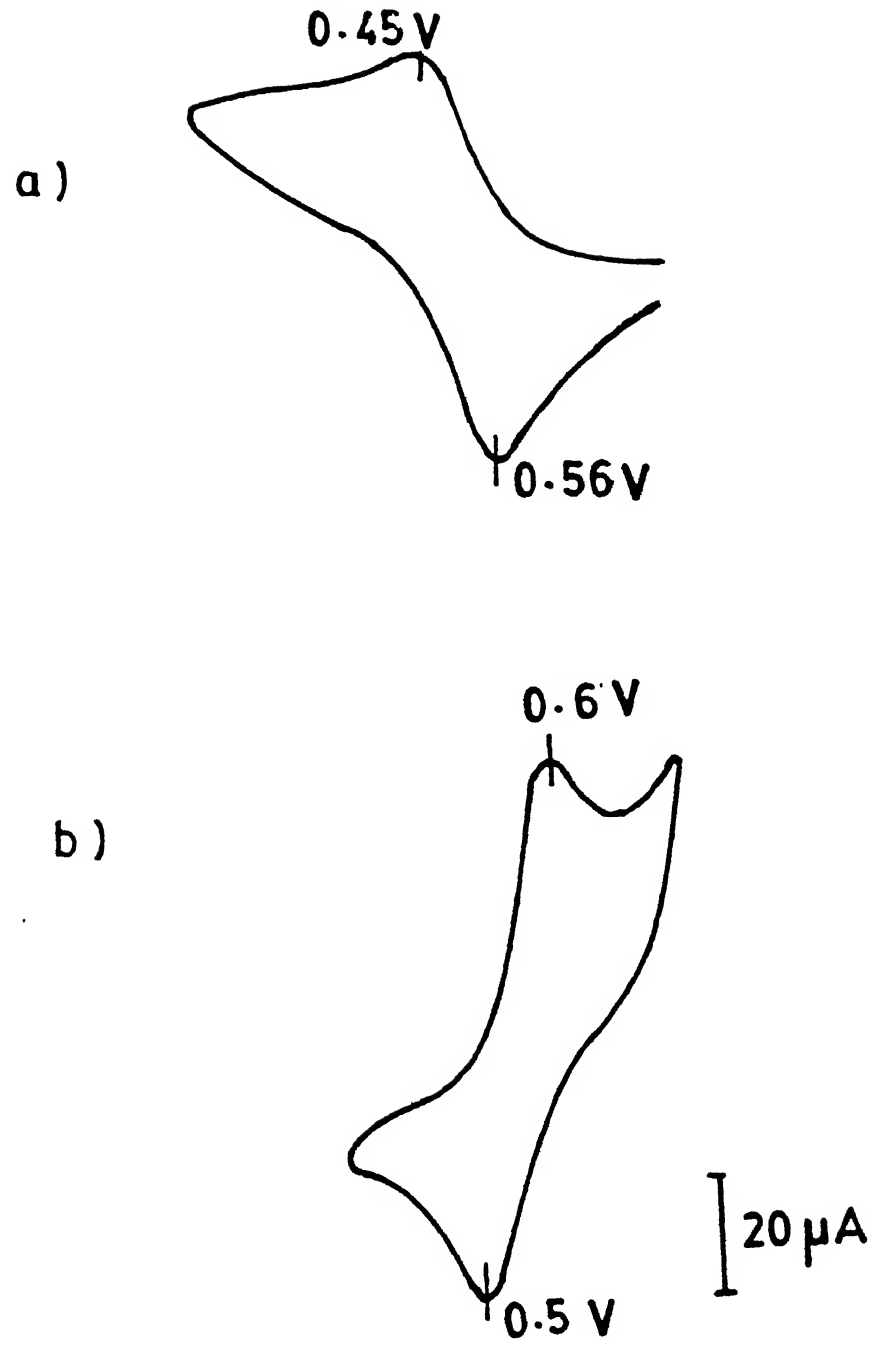

Fig 3.22 Cyclic voltammograms for the complexes 3 and 4 in CH_3CN (Ca 1 x 10^{-3}M) at the scan rate of 100mVs^{-1} using a glassy carbon working electrode a) for complex 3 b) for complex 4

The ligand based nature of these redox couples are ruled out by the fact $E_{1/2}$ value does not differ to any significant extent for the two complexes in spite of L_4 having two aromatic groups while L_3 having none. Besides, in case of 3, the only other redox active parts will be the thiols or the disulfide groups. Thiols will not give quasi-reversible cyclic voltammograms due to bond making/bond breaking processes involved. The N_4-analogue (L_5) of the ligand, L_3 where the two thiols were replaced by aliphatic amines was prepared. Copper(II) complex of this ligand was found to be pseudotetrahedral based on electronic spectral studies which showed a quasi-reversible Cu(II)/Cu(I) couple with $E_{1/2}$ = 0.28 V vs SCE and ΔE_p = 80 mV. Had it been due to disulfide group, both the CuN_4 (5) and the present CuN_2S_2 complexes would have given similar cyclic voltammograms. The high positive value and quasi-reversibility for the Cu(II)/Cu(I) couple is attributable to the pseudotetrahedral coordination geometry present in both the complexes : as copper(I) ion has a strong liking for tetrahedral coordination, the ligand reorganizational requirement accompanying Cu(II) $\rightarrow$Cu(I) reduction will be minimum. Lower the reorganization following a redox change in copper complexes, the more positive will be its thermodynamic redox potential. Complex 6 (Fig. 3.23), which will be a planar CuN_4 complex, show a quasi-reversible couple at $E_{1/2}$ = -0.18 V vs SCE. Hence, the Cu(II)/Cu(I) potential is shifted to +450 mV (Table 3.7) in case of 5 (Fig. 3.23). The free ligands or their Zn(II) complexes do not show any esponse in the region, -0.8 to +1.0 V. The $E_{1/2}$ values obtained for the present complexes are substantially higher compared to known CuN_2S_2 complexes having square planar geometry

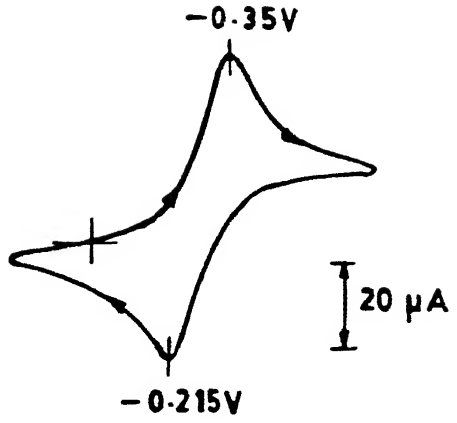

(a)

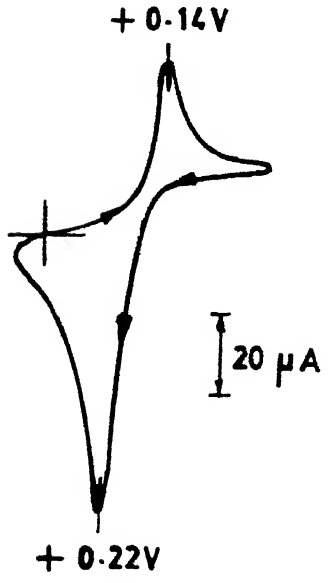

(b)

Fig 3.23 Cyclic voltammograms for the complexes 5 and 6 in CH_3CN (Ca 1 x 10^{-3}M) at the scan rate of 100mVs^{-1} using a glassy carbon working electrode a) for complex 6 b) for complex 5

[41-43] and very similar to the type 1 copper [9]. The high redox potential observed in case of the type 1 copper has been attributed to the substantially distorted geometry at the active site [22].

On scanning further in the positive side, no well-defined peak is observed. However, when scanned in the negative side, a small broad cathodic peak appears at about -0.8 V and on scan reversal an anodic peak of similar nature appears near -0.5 V. Also, a sharp anodic peak appears at -0.2 V. We did not probe any further the cathodic and anodic peaks which appear at -.8 V and at -0.5 V respectively. The sharp peak at -0.2 V is due to oxidation of metallic copper deposited at the electrode surface. Examples of this behaviour is known [118]. Coulometric data could not be collected for any of the complexes as they are unstable in the coulometric time-scale.

3.8 Conclusion

Part A

The complex 1 is a stable copper(II) complex with a ligand bearing two nitrogens, one thioether and one thiolate donors resembling the donor set present in some type 1 active sites of blue proteins. Variation of this ligand so as to get a complex with a long copper(II) thioether linkage would be an important step towards modelling the type 1 active site.

Part B

In the other set two neutral CuN_2S_2 complexes have been synthesized which are forced to adopt a pseudotetrahedral geometry

due to large bite angle and methyl substitutents of the two nitrogens.

The distorted geometry (3 and 4) raises the Cu(II)/Cu(I) couple and makes the EPR spectra (3) rhombically distorted by a significant amount. The amount of d_z2 mixing into the ground state wave function for the stellacyanin active site is estimated to be about 3%. This necessitates increased ligand field strength along the Z-direction which is possible if the local symmetry is more like C_{2V}. Cucumber basic protein (CBP) although having the same donor set as present in the plastocyanin gives a rhombic EPR signal. Studies of EPR characteristics of these blue sites alongwith their redox behaviour are likely to be facilitated by model Cu(II) thiolates where close to C_{2v} symmetry exists.

CHAPTER 4

HEXACOORDINATED Cu(II)-COMPLEXES

In the previous chapter tetracoordinated Cu(II)-complexes have been discussed. The present chapter reports the synthesis and characterization of hexacoordinated copper(II) complexes with ligands having $N_2S^*_2S_2$ (S^* =thioether) donors. The complexes described here represent the first set of examples of hexacoordinated copper(II) complexes having thiolate ligation. A hexacoordinated Cu(II)-ion is subject to Jahn-Teller distortion [87]. For a moderate to strong Jahn-Teller distortion, the singly occupied $d_{x^2-y^2}$ orbital will be destabilized due to strong bonding interactions equatorially. As a result, removal of the electron from $d_{x^2-y^2}$ orbital might be easier leading to oxidized species. With this idea, the complexes were synthesized to explore the possibility of having Cu(II)-thiolate species. A number of Cu(III)-complexes with deprotonated peptides as ligands have been characterized in the solid state [88]. A few Cu(III)-complexes with sulfur donor ligands like dithiolenes and dithiocarbamates are also known [119]. However, no complex having either simple aromatic or aliphatic thiolate bonded to Cu(III) has been reported. Cassella and coworkers obtained [76] oxidative cyclic responses with tetracoordinated thiolato complexes of Cu(II) which they have attributed to Cu(III)/Cu(II) couple without exploring the possibilities of ligand oxidations. Although no Cu(III)-thiolate bonding has been found in any of the copper proteins discovered todate, its involvement in the catalytic

cycles of some proteins has been implicated [88]. However, studies of Cu(III)-thiolate species are required to provide an important data base which will be of enormous use in detecting such species in biological systems. Besides, generation of Cu(III)-thiolate systems is interesting purely from the point of view of synthetic chemistry.

As discussed in the previous chapter, the ligands were synthesized with the thiols protected as their t-butyl derivatives. On refluxing with a Cu(II)-salt, the S-^{t}Bu linkage is cleaved forming the corresponding Cu(II)-thiolate bond. Here, two sets of hexadentate ligand systems are reported one bearing imine/amine, thioether and tertiarybutyl protected thiol groups and the other set has amide, thioether and tertiarybutyl protected thiols.

Non-thiolate complexes like 6, 6(A), 6(B) and 6(C) were synthesized to facilitate characterization of the copper (II) thiolato complexes. Two stable Nickel (II) thiolato complexes were also synthesized by breaking the S-tertiarybutyl group of the ligands L and L_8 to sort out possible ligand oxidations in these cases in the cyclic voltammetric studies. With other ligands, the S-t_{Bu} linkage cannot be broken by Ni(II).

4.1 Experimental Section

4.1.1 Solvents and Reagents

All solvents, tertiary butanol, and triethylamine were obtained from SD Fine Chemicals and purified prior to use following standard methods [92]. 2-Nitrobenzaldehyde,

2-mercaptoaniline, 1,2-dibromoethane, 1,3-dibromopropane, tertiary butylthiol, mercaptoacetic acid, mercaptopropionic acid, ethylchloroformate, thiosalicylic acid, and the Cu(II) salts were obtained from Aldrich and used as received.

4.1.2 Physical Measurements

The physical measurements were made on the complexes as described in chapter 3.

4.2 Syntheses of Ligands

Syntheses of ligands are shown schematically in Figs. 4.1, 4.2 and 4.3.

4.2.1 Synthesis of 1,2 di (o-aminophenolthio) ethane

This compound was prepared by following a published procedure [120]. Sodium (10 g, 0.4 mol) was dissolved in ethanol (150 ml) and to this, 2-mercaptoaniline (54.5 g, 0.4 mol) was added in hot condition (~50^{o}C). The resulting solution was allowed to reflux. 1,2,-dibromoethane (18.6 ml, 0.2 mol) in ethanol (50 ml) was added over a period of 30 minutes to the refluxing solution through a dropping funnel. Refluxing continued for another 30 minutes. The reaction mixture was then allowed to cool to room temperature and then poured into water (150 ml) with constant stirring. A light yellow solid precipitated. The solid was filtered and washed well with water and air dried. Yield 82%. Recrystallization from ethanol yielded 68% of the desired product

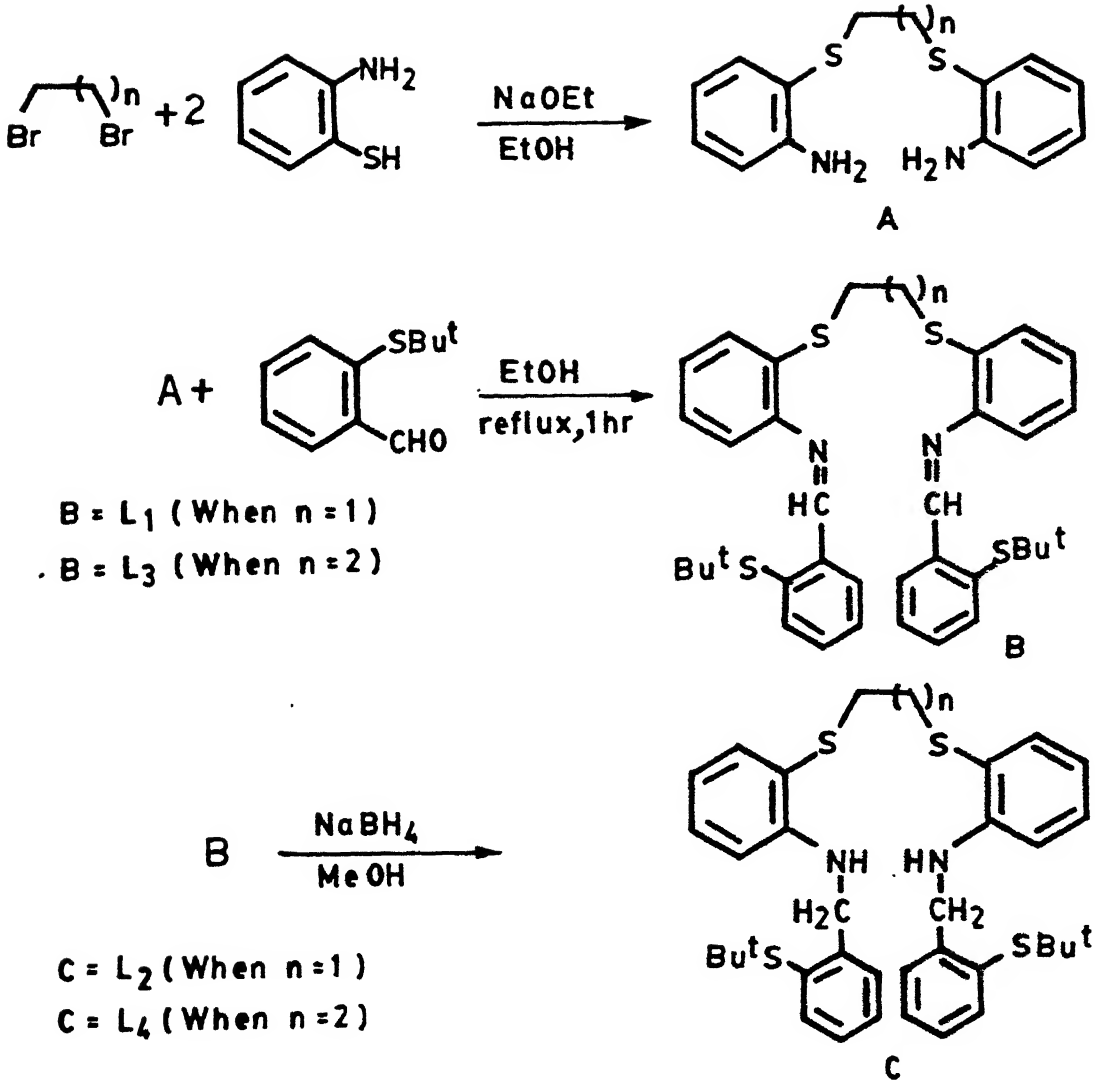

Fig 4.1 Synthetic scheme for the ligands L_1, L_2, L_3 and L_4

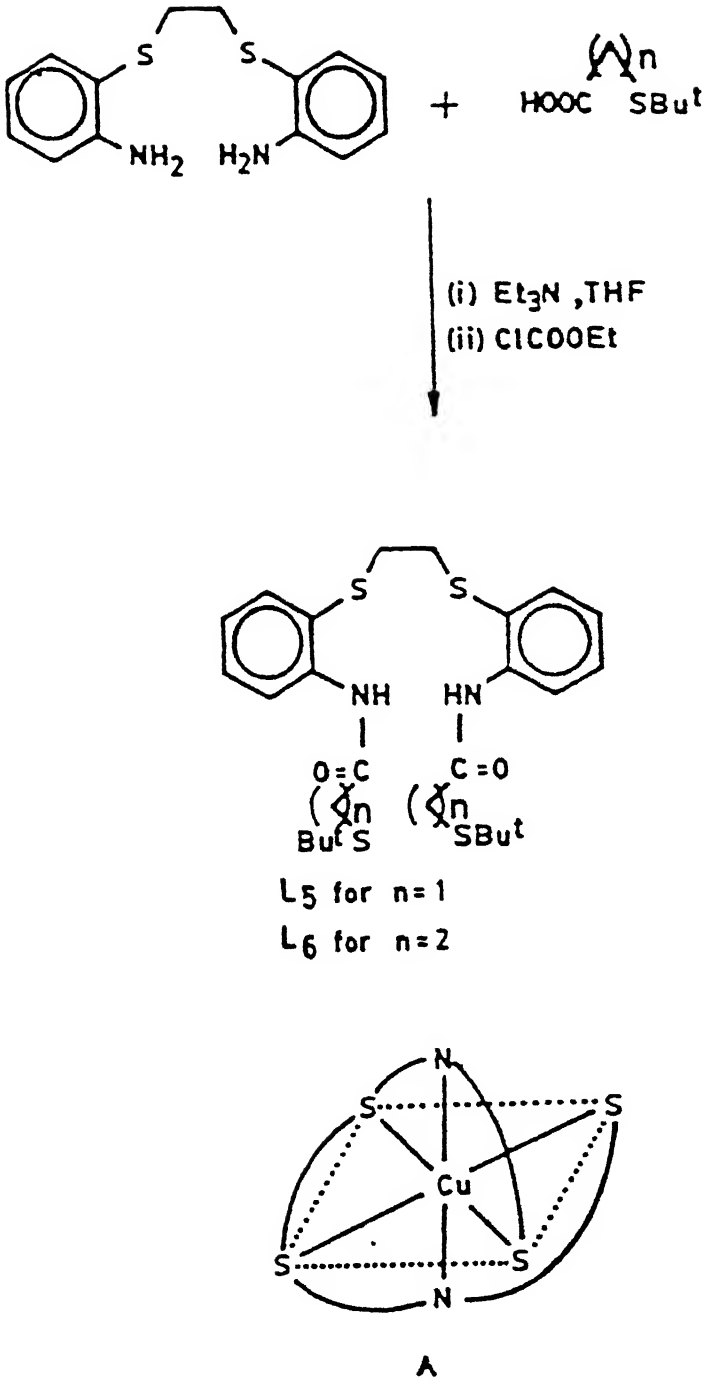

Fig 4.2 Synthetic scheme for the ligands L_5 and L_6 with binding mode (for complexes)

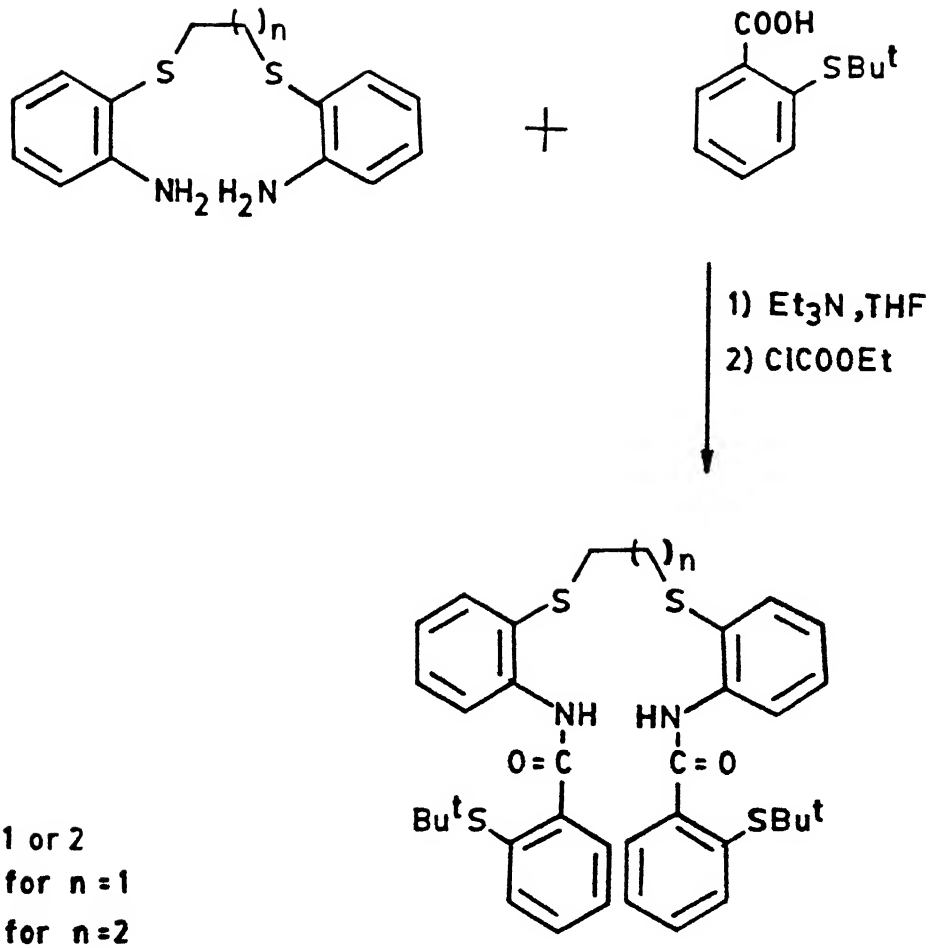

n = 1 or 2
L_7 for n = 1
L_8 for n = 2

Fig 4.3 Synthetic scheme for the ligands L_7 and L_8

m.pt. 77-78^{o}C (Lit 77.5-78.5^{o}C). ^{1}H-NMR (80MHz, $CDCl_3$, δ_{TMS}ppm) : 7.1 (m, 8H) aromatic, 4.35 (s, br, 4H) NH, 2.9 (s, 4H) CH_2 (Fig. 4.4).

4.2.2 Synthesis of 1,2 di(o-aminophenolthio)propane

This compound was synthesized following the above procedure. Sodium (4.6 g, 0.2 mol) was dissolved in ethanol (75 ml) and 2-mercaptoaniline (25 g, 0.2 mol) in ethanol (25 ml) was added to it in hot condition (~50^{o}C). The resulting solution was allowed to reflux. 1,3-Dibromopropane (20.2 g, 0.1 mol) diluted in ethanol (25 ml) was added dropwise through a dropping funnel during 30 minutes to the refluxing solution with stirring. After the addition was over, stirring continued for another 30 minutes. Then, the reaction mixture was allowed to cool to room temperature and poured into water (100 ml) with constant stirring. Brown oily liquid separated which could be collected with the help of a separatory funnel. It was purified by dissolving in ethanol followed by treatment with decolorizing charcoal and finally on evaporation, a light brown semi-solid product was obtained in 70% yield. ^{1}H-NMR (80MHz, $CDCl_3$, δ_{TMS}ppm) : ^{1}H-NMR 7.05 (m, 8H) aromatic, 4.2 (s, br, 4H) NH, 2.92 (t, 4H) -SCH_2, 1.9 (m, 2H) CH_2 (Fig. 4.5).

4.2.3 Synthesis of 2-t-Butylthiobenzaldehyde

This was prepared as described in chapter 3.

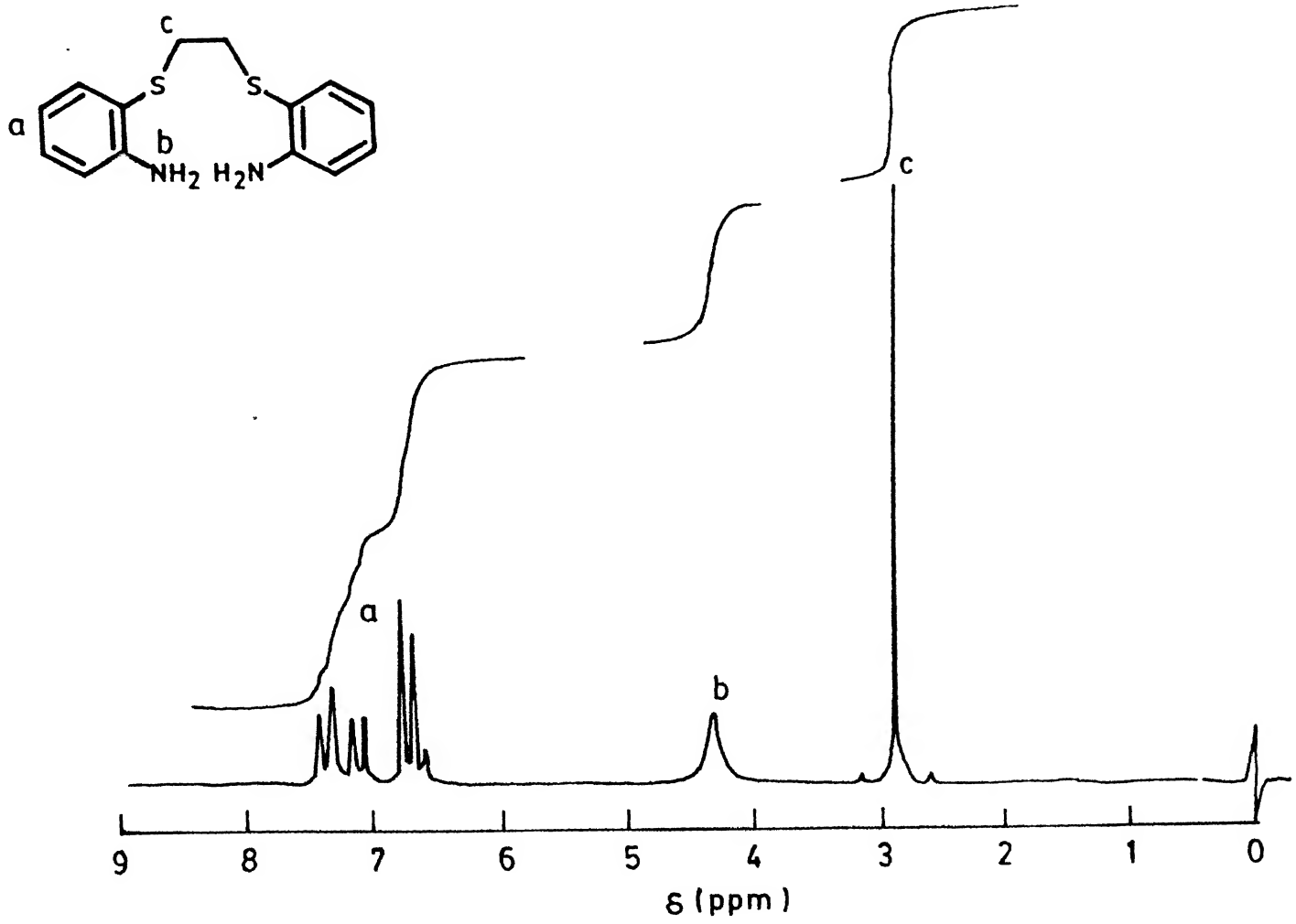

Fig 4.4 ^{1}H-NMR (80MHz) spectrum of 1,2 di (o-aminophenolthio)ethane in $CDCl_3$

4.2.4 Synthesis of S-tert-butyl-mercaptoacetic acid

This was prepared following the method of Pastuszak and Chimiak. A solution of mercaptoacetic acid (9.21 g, 100 mmol) in a mixture of 50 ml of 2(N) hydrochloric acid and 15 ml (11.8 g, 160 mmol) of tertiarybutyl alcohol was refluxed using a long reflux condenser. After 15 hours of reflux, the colorless reaction mixture was distilled at atmospheric pressure to remove water and butanol to obtain an oily liquid. This was subjected to fractional distillation under 5 mm pressure and the desired product was collected as a colorless oily liquid at 130-135^{o}C in 72% Yield. ^{1}H-NMR (80MHz, $CDCl_3$, δ_{TMS}ppm) : 11.1 (s, 1H) CO_2H, 3.3(s, 2H) CH_2, 1.26 (s, 9H) t-butyl (Fig. 4.6).

4.2.5 Synthesis of S-tertbutyl mercapto propionic acid

This was synthesized using the above procedure. Mercaptopropionic acid (10.16 g, 100 mmol) mixed with 50 ml of 2(N) HCl and tertiarybutyl alcohol (11.8 g, 160 mmol), was refluxed for 15 hours employing a long reflux condenser. The colorless reaction mixture was distilled at atmospheric pressure to remove water and t-butyl alcohol to obtain an oily liquid, which on fractional distillation afforded the desired product as a colorless oil (125-130^{o}C, 5 mm). Yield. 65%. ^{1}H-NMR (80MHz, $CDCl_3$, δ_{TMS}ppm) : 10.05 (s, 1H) CO_2H, 2.87 (t, 4H) CH_2CH_2, 1.25 (s, 9H) t-butyl.

4.2.6 Synthesis of S-Tertiarybutyl thiosalicylic acid

This was prepared following a similar procedure as adopted in case of the aliphatic analogues. Thiosalicylic acid

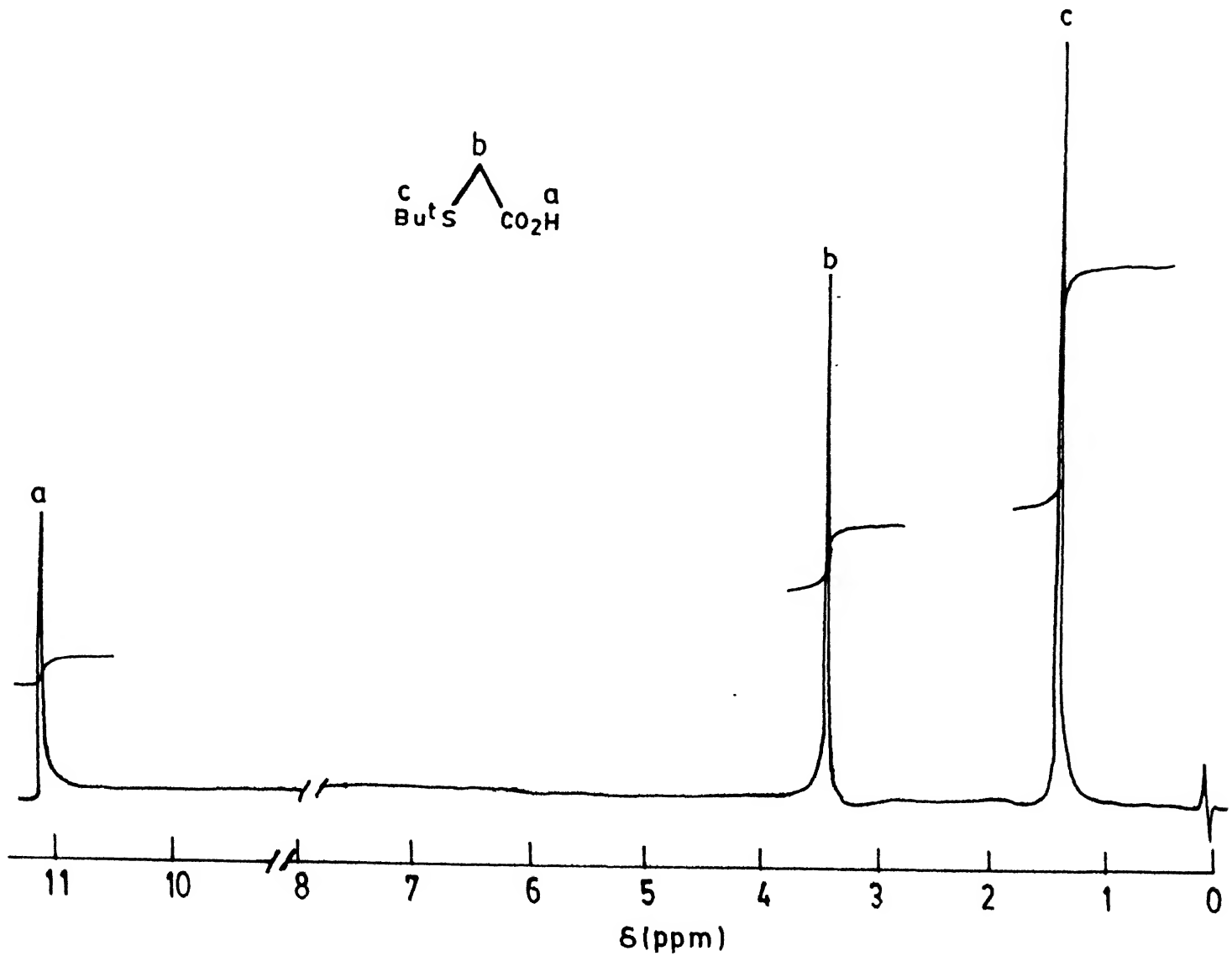

Fig 4.6 ^{1}H-NMR (80MHz) spectrum of S-tert-butyl mercaptoacetic acid in $CDCl_3$

(5 g, 0.032 mol) was taken in a 100 ml round bottom flask. 5 ml of tertiarybutyl alcohol and 15 ml of 2(N) HCl were added to it. The reaction mixture was allowed to reflux for 12 hours. Excess butanol was distilled off to get a light yellow solid at room temperature. The solid was collected by filtration, and washed several times using water. For further purification, the solid was dissolved in minimum amount of ethyl alcohol, filtered and the filtrate kept for slow evaporation. Light yellow crystalline solid appeared, which was collected by filtration and air-dried. Yield ~ 60%. m.pt. 67-68^{o}C. ^{1}H-NMR (80MHz, $CDCl_3$, δ_{TMS}ppm) : 7.5 (m, 4H) aromatic, 1.32 (s, 9H) t-butyl (Fig. 4.7).

4.2.7 Synthesis of the Ligand, L_1

The ligand L_1 was prepared by the Schiff base condensation of 1,2-di(o-aminophenolthio)ethane and 2-t-butylthiobenzaldehyde. In a typical reaction, 1,2-di (o-aminophenolthio)ethane (2 g, 7.2 mmol) was mixed with 2-t-butylthiobenzaldehyde (2.9 g, 14.4 mmol) in ethanol (40 ml) and refluxed for 1 hour. Color of the solution changed from light yellow to bright yellow. It was allowed to cool to room temperature and filtered. The filtrate on slow evaporation afforded a bright yellow crystalline product. Yield 85%. m.pt. 115^{o}C. ^{1}H-NMR (80MHz, $CDCl_3$, δ_{TMS}ppm) : 9.3 (s, 2H) CH, 7.4 (m, 16H) aromatic, 3.3 (s, 4H) CH_2, 1.2 (s, 18H) t-butyl (Fig. 4.8). I.R : 1654 cm^{-1} ($\nu_{C=N}$).

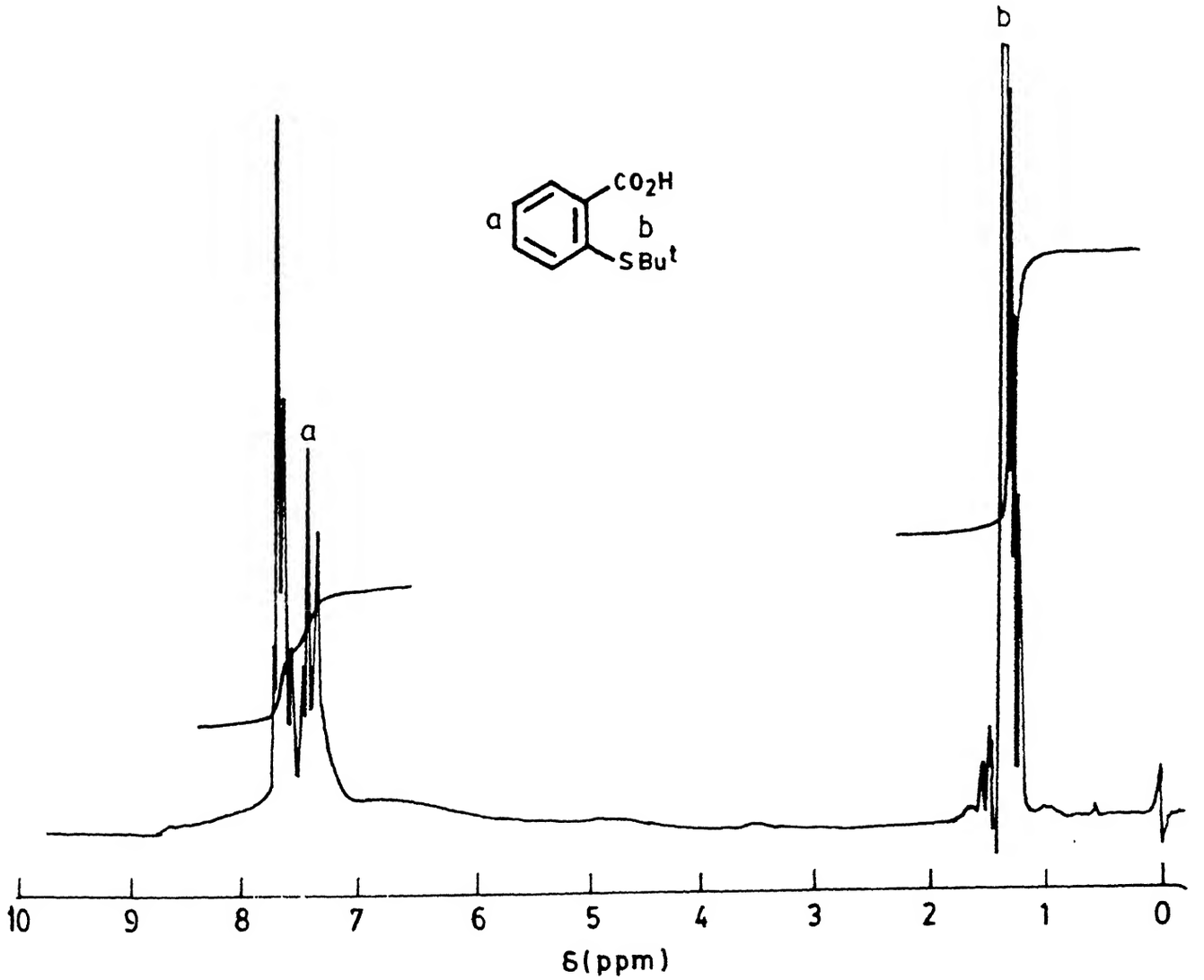

Fig 4.7 ^{1}H-NMR (80MHz) spectrum of S-tert-butyl thiosalicylic acid in $CDCl_3$

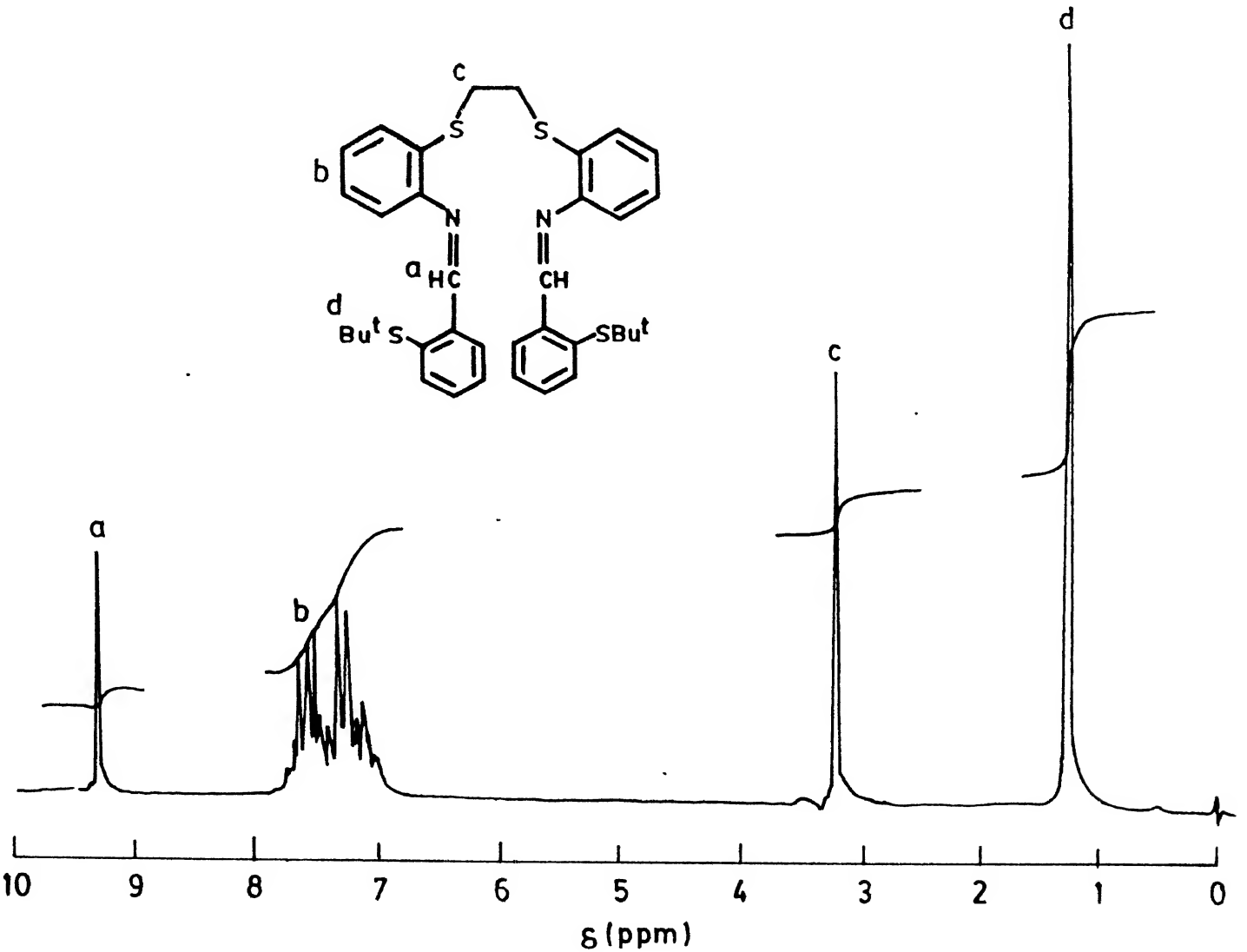

Fig 4.8 ^{1}H-NMR (80MHz) spectrum of the ligand L_1 in $CDCl_3$

4.2.8 Synthesis of the Ligand, L_3

This Schiff base was similarly prepared by refluxing 1,2-di(o-aminophenolthio)propane (3 g, 0.01 mol) with 2-t-butylbenzaldelyde (4 g, 0.02 mol) in ethanol (40 ml). The resulting light yellow solution was heated under reflux for 2 hours. Color of the solution changed to light orange. It was concentrated to about 15 ml,filtered, treated with ~15 ml of petroleum ether and finally placed in the freeze ($5^{o}C$). On keeping for 3 days a semisolid material formed which became solid after a period of 15 days. The product was isolated as a yellow solid, washed with diethyl ether and dried in vacuo. Yield 82%. I.R 1652 cm^{-1} ($\nu_{C=N}$). ^{1}H-NMR (80MHz, $CDCl_3$, δ_{TMS}ppm) : 9.2 (s, 2H) CH, 7.4 (m, 16H) aromatic, 3.05 (m, 4H)-SCH_2, 2.03 (m, 2H) CH_2, 1.2 (s, 18H) t-butyl (Fig. 4.9).

Syntheses of the reduced Schiff bases

4.2.9 Synthesis of Ligand, L_2

The Schiff base was reduced with sodium borohydride as follows:

The Schiff base L_1 (1.2 g, 1.9 mmol) was taken in methanol (120 ml) and treated with solid sodium borohydride (0.15 g, 4 mmol) in small portions with constant stirring. A vigorous reaction took place during addition. The reaction mixture was stirred for 2 h at RT and then heated to reflux for 8 h. After the reflux was over, excess $NaBH_4$ was quenched with 10 ml of H_2O and then evaporated to dryness. The golden yellow soild was

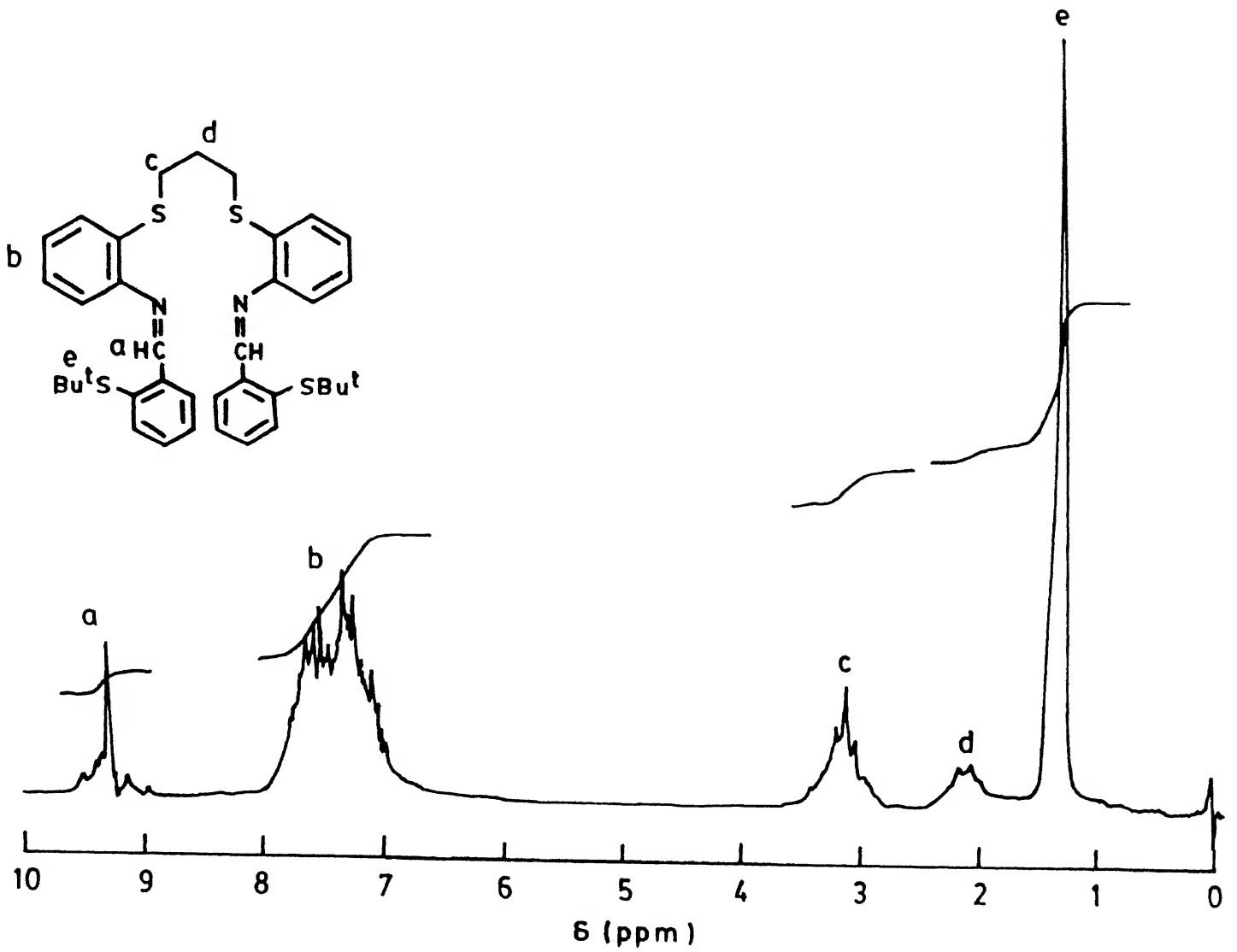

Fig 4.9 ^{1}H-NMR (80MHz) spectrum of the ligand L_3 in $CDCl_3$

shaken with 100 ml of $CHCl_3$ and 15 ml of H_2O. The organic layer separated, dried with anhydrous sodium sulfate and finally evaporated off $CHCl_3$ under reduced pressure to obtain the desired product as a light yellow semisolid. Yield 85%. ^{1}H-NMR (80MHz, $CDCl_3$, δ_{TMS}ppm) : 7.3 (m, 16H) aromatic, 4.97 (s, br, 2H) NH, 4.6 (s, 4H) N-CH_2, 3.05 (s, 4H) -S-CH_2, 1.2 (s, 18H) t-butyl.

4.2.10 Synthesis of Ligand, L_4

The Schiff base, L_3 (1.5 g, 2.3 mmol) taken in methanol (120 ml) and treated with solid sodium borohydride (0.18 g, 4.7 mmol). Vigorous reaction took place during addition. The reaction mixture was first stirred for 2 hours at RT and then refluxed for 8 hours. The product isolated as a light yellow semisolid following the above procedure in 80% yield. ^{1}H-NMR (80MHz, $CDCl_3$, δ_{TMS}ppm) : 7.4 (m, 16H) aromatic, 4.95 (s, br, 2H) NH, 4.6 (s, 4H) N-CH_2, 3.06 (m, 4H) -S CH_2, 2.03 (m, 2H) CH_2, 1.2 (s, 18H) t-butyl.

All amide ligands were synthesized by following the mixed anhydride method [121]. In this method first the acid was allowed to react with alkylchloro carbonates to form a reactive intermediate and then the intermediate was allowed to react with amine to form the desired amide along with carbondioxide and corresponding alcohol which can be easily removed from the reaction mixture.

Synthetic route :

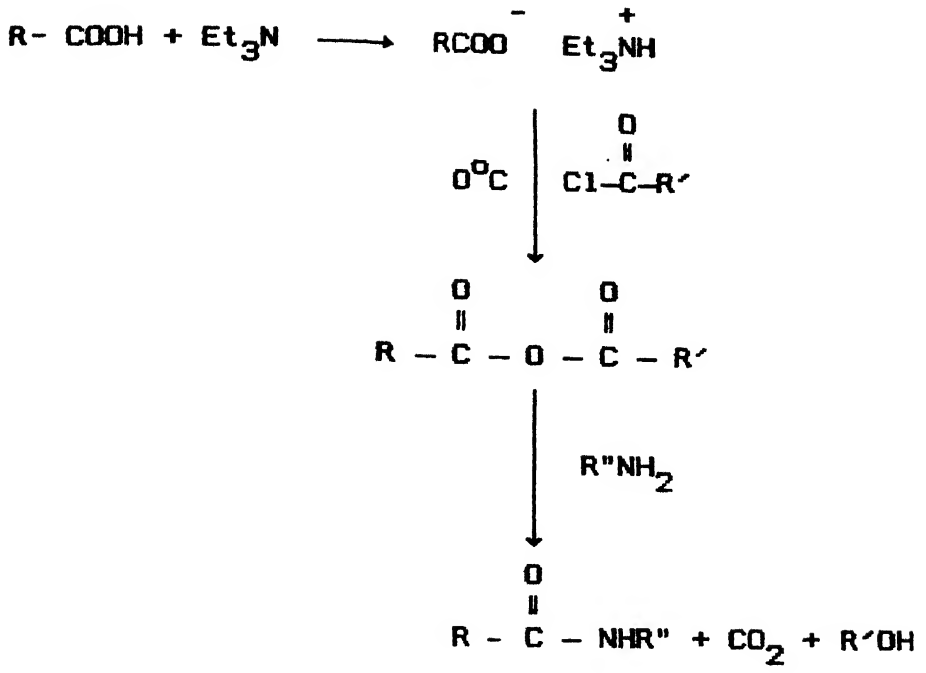

4.2.11 Synthesis of the Ligand, L_5

S-tert-butylmercaptoacetic acid (5 g, 34 mmol) disslolved in 30 ml tetrahydrofuran was taken in a three necked round bottom flask placed in an ice-salt bath. It was treated with triethyl amine (3.4 g, 34 mmol), and stirred for 10 minutes. Ethylchloroformate (3.7 g, 34 mmol) in 30 ml of tetrahydrofuran was added dropwise under an argon atmosphere through a dropping funnel. Total addition time was 30 minutes. After 15 minutes of additional stirring started the addition of a solution of 1,2-di(o-aminophenolthio)ethane (4.7 g, 17 mmol) in 30 ml of THF over a period of 40 minutes. Stirring continued at $0^{o}C$ for another hour and then at room temperature for 10 hours.

Triethylamine hydrochloride was filtered off and THF was removed completely to obtain a pale yellow oily liquid. The oily mass was dissolved in chloroform (30 ml) and washed with water (3x20 ml). The chloroform extract was dried over anhydrous sodium sulfate. Finally, $CHCl_3$ was removed completely in a rotary evaporator to obtain a pale yellow oily liquid in 75% yield. ^{1}H-NMR (80MHz, $CDCl_3$, δ_{TMS}ppm) : 7.1 (m, 8H) aromatic, 5.3 (s br, 2H) NH, 3.3 (s, 4H) aliphatic CH_2, 2.9 (s, 4H) S-CH_2, 1.2 (s, 18H) t-butyl (Fig. 4.10).

4.2.12 Synthesis of the Ligand L_6

This ligand was synthesized by using the above procedure. S-tertierybutyl mercaptopropionic acid (5.51 g, 34 mmol) in 30 ml of tetrahydrofuran was taken in a three necked round bottom flask placed in an ice-salt bath to which added triethylamine (3.4 g, 34 mmol). After stirring the reaction mixture for 10 minutes, ethylchloroformate (3.7 g, 34 mmol) taken in 30 ml of tetrahydrofuran was added dropwise in an argon atmosphere. Addition took 30 minutes. After a further 15 minutes of stirring started the addition of 1,2-di(o-aminophenolthio)ethane (4.7 g, 17 mmol) in 30 ml of tetrahydrofuran dropwise. Continued stirring at 0^oC for another one hour and then at room temperature for 10 hours. Finally, the reaction mixture was warmed to 40^oC for 30 minutes. White triethylamine hydrochloride was filtered off followed by complete evaporation of tetrahydrofuran under reduced pressure to obtain a pale yellow oily liquid. The oily liquid was taken in chloroform

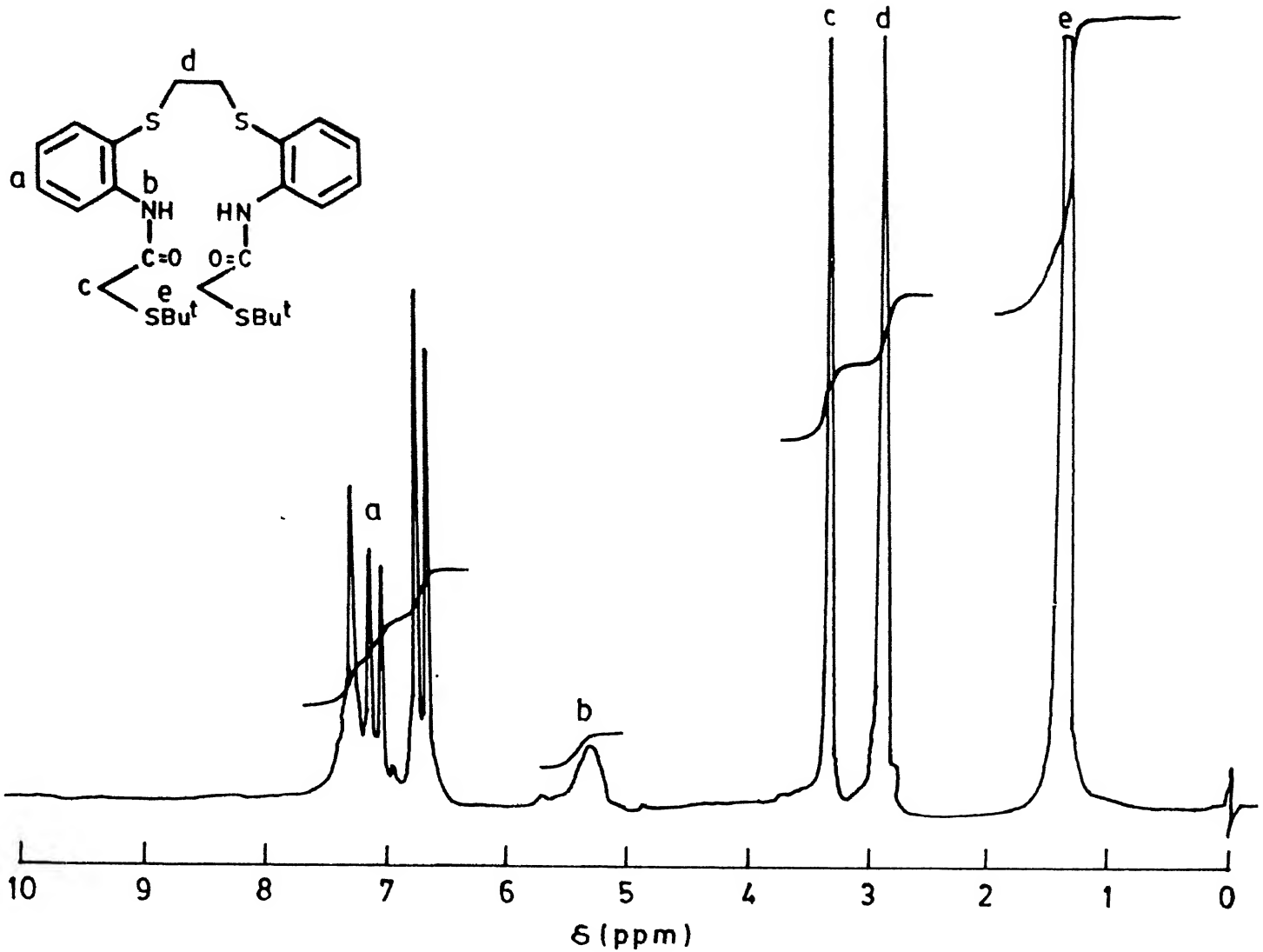

Fig 4.10 ^{1}H-NMR (80MHz) spectrum of the ligand L_5 in $CDCl_3$

(40 ml) and washed with water (3x20 ml). The chloroform extract was dried over sodium sulfate (anhydrous) and then the solvent was removed completely using a rotary evaporator. Pale yellow oily liquid obtained in high yield (~70%). ^{1}H-NMR (80MHz, $CDCl_3$, δ_{TMS}ppm) : 7.1 (m, 8H,) aromatic, 5.2 (s br, 2H) NH, 3.3 (m, 8H) aliphatic CH_2, 2.8 (s, 4H) aliphatic CH_2, 1.2 (s, 18H) t-butyl (Fig.4.11).

4.2.13 Synthesis of the Ligand, L_7

This was synthesized by the mixed anhydride method as above. To an ice-cold solution of S-t-butyl thiosalicylic acid (2 g; 9.5 mmol) and triethylamine (0.96 g; 9.5 mmol) was slowly added ethylchloroformate (1.03 g; 9.5 mmol) mixed with 30 ml of THF. The mixture was allowed to stir at ice cold temperature for 30 mintues and then allowed to react slowly with a THF solution (40 ml) of 1,2-di(o-aminophenolthio)ethane (1.31 g; 4.7 mmol) in an argon atmosphere. The reaction mixture was brought to room temperature after 2 hours and allowed to stir for 16 hours. White precipitate of triethylamine hydrochloride filtered off and THF evaporated off under reduced pressure to obtain a pale yellow semisolid. This semisolid dissolved in $CHCl_3$ and washed several times with H_2O and finally $CHCl_3$ removed to obtain the desired product as a pale yellow semisolid. Yield 78% ^{1}H-NMR (60MHz, $CDCl_3$, δ_{TMS}ppm) : 7.2 (m, 16H) aromatic, 5.5 (s br, 2H) NH, 2.9 (s, 4H) CH_2, 1.3 (s, 18H) t-butyl (Fig. 4.12).

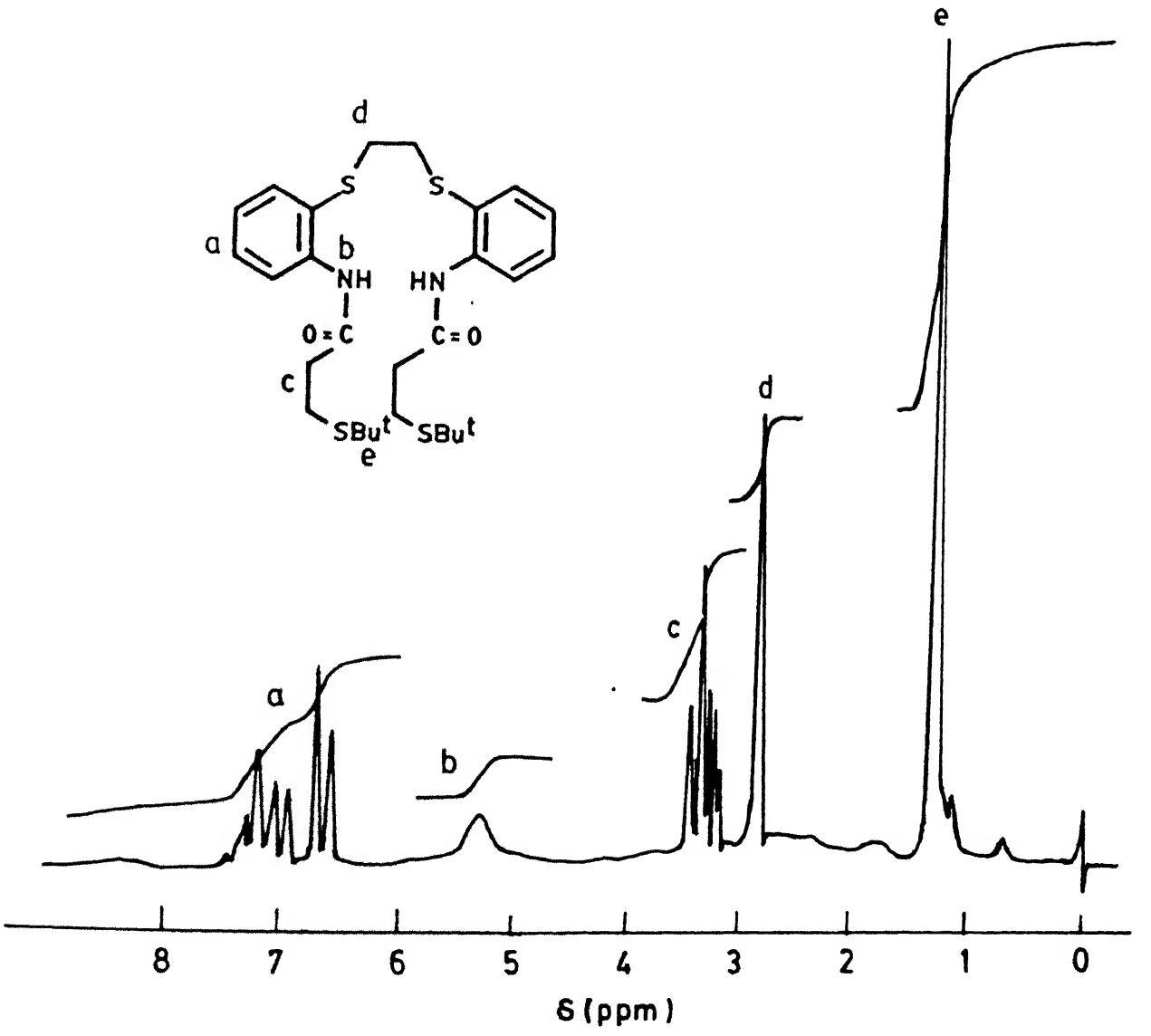

Fig 4.11 ^{1}H-NMR (80MHz) spectrum of the ligand L_6 in $CDCl_3$

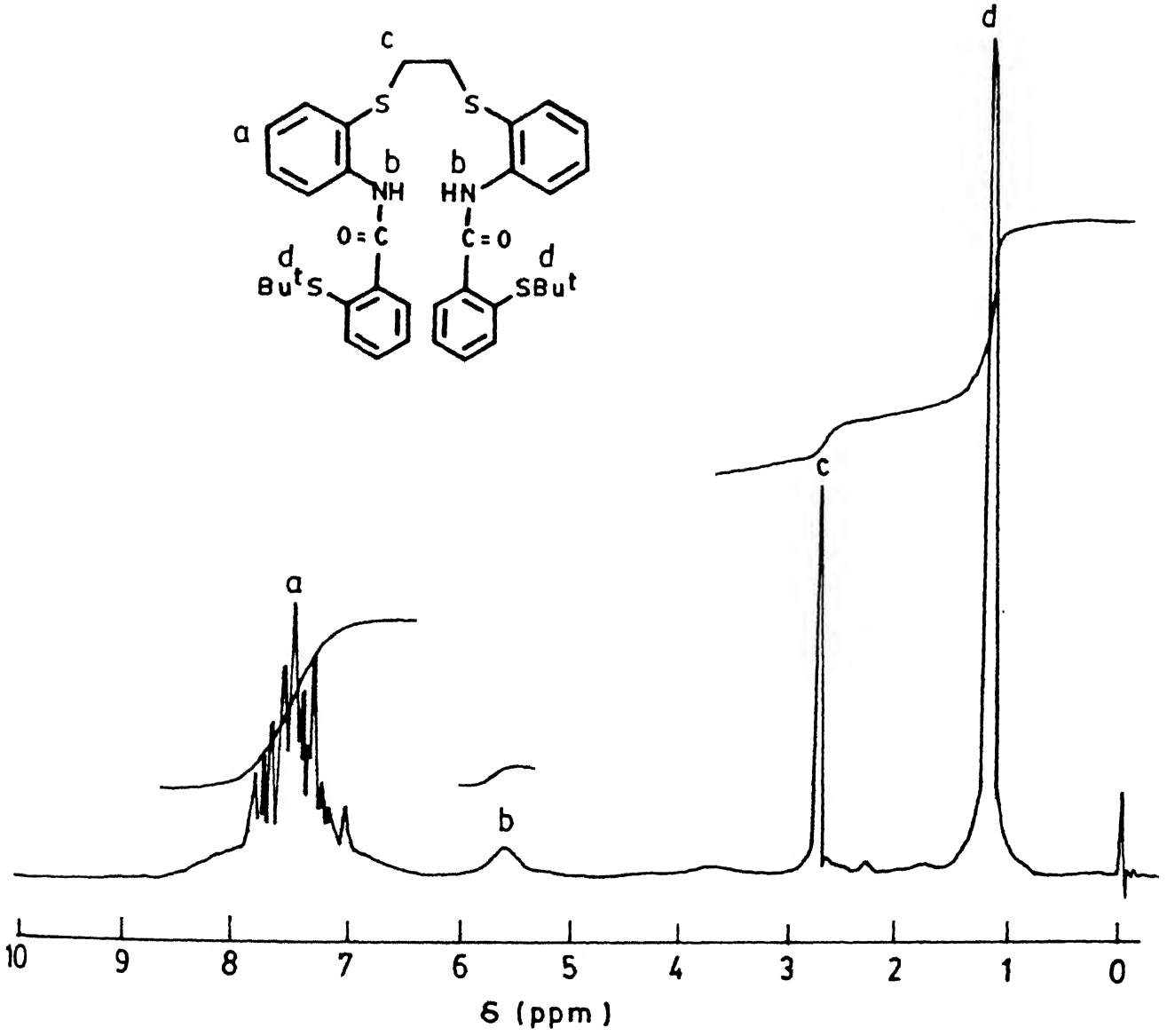

Fig 4.12 ^{1}H-NMR (80MHz) spectrum of the ligand L_7 in $CDCl_3$

4.2.14 Synthesis of the Ligand, L_8

The ligand L_8 was synthesized following the same mehtod as used for L_7 using 1,2-di(o-aminophenolthio)propane and S-tertiarybutyl thiosalicyclic acid. The product was obtained as a pale yellow semisolid in 75% yield. ^{1}H-NMR (60MHz, $CDCl_3$, δ_{TMS}ppm) : 7.3 (m, 16H) aromatic, 6.2 (s br, 2H) NH, 2.8 (t, 4H) $-SCH_2$, 1.9 (m, 2H) CH_2 1.3 (s, 18H) t-butyl (Fig. 4.13).

4.3 Syntheses of copper (II) complexes

The thiolato complexes (Figs. 4.14 and 4.15) were synthesized by breaking the S-^{t}Bu linkage utilizing Lewis acidity of Cu (II) ion as mentioned in chapter 3. Cu(II)-salts like chloride, acetate, nitrate etc. could be used. When copper perchlorate was used, the yield of the product decreased with increasing time of reflux due to oxidizing effect of the perchlorate.

4.3.1 Synthesis of the complex, 1

Ligand L_1 (2.35 g, ~3.7 mmol) was dissolved in ehthanol (30 ml) and a solution of copper (II)chloride dihydrate (0.63 g, ~3.6 mmol) in 10 ml of ethanol was added to it with constant stirring at room temperature. The color of the reaction mixture became violet immediately. This violet solution was allowed to reflux for 1 hour when the color changed to dark blue. The dark blue solution was reduced to about 10 ml by passing nitrogen gas through the solution at room temperature. Finally, on keeping at 5^oC overnight, a deep blue powdered solid separated which was

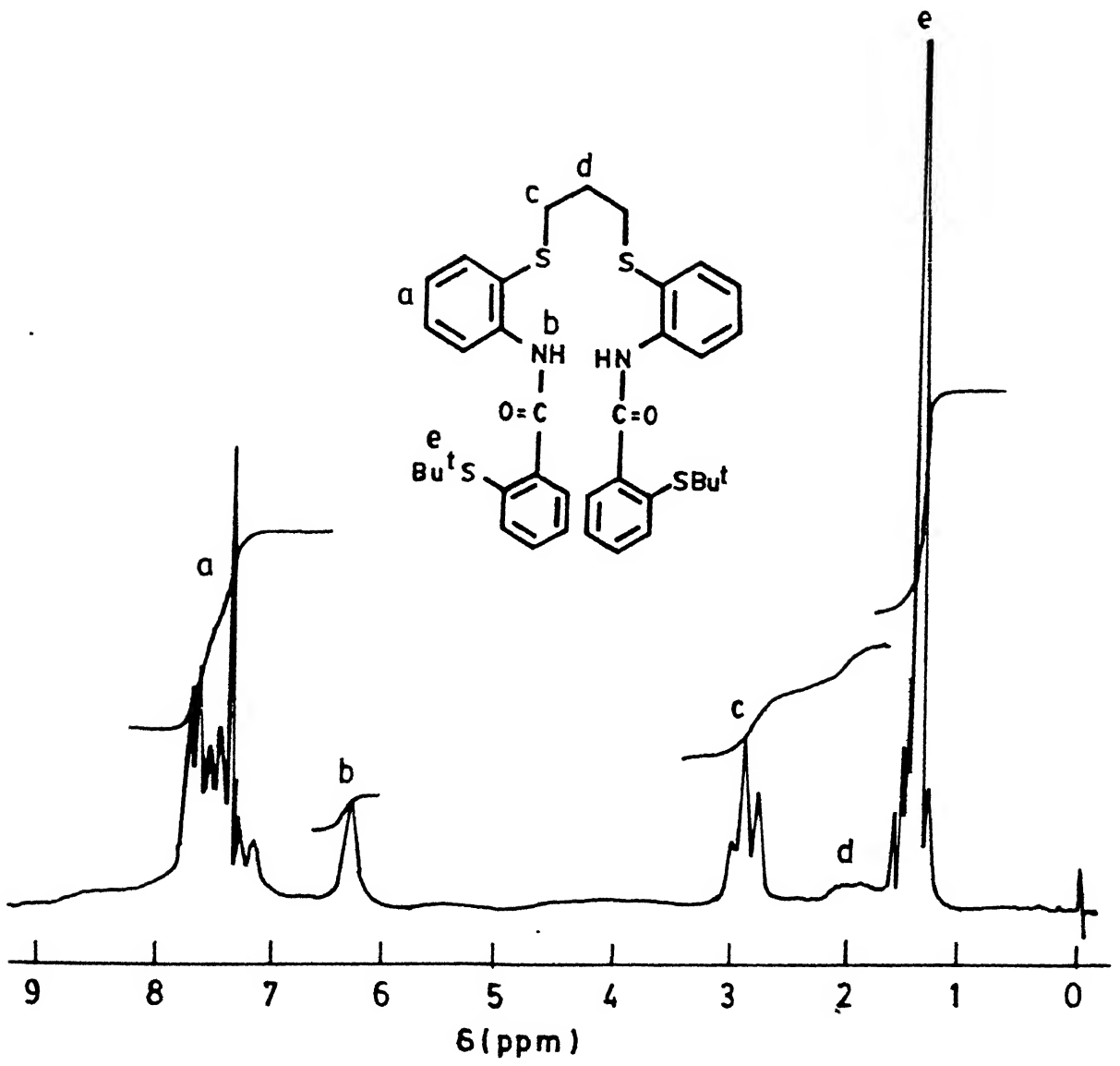

Fig 4.13 ^{1}H-NMR (80MHz) spectrum of the ligand L_8 in $CDCl_3$

collected by filtration, washed a couple of times with ether and finally dried in a stream of nitrogen. Yield ~64%.

4.3.2 Synthesis of the complex, 2

The ligand L_2 (1 g, 1.7 mmol) was dissolved in ethyl alcohol (25 ml) and treated with an ethanolic solution (25 ml) of copper (II) chloride dihydrate (0.26 g, 1.5 mmol) under argon atmosphere. Color of the reaction mixture became green. Upon refluxing for 1 hour the color of the solution became blue-violet. From this solution, a dark blue crystalline solid could be isolated following the above procedure. Yield ~55%.

4.3.3 Synthesis of the complex, 3

The ligand L_3 (1 g, 1.6 mmol) was dissolved in ethyl alcohol (25 ml) and treated with an ethanolic solution (20 ml) of copper (II) chloride dihydrate (0.26 g, 1.5 mmol) under an argon atmosphere. Upon refluxing for 1 hour color of the solution became dark blue green. From this solution a dark blue-green solid could be isolated following the procedure used for 1 in 61% yield.

4.3.4 Synthesis of the complex, 4

The ligand L_4 (1 g, 1.5 mmol) was taken in 30 ml of ethyl alcohol and added copper (II) chloride dihydrated (0.26 g, 1.5 mmol) in ethyl alcohol (15 ml) under an argon atmosphere. The color of the reaction mixture became blue violet after refluxing for 1 hour. Dark blue crystalline solid was obtained following

the procedure used for 1 in 57% yield.

4.3.5 Synthesis of the complex, 5

1,2-di(o-aminophenolthio)ethane (1 g, 3.6 mmol) was taken in methyl alcohol (40 ml) and was allowed to react with copper (II) chloride dihydrate (0.6 g, 3.5 mmol) in 40 ml of methyl alcohol. The initial green solution turned blue-violet after 20 minutes of refluxing. The desired product separated out as blue-violet crystalline solid on cooling to room temperature and it was isolated by filtration. A further crop of the product could be obtained on concentrating this solution. Yield ~80%.

4.3.6 Synthesis of the complex, 5(A)

1,2-di(o-aminophenolthio)ethane (1 g, 3 mmol) was taken in acetonitrile (5 ml) and added copper (II) perchlorate hexahydrate (1.1 g, 3 mmol) in acetonitrile (10 ml). Stirred the reaction mixture for 15 minutes while the color of the reaction mixture became violet-green. Dirty green solid precipitated out, which was collected by filtration. The solid was washed using cold acetonitrile (1ml) and air dried. Yield 75%.

4.3.7 Synthesis of the complex, 5(B)

1,2-di(o-aminoethanethio)propane (1 g, 3.4 mmol) was taken in acetonitrile (20 ml) and added copper (II) chloride dihydrate (0.58 g, 3.4 mmol) in 20 ml of acetonitrile with stirring. Color of the reaction mixture became greenish brown. The reaction mixture filtered after 30 minutes of stirring and

then allowed for slow evaporation. Dark brown solid which separated was collected by filtration, washed using cold acetonitrile (4 ml) and air-dried. Yield 85%.

4.3.8 Synthesis of the complex, 5(C)

1,2-di(o-aminoethanethio)propane (1 g, 3.4 mmol) was taken in acetonitrile (20 ml) and added copper (II) perchlorate hexahydrate (1.26 g, 3.4 mmol) in 25 ml of acetonitrile with stirring. Color of the reaction mixture became greenish violet. The reaction mixture was stirred for 30 minutes and filtered. The filtrate was kept for slow evaporation. Dark brown-violet solid that seperated was collected by filtration , washed using 5 ml of cold acetonitrile and air dried. Yield 80%.

4.3.9 Synthesis of the complex, 6

The ligand L_5 (0.5 g, 0.9 mmol) was dissolved in ethyl alcohol (30 ml) and a solution of copper (II) chloride dihydrate (0.16 g, 0.9 mmol) in ethanol (10 ml) was added to it with constant stirring at room temperature under an argon atmosphere. The resulting solution was heated to reflux for half an hour when it became deep blue. The deep blue solution was reduced to about 10 ml by constantly passing nitrogen gas through the solution at room temperature and filtered. Finally, on keeping at $5^{o}C$ overnight, a deep blue powdered solid separated which was collected by filtration and dried in a stream of nitrogen. Yield 65%.

4.3.10 Synthesis of the complex, 7

This complex was synthesized as above. The ligand L_6 (0.6 g, 1 mmol) was dissolved in ethyl alcohol (30 ml) and a solution of copper (II) chloride dihydrate (0.17 g, 1 mmol) in ethanol (10 ml) was added with constant stirring at room temperature under argon atmosphere. The color of the reaction mixture became blue after 30 minutes of reflux. From this solution a deep blue powdered solid was isolated following the above procedure. Yield 70%.

4.3.11 Synthesis of the complex, 8

Ligand L_7 (1.2 g, 1.8 mmol) was taken in ethyl alcohol (30 ml) and a solution of copper (II) chloride dihydrate (0.3 , ~1.8 mmol) in ethyl alcohol (10 ml) was added with constant stirring at room temperature under an argon atmosphere. The color of the reaction mixture became deep blue after 30 minutes of reflux. The deep blue solution was reduced to about 10 ml by passing nitrogen through the solution at RT. Finally on keeping at $5^{o}C$ for 2 hours, a dark blue powder separated which was collected by filtration, washed with diethyl ether and dried under vacuum. Yield ~60%.

4.3.12 Synthesis of the complex, 9

Ligand L_8 (1.0 g, 1.4 mmol) was taken in ethyl alcohol (20 ml) and a solution of copper (II) chloride dihydrate (0.25 gm, 1.4 mmol) in 10 ml of ethyl alcohol was added with constant stirring at room temperature under an argon atmosphere. Color of

the reaction mixture became brown after 5 minutes of reflux and finally became dark green after 20 minutes of reflux. Dark blue-green solid was collected from this reaction by using the above mentioned procedure. Yield 55%.

4.4 Syntheses of nickel (II) thiolate complexes

These complexes (Fig 4.15) were synthesized by using the same procedure as in the case of copper complexes by breaking the sulfur tertiary butyl linkage with a nickel (II) salt. [122].

4.4.1 Synthesis of the complex, 10

The ligand L_7 (1.5 g, ~2.3 mmol) was taken in isobutyl alcohol (25 ml) and added solid nickel(II) acetate tetrahydrate (0.56 g, ~2.3 mmol) under an argon atmosphere. Color of the reaction mixture became dark-brown after three hours of reflux. The solution was allowed to cool to room temperature and filtered. Isobutyl alcohol was evaporated partly under reduced pressure to make the volume to about 5 ml and then it was kept at $5^{o}C$ overnight. Orange solid that appeared was collected by filtration and washed the solid using petroleum ether ($60-80^{o}C$). The solid was dried under vacuum. Yield 31% .

4.4.2 Synthesis of the complex, 11

The ligand L_8 (1.5 g, 2.2 mmol) in isobutyl alcohol (25 ml) was allowed to react with nickel(II) acetate tetrahydrate (0.55 g, 2.2 mmol) under an argon atmosphere. Color of the reaction mixture became reddish-brown after three hours of reflux. Orange solid could be isolated from this solution by following the

above mentioned procedure. Yield ~ 34%.

4.5 Results and Discussion

All the ligands form 1:1 complexes with copper as can be inferred from the analytical data (Table 4.1). The qualitative test for the chloride ion is negative in all cases except in 5 and 5B when copper(II) chloride is used for complex formation with the ligands indicating complete cleavage of S-tertiarybutyl linkage and subsequent replacement of the chloride ions by thiolates. All the complexes except 5(A) and 5(C) behave as non electrolytes (Table 4.2) in dichloromethane, acetonitrile, dimethylformamide or in ethyl alcohol. Complexes 5(A) and 5(C) behave as 1:2 electrolytes in ethanol or in acetonitrile.

The Cu(II)-thiolates are air-stable in the solid state. In solution in an argon atmosphere, they are stable for days. However, on exposure to air they are only stable for a few hours, after which they begin to decompose slowly. Rest of the complexes are stable in the solid state as well as in solutions.

4.5.1 Infrared Spectra

Selected infrared spectral data are collected in Table. 4.2. For 1 and 3, the C=N stretching frequency is red-shifted by 30 cm^{-1} upon complexation signifying coordination through imine nitrogens. In case of hexacoordinated amides, the C=O and NH stretching frequencies appear around 1640 and 3330 cm^{-1} (except 5, which appears at around 1610 cm^{-1}) indicating the amides are not

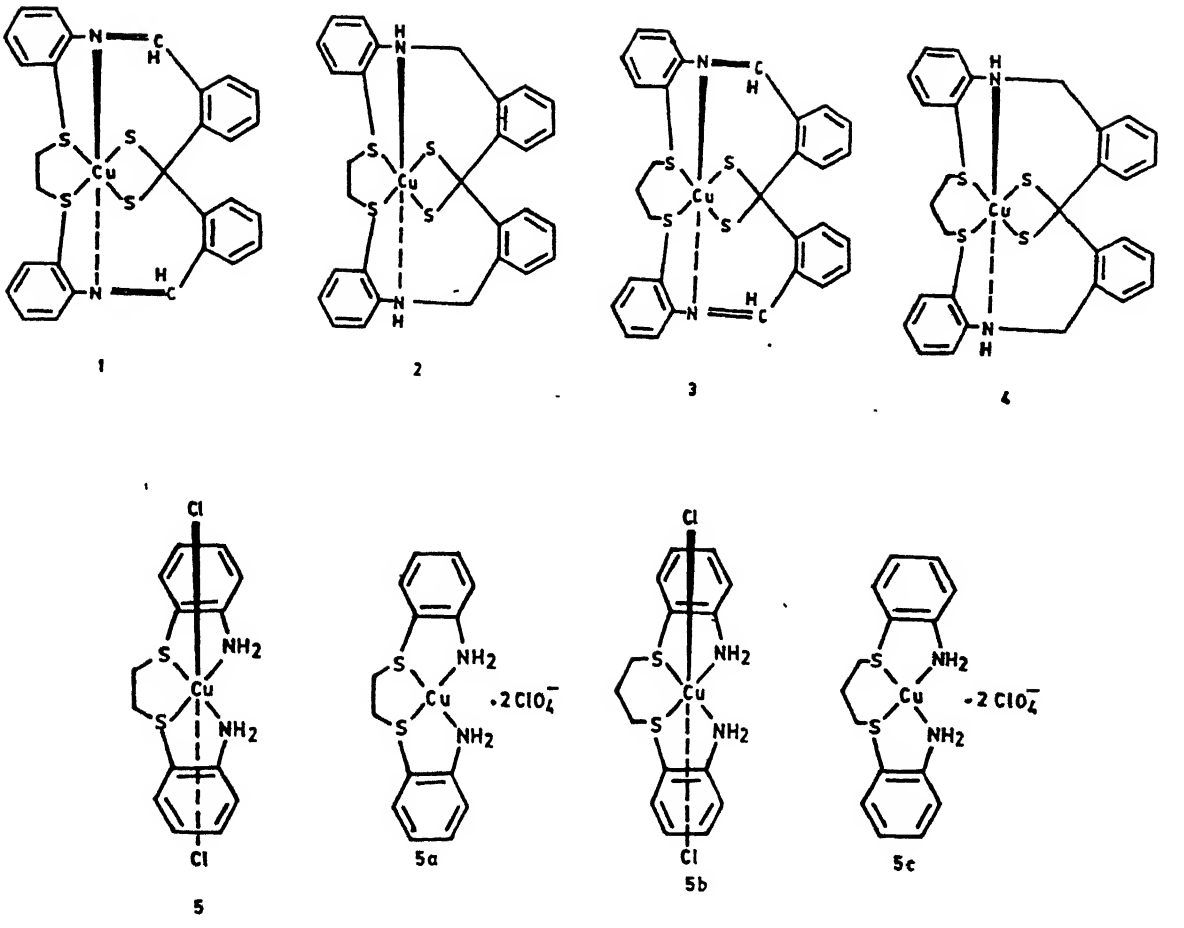

Fig 4.14 Complexes 1 to 5C

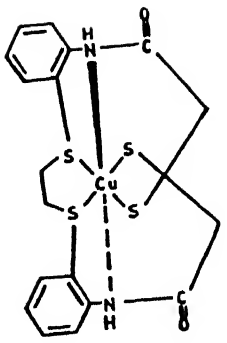

6

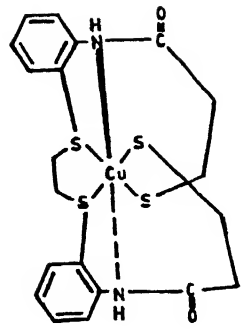

7

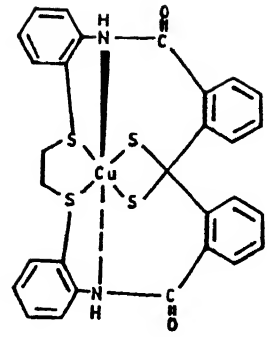

8

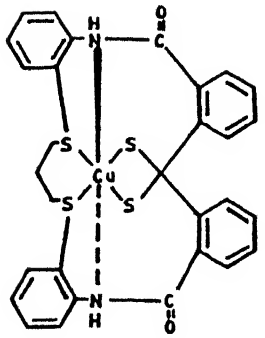

9

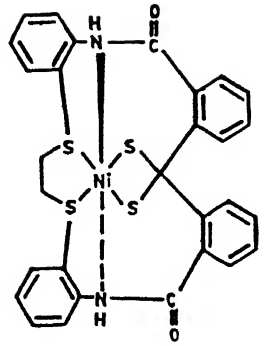

10

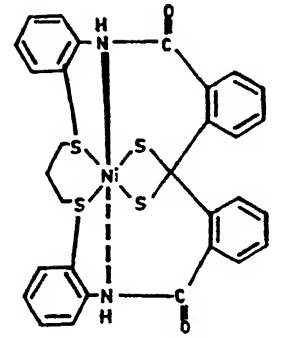

11

Fig 4.15 Complexes 6 to 11

Table 4.1

Microanalytical Data for the Copper (II) and Nickel(II) Complexes

Complex	Empirical Formula	Anal% Calcd				Found			
		C	H	N	S	C	H	N	S
1.	$C_{28}H_{22}N_2S_4Cu$	58.16	3.83	4.84	22.18	57.54	3.90	4.81	21.78
2.	$C_{28}H_{26}N_2S_4Cu$	57.75	4.50	4.81	22.02	57.18	4.36	4.62	21.73
3.	$C_{29}H_{24}N_2S_4Cu$	58.76	4.14	4.61	21.04	58.61	4.08	4.73	21.65
4.	$C_{29}H_{28}N_2S_4Cu$	58.19	4.27	4.60	21.13	58.41	4.41	4.71	21.58
5	$C_{14}H_{16}N_2S_2Cl_2Cu$	40.93	3.92	6.82	15.61	42.01	3.57	6.97	16.10
5(A)	$C_{14}H_{16}N_2S_2Cl_2O_8Cu$	31.20	2.97	5.19	11.88	30.90	3.05	5.32	11.91
5(B)	$C_{15}H_{18}N_2S_2Cl_2Cu$	42.40	4.24	6.95	15.07	41.98	4.31	5.95	15.40
5(C)	$C_{15}H_{18}N_2S_2Cl_2O_8Cu$	32.57	3.26	5.07	11.58	31.55	3.30	5.17	11.25
6	$C_{18}H_{18}N_2S_4O_2Cu$	44.48	3.71	5.76	26.36	44.81	3.43	5.79	26.60
7	$C_{19}H_{20}N_2S_4O_2Cu$	46.73	4.28	5.45	24.92	46.21	4.42	5.09	25.12
8	$C_{28}H_{22}N_2S_4O_2Cu$	55.12	3.61	4.59	20.99	54.20	3.81	4.29	21.22
9	$C_{29}H_{24}N_2S_4O_2Cu$	55.81	3.85	4.49	20.53	55.61	3.70	4.61	20.05
10	$C_{28}H_{22}N_2S_4O_2Ni$	55.56	3.64	4.63	21.17	55.31	3.42	4.30	21.22
11	$C_{29}H_{24}N_2S_4O_2Ni$	56.25	3.88	4.52	20.68	56.01	4.02	4.14	20.79

Table 4.2

Selective Infrared Bands, Yeild, Color and Conductivity Data for the Copper(II) & Nickel(II) Complexes

Complex	Infrared Bands (cm^{-1})	Yield %	Color	Conductance ($ohm^{-1}cm^{2}mol^{-1}$)
1	1615,s($\nu_{C=N}$)	64	Deep blue	10[a]
2	3320,s,br(ν_{NH})	55	Dark blue	9[a]
3	1620,s($\nu_{C=N}$)	61	Blue green	11[a]
4	3330,s,br(ν_{NH})	57	Dark blue	20[a]
5	3450,s,br(ν_{NH})	80	Blue violet	17[a]
5(a)	3441,s,br(ν_{NH}) ~1100,s,br(ν_{Cl-O})	75	Dirty green	249[a]
5(b)	3430,s,br(ν_{NH})	85	Dark brown	15[a]
5(c)	3435,s,br(ν_{NH}) ~1100,s,br(ν_{Cl-O})	80	Dark brown violet	265[a]
6.	1608,s($\nu_{C=O}$) 3157,s,br(ν_{NH})	65	Blue	5[a]
7.	1680,s($\nu_{C=O}$) 3162,s,br(ν_{NH})	70	Deep blue	6[a]
8.	1650,s($\nu_{C=O}$) 3110,s,br(ν_{NH})	60	Dark blue	2.3[b]
9.	1645,s($\nu_{C=O}$) 3142,s,br(ν_{NH})	55	Dark blue green	1.1[b]
10	1670,s($\nu_{C=O}$) 3340,s,br(ν_{NH})	45	Orange	1.2[b]
11	1660,s($\nu_{C=O}$) 3310,s,br(ν_{NH})	46	Orange	1.4[b]

a = acetonitrile; b = dimethyl formamide

deprotonated [123]. For the perchlorate salts of the complexes, 5(A) and 5(C), the IR spectra show a strong and broad absorption at 1100 cm^{-1} attributable to the presence of uncoordianted perchlorate anions [97].

4.5.2 Absorption Spectra

For the Cu(II)- and Ni(II)-thiolates, the electronic absorption band positions are found to be practically independent of the solvent used. Absorption bands (Figs. 4.16 to 4.25) obtained on acetonitrile/dimethylformamide solutions are listed in (Table 4.4). A prominent feature in the electronic spectra of all hexacoordinated Cu(II)-thiolates is the occurrence of an intense band centered around 600 nm due to which they look dark blue in color. A hexa-coordinated copper (II) ion is subject to Jahn-Teller distortion whereby the e_g set splits. The extent of distortion may be expressed in terms of tetragonality T defined as [87]

$$T = \frac{0.5\ (R_x + R_y)}{R_z} \qquad (1)$$

where R is the bond length along the axis denoted by the subscript. In general, greater the tetragonality greater will be the separation of d_z^2 and $d_{x^2-y^2}$. Depending upon the extent of distortion, several ligand field transitions may be expected [87] corresponding to transition from components of t_{2g} to $d_{x^2-y^2}$ in addition to the one from $d_{z^2} \rightarrow d_{x^2-y^2}$. For moderate tetragonal distortions, the lowest energy absorption can be identified with

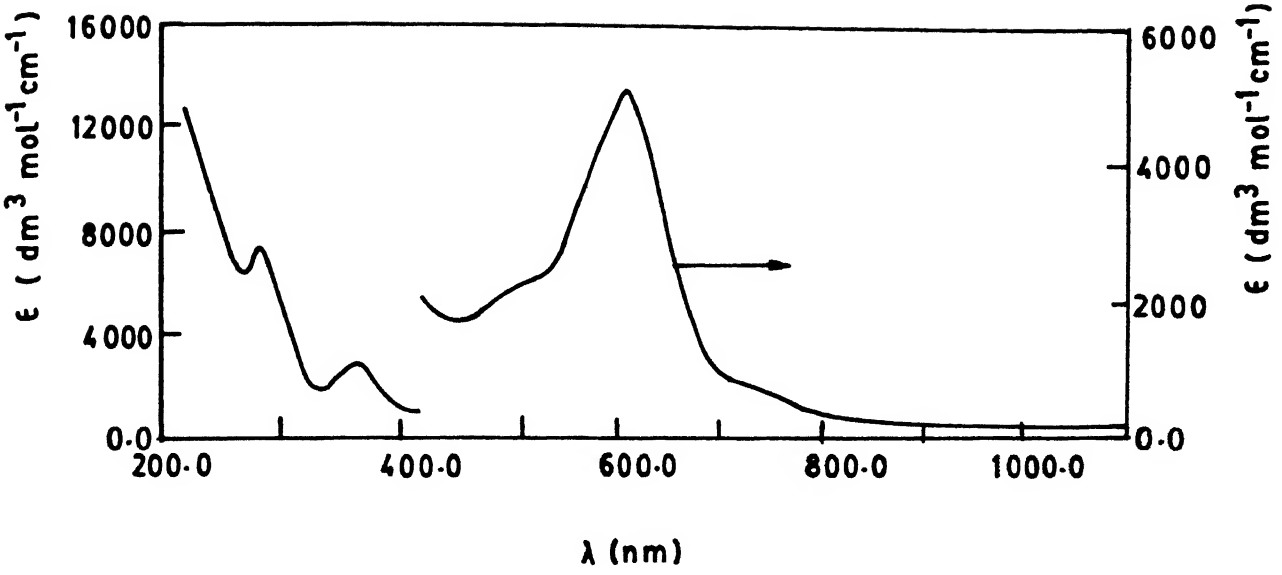

Fig 4.16 Electronic spectrum for the complex 1 in CH_3CN

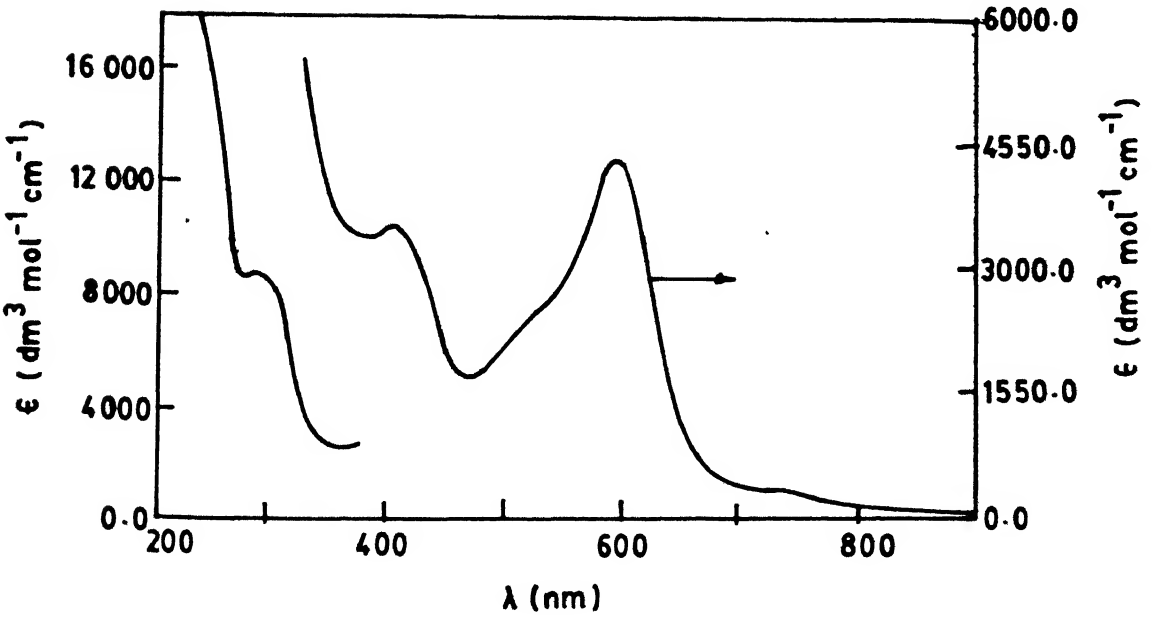

Fig 4.17 Electronic spectrum for the complex 2 in CH_3CN

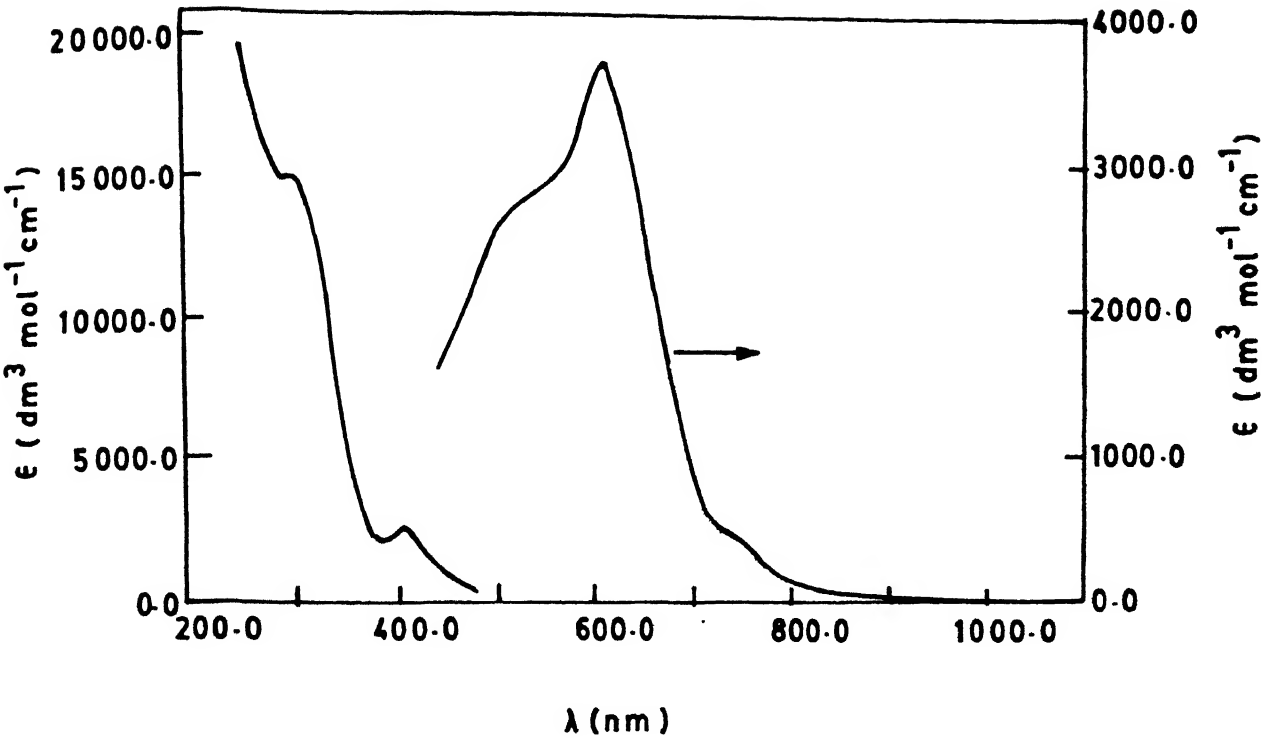

Fig 4.18 Electronic spectrum for the complex 3 in CH_3CN

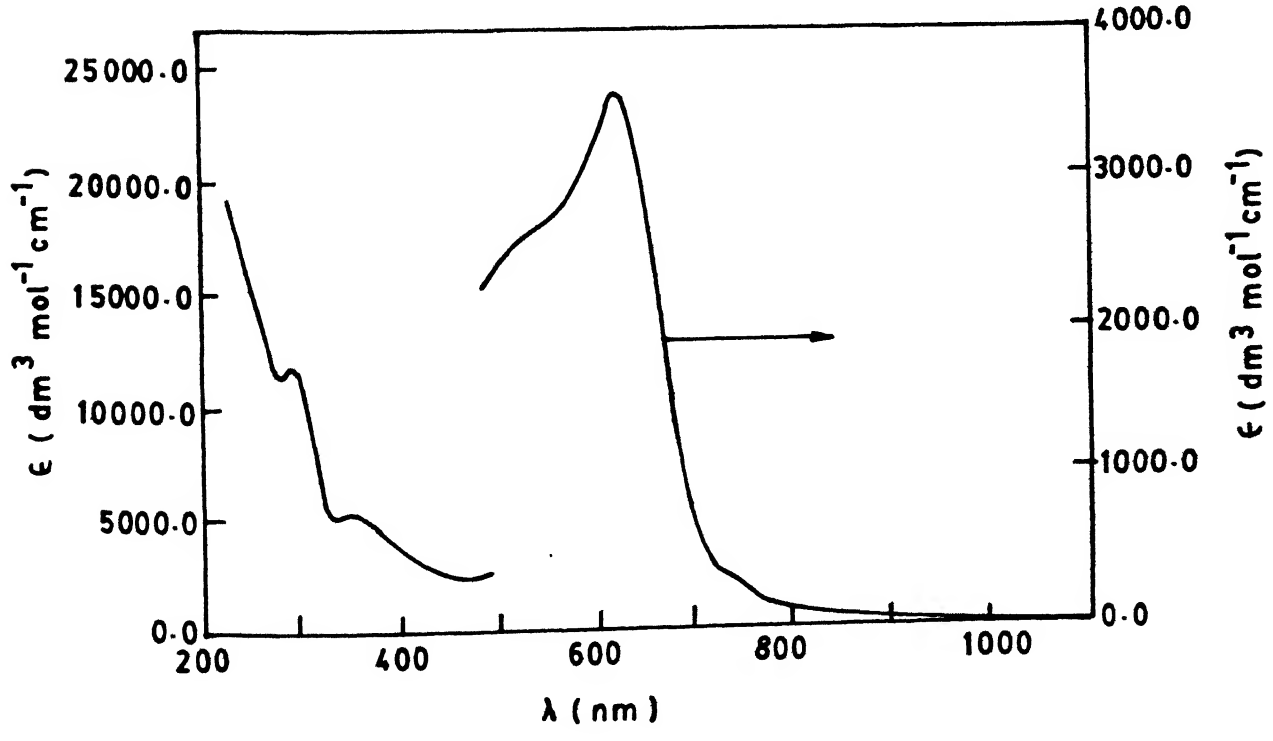

Fig 4.19 Electronic spectrum for the complex 4 in CH_3CN

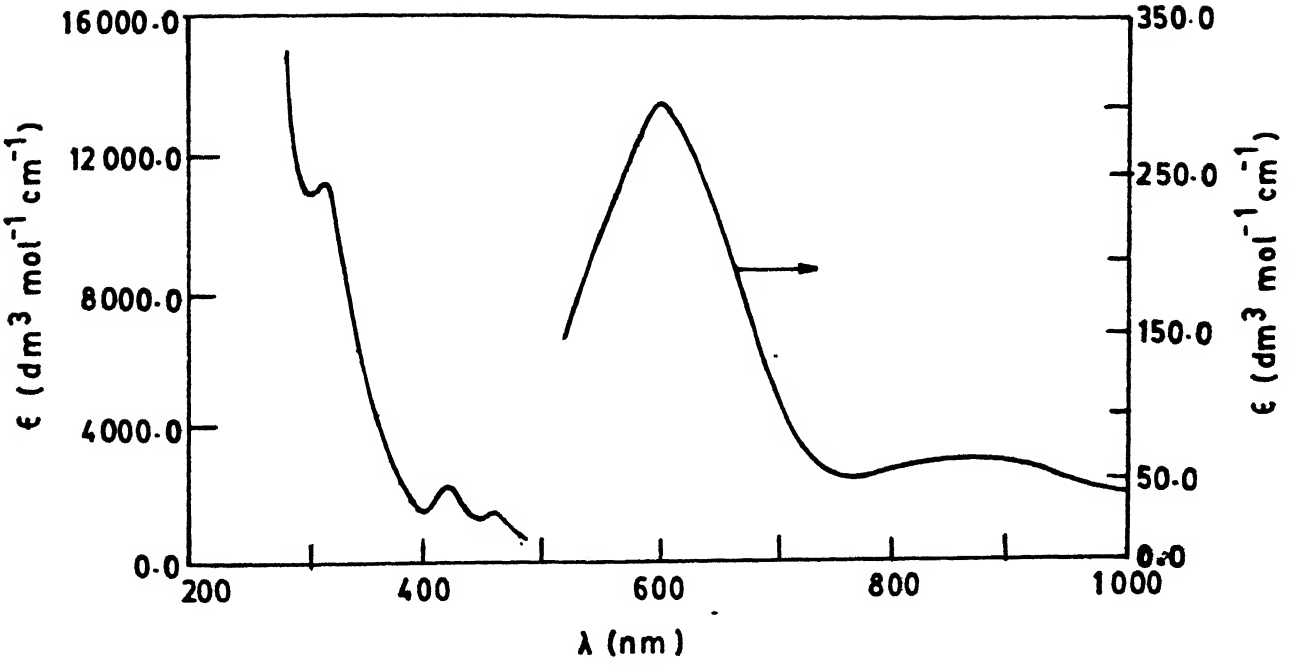

Fig 4.20 Electronic spectrum for the complex 5 in CH_3CN

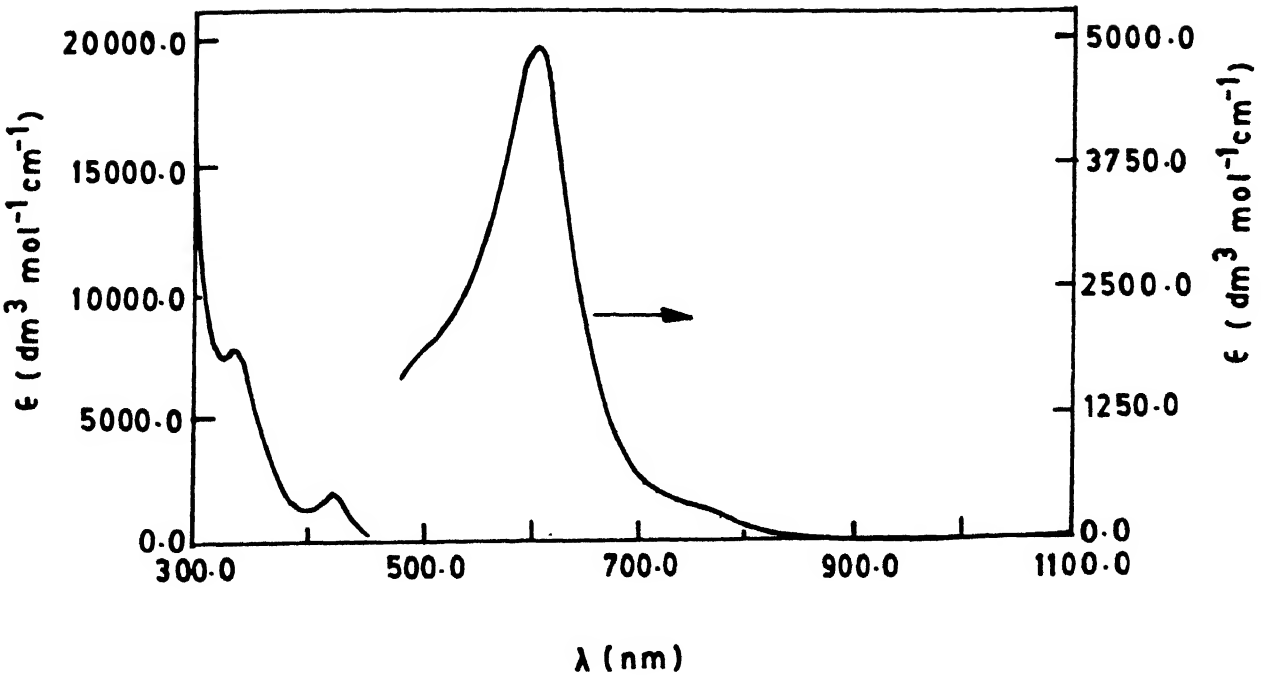

Fig 4.21 Electronic spectrum for the complex 6 in CH_3CN

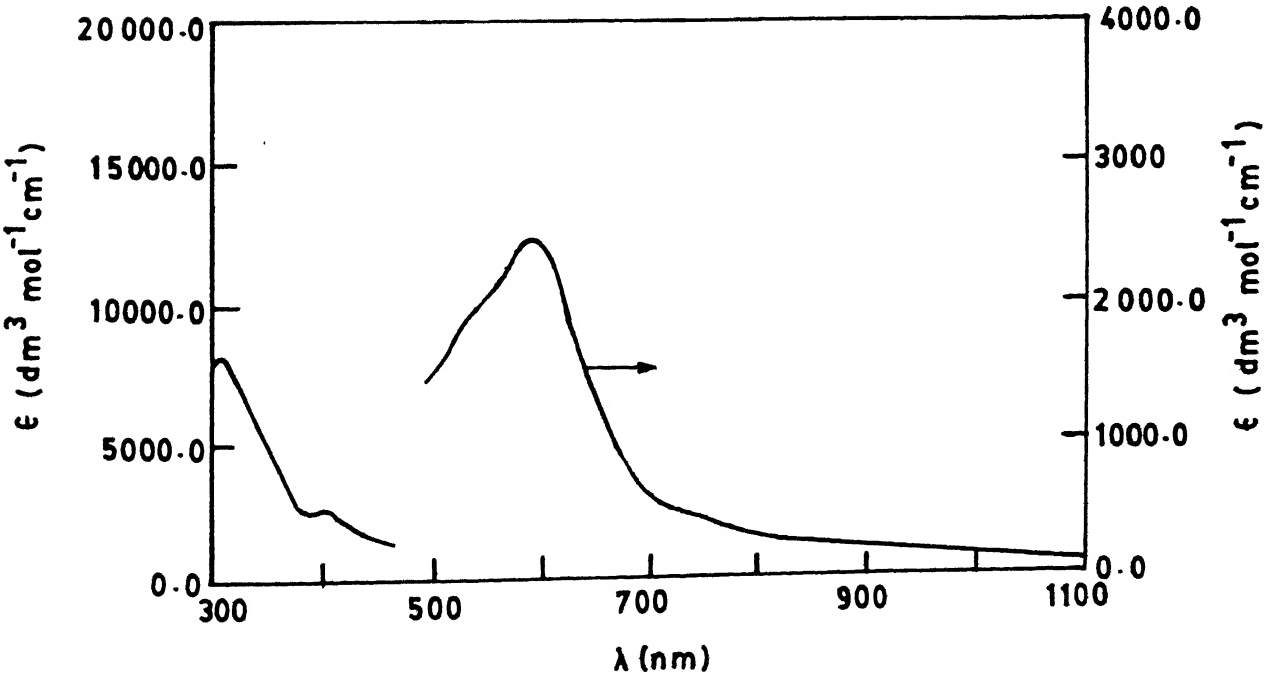

Fig 4.22 Electronic spectrum for the complex 7 in CH_3CN

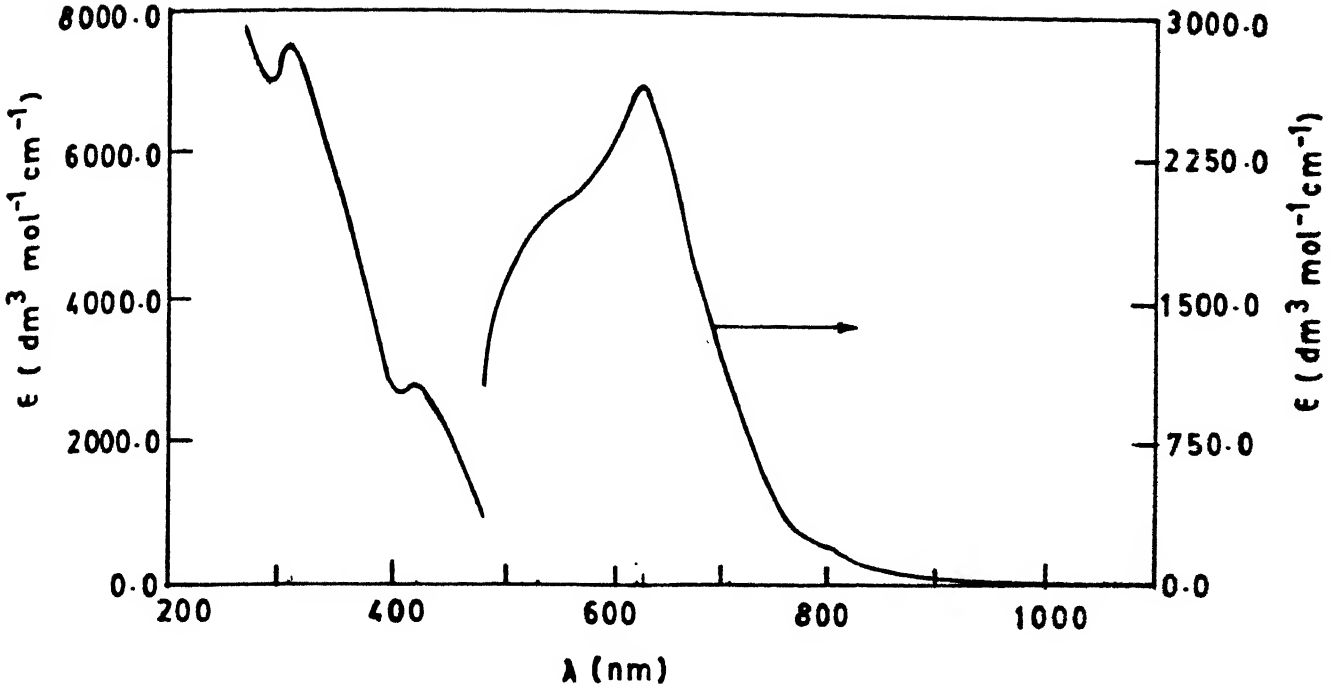

Fig 4.23 Electronic spectrum for the complex 8 in DMF

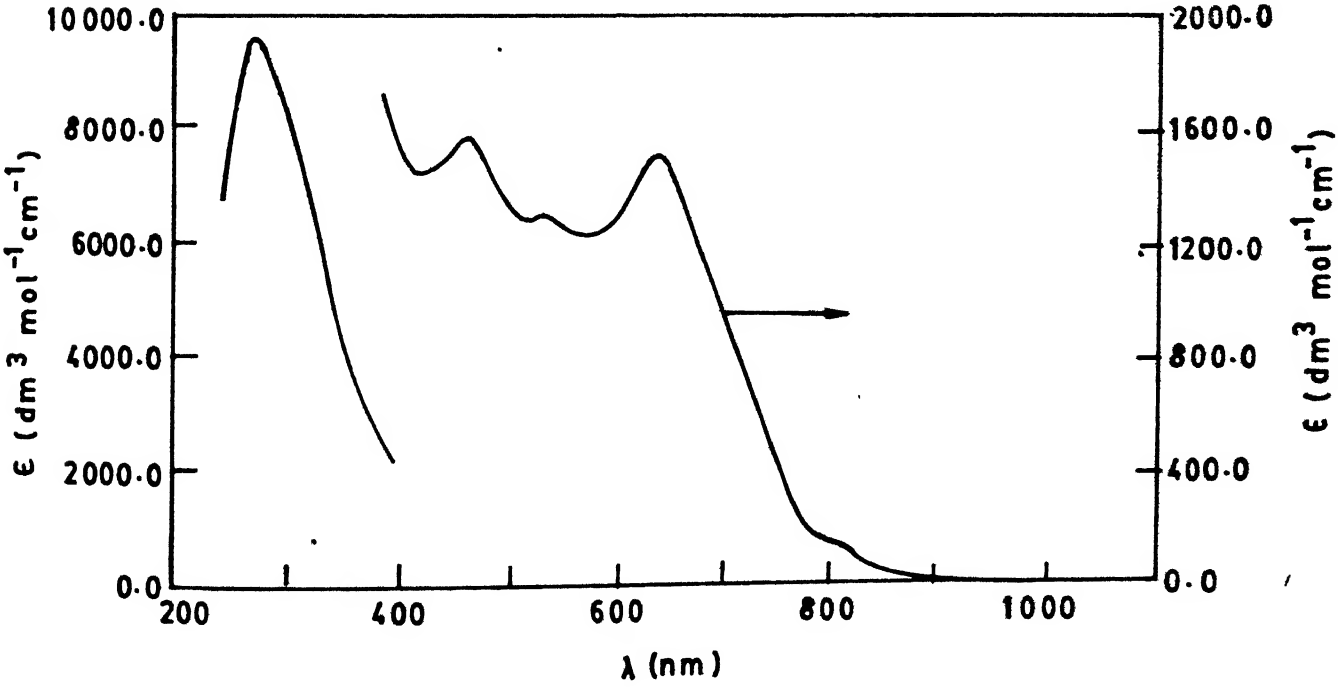

Fig 4.24 Electronic spectrum for the complex 9 in DMF

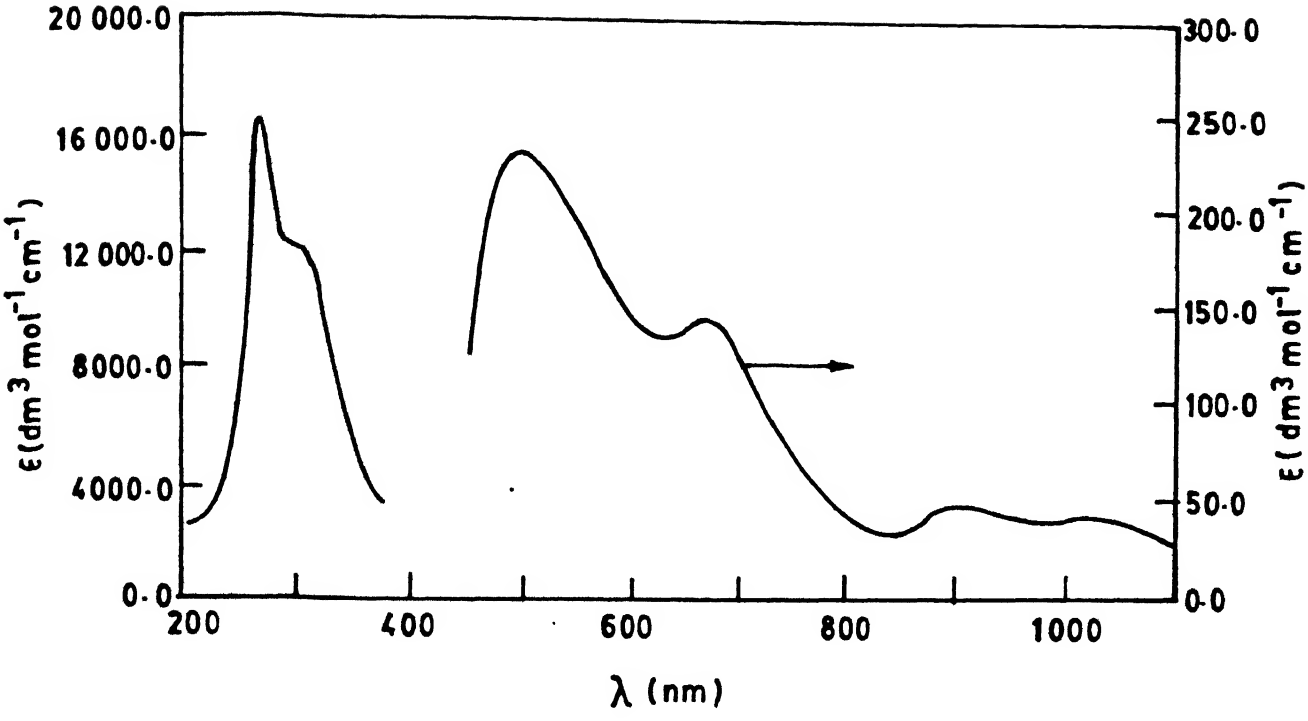

Fig 4.25 Electronic spectrum for the complex 10 in DMF

d_z2, $d_x2_{-y}2$ transition while an usually broad band at higher energy will contain $d_{xy} \rightarrow d_x2_{-y}2$ and d_{xz}, $d_{yz} \rightarrow d_x2_{-y}2$ transitions. With increasing tetragonal distortion all the ligand field bands will be blue-shifted. Compounds 5 and 5(B) show a weak band centered around 890 nm attributable to $d_z2 \rightarrow d_x2_{-y}2$ and for the Cu(II)-thiolates this band is blue shifted and appear as a shoulder between 730-750 nm. This reflects higher ligand field strength in these cases. Complexes 5 and 5(B) exhibit a broad band at about 600 nm with low intensity which is attributed to the transitions involving components of t_{2g} to the d-vacancy $d_x2_{-y}2$. All other complexes have absorption maxima near 600 nm with high extinction coefficients. Very high intensity of the band cannot be solely due to ligand field transitions. Charge transfer transitions should contribute significantly to this. Electronic spectral studies [124] on a number of structurally characterized tetragonal complexes with $CuS^*_2N_2X_2$(x = O, Cl and S^* = thioether) and CuN_4S_2 chromophores [125] have been reported where σ(N) $\longrightarrow$ Cu(II) Ligand to metal charge transfer transition (LMCT) occurs around 280 nm while σthioether $\longrightarrow$ Cu(II) transition could be located in the range 340-450 nm. Comparing electronic spectra of the Cu(II)-thiolates with 5 and 5(B) it can be concluded that the intense band around 600 nm should have significant contribution from σ thiolate $\rightarrow$ Cu(II) LMCT transition. High intensity of the band is made possible by good overlap of equatorially bound thiolate with the $3d_x2_{-y}2$ orbital of copper(II). The shoulder that appears between 500-540 nm should then be the higher energy π-thiolate $\longrightarrow$ copper (II) LMCT absorption [9]. The lower energy π-symmetry thiolate $\longrightarrow$Cu(II) LMCT transition may be mixed with the

shoulder at 730-750 nm. The low energy for σthiolate $\rightarrow$ copper (II) LMCT transition for tetragonal coordination geometry is quite remarkable. Oxo-analogue of the Schiff base ligand L_1 is known to coordinate in an octahedral manner. It has been pointed out that the least strained mode of coordination for complexes of the oxo-ligand is the one similar to A shown in Fig. 4.2. Examination of molecular models for the Cu(II)-and Ni(II)-thiolates show that least strained mode of binding in each case will be the one as illustrated in A. Electronic absorption bands observed for the hexacoordinated Ni(II) complexes are also listed in Table 4.4. Octahedral Ni(II) complexes show [126] three spin-allowed ligand field transitions corresponding to excitation from the $^3A_{2g}$ ground state to $^3T_{2g}$, $^3T_{1g}$and $^3T_{1g}$ (P) states. For an ideal octahedral coordination, the intensities of these d-d bands lie below 30 $M^{-1}cm^{-1}$. As the geometry distorts from the ideal centrosymmetric one, the intensities of these bands increase and may result in splitting of some of the bands [126]. The intensities of the ligand field bands observed are consistent with their structures, which are only slightly distorted from octahedral. For both the Ni(II)-complexes, solvent had no effect in the appearance of their electronic spectral bands. This means the ligands encapsulate the metal ion having no vacant site for possible solvent interactions. For a clear knowledge about the coordinating atom orientation in each case, single crystal x-ray structure is needed. Unfortunately, all efforts to grow single crystals of any of these complexes remain unachievable.

4.5.3 Magnetic Susceptibility and EPR Studies

Room temperature magnetic moment values (Table 4.3) for the Cu(II)-complexes after diamagnetic corrections are typical of discrete mononuclear Cu(II)-complexes [99]. The two Ni(II)-complexes show magnetic moment values (Table 4.3) which lie within normal ranges for octahedral Ni(II)-complexes [127]. In the solid state, each copper complex shows a broad EPR signal near g = 2 typical of magnetically concentrated systems and not indicative of their solid state structures. In acetonitrile solution at RT non-amide complexes exhibits a four-line spectrum which is again typical of Cu(II) solution species. Representative solid state spectrum at RT of complex 2 is in Fig. 4.27. The non-amide hexacoordinated complexes, in acetonitrile glass at liquid nitrogen temperature, show axial EPR specta. The shape of the spectra can be explained on the basis of tetragonally distorted octrahedral symmetry around Cu(II) ion. As a representative, the EPR spectrum of complex 1 in acetonitrile glass is reproduced in Fig. 4.26 which shows $g_{\parallel} > g_{\perp}$ corresponding to the $d_{x^2-y^2}$ ground state. The hyperfine coupling in the parallel region of the spectrum (Table 4.3) is somewhat smaller compared to typical tetragonal copper(II) complexes [9]. This could be due to strong equatorial coordination of two thioethers and two thiolates. A strongly bound sulfur to a Cu(II)-ion can delocalize [128] the single d-electron on to sulfur p_{π} orbitals as suggested [44] in case of the blue protein, plastocyanin. Other complexes show similar EPR results in liquid nitrogen temperatures (Table 4.3).

Table 4.3

Magnetic Moment (R T) and EPR Spectral Data (80 K) for the Copper(II) and Nickel(II) Complexes

Complex	μ_{eff}/μ_B	$g_{\parallel}$	$g_{\perp}$	$A_{\parallel}$	g_{aV}
1.	2.13	2.42	2.09	101	
2.	2.16	2.38	2.07	105	
3.	2.04	2.19	2.06	109	
4.	2.12	2.18	2.04	105	
5.	2.10	2.31	2.03	115	
6.	2.01				2.14
7.	2.07				2.18
8.	1.93				2.12
9.	1.98				2.07
10.	3.10				
11.	3.06				

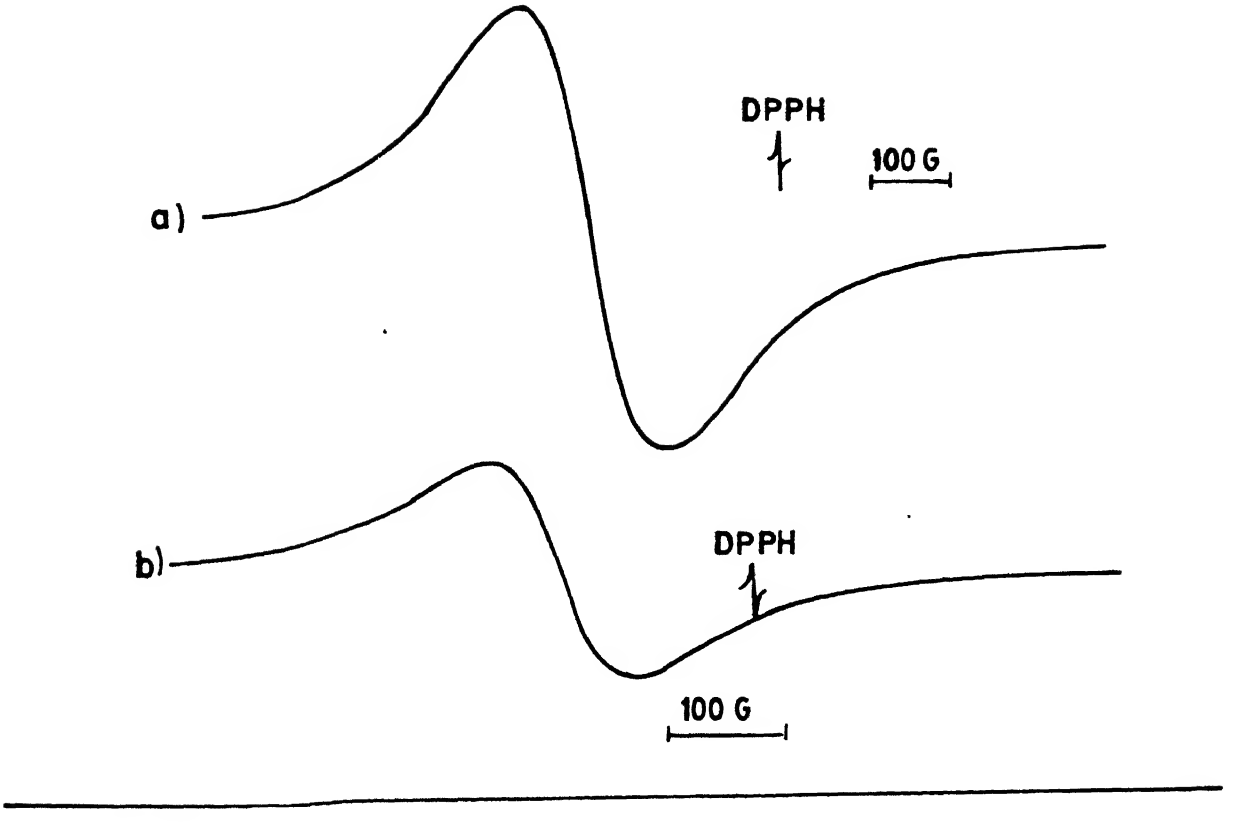

Fig 4.28 EPR spectrum of complex 6 in solid state (a) and in acetonitrile glass (b) at boiling liquid nitrogen temperature

EPR studies in acetonitrile glasses as well as in RT for the amide containing Cu(II)-complexes reveal only a broad signal near g = 2 with $g_{av} > g_e$. The spectral shape does not change upon change of solvent or temperature. Representative EPR spectra of complex 6 at L.N.T is shown in Fig.(4.28).

4.5.4 Electrochemistry

Cyclic voltammograms for the complexes are shown in Figs. 4.29-4.31, 4.33. while the redox data are collected in Table 4.4. For convenience, cyclic voltammetric studies for the non-amide and amide complexes are discussed separately.

All the non-amide complexes show (Fig. 4.29)well-defined cyclic responses although with different $E_{1/2}$ values which were found to be independent of sweep rate. The i_{pa}/i_{pc} ratio is found to be about 1.1 in each case which is also independent of sweep rate. The raio, $i_{p_c}/v^{1/2}$ is practically constant and the peak separation, ΔE_p increases slowly with increase in scan rate.

The peaks are assignable to the redox reactions

$$1^+ + e^- = 1 \qquad \text{(i)}$$

$$2^+ + e^- = 2 \qquad \text{(ii)}$$

$$3^+ + e^- = 3 \qquad \text{(iii)}$$

$$4^+ + e^- = 4 \qquad \text{(iv)}$$

$$5^+ + e^- = 5 \qquad \text{(v)}$$

For each complex, on scanning further in the positive side no peak can be observed either in the forward or in the reverse scan.

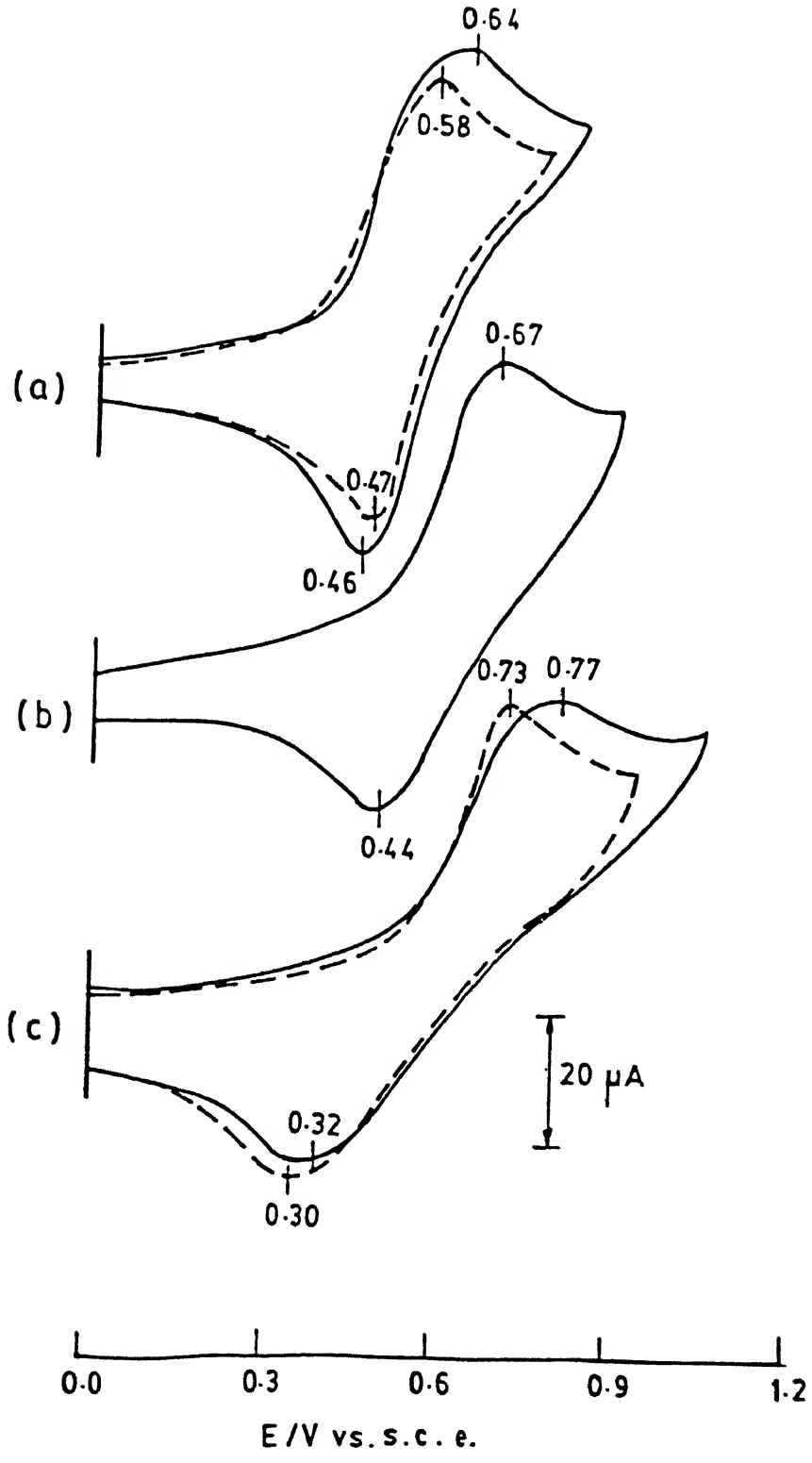

Fig 4.29 Cyclic voltammograms for the complexes : (a) broken line for 1, solid line for 2; (b) for 5 and (c) broken line for 3, solid line for 4 in CH_3CN (Ca 1 x 10^{-3}) at the scan rate of 100 mVs^{-1} using glassy carbon working electrode

Table 4.4

Electronic Spectral and Electrochemical Redox Potential Data for the Copper(II) and Nickel(II) Complexes

Complex	$\lambda_{max/nm}(\epsilon_{max}/dm^3mol^{-1}cm^{-1})$	E_{Pc} (V)	E_{Pa} (V)	$E_{1/2}$ (V)	ΔE_P (mV)
1.	750(sh), 615(4900), 500(sh), 365(3400), 290(7900)	0.47	0.58	0.53	110
2.	735(sh), 595(4450), 540(sh), 395(4060), 300(8400)	0.46	0.64	0.55	180
3.	755(sh), 610(3690), 540(sh), 405(2740), 300(15000)	0.30	0.73	0.51	430
4.	730(sh), 615(3540), 535(sh), 360(5360), 290(12240)	0.32	0.77	0.55	450
5.	890(65), 600(300), 460(1500), 420(2500), 305(11300)	0.44	0.67	0.56	230
5(a)	564(1914), 413(1971), 305(4285)	irreversible			
5(b)	747(305), 615(460), 510(603) 395(873), 309(7680)	irreversible			
5(c)	620(441), 420(1279), 304(15,269)	irreversible			
6.	770(sh), 615(4900), 510(sh), 415(1890), 330(7900)	0.47	0.53	0.50	60
6^+.	600(5800), 560(sh), 420(2740) 300(15,000)	0.53	0.47	0.50	60
7.	760(sh), 595(2450), 540(sh), 395(3060), 305(8400)	0.46	0.62	0.54	160
8.	800(sh), 620(2625), 525(sh), 420(2800), 305(7515)	0.48	0.58	0.53	100
9.	805(sh), 625(1520), 525(1315), 465(1575), 280(9615)	0.42	0.54	0.48	120
10.	1035(40), 895(45), 670(145), 495(230), 295(1800), 270(16980)	no cyclic response			
11.	1030(15), 875(15), 660(60), 490(240), 300(9900), 270(13260)	no cyclic response			

sh = shoulder; Solvent used was Acetonirile except for complexes 8, 9, 10 and 11 for which the solvent was DMF. Standard electrode is the saturated calomel electrode (SCE)

When the voltage scan in the negative side is probed only broad cathodic peak appear but on scan reversal no corresponding anodic peak can be observed. This signifies that the reduced products are unstable in the CV time-scale. However, a sharp anodic peak appears near -0.2 V attributable to the oxidation of metallic copper deposited at the electrode surface. Similar observations have been made by other workers [118].

The oxidation and reduction waves are assignable to copper centers. If it were a case of ligand oxidation, then the aromatic amine or the aromatic imine would have been the redox active centers [129]. In that case, increasing the carbon chain between the two thioethers would not have any effect on the shape of cyclic voltammograms. Complex 5A shows only an irreversible response in the region -1.0 to +1.0 V which rules out the possibility of thioether oxidation. Thiol oxidation is ruled out as it will not give a cyclic response due to the formation of disulfide bond. An exhaustive constant potential coulometry performed on complex 1 at room temperature at 0.75 V gives n = 1.1 e^-. However, the oxidised product is quite unstable at room temperature to record its electronic spectrum. When quickly frozen in an EPR tube under anerobic condition, it gives no EPR signal. To get the oxidized species, easy removal of the unpaired electron of Cu(II) is needed. We conclude that strongly bound four sulfurs at the equatorial plane raise the singly occupied $3d_{x^2-y^2}$ orbital so that removal of this electron becomes easier. The increase in ΔE_p values on increasing the chelate size is due to the fact that oxidised metal-ligand ensemble do no longer hold

strongly. All four amide-complexes give well defined cyclic responses with $E_{1/2}$ values near 0.5 V. In case of complex 6 (Fig. 4.30), the response is reversible (ΔE_p = 60 mV) with $E_{1/2}$ = 0.50 V vs SCE and is found to be independent of scan rates employed (50, 100, 150 and 200 mV sec^{-1}). In case of each of the other three Cu(II)-complexes, the response is only quasi-reversible. The following common characteristics were observed : the ratio, i_{P_a}/i_{P_c} = 1.0 within experimental error for different scan rates, the ratio $i_{P_c}/v^{1/2}$ practically constant, and the peak separation, ΔE_p increases slowly (except for 6) with increase in scan rate. The peaks are assignable to the redox reactions.

$$6^+ + e^- = 6 \qquad \text{(vi)}$$

$$7^+ + e^- = 7 \qquad \text{(vii)}$$

$$8^+ + e^- = 8 \qquad \text{(viii)}$$

$$9^+ + e^- = 9 \qquad \text{(ix)}$$

For complex 6, on scanning in the positive side, one more anodic peak is observed near 0.9 V (Fig. 4.31) but no cathodic response is found on scan reversal. This anodic peak was not probed any further. When the voltage scan in the negative side is probed, no well-defined cathodic peak can be observed while the current increases steadily (Fig. 4.31). However, on scan revarsal, a peak appears near 0.2 V which is attributed to the oxidation of metallic copper deposited at the electrode surface. Similar observations have been made by other workers and also in case of non-amide complexes [118]. Complexes 7,8 and 9

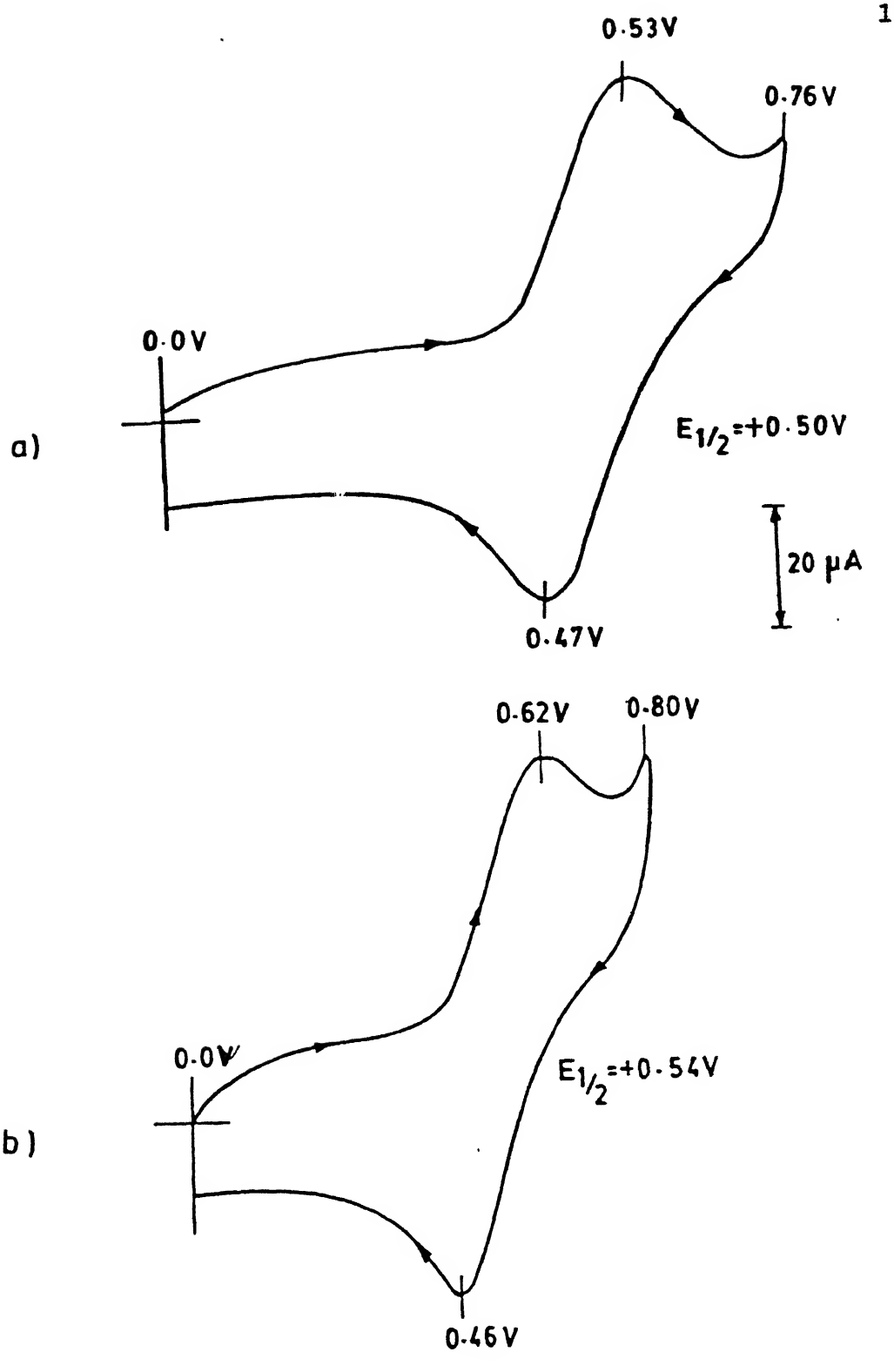

Fig 4.30 Cyclic voltammograms for the complexes : (a) for 6, (b) for 7 in CH_3CN (Ca 1 x 10^{-3} M) at the scan rate of 50 mVs^{-1} using glassy carbon working electrode,

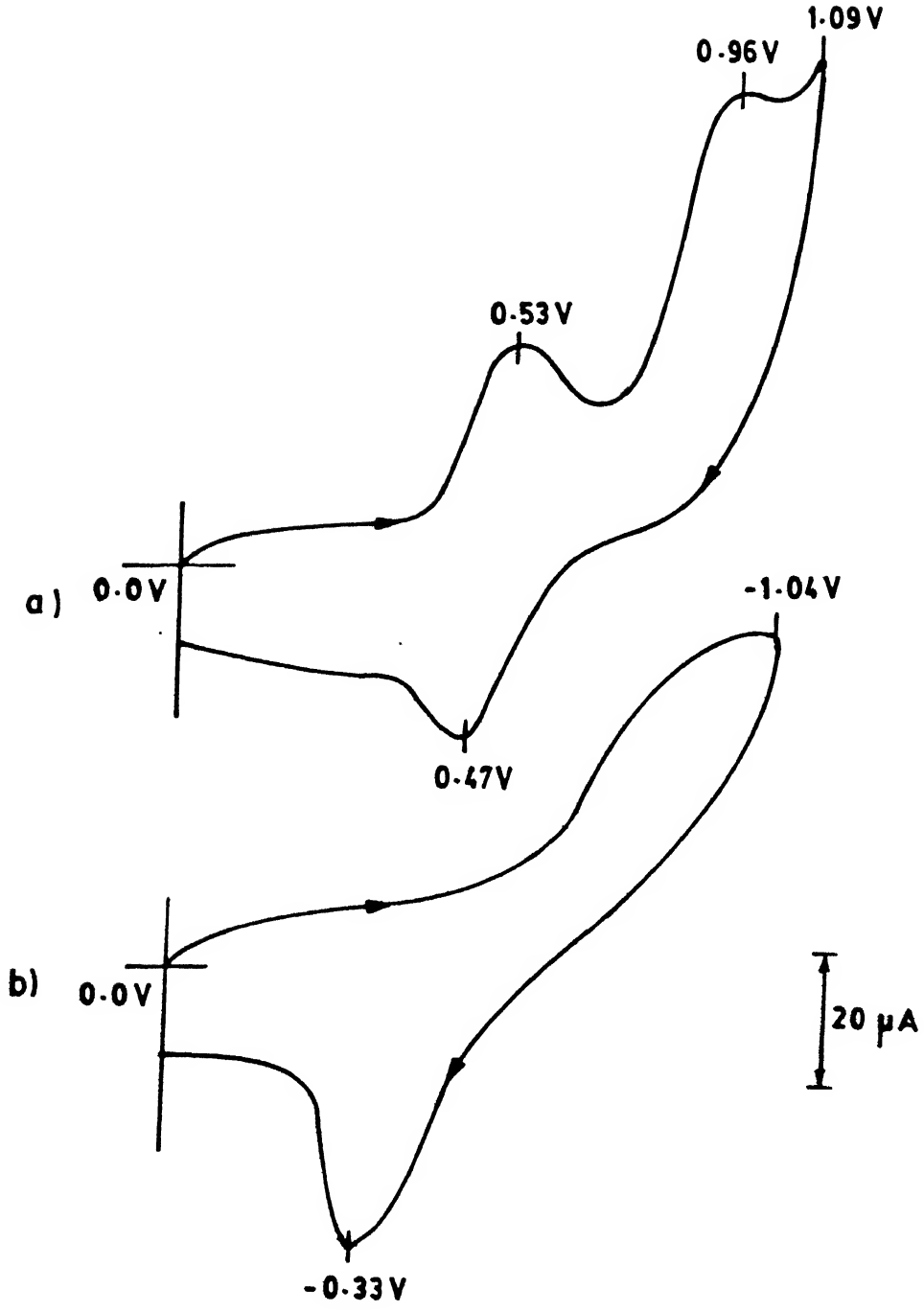

Fig 4.31 Cyclic voltammograms for the complex 6 : (a) for positive scan (0.0 to + 1.09 V), (b) for negative scan (0.0 to -1.04 V) in CH_3CN (Ca 1×10^{-3} M) at the scan rate of 50 mVs^{-1} using glassy carbon working electrode

behave similarly. The involvement of the metal centre in the redox reaction is probed in various ways some of which are already metnioned in case of non-amide complexes. For the present set of Cu(II)-complexes, the arguments in favour of oxidations being metal-centred are given in the following paragraphs.

The copper perchlorate complex, 5(A) shows only ill-defined peaks in the region -1.0 to + 1.0 V. The carbon chain between thioethers changes the response significantly which rules out the possibility of thioether oxidation. Also, if the oxidation wave is due to the aromatic amide, then varying the chain length between thiolate and amide nitrogen (as in 7 compared to 6) is not likely to affect the response as drastically as it has in the present situation. Thiol oxidation is not expected to give a reversible response due to disulfide bond formation. The Ni(II)-analogues of only 8 and 9 could be prepared and charcterized. When subjected to cyclic voltammetric investigations, none of the Ni(II)-complexes showed any well-defined peak in the region, -1.0 to +1.2 V. Only a broad anodic peak appears at about +1.0 V but on scan reversal no peak is seen. This indicates that the oxidized species undergo rapid chemical decomposition once it is generated electrochemically. Hence, the reversible/quasireversible response is expected to have a significant metal contribution if it is not entirely metal-centred. On exhaustive controlled potential coulometry of 6 at 0.7 V at room temperature of an acetonitrile solution (ca 1 x 10^{-3}M), color of the solution changed from dark blue to dark green. The experimental value for n is found to be 1.02 e^{-} and

the oxidation reduction cycle can be completed with about 96% recovery of the starting copper(II)-complex. The oxidized product when quickly frozen in liquid nitrogen in an EPR tube anaerobically, does not show any EPR signal. Also, when transferred at room temperature, it does not give any EPR spectrum. It is realized that diamagnetism could result from strong coupling of the unpaired electron localized on a copper(II) center and a free radical ligand, that is $[Cu(II)(L^{2-})] \rightarrow [Cu(II)(L^{\cdot -})]^{+}$(a)+e instead of $[Cu(III)(L^{2-})]$(b)+e^{-}. However, (a) and (b) may be regarded as two limiting forms of a resonance hybrid system. In that case, the question remains to be answered is which structure contribute more to the resonance hybrid.

Electronic spectrum of the oxidized product recorded at room temperature shows features different from the starting material (Fig 4.32). Moreover, if the cyclic response has significant metal contribution, then the difference in the redox behaviour of complexes, 6 and 7 can be more easily explained. In complex 6, the metal-ligand ensemble is strongly held together. On increasing the chain length between thiolate and amide nitrogen (complex 7), the chelate size is increased so that in the oxidized species, the ligand and the metal are not tightly held leading to higher ΔE_p values. When monitored spectrophotometrically at 600 and at 420 nm under anaerobic condition, the oxidized complex 6 did not decompose in acetonitrile to any noticeable extent in 45 minutes at RT. In case of the pair 8 and 9 (Fig. 4.33), although ΔE_p values are comparable, the $E_{1/2}$ values indicate the 9 is easier to oxidize compared to 8. Both the ligand's donor atoms

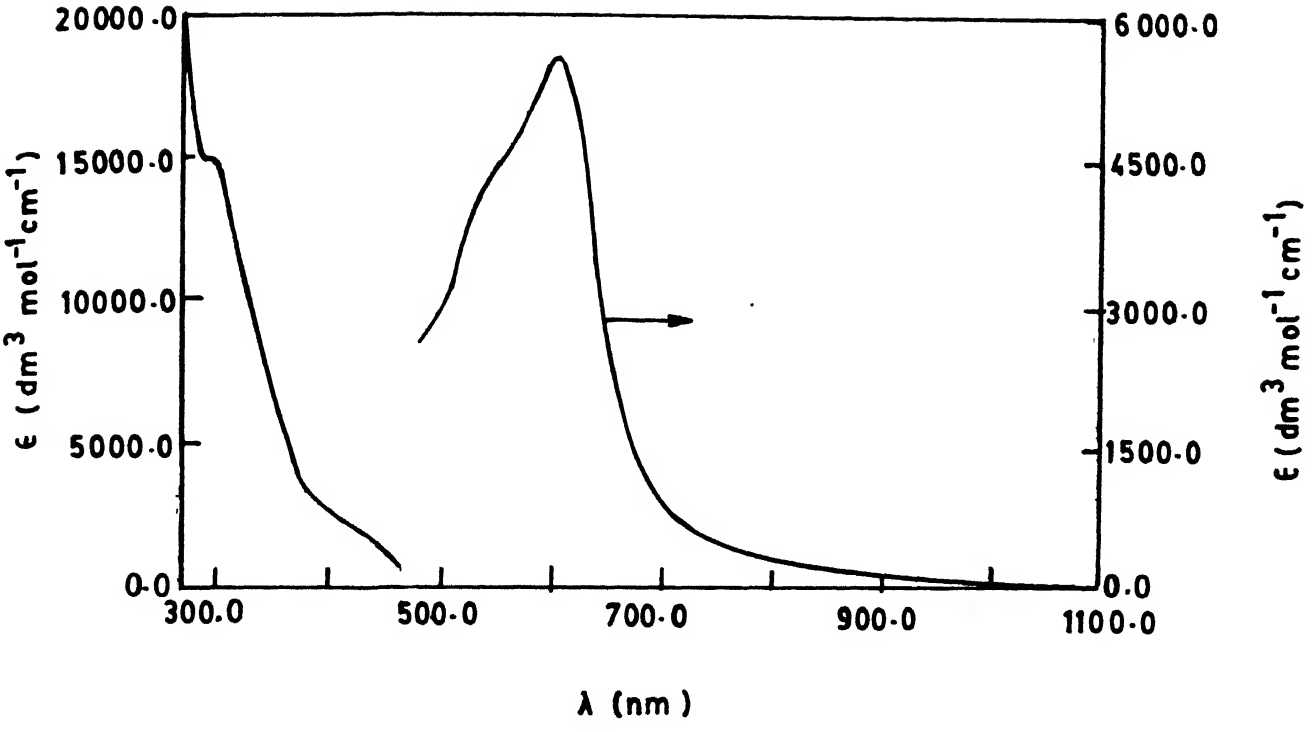

Fig 4.32 Electronic spectrum for 6^+ (Coulometrically oxidized species of 6) in CH_3CN

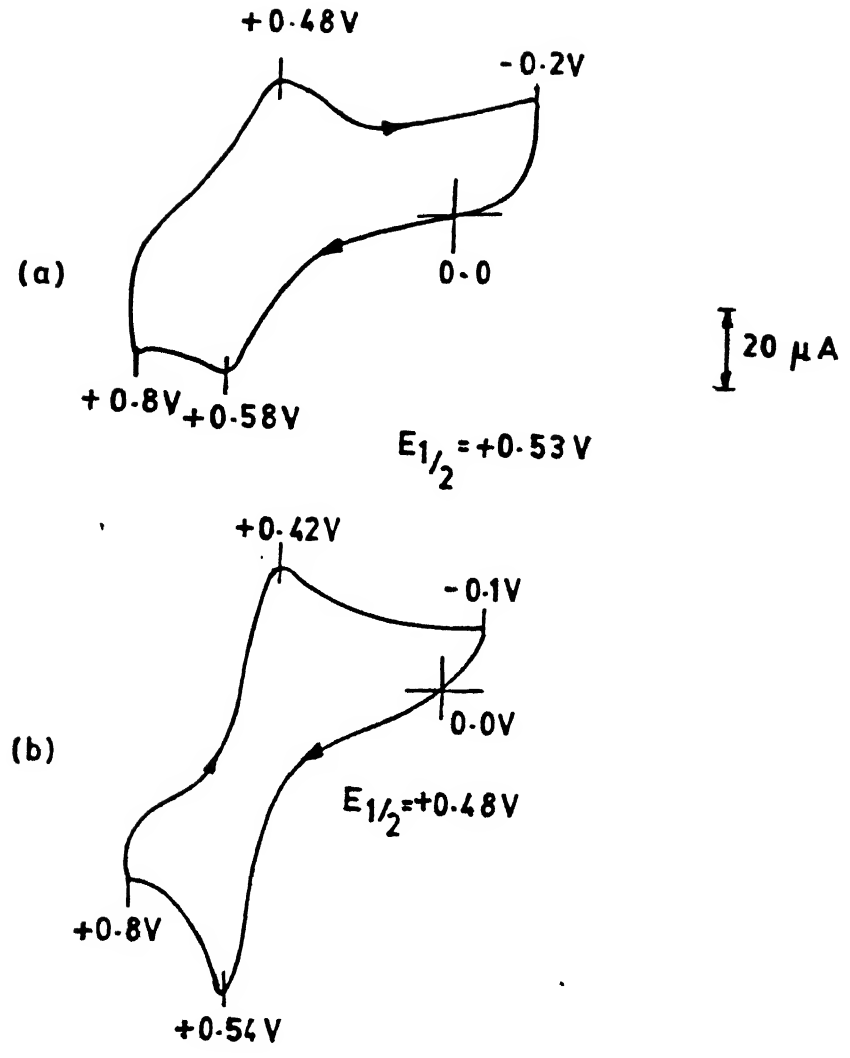

Fig 4.33 Cyclic voltammograms for the complexes : (a) for 8, (b) for 9 in DMF (Ca 1 x 10^{-3}M) at the scan rate of 100 mVs^{-1} using glassy carbon working electrode.

are somewhat rigid due to the aromatic rings. However, examination of molecular models show that in 8 the ligand is less rigid as the thioethers are separated by three carbon atoms thereby more easily able to reorganize itself upon oxidation resulting in lower $E_{1/2}$ value.

4.6 Conclusion

Hexacoordinated Cu(II)-thiolates having four equatorial sulfur ligation show reversible/quasi-reversible oxidation of the metal-ligand ensembles. The four equatorial bonds raise the energy of the singly occupied $d_{x^2-y^2}$ orbital. This not only lowers the Cu(II)/Cu(I) potential but also gives rise to easy removal of the electron to produce oxidized species at least in the cyclic voltametric time scale. With suitable modification of the ligand superstructure, metastable oxidized species can be generated electrochemically that allows spectroscopic probe. The oxidation is argued as mostly metal-centred if not completely so. The Cu(II)/Cu(I) couple is not seen in any of the complexes studied. Strong equatorial thiolate ligation gives rise to an intense σ (thiolate) $\longrightarrow$ Cu(II) LMCT absorption near 600 nm which gives blue color to these complexes. Whether non-sulfur ligation in the equatorial positions also makes possible the metastable generation of Cu(III) species remains to be seen. Obviously, Cu(III)-species with different types of equatorial and axial donors are needed for this purpose.

CHAPTER 5

INTERACTION OF DISULFIDES WITH COPPER(I) SALT : A NEW SYNTHETIC STRATEGY FOR COPPER(II) THIOLATES

This chapter describes a new synthetic route to Cu(II)-thiolato complexes. As discussed in chapter 1, a number of synthetic strategies are available to synthesize stable Cu(II)-thiolates. Adopting the method of Toftlund and coworkers a large number of thiolato complexes have been synthesized as described in the previous two chapters. However, it is always desirable to find a new route of synthesis of Cu(II)-thiolates which is important, at least, from the point of view of synthetic chemistry. Besides, a new route might allow synthesis of Cu(II)-thiolates with desired coordination geometries not possible following existing methods.

From the literature it is known that some specific disulfides can be cleaved by Ti(III) salts to form Ti(IV)-thiolato complexes [130]. It was, therefore, decided to probe whether a Cu(I)-salt can cleave a disulfide bond to result a Cu(II)-thiolate. Acyclic disulfides were found not to be cleaved by Cu(I) to give Cu(II) thiolates. Therefore, it was decided to try with cyclic disulfides. The idea was to have a macrocycle having a disulfide linkage in addition to amino nitrogens in the ring. The Cu(I) ion can anchor at the macrocycle through coordination to these nitrogens and can act as a reducing centre to cleave the disulfide bond. To test this idea, disulfide containing macrocycles, L_1 and L_2 have been synthesized and their

reactivities towards Cu(I) were probed.

5.1 Experimental Section

5.1.1 Solvents and Reagents

All solvents obtained from Glaxo Laboratories and were purified prior to use following standard methods [92]. 1,2 ethylenediamine (Glaxo Laboratories) was distilled before use. Isobutyraldehyde (Merck) was purified by distillation before use. Trans -1,2 diaminocyclohexane (Aldrich) and sulfurmonochloride (Fluka) were used as received

5.2 Syntheses of Ligands

The ligands were synthesized by using a route as shown schematically in Fig. 5.1.

5.2.1 Synthesis of diisobutyraldehyde disulfide

Synthesis of diisobutyraldehyde disulfide has already been described in the Chapter 3.

5.2.2 Synthesis of the Schiff base, L_1'

Ethylenediamine (2 g, 0.03 mol) in methyl alcohol (15 ml) was slowly added to diisobutyraldehyde disulfide (7 g, 0.03 mol) in methyl alcohol (20 ml) with stirring. The resulting solution was heated under reflux for 30 minutes and then cooled to room temperature. Volume of the solution was reduced to ~15 ml in a rotary evaporator and then kept in the freeze ($5^{o}C$) for 10 h. Desired product was obtained as colorless needles in 80% yield. m.pt. = $170^{o}C$, I.R. : 1652 cm^{-1} ($\nu_{C=N}$). ^{1}H-NMR (80MHz, $CDCl_3$, δ_{TMS}

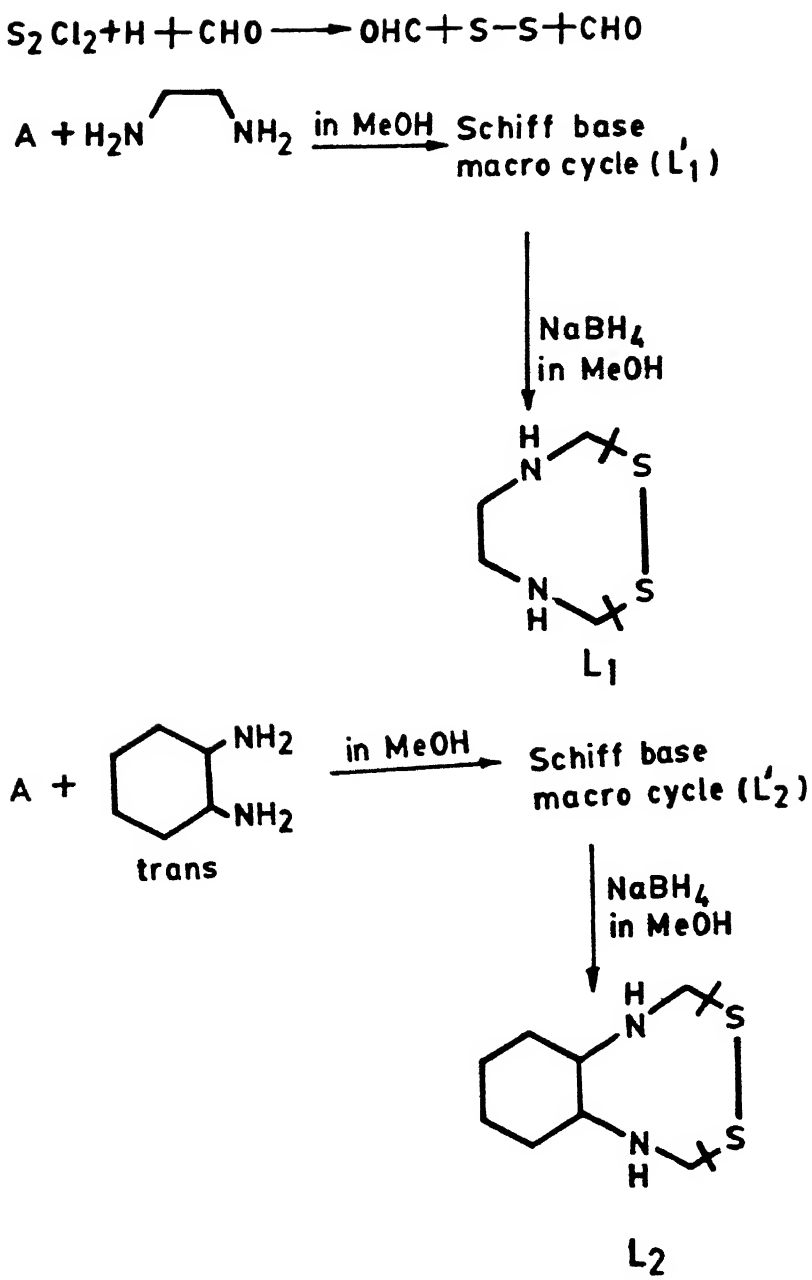

Fig 5.1 Synthetic scheme for the ligands L_1 and L_2

ppm) : 6.8 (s, 2H) imine, 4.1 and 3.2 (AB type, 4H) NCH_2CH_2N, 1.3 (d, 12H) CH_3.

5.2.3 Synthesis of the Schiff base, L'_2

It was synthesized following the above procedure. Trans-1,2 diaminocyclohexane (5 g, 44 mmol) mixed with ethyl alcohol (30 ml) and slowly added to a solution of di-isobutylraldehyde disulfide (9.03 g, 44 mmol) dissolved in 30 ml of ethyl alcohol with stirring. The colorless soution thus formed was heated to reflux for 10 minutes and then kept for slow evaporation at room temperature. Colourless needle-shaped crystals were collected by filtration. Yield 85%. m.pt. = 140°C, I.R. : 1654 cm^{-1} ($\nu_{C=N}$). ^{1}H-NMR (60MHz, $CDCl_3$, δ_{TMS} ppm) : 6.85 (s, 2H) imine, 2.8 (d, 2H) 2CH, 1.8 (m, 8H) $4CH_2$, 1.3 (d, 12H) CH_3.

5.2.4 Synthesis of the ligand, L_1

Ligand L_1 was synthesized by the reduction of the Schiff base, L'_1 using $NaBH_4$ as the reductant following the method of Joshua et.at [131]. The Schiff base L'_1 (3 g; 13 mmol) dissolved in 100 ml of dry ethanol to which added excess $NaBH_4$ (1.72 g, 45.5 mmol) in portions over 30 minutes. A vigorous reaction started immediately. After the addition was complete, the reaction mixture was allowed to reflux for 10 hrs. Ethanol evaporated off in a rotary evaporator and the colorless liquid was partitioned between water (40 ml) and dichloromethane (40 ml). The organic layer was removed and the aqueous layer extracted with

dichloromethane (5x20 ml). The combined extracts were dried over Na_2SO_4 and dichloromethane evaporated off. The residue was chromatographed on silica gel. Elution with chloroform-methanol (19:1) gave a bicyclic product (L_1''). The bicyclic product could be crystallized as the picrate derivaive. Slow evaporation from ethanol afforded single crystals of this compound suitable for x-ray structure determination as described later in this chapter. Elution with chloroform-methanol-ammonium hydroxide (79:20:1) afforded the desired product, L_1. It was purified by converting to the dihydrochloride by passing HCl gas through the ethanolic solution followed by crystallization. Yield 32%. The free ligand was obtained as a colorless oily liquid on treating the dihydrochloride with aqueous KOH followed by extraction with CH_2Cl_2 and finally evaporating off all CH_2Cl_2. ^{1}H-NMR (80MHz, $CDCl_3$, δ_{TMS} ppm) : 2.75 (m, 8H) $4CH_2$, 2.1 (s br, 2H) NH, 1.25 (d, 12H) CH_3.

Synthesis of the ligand, L_2

This ligand was synthesized using the same procedure as above. After refluxing the Schiff base L_2' (3.5 g; 12.3 mmol) with $NaBH_4$ (1.63 g, 43 mmol) in dry ethanol (100 ml) for 10 h, a colorless thick liquid was obtained upon removal of ethanol. This was chromatographed on silica gel after removal of borate as above. Elution with chloroform : methanol (19:1) yielded a bicyclic product. The desired macrocycle, L_2 was eluted as before with chloroform : methanol : ammonium hydroxide (79:20:1). After removal of solvent, it was dissolved in 25 ml dry ethanol and HCl

gas passed through. Upon concentration under vacuum, the dihydrochloride was obtained in 62% yield. Free ligand could be isolated as a colorless oily liquid from the dihydrochloride by treatment with aqueous KOH followed by extraction with CH_2Cl_2 and finally evaporating off CH_2Cl_2. ^{1}H-NMR (60MHz, $CDCl_3$ δ_{TMS} ppm) : 3.14-1.45 (m, 16H) all other protons, 1.2 (d, 12H) CH_3 (Fig. 5.2).

5.3 X-ray crystallographic studies

The macrocyclic Schiff base ligand, L_1 and the bicyclic compound L_1'' were subjected to single crystal x-ray structural studies to ascertain their structures. Structure of L_2 was confirmed by determining its lattice parameters and the space group and matched with the known structure [132]. Crystals suitable for x-ray studies were grown by slow evaporation of methanolic solutions at RT. Cell parameters and reflection intensities were measured at room temperature on a Stoe-Siemens diffractometer with graphite monochromated Mo-K_α radiation. A summary of crystal data, intensity measurements and structure solution and refinements are given in Table (5.1). Intensity data were corrected for decay and Lorentz-polarization effects. The structures were solved by direct methods [133] and refined on F by full-matrix least-squares calculations using the SHELXTL-PLUS program package [134]. In each case, a few hydrogen atoms could be located in successive Fourier difference maps while others were added at calculated positions. Anisotropic refinement of non-hydrogen atoms and isotropic refinement of hydrogen atoms were carried out.

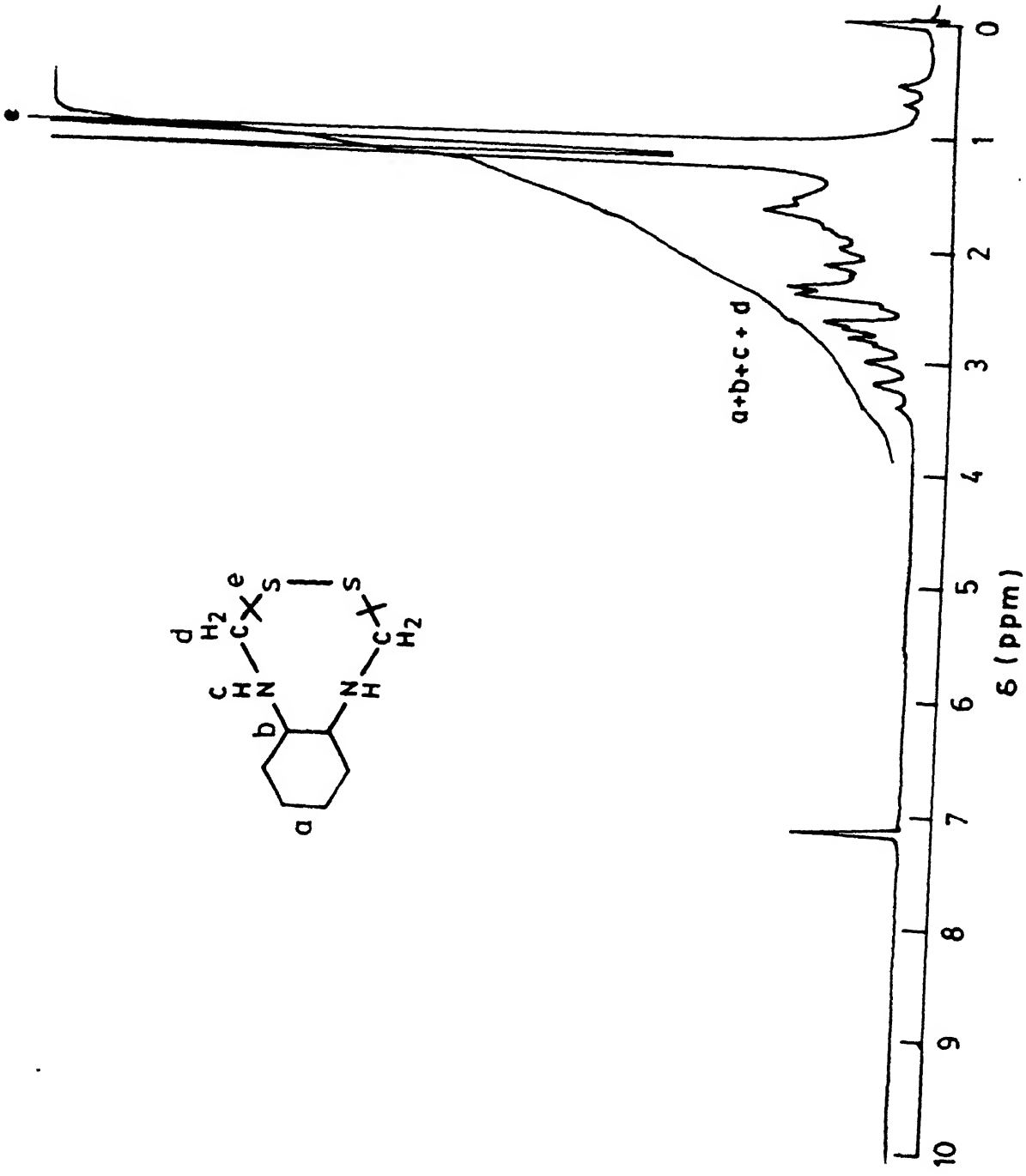

Fig 5.2 ^{1}H-NMR (60MHz) spectrum for L_2 in $CDCl_3$

Fractional atomic coordinates of the non-hydrogen atoms, bond distances and bond angles, anisotropic thermal parameters for the non-hydrogen atoms and fractional coordinates and isotropic thermal parameters for the hydrogen atoms are listed separately for L_1' and L_1'' structures. Perspective views of the molecular structures are shown in Figs. 5.3 to 5.5. A detailed discussion of the structures are not presented here as they are out of scope of the present thesis.

5.4 Syntheses of the complexes

Syntheses of complexes is shown schematically in Fig. 5.6.

5.4.1 Synthesis of copper(II) tetrafuroborate

25 ml fluroboric acid (40%) was taken in 200 ml of water. Large excess of cupric carbonate, (26 g) was added in scoops to the hot (~50^{o}C) solution of acid with stirring. Vigorous reaction started immediately. Addition took about 2 hours. Finally the reaction mixture was heated at about 70-80^{o}C for a further period of 2 hours. The reaction mixture allowed to cool to RT and then filtered to get a blue colored filtrate.

The filrate concentrated to about 40 ml and left in the freze at 5^{o}c for 5 hours. Blue tetrafluorobonate salt settled at the bottom which was collected by filtration, washed with acetone and air-dried. A further crop of the product could be isolated upon concentration of the solution to about 25 ml. Yield 65%.

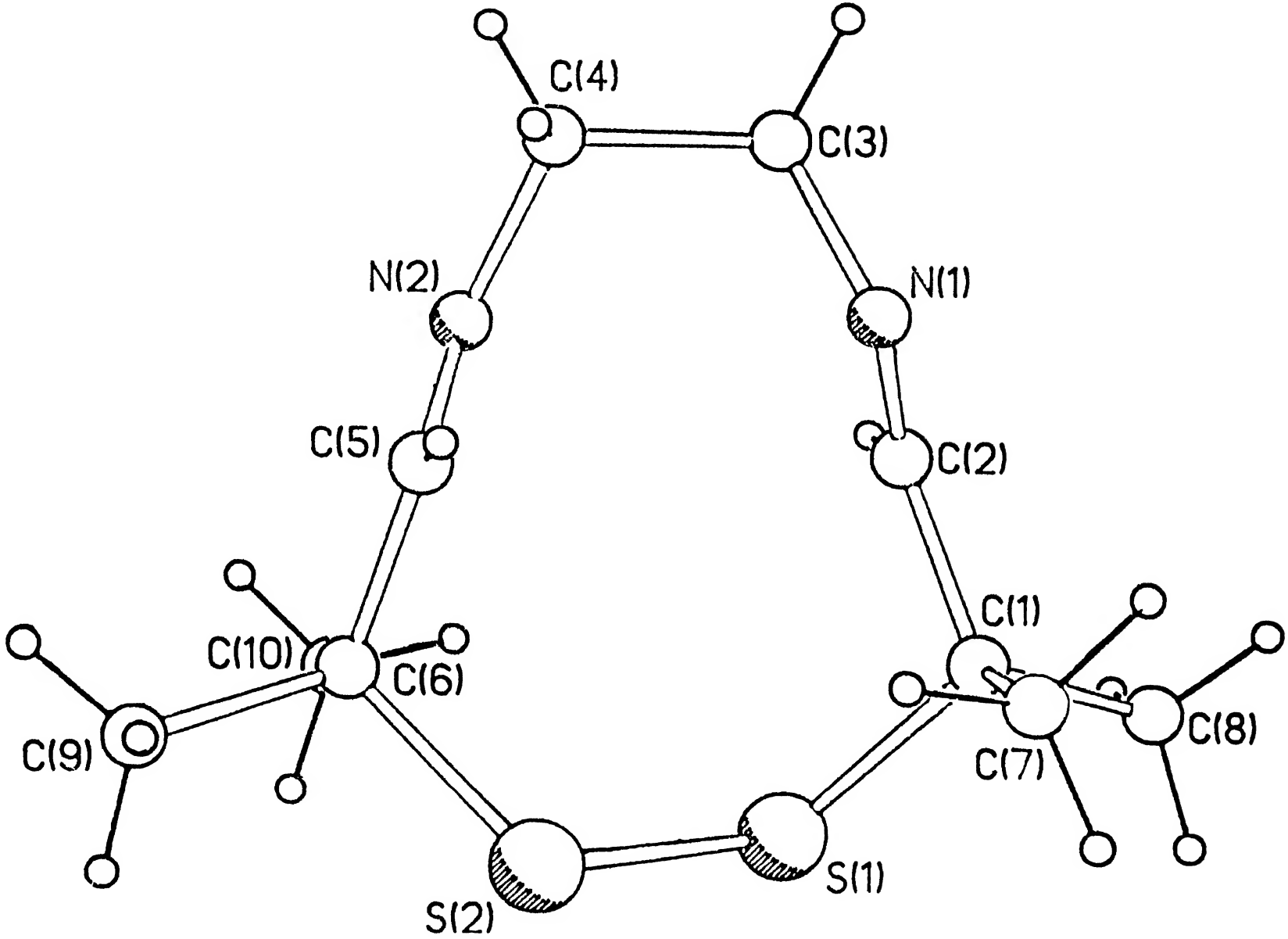

Fig 5.3 Perspective view of the macrocycle, L_1'

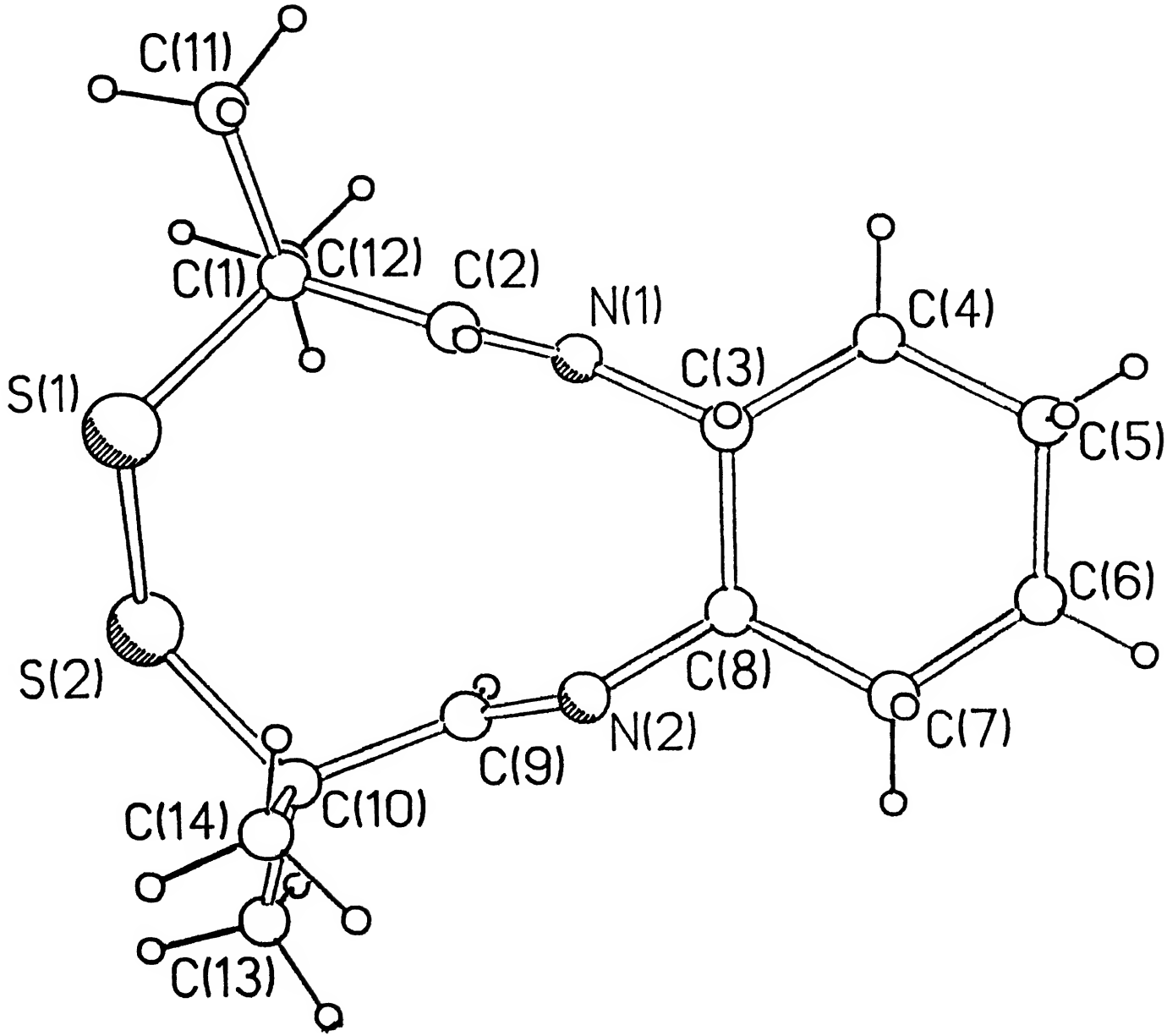

Fig 5.4 Perspective view of the macrocycle, L'_2

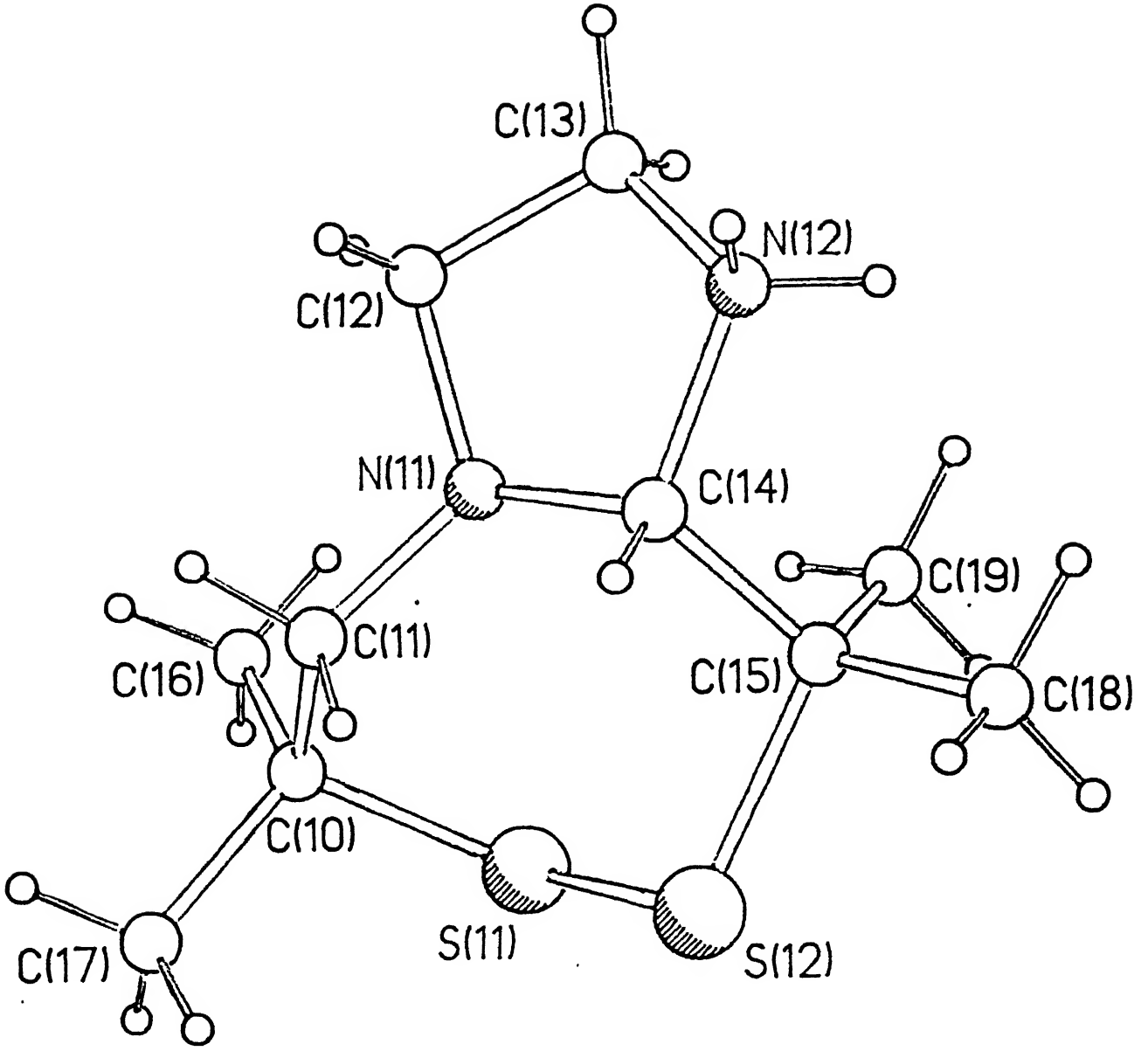

Fig 5.5 Perspective view of the cation, of L_1''

Table 5.1

Crystal and Refinement Data for L_1' and L_1''

Compund	L_1'	L_1''
Crystal System	Orthorhombic	monoclinic
Formula	$C_{10}H_{18}N_2S_2$	$[C_{10}H_{21}N_2S_2]$ $[C_6H_2N_3O_7]$
M	230.4	461.5
Space group	$P2_12_12_1$	$P2_1/c$
a, A^o	8.7054(7)	22.787(3)
b, A^o	8.8920(7)	8.431(2)
c, A^o	15.8238(13)	23.951(3)
v, A^{o3}	1224.9	4304.6
Z	4	8
d_c, g cm^{-3}	1.249	1.424
d_m, g cm^{-3}	1.26	1.40
μ/cm^{-1}	3.9	2.8
crystal dimensions(mm)	0.56x0.60x0.68	0.5x0.5x0.6
Scan type	θ-2θ	θ-2θ
Scan range	0.6+0.35tanθ	0.6+0.35tanθ
2θ range, deg	2-50	2-50
Index ranges	$0\leq h\leq 10$, $0\leq K\leq 10$ $0\leq 1\leq 18$	$-27\leq h\leq 27$, $0\leq k\leq 9$, $0\leq 1\leq 28$
Variation in standard intensity	<1%	<1%
Standard reflections	3 measured every 60 min	3 measured every 60 min
Reflection collected	2697	9133
Independent reflection	2159	7503
No. of reflections used $CF\geq 4\sigma(F)$	2124	5281
Data parameter Ratio	15.1	9.3
Weighting scheme	$w=4(F_o)^2/[\sigma(F_o)^2]^2$	$w=4(F_o)^2/[\sigma(F_o)^2]^2$
Final goodnes of fit	1.09	1.05
Final R_F	0.024	0.046
Final W_R	0.028	0.057
Largest and mean shift/esd	0.010	0.056
Highest peak in final difference map, eA^{o-3}	+0.35	+0.35

Table 5.2

Fractional Atomic Coordinates ($x10^4$) of the Non-Hydrogen Atoms in L_1'

Atom	x	y	z
S(1)	1015(1)	470(1)	6034(1)
S(2)	2987(1)	1462(1)	6412(1)
N(1)	2614(2)	-3165(1)	6779(1)
N(2)	4982(2)	-2034(2)	5732(1)
C(1)	654(2)	-1221(2)	6703(1)
C(2)	1645(2)	-2446(2)	6343(1)
C(3)	3621(2)	-4182(2)	6306(1)
C(4)	5188(2)	-3427(2)	6207(1)
C(5)	4971(2)	-833(2)	6157(1)
C(6)	4623(2)	683(2)	5788(1)
C(7)	926(2)	-924(2)	7633(1)
C(8)	1042(2)	-1561(2)	6511(1)
C(9)	5928(2)	1784(2)	5997(1)
C(10)	4282(2)	642(2)	4849(1)

Table 5.3

Bond Distances (Å) and Angles (°) in L_1'

S(1)-S(2)	2.020(1)	S(1)-C(1)	1.865(2)
S(2)-C(6)	1.865(2)	N(1)-C(2)	1.264(2)
N(1)-C(3)	1.465(2)	N(2)-C(4)	1.459(2)
N(2)-C(5)	1.263(2)	C(1)-C(2)	1.502(2)
C(1)-C(7)	1.513(2)	C(1)-C(8)	1.537(2)
C(3)-C(4)	1.529(2)	C(5)-C(6)	1.500(2)
C(6)-C(9)	1.536(3)	C(6)-C(10)	1.517(2)
S(2)-S(1)-C(1)	109.1(1)	S(1)-S(2)-C(6)	109.3(1)
C(2)-N(1)-C(3)	115.6(1)	C(4)-N(2)-C(5)	116.4(1)
S(1)-C(1)-C(2)	105.8(1)	S(1)-C(1)-C(7)	112.6(1)
C(2)-C(1)-C(7)	113.9(1)	S(1)-C(1)-C(8)	102.0(1)
C(2)-C(1)-C(8)	109.5(1)	C(7)-C(1)-C(8)	112.1(2)
N(1)-C(2)-C(1)	122.9(1)	N(1)-C(3)-C(4)	108.4(1)
N(2)-C(4)-C(3)	108.4(1)	N(2)-C(5)-C(6)	123.7(1)
S(2)-C(6)-C(5)	106.4(1)	S(2)-C(6)-C(9)	102.4(1)
C(5)-C(6)-C(9)	109.8(1)	S(2)-C(6)-C(10)	112.2(1)
C(5)-C(6)-C(10)	113.6(1)	C(9)-C(6)-C(10)	111.8(1)

Table 5.4

Anisotropic Thermal Parameters ($Å^2 \times 10^3$) for the Non-Hydrogen Atoms in L_1'

	U_{11}	U_{22}	U_{33}	U_{23}	U_{13}	U_{12}
S(1)	28(1)	31(1)	40(1)	9(1)	2(1)	4(1)
S(2)	39(1)	25(1)	40(1)	-7(1)	9(1)	-4(1)
N(1)	32(1)	27(1)	33(1)	3(1)	3(1)	1(1)
N(2)	29(1)	33(1)	32(1)	2(1)	5(1)	3(1)
C(1)	26(1)	30(1)	34(1)	4(1)	5(1)	0(1)
C(2)	29(1)	23(1)	30(1)	0(1)	-1(1)	-5(1)
C(3)	43(1)	25(1)	46(1)	1(1)	5(1)	6(1)
C(4)	35(1)	31(1)	43(1)	3(1)	4(1)	9(1)
C(5)	23(1)	35(1)	27(1)	5(1)	-1(1)	-2(1)
C(6)	27(1)	28(1)	30(1)	1(1)	3(1)	-4(1)
C(7)	48(1)	40(1)	31(1)	1(1)	10(1)	5(1)
C(8)	25(1)	51(1)	65(1)	13(1)	2(1)	-2(1)
C(9)	38(1)	41(1)	54(1)	3(1)	0(1)	-14(1)
C(10)	40(1)	38(1)	29(1)	7(1)	3(1)	4(1)

The anisotropic temperature factor exponent takes the form $-2\pi^2(h^2a^*U_{11} + \ldots + 2hka^*b^*U_{12})$

Table 5.5

Fractional Coordinates ($x10^4$) and Isotropic Thermal Parameters ($Å^2 x10^3$) for the Hydrogen Atoms in L_1'

	x	y	z	U
H(2)	1538	-2694	5755	33
H(3a)	3734	-5111	6609	46
H(3b)	3188	-4379	5759	46
H(4a)	5872	-4084	5907	44
H(4b)	5608	-3207	6754	44
H(5)	5199	-892	6750	34
H(7a)	222	-171	7830	48
H(7b)	1961	-594	7731	48
H(7c)	748	-1848	7931	48
H(8a)	-1642	-706	6680	56
H(8b)	-1360	-2427	6827	56
H(8c)	-1191	-1745	5919	56
H(9a)	5620	2771	5820	53
H(9b)	6845	1496	5702	53
H(9c)	6122	1788	6594	53
H(10a)	4052	1650	4671	43
H(10b)	3409	9	4745	43
H(10c)	5149	272	4537	43

Table 5.6

Fractional Atomic Coordinates ($x10^4$) of Non-Hydrogen Atoms in the Bicyclic Compound, L_1''

A. Bicyclic Cations

Atom	x	y	z
S(11)	1264(1)	5068(1)	2989(1)
S(12)	1479(1)	3436(1)	2473(1)
N(11)	954(1)	6556(3)	1745(1)
N(12)	462(1)	5351(3)	823(1)
C(10)	1574(1)	6986(4)	2190(1)
C(11)	1556(1)	7029(4)	2835(1)
C(12)	641(1)	7778(3)	1311(1)
C(13)	133(1)	6871(3)	854(1)
C(14)	970(1)	5101(3)	1427(1)
C(15)	849(1)	3586(3)	1730(1)
C(16)	1137(2)	8216(6)	2938(2)
C(17)	2249(2)	7209(6)	3258(2)
C(18)	956(2)	2124(4)	1399(2)
C(19)	206(1)	3579(4)	1790(1)
S(21)	3768(1)	1019(2)	2078(1)
S(22)	3555(1)	-599(1)	2599(1)
N(21)	4110(1)	2488(3)	3342(1)
N(22)	4626(1)	1239(3)	4250(1)
C(20)	3502(1)	2963(5)	2259(1)
C(21)	3509(1)	2957(4)	2898(1)
C(22)	4412(1)	3699(4)	3788(1)
C(23)	4933(1)	2780(4)	4231(1)
C(24)	4103(1)	1010(3)	3650(1)
C(25)	4208(1)	-485(4)	3330(1)
C(26)	3966(3)	4164(7)	2182(2)
C(27)	2837(2)	3285(7)	1827(2)
C(28)	4111(2)	-1949(5)	3662(2)
C(29)	4837(1)	-493(5)	3247(1)

Contd.

B. Picrate Anions

Atom	x	y	z
O(31)	5764(1)	-320(3)	4827(1)
C(31)	6221(1)	-666(3)	4667(1)
C(32)	6692(1)	457(3)	4655(1)
C(33)	7157(1)	132(4)	4433(1)
C(34)	7200(1)	-1374(3)	4226(1)
C(35)	6778(1)	-2539(3)	4219(1)
C(36)	6308(1)	-2191(3)	4439(1)
N(31)	6669(1)	2083(3)	4863(1)
O(32)	6790(2)	3172(3)	4581(1)
O(33)	6536(2)	2278(4)	5302(1)
N(32)	7699(1)	-1729(4)	3997(1)
O(34)	8027(1)	-628(4)	3948(2)
O(35)	7775(1)	-3089(3)	3872(1)
N(33)	5861(1)	-3438(3)	4407(1)
O(36)	5727(1)	-4342(3)	3986(1)
O(37)	5615(1)	-3519(4)	4784(1)
O(41)	676(1)	3842(3)	4813(1)
C(41)	1157(1)	3480(3)	4689(1)
C(42)	1644(1)	4567(3)	4703(1)
C(43)	2126(1)	4219(3)	4504(1)
C(44)	2157(1)	2715(3)	4290(1)
C(45)	1721(1)	1574(3)	4272(1)
C(46)	1244(1)	1946(3)	4475(1)
N(41)	1622(1)	6173(3)	4919(1)
O(42)	1425(1)	6376(3)	5327(1)
O(43)	1792(1)	7267(3)	4675(1)
N(42)	2657(1)	2324(3)	4066(1)
O(44)	3051(1)	3331(3)	4100(1)
O(45)	2669(1)	1002(3)	3867(1)
N(43)	793(1)	689(3)	4447(1)
O(46)	648(1)	-197(4)	4022(1)
O(47)	583(2)	580(4)	4839(2)

Table 5.7

Bond Distances (Å) in L_1''

A. Bicyclic Cations

S(11)-S(12)	2.021(2)	S(11)-C(10)	1.853(4)
S(12)-C(15)	1.856(2)	N(11)-C(11)	1.465(3)
N(11)-C(12)	1.458(3)	S(11)-C(14)	1.451(3)
N(12)-C(13)	1.499(4)	N(12)-C(14)	1.514(3)
C(10)-C(11)	1.530(4)	C(10)-C(16)	1.517(7)
C(10)-C(17)	1.527(5)	C(12)-C(13)	1.493(4)
C(14)-C(15)	1.542(4)	C(15)-C(18)	1.531(5)
C(15)-C(19)	1.521(5)	S(21)-S(22)	2.020(2)
S(21)-C(20)	1.850(4)	S(22)-C(25)	1.856(3)
N(21)-C(21)	1.460(3)	N(21)-C(22)	1.462(4)
N(21)-C(24)	1.451(4)	N(22)-C(23)	1.483(4)
N(22)-C(24)	1.521(3)	C(20)-C(21)	1.526(5)
C(20)-C(26)	1.521(7)	C(20)-C(27)	1.527(5)
C(22)-C(23)	1.501(4)	C(24)-C(25)	1.537(4)
C(25)-C(28)	1.527(6)	C(25)-C(29)	1.515(5)

Contd..

B. Picerate Anions

O(31)-C(31)	1.266(4)	C(31)-C(32)	1.438(4)
C(31)-C(36)	1.436(4)	C(32)-C(33)	1.372(4)
C(32)-N(31)	1.466(4)	C(33)-C(34)	1.378(4)
C(34)-C(35)	1.371(4)	C(34)-N(32)	1.458(4)
C(35)-C(36)	1.382(4)	C(36)-N(33)	1.447(4)
N(31)-O(32)	1.226(5)	N(31)-O(33)	1.204(4)
N(32)-O(34)	1.222(4)	N(32)-O(35)	1.213(4)
N(33)-O(36)	1.213(4)	N(33)-O(37)	1.220(5)
O(41)-C(41)	1.270(3)	C(41)-C(42)	1.430(4)
C(41)-C(46)	1.431(4)	C(42)-C(43)	1.377(4)
C(42)-N(41)	1.456(4)	C(43)-C(44)	1.378(4)
C(44)-C(45)	1.373(4)	C(44)-N(42)	1.459(4)
C(45)-C(46)	1.373(4)	C(46)-N(43)	1.461(4)
N(41)-O(42)	1.224(5)	N(41)-O(43)	1.225(4)
N(42)-O(44)	1.217(4)	N(42)-O(45)	1.217(4)
N(43)-O(46)	1.210(4)	N(43)-O(47)	1.200(6)

Table 5.8

Bond Angles (°) in L_1''

A. Bicyclic Cations

S(12)-S(11)-C(10)	106.3(1)	S(11)-S(12)-C(15)	105.5(1)
C(11)-N(11)-C(12)	115.0(2)	C(11)-N(11)-C(14)	115.0(2)
C(12)-N(11)-C(14)	108.7(2)	C(13)-N(12)-C(14)	107.4(2)
S(11)-C(10)-C(11)	110.2(2)	S(11)-C(10)-C(16)	104.3(3)
C(11)-C(10)-C(16)	111.3(3)	S(11)-C(10)-C(17)	109.9(3)
C(11)-C(10)-C(17)	109.1(3)	C(16)-C(10)-C(17)	111.9(3)
N(11)-C(11)-C(10)	114.4(3)	N(11)-C(12)-C(13)	102.6(2)
N(12)-C(13)-C(12)	101.7(2)	N(11)-C(14)-N(12)	103.4(2)
N(11)-C(14)-C(15)	114.3(2)	N(12)-C(14)-C(15)	111.2(2)
S(12)-C(15)-C(14)	107.6(2)	S(12)-C(15)-C(18)	103.4(2)
C(14)-C(15)-C(18)	109.6(3)	S(12)-C(15)-C(19)	110.7(2)
C(14)-C(15)-C(19)	112.7(2)	C(18)-C(15)-C(19)	112.4(3)
S(22)-S(21)-C(20)	106.5(1)	S(21)-S(22)-C(25)	105.1(1)
C(21)-N(21)-C(22)	114.8(2)	C(21)-N(21)-C(24)	115.2(2)
C(22)-N(21)-C(24)	108.4(2)	C(23)-N(22)-C(24)	107.7(2)
S(21)-C(20)-C(21)	110.1(2)	S(21)-C(20)-C(26)	105.3(3)
C(21)-C(20)-C(26)	111.2(3)	S(21)-C(20)-C(27)	109.1(3)
C(21)-C(20)-C(27)	109.7(3)	C(26)-C(20)-C(27)	111.4(4)
N(21)-C(21)-C(20)	114.0(3)	N(21)-C(22)-C(23)	101.9(2)
N(22)-C(23)-C(22)	102.1(2)	N(21)-C(24)-N(22)	103.0(2)
N(21)-C(24)-C(25)	114.8(2)	N(22)-C(24)-C(25)	111.5(2)
S(22)-C(25)-C(24)	107.3(2)	S(22)-C(25)-C(28)	103.5(2)
C(24)-C(25)-C(28)	109.0(3)	S(22)-C(25)-C(29)	110.9(2)
C(24)-C(25)-C(29)	113.0(3)	C(28)-C(25)-C(29)	112.5(3)

Contd..

B Picrate Anions

O(31)-C(31)-C(32)	123.6(3)	O(31)-C(31)-C(36)	124.0(2)
C(32)-C(31)-C(36)	112.2(2)	C(31)-C(32)-C(33)	124.1(3)
C(31)-C(32)-N(31)	119.5(3)	C(33)-C(32)-N(31)	116.3(3)
C(32)-C(33)-C(34)	119.1(3)	C(33)-C(34)-C(35)	121.7(3)
C(33)-C(34)-N(32)	119.2(3)	C(35)-C(34)-N(32)	119.0(3)
C(34)-C(35)-C(36)	118.5(3)	C(31)-C(36)-C(35)	124.3(3)
C(31)-C(36)-N(33)	118.8(3)	C(35)-C(36)-N(33)	116.8(3)
C(32)-N(31)-O(32)	118.1(3)	C(32)-N(31)-O(33)	118.3(3)
O(32)-N(31)-O(33)	123.5(3)	C(34)-N(32)-O(34)	117.7(3)
C(34)-N(32)-O(35)	119.0(3)	O(34)-N(32)-O(35)	123.3(3)
C(36)-N(33)-O(36)	117.8(3)	C(36)-N(33)-O(37)	119.9(3)
O(36)-N(33)-O(37)	122.2(3)	O(41)-C(41)-C(42)	124.5(3)
O(41)-C(41)-C(46)	122.8(2)	C(42)-C(41)-C(46)	112.5(2)
C(41)-C(42)-C(43)	124.3(3)	C(41)-C(42)-N(41)	118.8(3)
C(43)-C(42)-N(41)	116.9(3)	C(42)-C(43)-C(44)	118.5(3)
C(42)-C(44)-C(45)	121.7(3)	C(43)-C(44)-N(42)	119.5(3)
C(45)-C(44)-N(42)	118.8(3)	C(44)-C(45)-C(46)	118.9(3)
C(41)-C(46)-C(45)	124.1(3)	C(41)-C(46)-N(43)	119.2(3)
C(45)-C(46)-N(43)	116.6(3)	C(42)-N(41)-O(42)	118.7(3)
C(42)-N(41)-O(43)	118.4(3)	O(42)-N(41)-O(43)	122.9(3)
C(44)-N(42)-O(44)	118.1(3)	C(44)-N(42)-O(45)	118.6(3)
O(44)-N(42)-O(45)	123.2(3)	C(46)-N(43)-O(46)	117.7(3)
C(46)-N(43)-O(47)	119.2(3)	O(46)-N(43)-O(47)	123.0(3)

Table 5.9

Anisotropic Thermal Parameters ($Å^2 \times 10^3$) for the Non-Hydrogen Atoms in L_1''

A. Bicyclic Cations

	U_{11}	U_{22}	U_{33}	U_{23}	U_{13}	U_{12}
S(11)	84(1)	113(1)	37(1)	-1(1)	21(1)	-33(1)
S(12)	73(1)	68(1)	57(1)	20(1)	7(1)	0(1)
N(11)	44(1)	42(1)	43(1)	-2(1)	17(1)	-2(1)
N(12)	43(1)	47(1)	36(1)	1(1)	18(1)	-4(1)
C(10)	67(2)	76(2)	44(1)	-15(1)	18(1)	-15(2)
C(11)	49(1)	53(2)	46(1)	-6(1)	16(1)	-9(1)
C(12)	56(2)	42(1)	66(2)	2(1)	23(1)	4(1)
C(13)	48(1)	55(2)	54(1)	6(1)	16(1)	8(1)
C(14)	38(1)	44(1)	37(1)	0(1)	17(1)	-1(1)
C(15)	54(1)	45(1)	45(1)	4(1)	18(1)	-6(1)
C(16)	123(4)	124(4)	81(3)	-39(3)	52(3)	0(3)
C(17)	88(3)	124(4)	55(2)	-14(2)	5(2)	-39(3)
C(18)	93(2)	43(2)	82(2)	0(2)	31(2)	-2(2)
C(19)	63(2)	77(2)	46(1)	5(1)	23(1)	-22(2)
S(21)	88(1)	139(1)	41(1)	2(1)	21(1)	48(1)
S(22)	81(1)	81(1)	72(1)	-21(1)	-3(1)	2(1)
N(21)	46(1)	46(1)	47(1)	8(1)	19(1)	5(1)
N(22)	44(1)	56(1)	41(1)	5(1)	21(1)	8(1)
C(20)	66(2)	98(3)	51(2)	24(2)	26(1)	25(2)
C(21)	53(1)	67(2)	52(1)	13(1)	22(1)	21(1)
C(22)	59(2)	48(2)	71(2)	3(1)	24(1)	-2(1)
C(23)	51(1)	60(2)	59(2)	-1(1)	17(1)	-7(1)
C(24)	37(1)	50(1)	43(1)	4(1)	19(1)	3(1)
C(25)	58(2)	50(2)	51(1)	0(1)	13(1)	7(1)
C(26)	133(4)	147(5)	91(3)	47(3)	56(3)	-4(4)
C(27)	89(3)	156(5)	59(2)	24(3)	16(2)	59(3)
C(28)	111(3)	54(2)	102(3)	4(2)	27(2)	-3(2)
C(29)	66(2)	101(3)	51(2)	-4(2)	22(1)	34(2)

Contd.

B. Picrate Anions

	U_{11}	U_{22}	U_{33}	U_{23}	U_{13}	U_{12}
O(31)	47(1)	73(1)	48(1)	7(1)	25(1)	15(1)
C(31)	37(1)	60(2)	33(1)	3(1)	11(1)	6(1)
C(32)	42(1)	56(2)	40(1)	-7(1)	11(1)	1(1)
C(33)	41(1)	61(2)	48(1)	-4(1)	15(1)	-6(1)
C(34)	36(1)	62(2)	44(1)	-2(1)	18(1)	3(1)
C(35)	46(1)	55(2)	42(1)	-6(1)	16(1)	5(1)
C(36)	39(1)	54(2)	44(1)	1(1)	15(1)	-2(1)
N(31)	58(1)	68(2)	66(1)	-19(1)	20(1)	3(1)
O(32)	134(2)	58(2)	126(2)	-3(2)	62(2)	-6(2)
O(33)	155(3)	103(2)	96(2)	-43(2)	64(2)	-3(2)
N(32)	50(1)	77(2)	65(1)	-2(1)	33(1)	3(1)
O(34)	85(2)	100(2)	163(3)	-13(2)	89(2)	-17(2)
O(35)	88(2)	83(2)	107(2)	-12(1)	64(2)	15(1)
N(33)	54(1)	61(2)	75(2)	-10(1)	32(1)	-7(1)
O(36)	100(2)	83(2)	138(2)	-49(2)	71(2)	-40(2)
O(37)	93(2)	103(2)	107(2)	-12(2)	65(2)	-37(2)
O(41)	41(1)	77(1)	44(1)	-7(1)	18(1)	11(1)
C(41)	34(1)	59(2)	34(1)	-3(1)	12(1)	7(1)
C(42)	44(1)	49(1)	35(1)	-5(1)	12(1)	1(1)
C(43)	41(1)	60(2)	39(1)	0(1)	14(1)	-5(1)
C(44)	33(1)	60(2)	41(1)	-3(1)	16(1)	4(1)
C(45)	41(1)	52(2)	47(1)	-8(1)	17(1)	3(1)
C(46)	37(1)	54(2)	48(1)	-5(1)	17(1)	-3(1)
N(41)	61(1)	54(2)	60(1)	-11(1)	23(1)	-2(1)
O(42)	137(2)	72(2)	78(2)	-22(1)	62(2)	-1(2)
O(43)	108(2)	56(1)	114(2)	-9(1)	59(2)	-13(1)
N(42)	41(1)	81(2)	55(1)	-5(1)	25(1)	4(1)
O(44)	66(1)	106(2)	112(2)	-19(2)	61(1)	-20(1)
O(45)	82(2)	89(2)	126(2)	-30(2)	71(2)	3(1)
N(43)	52(1)	64(2)	98(2)	-14(1)	43(1)	-6(1)
O(46)	94(2)	92(2)	142(3)	-58(2)	60(2)	-44(2)
O(47)	140(3)	120(3)	169(3)	-42(2)	120(3)	-60(2)

The anisotropic Temperature factor exponent takes the form $-2\pi^2(h^2a^{*2}U_{11} + \ldots + 2hka^*b^*U_{12})$

H(26a)	3958	3951	1786	143
H(26b)	4377	3944	2465	143
H(26c)	3865	5259	2212	143
H(27a)	2811	3271	1418	125
H(27b)	2719	4315	1922	125
H(27c)	2559	2501	1884	125
H(28a)	4130	-2889	3443	111
H(28b)	3700	-1852	3684	111
H(28c)	4417	-2018	4058	111
H(29a)	4863	-1478	3056	87
H(29b)	5172	-435	3627	87
H(29c)	4872	373	3001	87
H(33)	7449	941	4422	60
H(35)	6808	-3575	4065	57
H(43)	2435	5005	4514	56
H(45)	1748	534	4120	55

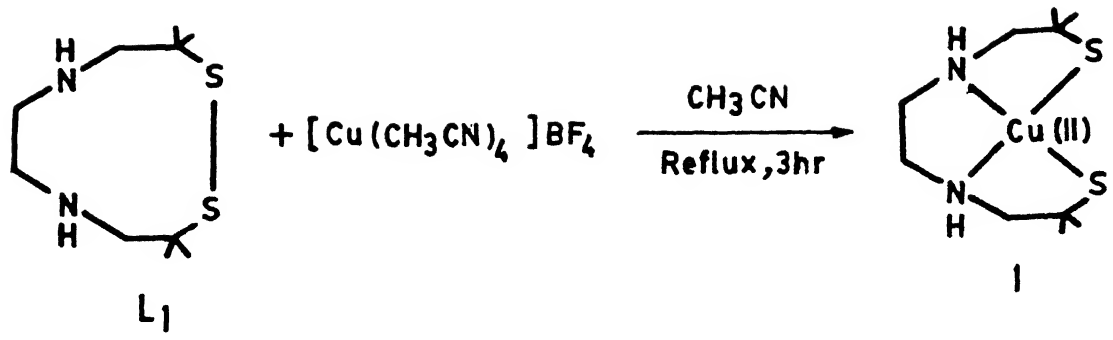

L_1 1

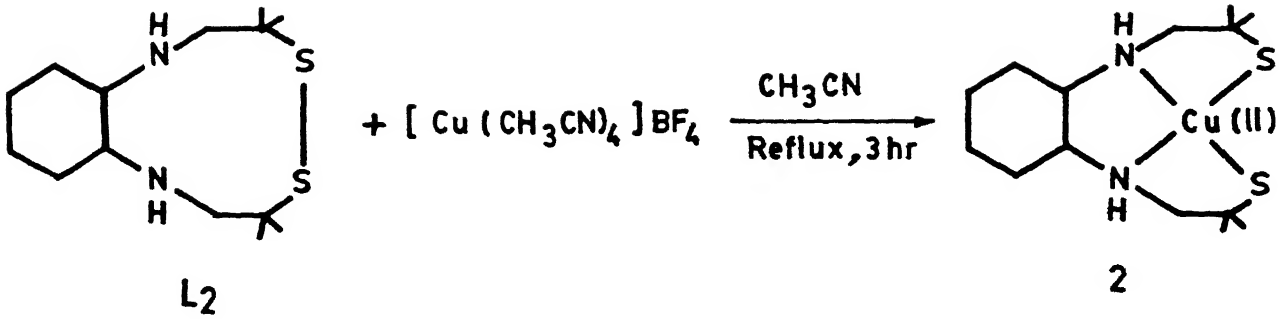

L_2 2

Fig 5.6 Synthetic scheme for the complexes 1 and 2

5.4.2 Synthesis of $[Cu(CH_3CN)_4]BF_4$

It was synthesized by the reaction between copper (II) tetrafluroborate and metallic copper in refluxing acetonitrile [32]. Copper(II) tetrafluroborate was dried in an Abarholden at about 100°C for 2 hours before use. Dry copper(II) tetrafluroborate (5 g, 21 mmol) was allowed to react with excess of copper wire in acetonitrile (250 ml) under reflux for 12 hours. The reaction mixture was then filtered to get a colorless filtrate. The solution concentrated to about 20 ml and left in the freeze at 5°C. Overnight, the desired product appeared as colorless rectangular plates. They were collected by filtration just before use in subsequent reactions. In acetonitrile, the copper(I) complex was found to be stable indefinitely.

5.4.3 Synthesis of the complex, 1

It was synthesized by the reaction between $[Cu(CH_3CN)_4]BF_4$ and ligand L_1. The ligand L_1 (0.47 g, 2 mmol) dissolved in 30 ml of acetronitrile. To this solution the Cu(I)-salt (0.63 g, 2 mmol) was added as solid. The reaction mixture was refluxed for 3 hours under nitrogen atmosphere. Color of the reaction mixture gradually changed to dark red brown. The solution was allowed to cool to room temperature and the volume reduced to about 10 ml by constantly passing a stream of N_2 gas through the flask. A red-brown solid obtained which was collected by filtration and dried in a stream of nitrogen gas. Yield 54%.

5.4.4 Synthesis of the complex, 2

Complex 2 was synthesized using the same procedure as above. Ligand L_2 (0.72 g, 2.5 mmol) was taken in 40 ml of acetonitrile and to this was added the Cu(I)-salt (0.78 g, 2.5 mmol) under nitrogen atmosphere. Colour of the reaction mixture changed to green. The reaction mixture was refluxed for 3 hours when color further changed to red-brown. The red-brown solution was filtered, reduced the volume to about 10 ml and finally kept in the freeze. Dark brown crystalline solid appeared overnight which was collected by filtration and dried in a stream of nitrogen gas. Yield 58%. Analytical data of the complexes are given in Table 5.11.

5.4.5 Physical Measurements

Physical measurements made on the complexes as described in chapter 3.

5.5 Results and Discussion

The complexes once formed, are stable in air in the solid state. In acetonitrile solutions they are stable for weeks. In solvents like DMSO, they are stable at least for one week. Both the complexes behave as non-electrolytes in solvents like dichloromethane, methanol, acetonitrile etc. Moreover, the infrared spectra of the complexes do not show any absorption around 775 cm^{-1} typical of the BF_4^- anion [135]. Magnetic moment values for 1 and 2 are found to be 2.01 and 1.97 (μ_{eff}/μ_B) respectively at room temperature after applying diamagnetic corrections. The values are typical of discrete mononuclear

Table 5.1

Microanalytical Data for the Complexes 1 and 2

Complex	Empirical Formula	Anal% Calcd				Found			
		C	H	N	S	C	H	N	S
1.	$C_{10}H_{22}N_2S_2Cu$	40.33	7.39	9.41	21.51	41.03	7.21	9.70	21.62
2.	$C_{14}H_{28}N_2S_2Cu$	47.79	7.96	7.96	18.20	48.17	8.10	7.75	18.61

Cu(II) complexes [99]. Also, the elemental analyses (C,H,N) of the complexes match with the formula, CuL (L = ligand) signifying the formation of 1:1 complexes.

5.5.1 Electronic Absorption Spectra

Each complex shows (Figs. 5.7 and 5.8) a broad absorption band with λ_{max} near 580 nm. For four coordinate copper(II) complexes the d-d bands may occur in the range 500-850 nm depending upon the stereochemistry and nature of donor atoms as well. For a square planar copper(II) complex with a N_2S_2 donor set [104], the ligand field transition has been found to occur at about 550 nm. X-ray crystallographic results indicated that in this complex the dihedral angle between the planes described by CuN_2 and CuS_2 fragments is 21^o (for a square planar geometry this angle should be equal to 0^o).So, from the band positions (Table 5.13) in the complexes, 1 and 2 it is clear that the coordination geometry around Cu(II) in each is nearly square planar or slightly distorted from square planar.

The electronic spectra of copper(II) complexes of primary amines like ethylenediamine and its alkyl derivatives have been studied in great detail [41, 102]. The parent $[Cu(en)_2]^{+2}$ complex exhibits a high intensity σ(N)-Cu(II) LMCT at 240 nm; alkylation of the amine lowers the ionization potential of the amine and results in a systematic red shift of this absorption. Hence, the strong absorption bands that occur at 285 and 280 nm for complexes 1 and 2 respectively may be assigned to σ(N) $\rightarrow$

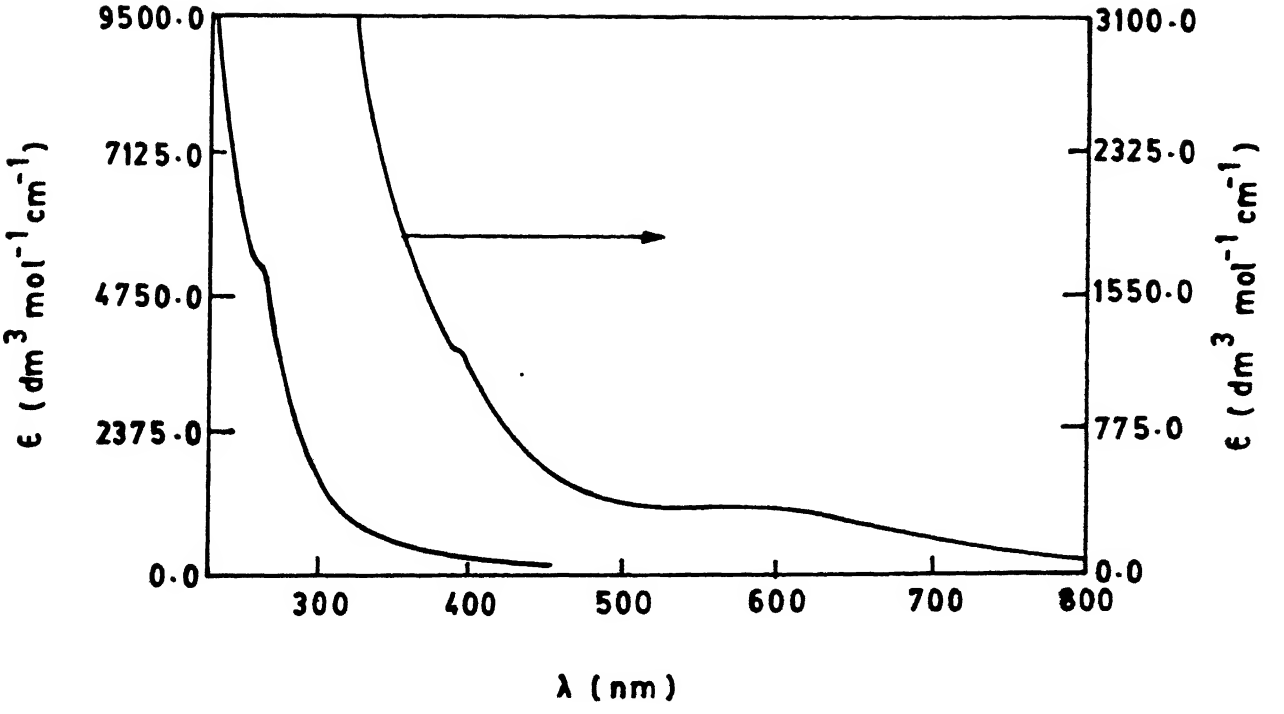

Fig 5.7 Electronic spectrum for the complex 1 in CH_2Cl_2

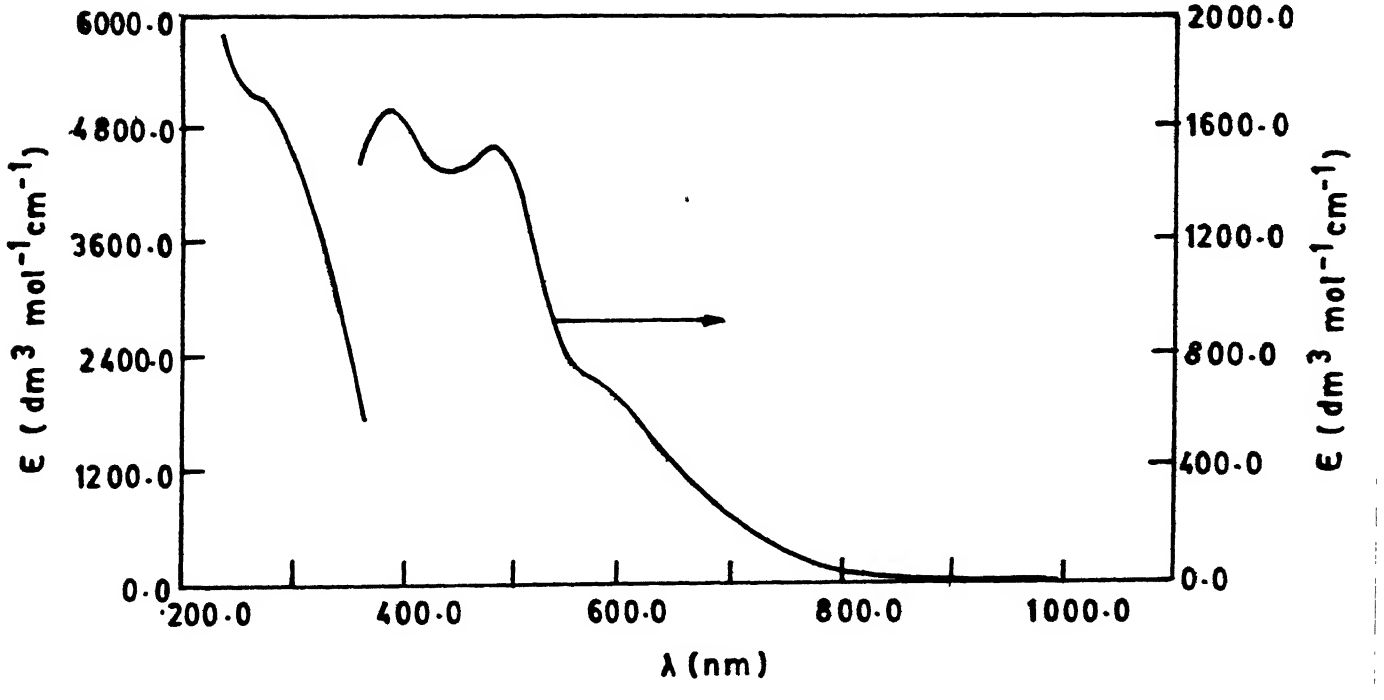

Fig 5.8 Electronic spectrum for the complex 2 in CH_2Cl_2

Table 5.2

Yield, Color, Magnetic Moment (R T) & EPR Data (R T) for the Complexes 1 and 2

Complex	Yield %	Color	Magnetic Moment(RT) μ_{eff}/μ_B	EPR data (RT) g_{av}
1.	54	Red-brown	2.01	2.046[a]
				2.136[b]
2.	58	Dark-brown	1.97	2.076[a]
				2.057[b]

a = solid; b = solution (dichloromethane)

Cu(II) LMCT transitions.

For tetragonal thiolato complexes, the σ(thiolate) $\rightarrow$ Cu(II) LMCT transition occurs around 350 nm [104]. So the bands at 370 (for 1) and 390 nm (for 2) can be assigned as σ(thiolate) $\rightarrow$Cu(II) LMCT absorption. However, a thiolate has two π symmetry lone pairs on sulfur which may give rise to π symmetry LMCT transition on either side of the transition as discussed earlier in chapters 1 and 3. The lower energy π transition occurs at approximately 450 nm. For 2, a band appears at 475 nm. This is well separated from the ligand field band and is quite close in energy to that of π(thiolate) $\rightarrow$ Cu(II) LMCT transition. Therefore, we assign this absorption as due to the lower energy π(thiolate) $\rightarrow$Cu(II) LMCT transition. For complex 1 this transition is not observable. Also, in neither case, the higher energy π(thiolate) $\rightarrow$ Cu(II) transition is seen.

5.5.2 Electron Paramagnatic Resonence

EPR spectral results on 1 and 2 are given in Table 5.12 while the representative spectra (at R.T) of 1 in solid state as well as in solution are shown in Fig. 5.9. Both the complexes show a broad signal in solid state. The spectral shape does not change on lowering the temperature. In solution at RT, a characteristic four-line spectrum is obtain for complex 1 while a broad signal observed from complex 2. At liquid nitrogen temperature a broad signal appears for both the complexes with g $\approx$ 2.

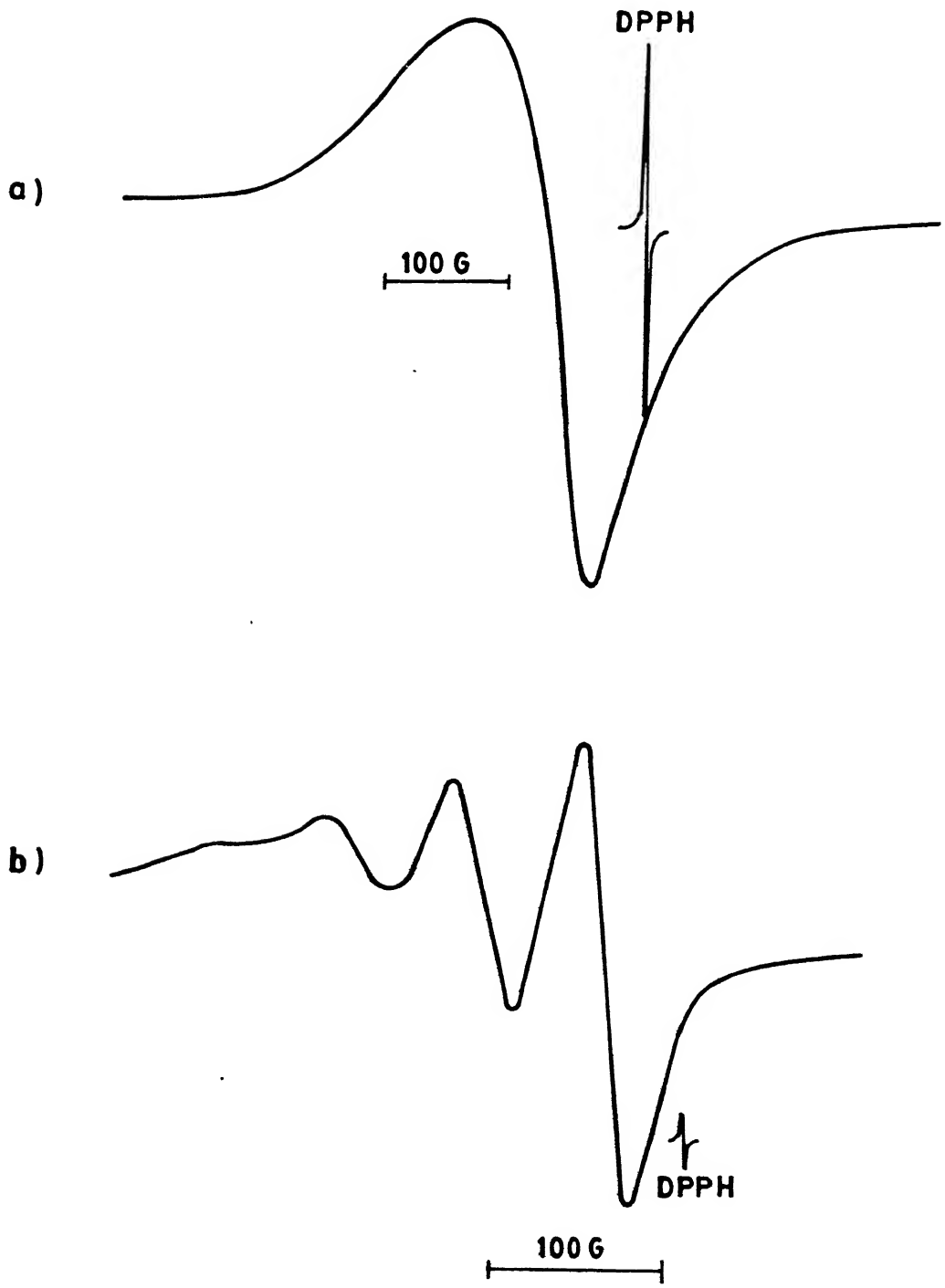

Fig 5.9 EPR spectrum of complex 1 at R.T.
a) for solid state b) solution (CH_2Cl_2)

Table 5.3

Electronic Spectral and Electrochemical Redox Potential Data for the Complexes 1 and 2

Complex	λ_{max}/nm (ϵ_{max} $dm^3 mol^{-1} cm^{-1}$)	Assignment	E_{pc} (V)	E_{pa} (V)	$E_{1/2}$ (V)	ΔE_p (mV)
1.	570(375)	d-d	-0.462	-0.275	-0.368	187
	370(sh)(1250)	σ(thiolate)→ Cu(II)LMCT				
	270(sh)(5100)	σ(N)→Cu(II)LMCT +Ligand absorption				
2.	587(sh)(667)	d-d	-0.410	-0.210	-0.340	140
	476(1557)	π(thiolate)→ Cu(II)LMCT				
	393(1674)	σ(thiolate)→ Cu(II)LMCT				
	280(sh)(5220)	σ(N)→Cu(II)LMCT +Ligand absorption				

5.5.3 Electrochemistry

Cyclic voltammograms for the complexes are shown in Fig. 5.10 while the redox data are collected in Table 5.13. Both the complexes give well defined quasi-reversible cyclic responses. In case of complex 2, $E_{1/2}$ = -0.34 V vs SCE and is found to be almost independent of scan rates employed (20, 50 and 100 mV s^{-1}). The ratio i_{pa}/i_{pc} is found to be almost 1.0 within experimental error for all the scan rates employed. In case of complex 1, $E_{1/2}$ = -0.37 V vs SCE at the scan rate 20mV s^{-1}, and the ratio, i_{pa}/i_{pc} is found to be around 0.95 for all the scan rates. The ΔE_p value for each complex increases somewhat on increasing the scan rate as expected. The peaks are assignable to the redox reactions

$$1^{+} + e^{-} = 1^{-} \qquad (1)$$

$$2^{+} + e^{-} = 2^{-} \qquad (2)$$

For the complex 1, on scanning further in the negative side, one more cathodic peak is observed near -1.26 v. However, on scan reversal the corresponding anodic peak is not observed. Instead, a broad and intense anodic peak is observed at about -0.27 v. The peak at -1.26 v may be due to reduction [136] of Cu(I) to formally Cu(0) when it undergoes chemical decomposition and the metallic copper gets deposited at the electrode surface. The peak at -0.27 v is then attributable to the oxidation of metallic copper deposited at the electrode surface. Similar observations have been made in earlier studies as mentioned in chapter 4. Same behaviour is observed for the complex 2. Complex 2, on scanning further in the negative side shows, one cathodic peak at about -0.72 V which can be attributed, like in case of complex 1, to

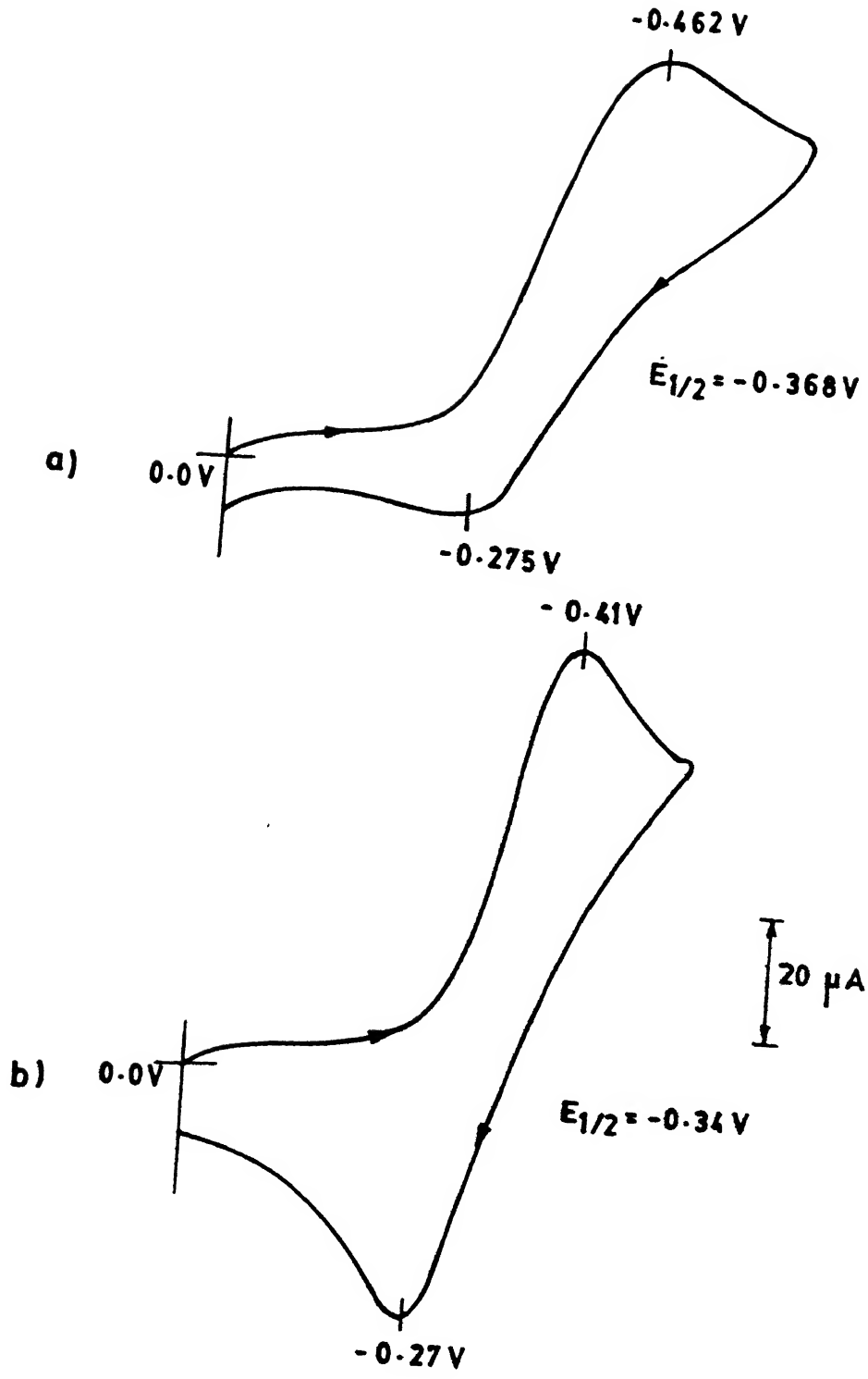

Fig 5.10 Cyclic voltammograms for the complexes : (a) for 1 (b) for 2 in CH_2Cl_2 (Ca 1 x 10^{-3}M) at the scan rate of 100 mVs^{-1} using glassy carbon working electrode.

the reduction of Cu(I) to formally Cu(0) state. On scan reversal, no corresponding anodic peak appears. However, one broad and intense anodic peak is observed at -0.25 v which is attributed to the oxidation of metallic copper deposited at the electrode surface. No peak is seen in the positive side for either complex.

The complexes show $E_{1/2}$ values which are very close to each other reflecting nearly the same coordination geometry. Amines do not undergo reduction at the low potentials observed. Also, thiolates cannot be reduced further. So, the cyclic responses (eqns. 1 and 2) are expected to have a significant metal contribution if they are not entirely metal centred. In the exhaustive controlled potential coulometry experiments performed at ~-0.5 v at RT, both the systems were found to be unsatble.

5.6 Conclusion

Spectroscopic and electrochemical studies on complexes 1 and 2 indicate that indeed discrete,neutral mononuclear copper(II) complexes having the chromophore, CuN_2S_2 have been formed. These complexes are tetragonal in nature. As the reactions between the disulfides and Cu(I) take place cleanly, it proves that this route is a viable one in synthesizing stable copper(II) thiolato complexes. Thus, the aim of having a new method of synthesizing stable Cu(II)-thiolates has been realised.

CHAPTER 6

HEXA COORDINATED Ni(II) COMPLEXES

In this chapter, the synthesis and characterization of two hexacoordinated nickel(II) complexes using tripodal ligands are described. The recent findings [79,80,86] of the presence of distorted octahedral nickel complexes with sulfur and nitrogen ligation at the active sites of several hydrognases and carbon-monoxide dehydrogenses led to an unprecedented interest in nickel chemistry with mixed sulfur and nitrogen donor ligands. Quite a few cyclic as well as acyclic ligands have been used to complex Ni(II) in order to model these sites [81-84]. A new approach in modelling these sites might be the use of tripodal ligands bearing sulfur and nitrogen donors. A hexadentate tripodal ligand is capable of completely wrapping around the metal ion. The coordination geomery of such a system depends upon factors [137] like (i) the electronic configuration and size of the metal ion, (ii) repulsions between non-bonded atoms in different ligand arms, (iii) inherent rigidity due to the presence of aromatic rings, etc. Therefore, through ligand design it is possible to effect a certain desired geometry on to the Ni(II) ion. Besides, complexes with tripodal ligands are capable of exhibiting high thermodynamic stability and kinetic inertness [89].

Thus, it is worthwhile to study nickel(II) complexes with mixed N, S donor ligands to probe their electrochemical as well as chemical properties. We are not aware of prior studies of

nickel (II) complexes with such tripodal ligands except the two synthesized from our laboratory [138]. Single crystal x-ray structural analysis was performed for the complex 1 where all six donors are coordinated in pseudo-octahedral manner. Other spectrochemical studies done for both the complexes include electronic spectral, magnetic susceptibility, conductivity and electrochemical studies.

6.1 Experimental Section

6.1.1 Solvents and Reagents

All the solvents used including n-butanol and pyridine were obtained from Glaxo Laboratories and were purified prior to use following standard procedures [92]. Toluene-4-sufonyl chloride,1,1,1 Tris-(hydroxymethyl)ethane cysteamine hydrochloride, 2-aminothiophenol and nickel(II) perchlorate hexahydrate were obtained from Aldrich and used as received.

6.1.2 Physical Measurements :

The physical measurements made on the complexes as described in chapter 3.

6.2 Syntheses of Ligands

Syntheses of ligands was achieved in stages as shown schematically in Fig. 6.1.

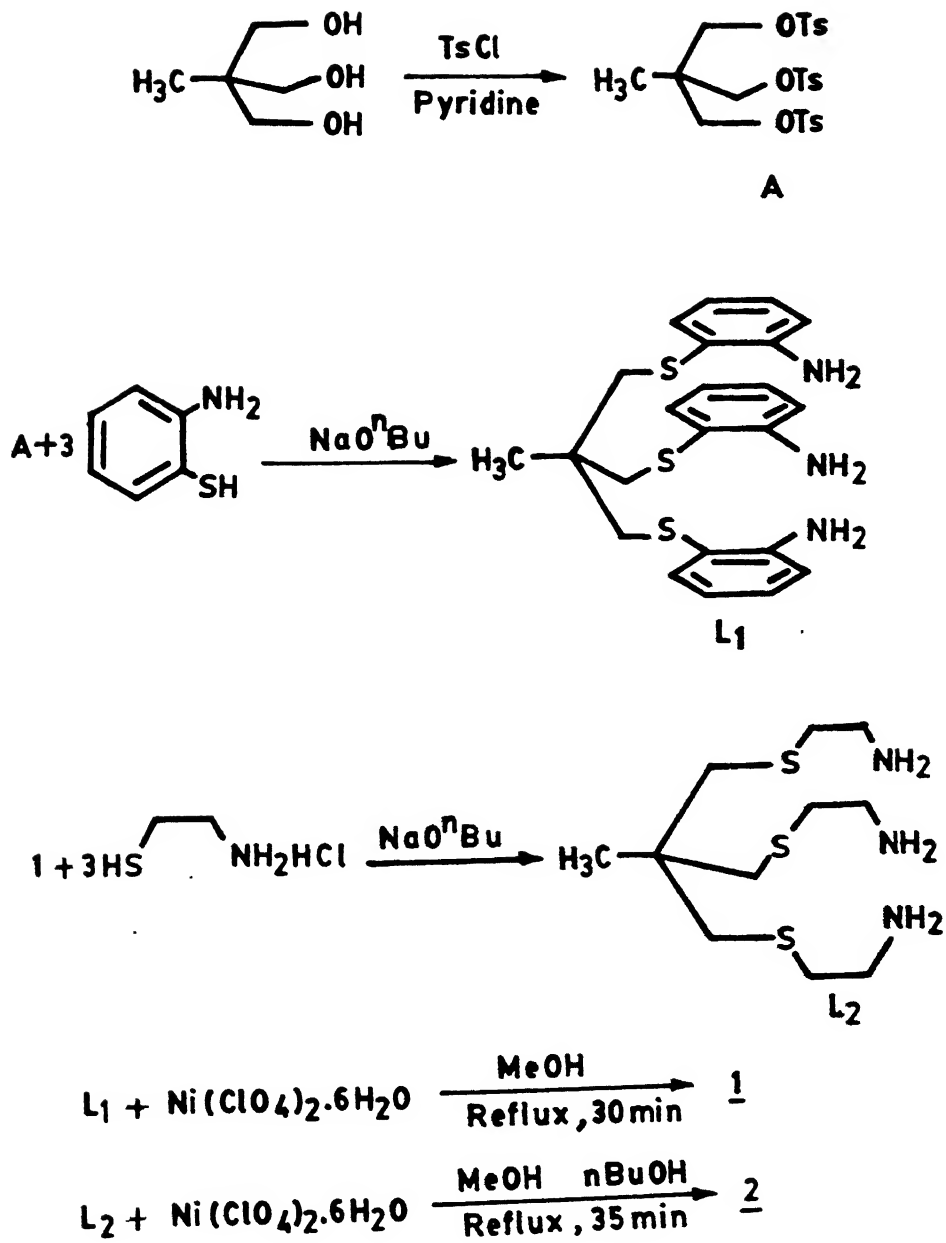

Fig 6.1 Synthetic scheme for the ligands L_1 and L_2 and complexes 1 and 2

6.2.1 Synthesis of the tritosylate of 1,1,1 Tris-(hydroxy methyl)ethane

Toluene-4-sulfonyl chloride (57.6 g, 0.3 mol) was taken in pyridine (50 ml) and cooled to - 10^{o} in an ice-salt bath for half an hour. An ice cold solution of 1,1,1 Tris-(hydroxymethyl) ethane (12.1 g, 0.1 mol) in pyridine (25 ml) was added portion wise through a syringe over a period of 2 hours maintaining the temperature at -10^{o}C while stirring continuously. After the addition was complete, the mixture was allowed to stir for another 30 mins and then left at 5^{o}C overnight. The reaction mixture was then poured into crushed ice and stirred vigorously. Liquid product became semisolid after 45 minutes of stirring and finally semisolid became solid after 2 hours of stirring. The white solid was collected by Filtration, washed thoroughly using water (10 x 200 ml) and finally dried under reduced pressure. Yield 85%. m.pt. = 106^{o}C (Lit = 108-108.5^{o}C) [139]. ^{1}H-NMR (60 MHz, $CDCl_3$, δ_{TMS} ppm) : 7.5 (m, 12H) aromatic, 3.8 (s, 6H) CH_2, 2.5 (s, 9H) CH_3 (tosyl), 1.0 (s, 3H) CH_3 (Fig. 6.2).

6.2.2 Synthesis of the ligand, L_1

n-Butanol (15 ml) was taken in a three-necked round bottom flask and to this was added sodium metal (0.81g, 35.2 mmol) portionwise to dissolve. A vigorous reaction started immediately and all the metal reacted in about 20 mins. Cysteamine hydrochloride (2 g, 17.6 mmol) was added to the hot (~60^{o}C) reaction mixture under an argon atmosphere with constant stirring. After the addition was complete, the reaction mixture was heated to reflux for 10 mins. Solid 1,1,1 tris-(hydroxymethyl)ethane

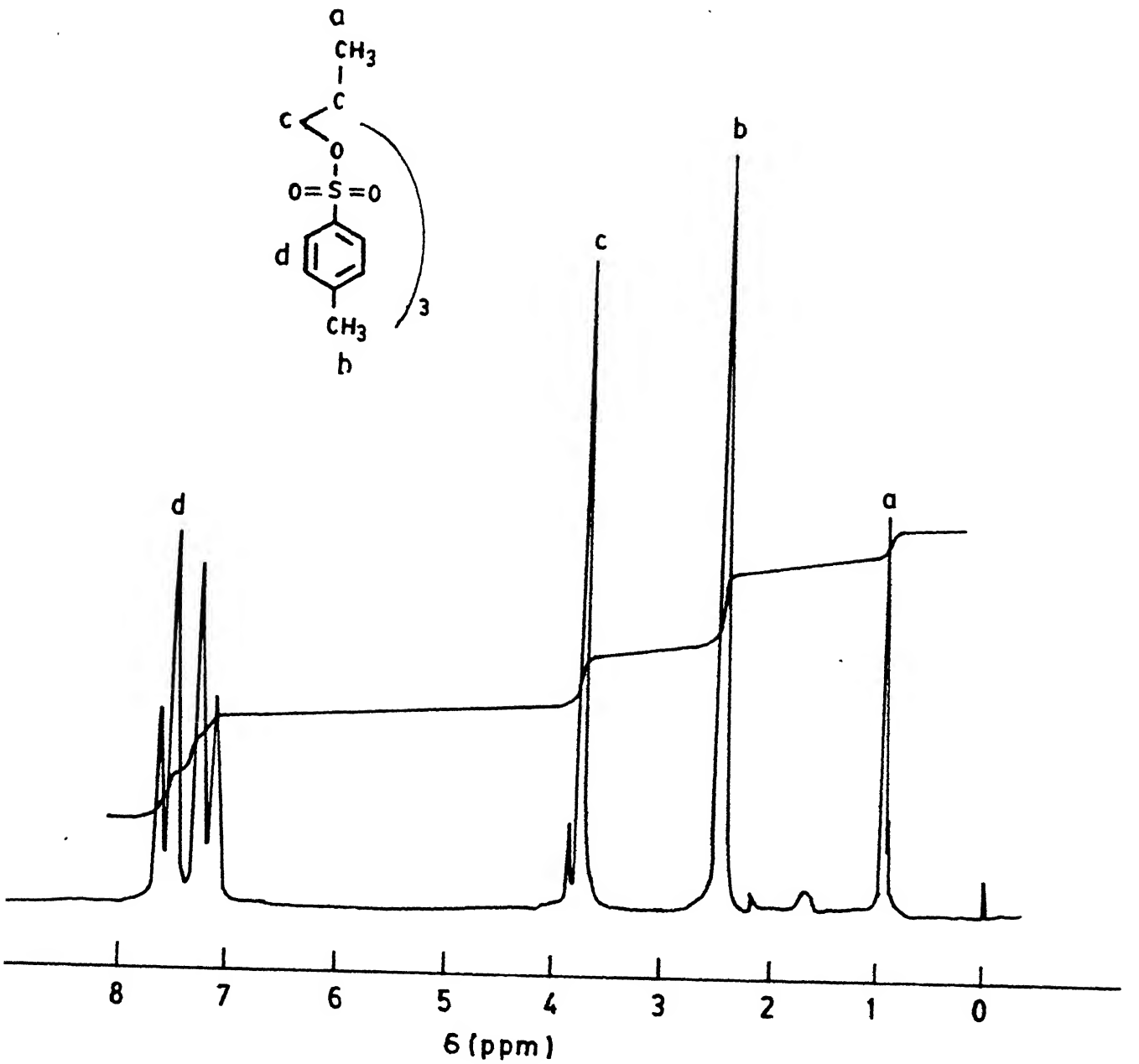

Fig 6.2 ^{1}H NMR (60MHz) spectrum for tritosylate of 1,1,1 Tris(hydroxymethyl) ethane in $CDCl_3$

tritosylate (3.4 g, 5.8 mmol) was added in portions to the refluxing solution over a period of 20 minutes. A white solid began to appear immediately. After refluxing for a further period of 2.5 hours, the reaction mixture was allowed to cool to room temperature and the solid sodium tosylate was removed by filtration. Treatment of the light brown filtrate with decolorizing charcoal afforded a very light yellow solution. n-Butanol was then evaporated off under reduced pressure to obtain light yellow oily mass. The oily mass was dissolved in chloroform (10 ml), washed using water (3 x 15 ml) and finally dried over anhydrous sodium sulfate. On removal of chloroform under reduced pressure a very light yellow oily mass in 70% yield was obtained. ^{1}H-NMR (80MHz, $CDCl_3$, δ_{TMS} ppm) : 3.5 (s, br, 6H) NH_2, 3.0 (m, 18H) all CH_2, 1.0 (s, 3H) CH_3.

6.2.3 Synthesis of the ligand, L_2

The ligand L_2 was synthesized in about 65% yield as a yellow oil following the above procedure except that 2-mercapto aniline was used instead of cysteamine hydrochloride. ^{1}H-NMR (80MHz, $CDCl_3$, δ_{TMS} ppm) : 7.2 (m, 12H) aromatic, 4.2(s, br, 6H) NH_2, 3.0 (s, 6H) CH_2, 1.0 (s, 3H) CH_3.

6.3 Syntheses of the Ni(II) complexes

6.3.1 Synthesis of complex, 1

To a warm (50^{o}C) stirred solution of ligand L_1 (0.5 g, 1.7 mmol) in methanol (25 ml) was added a methanolic solution (20 ml) of nickel(II) perchlorate hexahydrate (0.61 g, 1.7 mmol). The

solution turned purple during the addition of nickel salt. The reaction mixture was allowed to reflux for 30 min. Then it was allowed to cool to RT anhd filtered. After concentrating the filtrate to about 5 ml, the solution was kept in the freeze at $5^{o}C$ for 2 hours. Purple solid settled at the botom which was collected by filtration and air-dried. Yield 80%. Purple crystals of the complex suitable for x-ray diffraction studies were grown by slow evaporation of an acetonitrile solution at room temperature. I.R. : ~1100 cm^{-1},sbr(ν_{Cl-O}).

6.3.2 Synthesis of complex, 2

The ligand L_2 (1 g, 2.27 mmol) was dissolved in n-butanol (15 ml). Nickel(II) perchlorate hexahydrate (0.83 g, 2.27 mmol) in methanol (7 ml) was added to the warm ($40^{o}C$) stirred solution of the ligand. Color of the reaction mixture became green. It was allowed to reflux for 35 mins when the color changed to light brown. Blue solid appeared when the reaction mixture was allowed to cool to room temperature. The blue solid was collected by filtration, washed using methanol (2 ml) and air-dried. Yield 60%. I.R : ~1100 cm^{-1},sbr (ν_{Cl-O}). Analytical data of the complexes are given in Table 6.1.

CAUTION : Care must be taken when treating organic compounds with nickel(II) perchlorate as potentially explosive mixture may be formed.

6.4 X-ray Crystallography

Dark purple crystals suitable for x-ray diffraction studies were obtained from an acetonitrile solution on slow

Table 6.1

Color, Yield and Microanalytical Data for the Ni(II) Complexes

Complex	Color	Yield %	Empirical Formula	Anal% Calcd				Found			
				C	H	N	S	C	H	N	S
1.	Purple	80	$C_{11}H_{27}N_3O_8S_3Cl_2Ni$	23.79	4.86	7.57	17.31	23.81	4.79	7.54	17.40
2.	Blue	60	$C_{23}H_{27}N_3O_8S_3Cl_2Ni$	39.50	3.86	6.01	13.74	39.41	3.77	5.93	13.90

evaporation at room temperature. Crystal data, data collection, structure solution and refinement details are given in Table 6.2. All diffraction measurements were made at RT (21^{o}C) with a Nicolet R2m/V diffractometer system using graphite monochromated MoK$_{\alpha}$ radiation. Intensity data were corrected for decay, L_p and absorption effects. The structure was solved by heavy atom method [133] and refined on F by full-matrix least squares techniques using the SHELXTL-PLUS program package [134] on a DEC microVax-II computer. Difficulty was encountered in refining the S atoms of the tripodal ligand and two O atoms of one of the perchlorates owing to disorder. The two disordered O atoms were isotropically refined while all other nonhydrogen atoms were refined anisotropically. The site occupancy of the disordered atoms were kept at 0.5. All the hydrogen atoms were generated geometrically (C-H 0.96 Å ; N-H 0.87 Å), assigned isotropic thermal factors, and included in the structure-factor calculations. Analytic expressions of neutral-atom scattering factors were employed [140] and anomalous dispersion corrections [141] were incorporated. The highest peak (0.94 eA^{3}) was located near the Ni(II) ion. Fractional coordinates for non-hydrogen and hydrogen atoms, bond lengths, bond angles involving non-hydrogen atoms, and anisotropic thermal prameters are listed separately.

6.5 RESULTS AND DISCUSSION

A perspective view of one of the complex cations of 1 is shown in Fig. 6.3 showing the atom numbering scheme. The asymmetric unit consists of two independent complex units. The cation is formed through coordination to Ni(II) of all three pairs

Table 6.2 Crystal and Refinement Data for 1

Molecular formula	$C_{11}H_{27}N_3S_3Ni.2ClO_4$
Molecular weight	555.15
Color and habit	black-green prism
Unit cell parameters	a = 12.760(5)Å α = 90 °
	b = 17.932(6) β = 92.70(2)
	c = 19.333(4) γ = 90
	V = 4418.7Å^3 Z = 8 $F(000)$ = 2304
Density (calcd)	1.84 gcm^{-3}
Crystal system	monoclinic
Space group	$P2_1/n$ (No. 14)
Crystal size	0.22 x 0.18 x 0.32 mm^3
Radiation	graphite-monochromatized Mo$K\alpha$, λ = 0.71073 Å
Standard reflections	(1,0,7); (0,-3,-3)
Intensity variation	±1.2%
R_{int} (from merging of equiv. reflections)	0.0193
Absorption coefficient	14.5 cm^{-1}
Mean μr	0.17
Transmmision factors	0.647 to 0.779
Scan type and rate	ω-scan; 4.0 deg min^{-1}
Scan range	0.80° below $K\alpha_1$ to 0.80° above $K\alpha_2$
Background counting	stationary counts for one-fifth of scan time at each end of scan range
Collection range	$h,k,\pm\ell$; $2\theta_{max}$ = 47°
Unique data measured	5817
Obs. data with $\|F_o\| \geq 3\sigma(\|F_o\|)$, n	3187
No. of variables, p	554
Weighting scheme	$w = [\sigma^2\|F_o\| + 0.00015\|F_o\|^2]$
$R_F = \sum\|\|F_o\| - \|F_o\|\| / \sum\|F_o\|$	0.076
$wR = [\sum w^2(\|F_o\| - \|F_c\|)^2 / \sum w^2\|F_o\|^2]^{1/2}$	0.088
$S = [\sum w(\|F_o\| - \|F_c\|^2/(n-p)]^{1/2}$	1.63
Residual extrema in final difference map	+0.94 to -0.62 eÅ^{-3}

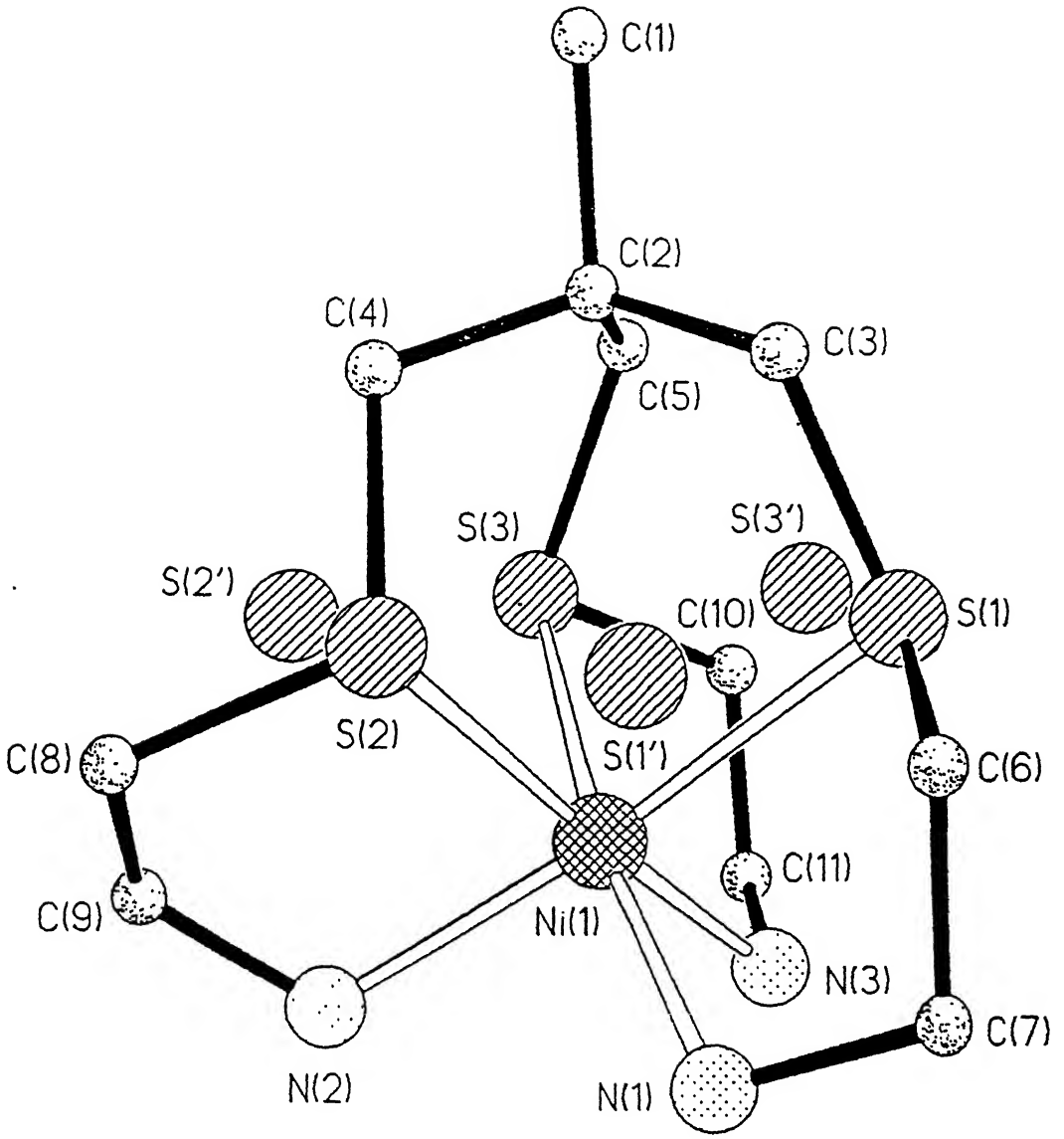

Fig 6.3 **Perspective view of 1 without hydrogen atoms for clarity**

Table 6.3 Fractional Atomic Coordinates (A° $\times 10^4$) and Equivalent Isotropic Temperature Factors ($A^{\circ 2}$ $\times 10^3$) for 1

Atom	x	y	z	U_{eq}
Ni(1)	2248(2)	4792(1)	6822(1)	44(1)
S(1)	1455(3)	4823(3)	5656(2)	51(1)
S(2)	2386(4)	3462(3)	6673(3)	59(2)
S(3)	3947(4)	4979(3)	6365(3)	60(2)
S(1')	1243(35)	3757(27)	6245(25)	63(3)
S(2')	3877(35)	3978(28)	6862(28)	72(3)
S(3')	2695(33)	5291(26)	5764(22)	49(3)
C(1)	3610(15)	3425(10)	4768(9)	90(3)
C(2)	3167(13)	3873(9)	5401(8)	60(2)
C(3)	2025(12)	4017(11)	5202(8)	68(2)
C(4)	3350(14)	3333(9)	6015(9)	69(2)
C(5)	3862(14)	4585(10)	5472(8)	64(2)
C(6)	207(13)	4381(12)	5928(10)	88(3)
C(7)	-92(13)	4874(12)	6543(9)	86(3)
C(8)	3095(18)	3214(13)	7476(10)	110(3)
C(9)	3415(20)	3847(14)	7854(12)	147(3)
C(10)	3732(17)	5982(11)	6185(10)	106(3)
C(11)	3200(17)	6310(12)	6760(14)	130(3)
N(1)	700(10)	4753(9)	7145(7)	78(2)
N(2)	2909(13)	4564(9)	7819(7)	95(3)
N(3)	2268(11)	5959(8)	6903(7)	70(2)
Ni(2)	2306(2)	8479(1)	3747(1)	56(1)
S(4)	2482(5)	9291(4)	4690(3)	64(2)
S(5)	3274(5)	9345(3)	3016(3)	61(2)
S(6)	715(5)	9070(4)	3370(3)	71(2)
S(4')	3546(14)	9388(11)	4137(11)	83(3)
S(5')	1625(17)	9246(10)	2836(9)	88(3)
S(6')	1013(12)	9292(9)	4537(8)	64(2)
C(12)	1768(18)	11250(11)	3651(12)	130(3)
C(13)	1923(14)	10410(9)	3694(10)	73(3)
C(14)	2696(15)	10266(9)	4320(9)	74(2)
C(15)	2404(17)	10212(9)	2994(9)	89(3)
C(16)	800(16)	10080(12)	3759(13)	117(3)
C(17)	3831(15)	9065(10)	4983(9)	81(3)
C(18)	3890(16)	8230(10)	4923(9)	88(3)
C(19)	2854(19)	8905(12)	2230(10)	110(3)
C(20)	2933(18)	8131(11)	2309(10)	108(3)
C(21)	-104(13)	8680(13)	4090(13)	111(3)
C(22)	286(17)	7824(13)	3960(11)	127(3)
N(4)	3762(14)	7976(11)	4150(9)	131(3)
N(5)	2426(15)	7796(9)	2851(9)	115(3)
N(6)	1341(15)	7699(10)	4186(10)	122(3)

Contd.

Cl(1)	340(4)	7192(3)	5869(2)	74(2)
O(1)	843(15)	6642(9)	5507(9)	206(3)
O(2)	775(13)	7925(7)	5746(7)	149(3)
O(3)	-758(10)	7225(11)	5628(9)	206(3)
O(4)	360(12)	7055(9)	6604(6)	152(3)
Cl(2)	6499(4)	8895(3)	3754(2)	75(2)
O(5)	7522(9)	8786(10)	3508(9)	176(3)
O(6)	5762(11)	8561(9)	3255(7)	146(3)
O(7)	6393(14)	8577(8)	4415(6)	156(3)
O(8)	6270(13)	9686(6)	3759(9)	167(3)
Cl(3)	1799(3)	1013(2)	1173(2)	59(1)
O(9)	1125(10)	1298(7)	1700(6)	118(2)
O(10)	2834(8)	1270(8)	1343(8)	124(3)
O(11)	1396(11)	1275(6)	515(5)	107(2)
O(12)	1752(11)	210(5)	1178(7)	120(2)
Cl(4)	-104(4)	3072(3)	8183(3)	78(2)
O(13)	983(9)	3269(9)	8320(8)	169(4)
O(14)	-292(20)	3047(17)	7447(7)	167(4)
O(15)	-418(15)	2432(10)	8523(11)	88(4)
O(16)	-660(19)	3734(12)	8461(16)	226(5)
O(14′)	-625(14)	3438(11)	7613(10)	80(4)
O(15′)	-111(21)	2265(8)	8015(16)	205(5)
O(16′)	-661(17)	3171(17)	8808(12)	141(4)

*U_{eq} defined as one third of the trace of the orthogonalized U tensor.

Atoms O(14) to O(16′) have isotropic thermal parameters.

All six S atoms and atoms O(14) to O(16′) have the same site occupancy factor of 1/2.

Table 6.4 Bond Distences (A°) in 1

Ni(1)-S(1)	2.428(5)	Ni(1)-S(2)	2.409(5)
Ni(1)-S(3)	2.403(5)	Ni(1)-S(1')	2.49(5)
Ni(1)-S(2')	2.54(5)	Ni(1)-S(3')	2.33(4)
Ni(2)-S(4)	2.336(6)	Ni(2)-S(5)	2.469(7)
Ni(2)-S(6)	2.374(7)	Ni(2)-S(4')	2.37(2)
Ni(2)-S(5')	2.37(2)	Ni(2)-S(6')	2.72(2)
Ni(1)-N(1)	2.10(1)	Ni(1)-N(2)	2.11(2)
Ni(1)-N(3)	2.10(1)	Ni(2)-N(4)	2.18(2)
Ni(2)-N(5)	2.13(2)	Ni(2)-N(6)	2.07(2)
S(1)-C(3)	1.86(2)	S(1)-C(6)	1.88(2)
S(2)-C(4)	1.83(2)	S(2)-C(8)	1.82(2)
S(3)-C(5)	1.86(2)	S(3)-C(10)	1.85(2)
S(1')-C(6)	1.82(5)	S(2')-C(4)	2.09(5)
S(2')-C(8)	2.10(6)	S(3')-C(5)	2.05(5)
S(3')-C(10)	1.96(5)		
C(1)-C(2)	1.59(2)	C(2)-C(3)	1.51(2)
C(2)-C(4)	1.54(2)	C(2)-C(5)	1.56(2)
C(6)-C(7)	1.54(3)	C(7)-N(1)	1.52(2)
C(8)-C(9)	1.40(3)	C(9)-N(2)	1.44(3)
C(10)-C(11)	1.45(3)	C(11)-N(3)	1.38(3)
S(4)-C(14)	1.91(2)	S(4)-C(17)	1.83(2)
S(5)-C(15)	1.91(2)	S(5)-C(19)	1.77(2)
S(6)-C(16)	1.96(2)	S(6)-C(21)	1.91(2)
S(4')-C(14)	1.95(2)	S(4')-C(17)	1.76(3)
S(5')-C(15)	2.01(3)	S(5')-C(19)	2.09(3)
S(6')-C(16)	2.07(3)	S(6')-C(21)	1.97(3)
C(12)-C(13)	1.52(3)	C(13)-C(14)	1.55(3)
C(13)-C(15)	1.55(3)	C(13)-C(16)	1.56(3)
C(17)-C(18)	1.51(3)	C(18)-N(4)	1.56(2)
C(19)-C(20)	1.40(3)	C(20)-N(5)	1.39(3)
C(21)-C(22)	1.64(3)	C(22)-N(6)	1.42(3)
Cl(1)-O(1)	1.39(2)	Cl(1)-O(2)	1.45(1)
Cl(1)-O(3)	1.46(1)	Cl(1)-O(4)	1.44(1)
Cl(2)-O(5)	1.42(1)	Cl(2)-O(6)	1.44(1)
Cl(2)-O(7)	1.41(1)	Cl(2)-O(8)	1.45(1)
Cl(3)-O(9)	1.45(1)	Cl(3)-O(10)	1.42(1)
Cl(3)-O(11)	1.43(1)	Cl(3)-O(12)	1.44(1)
Cl(4)-O(13)	1.44(1)	Cl(4)-O(14)	1.43(1)
Cl(4)-O(15)	1.39(2)	Cl(4)-O(16)	1.49(2)
Cl(4)-O(14')	1.42(2)	Cl(4)-O(15')	1.48(2)
Cl(4)-O(16')	1.44(2)		

Table 6.5 Bond Angles (°) in 1

S(1)-Ni(1)-S(2)	86.6(2)	S(1)-Ni(1)-S(3)	89.9(2)
S(2)-Ni(1)-S(3)	91.3(2)	S(1')-Ni(1)-S(2')	89.4(15)
S(1')-Ni(1)-S(3')	92.0(16)	S(2')-Ni(1)-S(3')	90.8(16)
S(1)-Ni(1)-N(1)	85.4(4)	S(2)-Ni(1)-N(1)	94.5(4)
S(3)-Ni(1)-N(1)	172.4(4)	S(1)-Ni(1)-N(2)	170.1(5)
S(2)-Ni(1)-N(2)	83.6(5)	S(3)-Ni(1)-N(2)	92.0(5)
N(1)-Ni(1)-N(2)	93.6(6)	S(1)-Ni(1)-N(3)	92.9(4)
S(2)-Ni(1)-N(3)	174.4(4)	S(3)-Ni(1)-N(3)	83.1(4)
N(1)-Ni(1)-N(3)	91.1(6)	N(2)-Ni(1)-N(3)	97.0(6)
Ni(1)-S(1)-C(3)	105.4(5)	Ni(1)-S(1)-C(6)	93.0(6)
C(3)-S(1)-C(6)	99.3(9)	Ni(1)-S(2)-C(4)	105.3(5)
C(4)-S(2)-C(8)	103.9(9)	Ni(1)-S(3)-C(5)	105.9(6)
Ni(1)-S(3)-C(10)	94.4(7)	C(5)-S(3)-C(10)	101.1(8)
C(1)-C(2)-C(3)	105.3(13)	C(1)-C(2)-C(4)	103.3(13)
C(3)-C(2)-C(4)	114.4(14)	C(1)-C(2)-C(5)	105.1(13)
C(3)-C(2)-C(5)	114.8(14)	C(4)-C(2)-C(5)	112.5(13)
S(1)-C(3)-C(2)	114.0(12)	C(6)-C(7)-N(1)	109.2(14)
S(3)-C(10)-C(11)	108.7(15)	C(10)-C(11)-N(3)	113.9(18)
Ni(1)-N(1)-C(7)	111.6(10)	Ni(1)-N(2)-C(9)	112.0(13)
Ni(1)-N(3)-C(11)	116.5(12)		
S(4)-Ni(2)-S(5)	91.3(2)	S(4)-Ni(2)-S(6)	90.6(2)
S(5)-Ni(2)-S(6)	89.3(2)	S(4)-Ni(2)-N(4)	86.0(5)
S(5)-Ni(2)-N(4)	91.4(5)	S(6)-Ni(2)-N(4)	176.5(5)
N(4)-Ni(2)-N(5)	87.7(7)	S(4)-Ni(2)-N(6)	97.9(5)
S(5)-Ni(2)-N(6)	169.1(5)	S(6)-Ni(2)-N(6)	84.9(5)
N(4)-Ni(2)-N(6)	95.0(7)	N(5)-Ni(2)-N(6)	90.7(7)
Ni(2)-S(4)-C(14)	106.7(6)	C(14)-S(4)-C(17)	99.7(9)
Ni(2)-S(5)-C(15)	102.6(7)	Ni(2)-S(5)-C(19)	94.1(7)
Ni(2)-S(6)-C(16)	105.3(7)	Ni(2)-S(6)-C(21)	95.9(6)
C(16)-S(6)-C(21)	94(1)		
C(14)-C(13)-C(16)	115(2)	C(15)-C(13)-C(16)	113(2)
S(4)-C(14)-C(13)	110(1)	S(5)-C(15)-C(13)	115(1)
C(17)-C(18)-N(4)	111(1)	S(5)-C(19)-C(20)	109(1)
S(6)-C(21)-C(22)	93(1)	C(21)-C(22)-N(6)	113(2)
Ni(2)-N(4)-C(18)	106(1)	Ni(2)-N(5)-C(20)	115(1)
Ni(2)-N(6)-C(22)	110(1)		

Contd.

O(1)-Cl(1)-O(2)	112(1)	O(1)-Cl(1)-O(3)	109(1)
O(2)-Cl(1)-O(3)	106(1)	O(1)-Cl(1)-O(4)	113(1)
O(2)-Cl(1)-O(4)	109(1)	O(3)-Cl(1)-O(4)	107(1)
O(5)-Cl(2)-O(6)	107.3(9)	O(5)-Cl(2)-O(7)	112(1)
O(6)-Cl(2)-O(7)	110.5(9)	O(5)-Cl(2)-O(8)	109(1)
O(6)-Cl(2)-O(8)	106.6(9)	O(7)-Cl(2)-O(8)	111.2(9)
O(9)-Cl(3)-O(10)	107.3(8)	O(9)-Cl(3)-O(11)	107.9(8)
O(10)-Cl(3)-O(11)	113.0(8)	O(9)-Cl(3)-O(12)	108.7(8)
O(10)-Cl(3)-O(12)	111.1(8)	O(11)-Cl(3)-O(12)	108.8(7)
O(13)-Cl(4)-O(14)	108(1)	O(13)-Cl(4)-O(15)	114(1)
O(14)-Cl(4)-O(15)	114(1)	O(14)-Cl(4)-O(16)	109(2)
O(15)-Cl(4)-O(16)	109(1)		

Table 6.6 Anisotropic Thermal Parameters ($A^{0\,2} \times 10^3$) for the Non-Hydrogen Atoms for 1

Atom	U_{11}	U_{22}	U_{33}	U_{23}	U_{13}	U_{12}
Ni(1)	46(1)	43(1)	43(1)	3(1)	7(1)	6(1)
S(1)	46(2)	62(3)	46(2)	0(2)	0(2)	6(2)
S(2)	71(3)	42(2)	67(3)	5(2)	25(2)	14(2)
S(3)	42(2)	68(3)	69(3)	-5(2)	10(2)	0(2)
S(1')	85(5)	50(5)	56(5)	-12(5)	30(5)	-32(5)
S(2')	78(5)	55(5)	84(5)	15(5)	12(5)	9(5)
S(3')	71(5)	49(5)	26(5)	-1(5)	-11(5)	5(5)
C(1)	122(4)	63(4)	89(4)	20(4)	52(4)	-6(4)
C(2)	70(4)	62(4)	50(4)	5(4)	25(4)	-19(4)
C(3)	55(4)	106(4)	41(4)	-1(4)	-3(4)	-23(4)
C(4)	111(4)	37(4)	62(4)	13(4)	39(4)	4(4)
C(5)	81(4)	73(4)	41(4)	-2(4)	27(4)	9(4)
C(6)	48(4)	132(4)	86(4)	-22(4)	13(4)	-33(4)
C(7)	43(4)	136(4)	82(4)	-1(4)	16(4)	-3(4)
C(8)	155(5)	110(4)	67(4)	51(4)	28(4)	18(4)
C(9)	179(5)	126(5)	125(4)	-8(5)	-93(4)	21(4)
C(10)	156(4)	75(4)	92(4)	-72(4)	64(4)	-40(4)
C(11)	102(4)	87(4)	204(5)	-2(4)	34(5)	18(4)
N(1)	61(4)	86(4)	88(4)	5(4)	31(4)	-13(4)
N(2)	130(4)	92(4)	63(4)	34(4)	6(4)	7(4)
N(3)	73(4)	81(4)	58(4)	9(4)	5(4)	-4(4)
Ni(2)	61(1)	54(1)	53(1)	-11(1)	-10(1)	9(1)
S(4)	82(3)	65(3)	44(3)	4(3)	7(3)	-6(3)
S(5)	62(3)	46(3)	76(3)	-5(3)	21(3)	1(3)
S(6)	52(3)	87(3)	72(3)	-4(3)	-4(3)	5(3)
S(4')	59(4)	76(4)	117(4)	7(4)	21(4)	11(4)
S(5')	139(4)	79(4)	44(4)	18(4)	-9(4)	16(4)
S(6')	58(4)	68(4)	68(4)	-1(4)	33(4)	-2(4)
C(12)	140(5)	75(4)	176(5)	30(4)	31(5)	6(4)
C(13)	67(4)	33(4)	120(4)	9(4)	7(4)	3(4)
C(14)	107(4)	28(4)	84(4)	3(4)	-21(4)	-24(4)
C(15)	165(5)	36(4)	66(4)	3(4)	9(4)	4(4)
C(16)	64(4)	93(4)	194(5)	13(4)	12(4)	24(4)
C(17)	101(4)	70(4)	68(4)	5(4)	-36(4)	-10(4)
C(18)	127(4)	70(4)	61(4)	10(4)	-43(4)	-11(4)
C(19)	187(5)	80(4)	68(4)	-22(4)	53(4)	-15(4)
C(20)	167(5)	77(4)	84(4)	-21(4)	51(4)	-6(4)
C(21)	35(4)	111(4)	190(5)	-15(4)	18(4)	52(4)
C(22)	108(4)	151(5)	118(4)	-65(4)	-39(4)	32(4)
N(4)	128(4)	123(4)	140(4)	13(4)	-31(4)	24(4)
N(5)	158(4)	77(4)	117(4)	26(4)	81(4)	19(4)
N(6)	162(4)	87(4)	123(4)	-14(4)	68(4)	-9(4)

Contd.

Cl(1)	91(3)	66(3)	65(3)	6(2)	-1(2)	-6(2)
O(1)	299(5)	138(4)	185(4)	101(4)	55(4)	-48(4)
O(2)	231(4)	113(4)	105(4)	-54(4)	41(4)	4(4)
O(3)	179(4)	229(5)	201(4)	-13(4)	-82(4)	-47(4)
O(4)	161(4)	187(4)	109(4)	-17(4)	19(4)	40(4)
Cl(2)	102(3)	63(3)	62(3)	4(2)	19(2)	2(2)
O(5)	82(4)	217(5)	231(5)	54(4)	32(4)	77(4)
O(6)	149(4)	177(4)	111(4)	-19(4)	-11(4)	-32(4)
O(7)	265(5)	111(4)	95(4)	-20(4)	31(4)	18(4)
O(8)	198(4)	117(4)	191(4)	28(4)	63(4)	-6(4)
Cl(3)	67(2)	48(2)	63(2)	1(2)	-6(2)	-5(2)
O(9)	129(4)	105(4)	122(4)	21(4)	17(4)	-30(4)
O(10)	71(4)	111(4)	188(4)	-5(4)	-30(4)	5(4)
O(11)	173(4)	71(4)	72(4)	-4(4)	-41(4)	11(4)
O(12)	158(4)	98(4)	101(4)	22(4)	-31(4)	-18(4)
Cl(4)	77(3)	83(3)	74(3)	-6(3)	-1(2)	26(2)

*The exponent takes the form: $-2\pi^2 \sum\sum U_{ij} h_i h_j a^*_i . a^*_j$.

Table 6.7 Fractional Coordinates ($Å \times 10^4$) and Isotropic Thermal Parameters ($Å^2 \times 10^3$) for the Hydrogen Atoms of 1.

	x	y	z	U
H(1A)	3542	3724	4357	120
H(1B)	3219	2971	4699	120
H(1C)	4336	3308	4866	120
H(7A)	-780	4740	6680	150
H(7B)	-89	5387	6402	150
H(9A)	4119	3952	7728	150
H(9B)	3420	3696	8331	150
H(11A)	3052	6822	6646	150
H(11B)	3655	6288	7169	150
H(1NA)	610	5136	7484	120
H(1NB)	579	4274	7348	120
H(2NA)	2353	4552	8137	120
H(2NB)	3394	4954	7951	120
H(3C)	2097	6086	7367	120
H(3D)	1736	6150	6583	120
H(12A)	1461	11417	4067	150
H(12B)	1316	11380	3259	150
H(12C)	2439	11483	3610	150
H(18A)	4561	8061	5106	150
H(18B)	3346	8015	5186	150
H(20A)	2631	7930	1885	150
H(20B)	3660	7993	2357	150
H(22A)	195	7694	3479	150
H(22B)	-145	7507	4228	150
H(4NA)	4343	8145	3894	150
H(4NB)	3714	7442	4121	150
H(5NA)	1728	7667	2686	150
H(5NB)	2802	7351	2984	150
H(6NA)	1412	7741	4681	150
H(6NB)	1549	7208	4049	150

*the exponent takes the form: $-8\pi^2 U \sin^2\theta / \lambda^2$

of sulfurs and nitrogens from the tripod. The two perchlorate anions remain uncoordinated. As the cationic structure shows, there is a definite equilibrium between trigonal antiprismatic (TAP) and trigonal prismatic (TP) arrangements of the six donors around Ni(II). An occupancy factor of 0.5 for each S indicates that both structures are equally probable at RT. The observed Ni-S bond lengths (range, 2.403 - 2.423 Å) in the TAP conformation are shorter compared to those (2.461-2.490 Å) found in a tripodal complex of Ni(II) with the same chromophore [138]. In the TP arrangement, the bond lengths vary widely and lie in the range, 2.33-2.54 Å. The Ni-N bond lengths are quite comparable to those found in similar complexes [138, 142]. For the ligand moiety, the bond lengths and angles are normal within statistical errors except the S-C lengths in the TP arrangement which are appreciably longer [147] than normal values (Table 6.4). The bond lengths and angles of the second cation are found to vary in a similar fashion although the magnitudes are different (Tables 6.4 and 6.5). Out of the four perchlorate anions in the asymmetric unit, one is disordered (Table 6.3).

Conductivity data for the complexes in acetonitrile are given in Table 6.8. As the data indicate, both 1 and 2 behave as 1:2 electrolytes. We have carried out conductance measurements in methanol and DMF. In both these solvents as well, the complexes behave as 1:2 electrolytes.

In the infrared spectra of the complexes, a strong and broad absorption occurs at 1100 cm^{-1} which is attributable to the anionic perchlorates.

Electronic absorption bands (Figs. 6.4 and 6.5) observed for the complexes in acetonitrile solutions are collected in Table 6.8 with assignments. No appreciable change in the band positions occur on changing the solvent indicating that the solvent molecules do not coordinate to the metal ion. Octahedral Ni(II) complexes exhibit three spin allowed ligand field bands [126] corresponding to the transitions from the $^3A_{2g}$ ground state to the $^3T_{2g}$, $^3T_{1g}$ and $^3T_{1g}(P)$ excited states. For complexes with usual octahedral or TAP (D_{3d}) complexes, the extinction coefficients for these bands lie [143] below 30 dm^3mol^{-1} cm^{-1}. As the geometry distorts from ideal ones, the intensities increase slowly and sometimes may result in splitting of the bands as well [126]. For Ni(II) complexes having TP (D_{3h}) geometry, the intensities of the the corresponding ligand field bands are usually higher [143]. Thus, intensities of the three ligand field bands obtained in case of complex, 1 are consistent with its solid state structures which is an equilibrium mixture of TAP and TP microsymmetry. For 2, however the intensities are significantly lower (Table 6.8) due to the fact that for 2, TAP geometry is predominating over TP geometry which is a result of extra rigidity in the ligand superstructure. This rigidity is due to the presence of three aromatic rings in the tripod.

Room temperature magnetic moment (μ_{eff}/μ_B) values for 1 and 2 after diamagnetic corrections are found to be 3.06 and 3.01 respectively. The values are within normal ranges found for octahedral Ni(II) complexes with mixed S,N-donor ligands [138, 144].

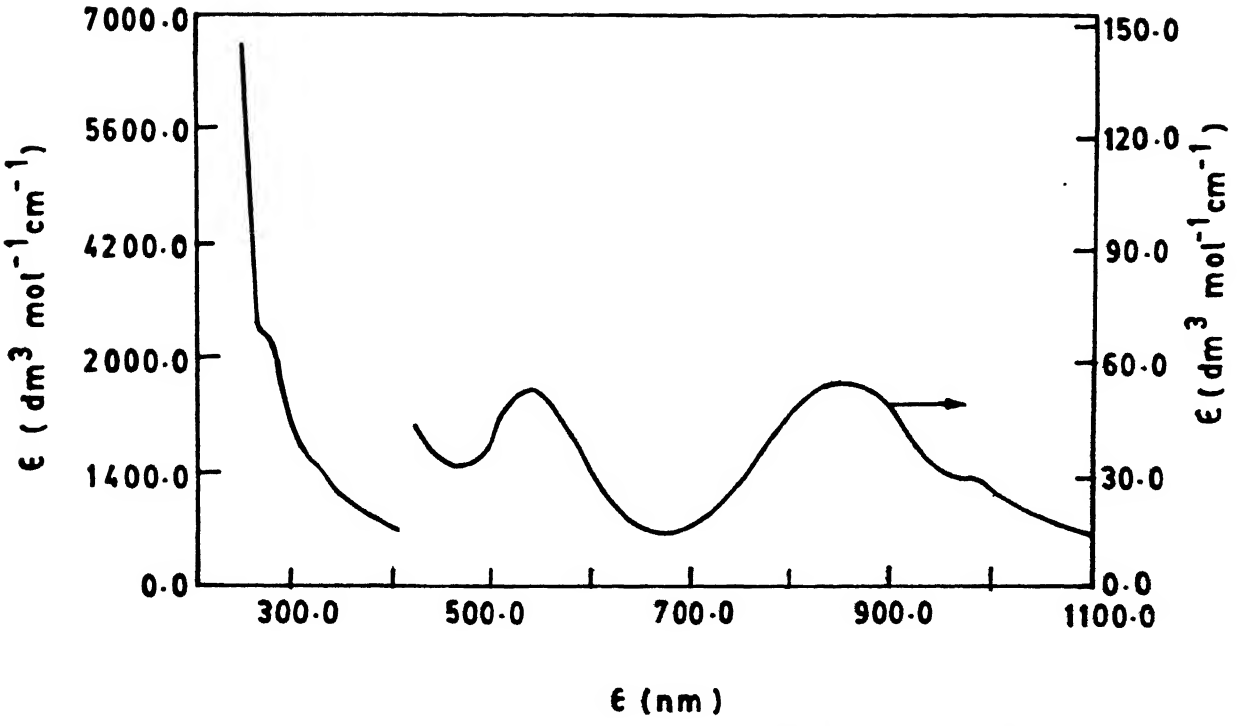

Fig 6.4 Electronic spectrum for the complex 1 in CH_3CN

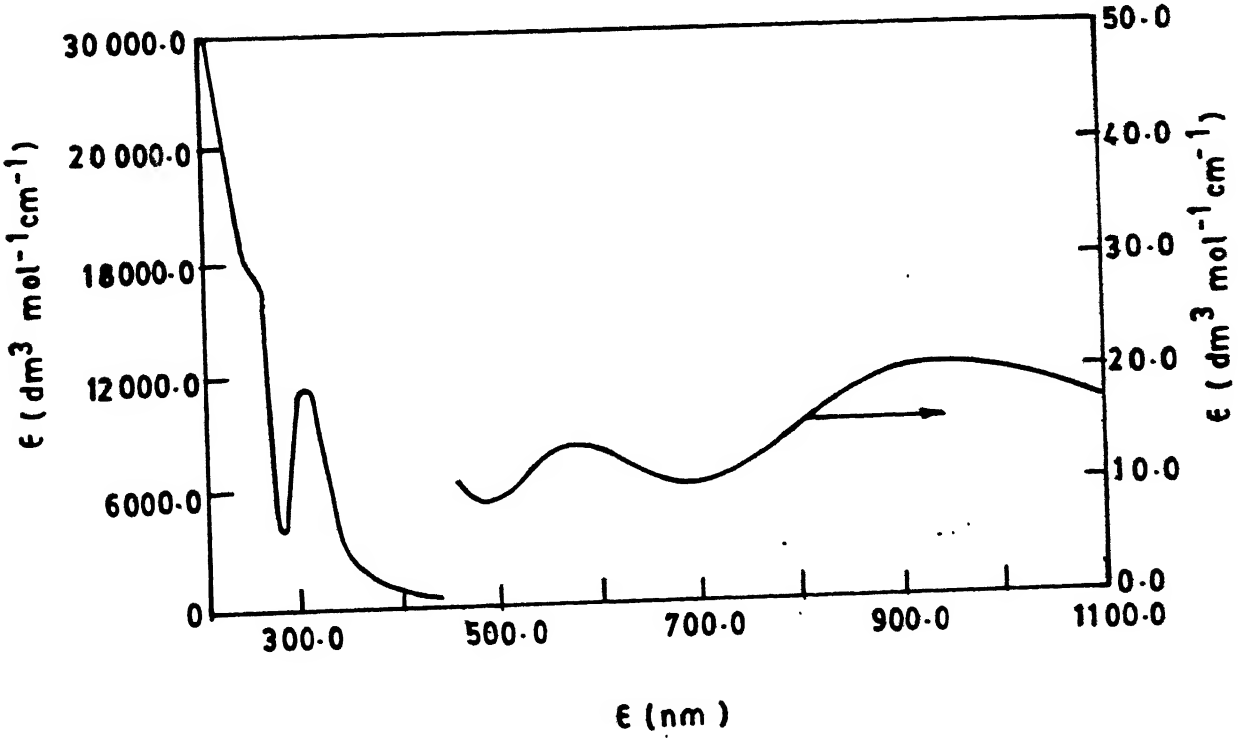

Fig 6.5 Electronic spectrum for the complex 2 in CH_3CN

Table 6.8

Molar Conductance, Magnetic Moment (R T) and UV-Vis Data for the Ni(II) Complexes

Complex	Conductance ($ohm^{-1}cm^{2}mol^{-1}$)	μ_{eff}/μ_B	λ_{max}/nm (ϵ_{max}, $dm^3mol^{-1}cm^{-1}$)	Assignment
1.	246	3.06	974(28)	$^3A_{2g} \rightarrow {}^3T_{2g}$
			848(53)	$^3A_{2g} \rightarrow {}^3T_{1g}$
			541(51)	$^3A_{2g} \rightarrow {}^3T_{1g}(P)$
			334(sh)(1419)	LMCT + Ligand absorption
			282(3122)	LMCT + Ligand absorption
2.	249	3.01	933(21)	$^3A_{2g} \rightarrow {}^3T_{2g}$ / $^3A_{2g} \rightarrow {}^3T_{1g}$
			577(14)	$^3A_{2g} \rightarrow {}^3T_{1g}(P)$
			306(11678)	LMCT + Ligand absorption
			260(sh)(17718)	LMCT + Ligand absorption

REFERENCES

1. T.P. Singer and E.B. Kearney, in *The Proteins*, 1st ed., Vol. 2, Part A, H. Neurath and K. Bailey, Eds., Academic, New York, 1954, p. 124.

2. B.C. Starcher, *J. Nutr*, 1969, 97, 321.

3. T. Mann and D. Keilin, *Proc. Roy, Soc. (London) Ser. B*, 1938, 126, 303.

4. G. Avigad, D. Amaral, C. Asensio and B.L. Horecker, *J. Biol. Chem.*, 1962, 237, 2736.

5. F. Ghiretti, ed., *Physiology and Biochemistry of Hemocyanins*, Academic Press, New York, 1968.

6. S. Katoh, *Nature (London)*, 1960, 186, 533.

7. M.R. Lemberg and J. Barrett, *Cytochromes*, Academic Press, New York, 1973.

8. J.A.D. Copper, W. Smith, M. Bacila, and H. Medina, *J. Biol. Chem.*, 1959, 234, 445.

9. E.I. Solomon, K.W. Penfield, and D.E. Wilcox, *Struct. Bonding*, 1983, 53, 1.

10. B.L. Vallee and R.J.P. Williams, *Proc. Natl. Acad. Sci. (USA)*, 1968, 59, 398.

11. J.M. Guss and H.C. freeman, *J. Mol. Biol*, 1983, 169, 521; J.M. Guss, P.R. Harrowell, M. Murata, V.A. Norris, and H.C. Freeman, J. Mol. Biol., 1986, 192, 361.

12. G.E. Norris, B.F. Anderson and E.N. Baker, *J. Am. Chem. Soc.*,1986, 108, 2784; E.N. Baker, J. Mol. Biol., 1988, 203, 1071.

13. J.M. Guss, E.A. Merritt, R.P. Phizackerley, B. Hedman, M. Murata, K.O. Hodgson and H.C. Freeman, *Science*, 1988, 241,806.

14. K. Petratos, Z. Dauter, K.S. Wilson, A. Lommen, J. Van Beekmen and G.W. Canters, *J. Mol. Biol.*, 1988, 199, 545.

15. A. Messerschmidt, A. Rossi, R. Ladenstein, R. Huber, M. Bolognesi, G. Gatti, A. Marchesini, T. Petruzzelli, and A. Finazzi-Agno, *J.Mol. Biol*, 1989, 206, 513.

16. N. Ito, S.E.V. Phillips, C. Stevens, Z.B. Orgel, M.J. McPherson, J.N. Keen, K.D.S. Yadav and P.F. Knowles, *Nature (London)*, 1991, 350, 87.

17. J.S. Richardson, K.A. Thomas, B.H. Rubin and D.C. Richardson, *Proc. Natl. Acad. Sci. (USA)*, 1975, 72, 1349.

18. E.L. Ulrich and J.L. Markey, *Coord. Chem. Rev.*, 1978, 27, 109.

19. R.A. Bradshaw, W.T. Shearer and F.R.N. Gurd, *J. Biol. Chem.*, 1968, 243, 3817.

20. R.D. Bereman and D.J. Kosman, *J. Am. Chem. Soc.*, 1977, 99, 7322.

21. G. Palmar, G.T. Babcock and L.E. Vickery, *Proc. Natl. Acad. Sci (USA)*, 1976, 73, 2206.

22. J.A. Fee, *Struct. Bonding*, 1975, 23, 1.

23. T.B. Freedman, J.A. Loehr and J.M. Loehr, *J. Am. Chem. Soc.*, 1976, 98, 2809.

24. K.W. Penfield, R.R. Gay, R.S. Himmelwright, N.C. Eickman, V.A. Norris, H.C. Freeman and E.I. Solomon *J. Am. Chem. Soc.* 1981, 103, 4382.

25a. E.I. Solomon, J.W. Hare and H.B. Gray, *Proc. Natl. Acad Sci*, 1976, 73, 1389.

25b. E.I. Solomon, J.W. Hare, D.M. Dooley, J.H. Dawson, P.J. Stephens and H.B. Gray, *J. Am. Chem. Soc.*, 1980, 102, 168.

26. C.A. Bates, W.S. Moore, K.J. Standley and W.H.K. Stevens *Proc. Phys. Soc.*, 1962, 79, 73-83.

27. J.E. Roberts, T.G. Borwn, B.M. Hoffman, J and Peisach, *J. Am. Chem. Soc.*, 1980, 102, 825.

28. R.J. Sundherg and R.B. Martin, *Chem. Rev.*, 1974, 74, 471.

29. L. Casella and M. Gullotti, *Inorg. Chem.* 1985, 24, 84 and references cited therein.

30. E.E. Bernarducci, P.K. Bharadwaj, K. Krogh-Jespersen, J.A. Potenza and H.J. Schugar, *J.Am. Chem. Soc.*, 1983, 105, 3860; H.J. Schugar in *Copper Coordination Chemistry : Biochemical and Inorganic perspectives*, K.D. Karlin and J. Zubieta, Eds., Adenine Press, New York, 1983.

31. E.E. Bernarducci, P.K. Bharadwaj, R.A. Lalancette, K. Krogh-Jespersen, J.A. Potenza and H.J. Schugar, *Inorg. Chem.*, 1983, 22, 3911.

32. S. Knapp, T.P. Keenan, X. Zhang, R. Fikar, J.A. Potenza and H.J. Schugar, *J. Am Chem. Soc.*, 1990, 112, 3452.

33. P.K. Bharadwaj, H.J. Schugar and J.A. Potenza, *Acta Cryst.*, 1991, C47, 754.

34. A.A. Gewirth, S.L. Cohen, H.J. Schugar and E.I. Solomon, *Inorg. Chem.*, 1987, 26, 1133.

35. E.I. Solomon, A.A. Gewirth, and T.D. Westmoreland, in *Advanced EPR- Applications in Biology and Biochemistry*, A.J. Hoff ed., Elsevier, Amsterdam, 1989.

36. J. Del Bene and H.H. Jaffe, *J.Chem. Phys.*, 1968, 48, 4050.

37. F.G. Herring, D.J. Patmore and A. Storr, *J. Chem. Soc. Dalton Trans.*, 1975, 711.

38. T.N. Sonrell, D.L. Jameson and C.J. O'connor, *Inorg. Chem.* , 1984, 23, 190 and references cited therein.

39. T. K. Ha, *J. Mol. Struct.*, 1979, 51, 87.

40. H. Yokoi and A.W. Addison, *Inorg. Chem.*, 1977, 16, 1341.

41. Y. Yokoi and T. Isobe, *Bull. Chem. soc. Jpn.*, 1969, 42, 2187.

42. C.E. Baxter, O.R. Rodig, R.K. Schlatzer and E. Sinn, *Inorg. Chem.*, 1979, 18, 1918; E.M. Gouge and J.F. Geldard, *Inorg. Chem.* , 1978, 17, 270.

43. W.M. Davis, A. Zask, K. Nakanishi and S.J. Lippard, *J. Am. Chem. Soc.*, 1985, 107, 3864.

44. K.W. Penfield, A.A. Gewirth and E.I. Solomon, *J. Am. Chem. Soc.* , 1985, 107, 4519.

45. C.C. Ou, V.M. Miskowski, R.A. Lalancette, J.A. Potenza and H.J. Schugar, *Inorg. Chem.* , 1976, 15, 3157; J.V. Dagdigian, V. McKee, and C.A. Reed, *Inorg. Chem*, 1982, 21, 1332; A.W. Addison, T.N. Rao, J. Reedijk, J. Van Rijn and G.C. Verschoor, *J. Chem. Soc. Dalton Trans.*, 1984, 1349; K.D. Karlin, R.W. Cruse, J.W. McKown, J.C. Hayes, P.L. Dahlstrom and J. Zubieta, *Trans. Met. Chem.*, 1984, 9. 404.

46. H. Sigel, K.H. Scheller, V.M. Rheinberger and B.E. Fischer, *J. Chem. Soc.Dalton Trans.*, 1980, 1022.

47. H.J. Prochaska, W.F. Schwindinger, M. Schwartz, M.J. Burk, E.E. Bernraducci, R.A. Lalancette, J.A. Potenza and H.J. Schugar, *J. Am. Chem. Soc.*, 1981, 103, 3446.

48. E.T. Adman, S. Turley, R. Branson, K. Petratos, D. Banner, D. Tsernoglou, T. Beppu and H. Watanabe, *J. Biol. Chem.*, 1989, 264, 87.

49. A.G. Sykes, *Advances in Inorganic Chemistry*, 1991, 36, 377; B. Reinhammar and B.G. Malmström in *copper proteins*, T.G.Spiro, ed., John Wiley, New York, 1981, 3, 109.

50a. T.H. Stevens, C.T. Martin, H. Wang, G.W. Brudvig, C.P. Scholes and S.I. Chan, *J. Biol. Chem.*, 1982, 257, 12106.

50b. G. Palmer, *Pure and Appl. chem.*, 1987, 59, 749 and references cited threin.

51. I. Bertini and A. Scozzafava, *Metal Ions in Biological systems*, 1981, 12, 31.

52. H.B. Gray and E.I. Solomon, in *Copper Proteins*, T.G. Spiro, ed. John Wiley, New York, 1981, *3*, 1.

53. K.W. Penfield, A.A. Gewirth and E.I. Solomon, *J. Am. Chem. Soc.*, 1985, 107, 4519; A.A. Gewirth and E.I. Solomon, *J. Am. Chem. Soc.*, 1988, 110, 3811.

54. E.I. Solomon, A.A. Gewirth and T.D. Westmoreland, in *Advanced EPR- Applications in Biology and Biochemistry*, A.J. Hoff ed., Elsevier, Amsterdam, 1989.

55. B. Sarkar, *Metal Ions in Biological Systems*, 1981, 12, 270.

56. M. Younes and U. Wener, *Biochem. Biophys. Res. Commun.* , 1977, 78, 1247.

57a. H.K. Back, R.L. Cooper, and R.A. Holwerda, *Inorg. Chem.*, 1985, 24, 1077.

57b. F.J. Davis, B.C. Gilbert, and R.O.C. Norman, *J. Chem. Soc. Perkin Trans. II*, 1983, 1763.

58. A.R. Amundsen, J. Whelan, and B.Bosnich, *J.Am. Chem. Soc.*, 1977, 99, 6730.

59. K. Miyoshi, Y. Sugiura, K. Ishizu, Y. Itaka and H. Nakamura, *J. Am. Chem. Soc.*, 1980, 102, 6130.

60. M.F. Corrigan, K.S. Murray, B.O. West and J.R. Pillerow, *Aust. J. Chem.*, 1977, 30, 2455.

61. J.L. Hughey, T.G. Fawcett, S.M. Rudich, R.A. Lalancette, J.A. Potenza and H.J. Schugar, *J. Am. Chem. Soc.*., 1979, 101, 2617.

62. A.A. Addison and E. Sinn., *Inorg. Chem*, 1983, 22, 1225.

63. O.P. Anderson, C.M. Perkins, and K. Brito *Inorg. Chem.*, 1983, 22, 1267.

64. N. Aoi, Y. Takano, H. Ogino, G. Matsubayashi and T. Tanaka, *J. Chem. Soc. Chem. Commun*, 1985, 703.

65. R. Gleiter and J. Spanget-Larsen, *Top. Curr. Chem.*, 1979, 86, 147.

66. E. John, P.K. Bharadwaj, J.A. Potenza and H.J. Schugar, *Inorg. Chem.*, 1986, 25, 3065.

67. E. John, P.K. Bharadwaj, J.A. Potenza, K. Krög-Jespersen and H.J. Schugar, *J. Am. Chem. Soc.*, 1986, 108, 5015.

68. A.B.P. Lever and H.B. Gray, *Acc. Chem. Res.*, 1978, 11, 348.

69. J. Becher, H. Toftlund and P.H. Olesen, *J. Chem. Soc. Chem. Commun.*, 1983, 740.

70. H. Toftlund, J. Becher, P.H. Olesen and J.H. Pedersen, *Isr. J. Chem.*, 1985, 25, 56.

71. O.P. Anderson, J. Becher, H. Frydendahl, L.F. Taylor and H. Toftlund, *J. Chem. Soc. Chem. Commun.*, 1986, 699.

72. J.S. Thompson, T.J. Marks and J. Ibers, *J. Am. Chem. Soc.*, 1979, 101, 4180.

73. N. Kitajima, K. Fujisawa and Y. Moro-oka, *J. Am. Chem, Soc.* 1990, 112, 3210.

74. J. Becher, D.J. Brockway, K.S. Murray, P.J. Newman and H. Toftlund, *Inorg. Chem.*, 1982, 21, 1791.

75. L. Casella, *Inorg. Chem.*, 1984, 23, 2781; L. Casella, M. Gullotti, E. Suardi, M. Sisti, R. Pagliarin and P. Zanello, *J. Chem. Soc. Dalton Trans*, 1990, 2843 and references cited therein.

76. P.K. Bharadwaj, J.A. Potenza and H.J. Schugar, *J. Am. Chem. Soc.*, 1986, 108, 1351.

77. J.M. Berg, D.J. Spira, K.O. Hodgson, A.E. Bruce, K.F. Miller, K.L. Corbin and E.I. Stiefel, *Inorg Chem.*, 1984, 23, 3412.

78. P.K. Bharadwaj, E. John, C. Xie, D. Zhang, D.N. Hendrickson, J.A. Potenza , and H.J. Schugar, *Inorg. Chem.*, 1986, 25, 4541.

79. R. Cammack, in *The Bioinorganic Chemistry of Nickel*, J.R. Lancaster Jr. ed., VCH Publishers, New York, 1988, Ch. 8.

80. S.W. Ragsdale, H.G. Wood, J.A. Morton, L.G. Ljungdahl and D.V. DerVartanian, in *The Bioinorganic Chemistry of Nickel*, J.R. Lancaster Jr. ed., VCh Publishers, New York, 1988, Ch. 14.

81a. S. Fox, Y. Wang, A.Silver and M. Millar, *J. Am. Chem. Soc.*, 1990, 112, 3218.

81b. H.J. Krugar and R.H. Holm *Inorg. Chem.*, 1987, 26, 3645.

82. H.J. Krugar and R.H. Holm, *J. Am. Chem. Soc.*, 1990, 112, 2955; P. Starropoulous, M. Carrie, M.C. Muetterites and R.H. Holm, *J. Am. Chem. Soc.*, 1990, 112, 5385; H. J. Krugar, G. Peng and R.H. Holm, *Inorg. Chem.*, 1991, 30, 734.

83. S.B. Choudhury, D. Ray, and A. Chakravorty, *Inorg. Chem.*, 1991, 30, 4354 and references cited therein.

84. N. Baidya, D. Ndreu, M.M. Olmstead and P.K. Mascharak, *Inorg. Chem.*, 1991, 30, 2448.

85. R. Cammack, D. Patil, R. Aguirre and E.C. Hatchikian, *FEBS LETT.*, 1982, 142, 289; J.J. Moura, I. Moura, B.H. Huynh, H.J. Krugar, M. Teixera, R.C. MuVarny, D.V. DerVartannian, A.V. Xavier, H.D. Peck and J. Le Gall, *Biophys. Biochem. Res. Commun.* 1982, 108, 1388.

86. M.K. Eidsness, R.J. Sullivan and R.A. Scott, in *The Bioinorganic Chemistry of Nickel*, J.r. Lancaster Jr. ed., VCH publishers, New York, 1988, Ch. 4.

87. M.A. Hitchman and T.D. Waite, *Inorg. Chem.*, 1976, 15, 2150.

88. D.W. Margerum and G.D. Owens, *Metal Ions in Biological Systems*, 1981, 12, 75.

89. C. Orvig, D.J. Berg and S.J. Rettig, *J. Am. Chem. Soc.*, 1991, 113, 2528; R.M. Kirchner, C. Mealli, M. Bailey, M. Howe, L.P. Torre, L.J. Wilson, L.C. Andrews, N.J. Rose and E.C. Lingafelter, *Coord. Chem. Rev.*, 1987, 77, 89.

90. L. Cassella, M. Gullotti, E. Suardi, M. Sisti, R. Pagliarin and P. Zanello, *J. Chem. Soc., Dalton Trans.*, 1990, 2843 and references cited therein.

91. R.J. Deeth, M.A. Hitchman, G. Lehman and H. Sachs, *Inorg. Chem.*, 1984, 23, 1310.

92. D.D. Perrin, W.L.F. Armarego and D.R. Perrin, *Purification of Laboratory Chemicals*, Ist Edition, Pergamon Press, Oxford, 1966.

93. M.A. Weiner and A. Basu, *Inorg. Chem.*, 1980, 19, 2797.

94. S.L. Kelly and K.M. Kadish, *Inorg. Chem.*, 1984, 23, 679.

95. O. Mehn-Cohn and B. Tarkowski, *Synthesis*, 1978, 56.

96. A.R. Amundsen, J. Whelan and B. Bosnich, *Inorg. Chem.*, 1979, 18, 206.

97. K. Nakamoto, *Infrared and Raman Spectra of Inorganic and Coordination Compounds*, 4th Edn. Wiley, New York, 1986, p. 251.

98. W.J. Grey, *Coord. Chem. Rev.*, 1971, 7, 81.

99. F.A. Cotton and G. Wilkinson, *Advanced Inorganic Chemistry*, 5th Edn. John Wiley, New York, 1988, p. 768.

100. B.J. Hathaway and D.E. Billing, *Coord. Chem. Rev.*, 1970, 5, 43.

101. B.J. Hathaway, *J. Chem. Soc. Dalton Trans.*, 1972, 1196.

102. B.P. Kennedy and A.B.P. Lever, *J. Am. Chem. Soc.*, 1973, 95, 6907.

103. U.M. Miskowski, J.A. Thich, R. Solomon and H.J. Schugar, *J. Am. Chem. Soc.*, 1976, 98, 8344.

104. H.J. Schugar in *Copper Coordination Chemistry : Biochemical and Inorganic Perspectives*, K.D. Karlin and J. Zubieta eds, Adenine Press, New York, 1983.

105. A.B.P. Lever, *Inorganic Electronic Spectroscopy*, 2nd. Edn., Elsevier, New York, 1984, p. 353.

106 J.J. D'Amico and W.E. Dahl, *J. Org. Chem.* 1975, 40, 1224.

107. J.J. Pastuszak and A. Chimiak, *J. Org. Chem.*, 1981, 46, 1868.

108. B.R. McGarvey, *Trans. Met. Chem*, 1966, 3, 89.

109. M. Gerloch and J.R. Miller, *Progr. Inorg. Chem.*, 1968, 10, 1.

110. M.A. Hitchman, C.D. Olson and R.L. Belford, *J. Chem. Phys.*, 1969, 50, 1195.

111. P. Beardwood and J.F. Gibson, *J. Chem. Soc., Chem. Commun.*, 1983, 1099.

112. R.D. Bereman, M.R. Churchill and G.D. Shields, *Inorg. Chem.*, 1979, 18, 3117.

113. D.W. Smith, *Coord. Chem. Rev.*, 1991, 109, 181.

114. R.A. Harlow, W.J. Wells III, G.W. Watt and S.H. Simonsen, *Inorg Chem.*, 1975, 14, 1768; L.P. Battaglia, A.B. Corradi, G. Marcotrigiano, L. Menabue and G.C. Pellacaui, *Inorg. Chem.*, 1979, 18, 148.

115. R.D. Bereman, G.D. Shields, J. Bordner and J.R. Dorfman, *Inorg. Chem.*, 1981, 20, 2165 and references cited therein.

116. M.B. Robin, *Higher Excited States of Polyatomic Molecules*, Vol.1, Academic Press, N.Y. (1975).

117. *Organic Electronic Spectral Data*, J.P. Phillps, D. Bates, H. Feuer and B.S. Thyagarajan, Eds., John Wiley, New York, 1982, Vol. XVIII, p.5.

118. M.I. Pilo, G. Manca, M.A. Zoroddu and R. Seeber, *Inorg. Chim. Acta.*, 1991, 180, 225.

119. W. Levasson and M.D. Spicer, *Coord. Chem. Rev.*, 1987, 76, 45.

120. R.D. Cannon, B. Chiswell and L.M. Venanzi, *J. Chem. Soc. (A)*, 1967, 1277.

121. J.R. Vaughan, Jr., *J. Am. Chem. Soc.*, 1951, 73, 3547.

122. T. Yamamura, M. Tadokoro and R. Kuroda, *Chem. Lett.*, 1989, 1245.

123. E. Kimura, Y. Kurogi, T. Tojo, M. Shiouoya and M. Shiro, *J. Am. Chem. Soc*, 1991, 113, 4857.

124. A.B.P. Lever, *Inorganic Electronic Spectroscopy*, 2nd Edn. Elsevier, New York, 1984, p. 553-555.

125. M. Dolwnes, J. Whelan and B. Bosnich, *Inorg. chem.*, 1981, 20, 1081.

126. E.I. Solomon and C.J. Ballhausen, *Mol. Phys.*, 1975, 29, 279.

127. M. Ciampolini, J. Gelsomini and N. Nardi, *Inorg. Chim. Acta*, 1968, 2, 343.

128. D. Ray, S. Pal and A. Chakravorty, *Inorg. Chem.*, 1986, 25, 2676.

129. A.L. Balch and R.H. Holm, *J. Am. Chem. Soc.*, 1966, 88, 5201.

130. H.A. Akers, M.C. Vang and T.D. Updike, *Can. J. Chem.*. 1987, 65, 1364.

131. A.U. Joshua, J.R. Scott, S.M. Sondhi, R.G. Ball, and J.W. Lown, *J. Org.Chem*, 1987, 52, 2447.

132. P.K. Bharadwaj, J.A. Potenza and H.J. Schugar, *Acta Cryst.*, 1988, C43, 2365.

133. Direct Method Program MULTAN 82 by Main, Lessinger, Declercq, Woolfson and Germain.

134. G.M. Sheldrick in *Crystallographic Computing 3 : Data Collection, Structure Determination, Proteins and Databases*, G.M. Sheldrick, C. Krugar and R. Goddand eds., Oxford University Press, New York, 1985.

135. K Nakamoto, *Infrared and Raman Spectra of Inorganic and Coordination Compounds*, 4th Edn, Wilew, New York, 1986, P.167.

136. A.M. Bond and M.A. Khalifa, *Inorg. Chem.*, 1987, 26, 413 and references cited therein.

137. R.M. Kirchner, C. Mealli, M. Bailey, M. Howe, L.P. Torre, L.J. Wilson, L.C. Andrews, N.J. Rose and E.C. Lingafelter, *Coord. Chem. Rev.*, 1987, 77, 89.

138. K. Ragunathan and P.K. Bharadwaj, *J. Chem. Soc., Dalton Trans*, 1992,0000.

139. J. Buckigham, *Dictionary of Organic Compounds*, 5th Edn, Chapman and Hall, Newyork, 1982, H-02490.

140. D.T. Cromer and J.T. Waber, *Acta Cryst.*, 1965, 18, 104.

141. *International Tables for X-ray Crystallography*, Kynoch Press, Birmingham, 1974, Vol. 4 (present distributors, Kluwer Academic Publishers, Dordrect).

142. M. Kumar, G.J. Colpas, R.O. Day and M.J. Maroney, *J. Am. Chem. Soc.*, 1989, 111, 8323.

143. C.C. Ou, V.M. Mishowshi, R.A. Lalancette, J.A. Potenza and H.J. Chugar, *Inorg. Chem.*, 1976, 15, 3157.

144. E. Larsen, G.N. Lamar, B.E. Wagner, J.E. Paarhs and R.H. Holm, *Inorg. Chem*, 1972, 11, 2652.

LIST OF PUBLICATIONS

. Synthesis and Characterisation of Copper(II) Complexes Having N_2S^*S and N_2S^*O (S^* = Thioether) Donor Sets, S. Mandal and P. K. Bharadwaj, Ind.J.Chem., 1991, 30A, 948.

. Hexacoordinated Cu(II)-Complexes Having $CuN_2S^*{}_2S_2$ (S^*= thioether) Chromophore : Synthesis, Electrochemistry and Spectroscopy, S.K. Mandal, and P.K. Bharadwaj, Polyhedron, 1992, 11, 1037.

3. Reactivity of Bismuth(III) Dichlorodithiocarbamate : Synthesis and Spectroscopic Characterisation of Mixed Bismuth-Molybdenum and Bismuth-Tungsten Complexes, S. Mandal, G. Mandal, R. Shukla and P. K. Bharadwaj, Ind.J.Chem., 1992, 31A, 128.

. Hexacoordinated Copper(II)-Thiolates. Part 2. Synthesis and Characterisation of a Copper(II) Complex with a Reversible Oxidative Response, S. Mandal, R. Shukla and P. K. Bharadwaj, Polyhedron (in press).

5. Synthesis and Characterisation of Cu(II) and Ni(II) Complexes with Ligands Having $N_2S_2S_2$ (S =Thioether) donors: Pseudoreversible Cu(III)/Cu(II) Couple, S. Mandal, R. Shukla and P. K. Bharadwaj, Polyhedron (in press).

5. Rigidity of Donor Atoms' Topology: Synthesis and Spectroscopic Characterization of Cu(II) and Cu(II)-Doped Zn(II) Complexes Having the Chromophore MN_4, S. Mandal and P. K. Bharadwaj,

Polyhedron (in press).

*7. Crystal Structure of $[Ni(OH_2)_2(NH_2CH_2CH_2CH_2NH_2)_2][picrate]_2$ W. Clegg, P. K. Bharadwaj and S. Mandal, Acta Cryst.C (in press).

*8. Tetrakis(pyridine)Nickel(II)Chloride, R. E. Bachman, K. H. Whitmire, S.Mandal and P.K. Bharadwaj, Acta Cryst.C (in press).

9. Modelling the Blue Proteins' Active Sites: Synthesis and Characterisation of CuN_2S_2 Complexes Showing Rhombic EPR Spectra and High Cu(II)/Cu(I) Potential, S. Mandal, R. Shukla and P.K. Bharadwaj, J.Chem.Soc.Dalton Trans. (under revision).

10. Ni(II) Complexes with Hexadentate Tripodal Ligands Having S_3N_3 Donor Set, S. Mandal, P. K. Bharadwaj and T. C. W. Mak, (communicated).

11. A New Route to Cu(II)-Thiolates Through Interactions Between Cu(I) and Macrocyclic Disulfides:Synthesis and Characterisation of Planar CuN_2S_2 Complexes, S. Mandal and P. K. Bharadwaj (communicated).

*12. First Example of a Hepta-coordinated Bi(III) Complex: Crystal and Molecular Structure of Bi(III) with the Tripodal Ligand, SALTREN, S. Mandal, P. K. Bharadwaj and A. H. White (communicated).

*Not related to the present thesis